



Dissertation

Novel Long-Wavelength Photoinitiators for Dental Applications

ausgeführt zum Zwecke der Erlangung
des akademischen Grades eines Doktors der technischen
Wissenschaften
unter der Leitung von

Ao. Univ. Prof. Dr. Robert Liska
Institut 163
Institut für Angewandte Synthesechemie

eingereicht an der Technischen Universität Wien
Fakultät für Technische Chemie

von

Dipl.-Ing. Stephan Benedikt
0625752
Wallgasse 12/24, 1060 Wien

Wien, November 2015

Danksagung

Zuallererst möchte ich Prof. Robert Liska für die Möglichkeit danken, dass ich meine Dissertation am Institut für angewandte Synthesechemie durchführen durfte, für die Betreuung während der Arbeit und natürlich auch für das geduldige Korrekturlesen am Ende. Zusätzlich möchte ich mich für das interessante Thema bedanken.

Dieser Dank geht auch an Prof. Norbert Moszner von Ivoclar Vivadent, dessen fachkundige Unterstützung mich des Öfteren ein gutes Stück weitergebracht hat.

Natürlich möchte ich mich auch bei all meinen Kollegen, vor allem bei Paul, Davide, Pauli und György für die angenehme Arbeitsatmosphäre und viele schöne Tage auch abseits der Uni bedanken. Ein spezieller Dank geht dabei an Paul, für die fachliche und besonders die moralische Unterstützung während meiner Dissertation.

Nicht zuletzt möchte ich mich auch noch bei meinen beiden Bachelorstudenten Moritz und Patrick bedanken, die beide einen äußerst wertvollen Beitrag zu meiner Arbeit geleistet haben und schließlich auch an den Grundlagen und Denkanstößen für meine Publikationen mitgewirkt haben.

Besonders möchte ich mich an dieser Stelle bei meinem Vater und meiner Mutter bedanken, die immer an mich geglaubt haben und ohne deren Unterstützung in egal welcher Art und Weise ein Studium unmöglich gewesen wäre.

Selbstverständlich auch einen großen Dank an Sasha, die während dieser oft turbulenten Zeit immer für mich da war.

Abstract

Modern composite tooth fillings consist of inorganic filler and organic methacrylate matrix. This matrix is cured with a photoinitiator system to achieve a solid material. It is known that the state of the art photoinitiator system camphorquinone/ethyl-(dimethylamino) benzoate shows moderate reactivity and low solubility in general but especially in slightly acidic and aqueous primer mixtures. Furthermore higher penetration depth of light is desired, which could be solved by developing photoinitiators that initiate at longer wavelengths.

First studies with bisphosphylketones showed the desired red-shift but stability issues concerning water or temperature led to their elimination from the list of possible new photoinitiators.

Certain zirconium complexes also had potential but the zirconium central atom coordinated with the monomer double bonds leading to decomposition of the compounds.

Another concept is based on combination of diketone systems with heteroatoms with free d-orbitals. Even though the very interesting red-shift concept (λ_{\max} up to 490 nm) worked out, the reactivity was not in a reasonable range.

Benzoyl phenyltelluride was expected to be a red-shifted photoinitiator but instead was found to be a highly reactive TERP-reagent for visible light (400-500 nm) induced controlled radical polymerization. It provides polydispersities (1.2-1.3) among the lowest reported in literature and works best with acrylamides and acrylates.

In the field of water-soluble photoinitiators for primer mixtures an improvement could be achieved as well. Monoacylphosphine oxide (MAPO) and bisacylphosphine oxide (BAPO) salts based on sodium or lithium define an important and in the latter case a new class of water-soluble photoinitiators for radical polymerization. These compounds show excellent water-solubility, biocompatibility, storage stability and reactivity. Concerning these properties, the MAPO and BAPO salts are at least in the same range (biocompatibility, stability) or show even better results (reactivity) than state of the art photoinitiators.

Kurzfassung

Moderne Zahnfüllung auf Kompositbasis bestehen aus anorganischem Füller und organischer Methacrylatmatrix. Diese Matrix wird mit einem Photoinitatorsystem ausgehärtet. Es ist bekannt, dass das aktuelle Initiatorsystem auf der Basis von Campherchinon/Ethyl-(dimethylamino)benzoat generell eine geringe Reaktivität speziell in sauren und wässrigen Primer Mischungen aufweist. Außerdem wäre es wünschenswert eine höhere Eindringtiefe des Lichts zu erreichen, was durch die Entwicklung von Photoinitiatoren, die bei längeren Wellenlängen initiieren gelöst werden könnte.

Erste Studien zu den Bisphosphylketonen misslingen im Hinblick auf die geringe thermische und hydrolytische Stabilität dieser Verbindungsklasse.

Zirkonkomplexe zeigten zunächst ein gewisses Potential, allerdings stellte sich heraus, dass das Zirkonium Zentralatom mit den Monomerdoppelbindungen koordiniert, was zu einer Spaltung der Verbindung führt.

Diketonsysteme mit Heteroatomen mit freien d-Orbitalen wurden trotz interessantem Konzept und erreichtem Rotshift (λ_{\max} bis zu 490 nm) ebenfalls ausgeschlossen, da die Reaktivität zu gering war.

Benzoylphenyltellurid wurde als Photoinitiator mit höherem Rotshift entwickelt, stellte sich aber stattdessen als hochreaktives TERP-Reagenz für kontrollierte radikalische Polymerisation im sichtbaren Licht (400-500 nm) heraus. Damit können einige der niedrigsten Polydispersitäten (1.2-1.3) aus der Literatur erreicht werden und vor allem Acrylamide und Acrylate lebend polymerisiert werden.

Auch im Gebiet der wasserlöslichen Photoinitiatoren konnten Fortschritte erzielt werden. Mono- und Bisacylphosphinoxidsalze auf Basis von Natrium und Lithium definieren eine wichtige und in letzterem Fall sogar eine neue Klasse von wasserlöslichen Photoinitiatoren. Diese Verbindungen weisen exzellente Wasserlöslichkeit, Biokompatibilität, Lagerstabilität und Reaktivität auf. Im Hinblick auf diese Eigenschaften sind sie gleich gut (Biokompatibilität, Stabilität) oder sogar besser (Reaktivität) als die gängigen Photoinitiatoren.

Introduction	1
Objective	14
Results and Discussion	15
Experimental	119
Materials, Equipment and Analysis	145
Summary	148
Indices	154

	GP	EP
1. Bisphosphylketones	15	
1.1. State of the Art	15	
1.2. Syntheses	17	
1.2.1. Synthesis of Carbonylbis(diethoxyphosphine oxide) 9 (pathway A)	19	119
1.2.1.1. 2-Naphthalenesulfonyl Azide 13		119
1.2.1.2. Diazomethylenebis(diethoxyphosphine oxide) 14		120
1.2.1.3. Carbonylbis(diethoxyphosphine oxide) 9		120
1.2.2. Synthesis of Carbonylbis(diphenylphosphine oxide) 8	21	121
1.2.2.1. Synthesis via Diazotation and Hydrolysis (Pathway A)	21	121
1.2.2.2. Synthesis via Halogenation and Hydrolysis (Pathway B)	23	122
1.2.2.3. Synthesis with Phosgene (Pathway C)	26	
1.2.2.4. Synthesis via Direct Oxidation (Pathway D)	26	
1.3. Characterization and Interpretation	27	
2. Zirconium Complexes	32	
2.1. State of the Art	32	
2.2. Syntheses	37	
2.2.1. Bis(9-fluorenyl)ethane 26		123
2.2.2. (Ethylenebis(9-fluorenyl))zirconiumdichloride 25		124

2.3.	Characterization and Interpretation	41	
3.	Diketone Systems	43	
3.1.	State of the Art	43	
3.2.	Preliminary Experiments	46	
3.3.	Syntheses	49	
3.3.1.	Synthesis of Phenylglyoxylic Diethylphosphite 36 and Phenylglyoxylic Diphenylphosphine Oxide 32 (Pathway D)	51	125
3.3.1.1.	Phenylglyoxylic Acid Chloride 35		125
3.3.1.2.	Phenylglyoxylic Diphenylphosphine Oxide 32		126
3.3.2.	Synthesis of Oxalylbis(diphenylphosphine Oxide) 38 (Pathway E)	54	127
3.3.3.	Synthesis of Phenylglyoxylic Tri(m)ethylgermanium 33 and 39	55	128
3.3.3.1.	Synthesis with Pd-Catalyst (Pathway A)	55	
3.3.3.2.	Synthesis in Analogy to Phenylglyoxylic Trimethylsilicium 31 (pathway B)	56	127
3.3.3.3.	Synthesis via Grignard Reaction (Pathway C)	59	
3.3.3.4.	Synthesis via Organolithium Reaction (Pathway D)	60	
3.3.3.5.	Synthesis via Seebach Umpolung (Pathway F)	61	130
3.3.3.6.	Synthesis with a Copper Intermediate (Pathway G)	63	131
3.3.4.	Synthesis of Phenylglyoxylic Triphenylgermanium 46 (Pathway G)	64	132
3.3.5.	Synthesis of Phenylglyoxylic Trimethylsilyl Silicium 47 (Pathway H)	64	133
3.4.	Characterization & Interpretation	65	
3.4.1.	UV-VIS	66	
3.4.2.	Photo-DSC	70	
4.	Acyltellurides	73	
4.1.	State of the Art	73	
4.2.	Syntheses	74	
4.2.1.	Synthesis of Benzoyl Phenyltelluride BPT	76	
4.2.1.1.	Synthesis with a NaBH ₄ /NaOH Redox-System	76	134
4.2.1.2.	Synthesis with a Sm/ZrCl ₄ Redox-System	77	
4.2.2.	Synthesis of Pentafluorobenzoyl Phenyltelluride 50	77	135

4.2.3. Synthesis of Mesityl and Dimethoxybenzoyl Phenyltelluride 48 and 49	78	
4.2.4. Synthesis of Benzoyl Pentafluorophenyltelluride 51	79	
4.2.4.1. Grignard-Type Reaction	79	
4.2.4.2. Organolithium Reaction	81	
4.2.4.3. Synthesis from TeK ₂	82	136
4.2.5. Synthesis of Bis(2-methoxybenzoyl)telluride 56	83	137
4.3. Characterization	84	
4.4. TERP – State of the Art	86	
4.5. Characterization of BPT as TERP Reagent	89	
4.5.1. UV-VIS	90	
4.5.2. Controlled Living Radical Photopolymerization	92	138
4.5.3. Photo-DSC	94	
5. Water-Soluble Photoinitiators	99	
5.1. State of the Art	99	
5.2. Syntheses	101	
5.2.1. Syntheses of the MAPO-Salts Na-TPO and Li-TPO	102	
5.2.1.1. Synthesis of Na-TPO with an Ion-Exchange Resin	102	138
5.2.1.2. Synthesis of Na-TPO from NaI	103	139
5.2.1.3. Synthesis of Li-TPO from LiBr	103	140
5.2.2. Syntheses of the BAPO-Salts Na-BAPO and Li-BAPO	104	
5.2.3. Modification of Ivocerin	105	
5.2.3.1. Synthesis of ((3-(Chloromethyl)- 4-methoxybenzoyl)-diethylgermyl)- (4-methoxyphenyl)methanone 57	105	141
5.2.3.2. Attempted Introduction of –OH- and diethanolamino-groups	106	
5.3. Characterization	107	
5.3.1. Solubility	108	142
5.3.2. UV-VIS	109	
5.3.3. Storage Stability	111	143
5.3.4. Cytotoxicity and Cell Encapsulation	113	144
5.3.5. Photo-DSC	115	

Introduction

In the early 90's of the 20th century it was normal to use amalgam for tooth fillings. Dental amalgam^{1,2} is a mercury alloy that can be produced by mixing 50% mercury with other metals (min. 40% silver, max. 32% tin, max. 30% copper, max. 5% indium, max. 2% zinc) resulting in a kneadable mass that hardens within 3-5 minutes. The big advantage of amalgam is the high margin of error while application to the cavity, good stability and low price.

However, as soon as the 1830s people in Germany and the USA started to discuss the toxicity of amalgam³, especially considering the neurotoxicity of mercury, thus leading to first bans. Back then analytical data for the amount of mercury that is released from amalgam fillings was not available but with modern methods it became evident that those inlays lead to a higher concentration of mercury in the body. Electrochemical corrosion frees the mercury ions, which dissolve. Furthermore heavy metals like copper or tin get into the human organism by abrasion. According to a press release from 15.01.2009 the department of environment of Sweden decided to ban mercury. In October 2013 the Minamata-agreement was negotiated to make the reduction of mercury emission an international law. For these and also for esthetic (Figure 1) reasons many patients favor other inlay materials for their teeth.



Figure 1. Comparison between amalgam and composite filling

To understand what properties materials should show to be usable as dental inlays it is mandatory to understand how a tooth is built up (Figure 2).⁴

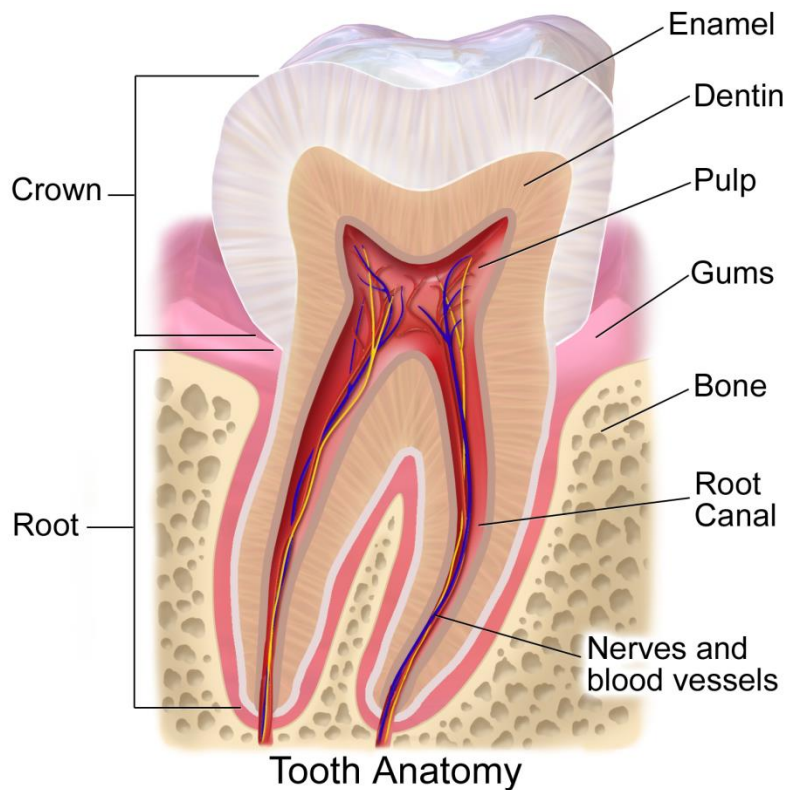


Figure 2. Scheme of a tooth⁵

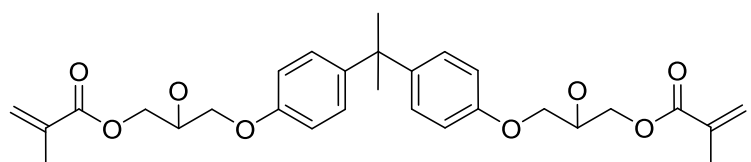
Enamel consists of a matrix of almost 100% hydroxyl apatite, glued together with collagen fibers leading to a great hardness but relatively low stability against acids. Dentin consists of the same materials but with a lower percentage of hydroxyl apatite. To substitute tooth material with artificial inlay material the following properties should be matched as well as possible:

- Low solubility in acidic environments
- Excellent mechanical properties concerning hardness and toughness
- Stability against abrasion
- Perfect fill of the cavity to hinder bacteria from getting into the tooth
- Tooth color to be visually appealing
- Easy handling
- Biocompatibility
- Ductile at ambient temperature and hardenable in the mouth
- Low cost

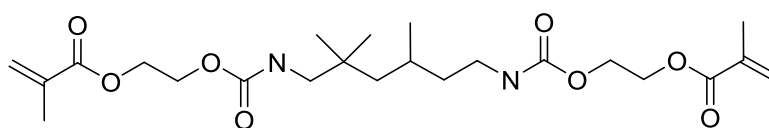
In the 2000s a lot of experimental inlays were tested and on the market for a while (ormocere, glass ionomer cement, polymer modified glass ionomer cement, compomer, ceramic inlays, composite inlays).⁴ Also hammered gold was used quite

frequently. Of all these only the ceramic and composite inlays are indicated today for stress-bearing regions.⁶ The cements are still sometimes used for temporary fillings but lost their importance on the market.

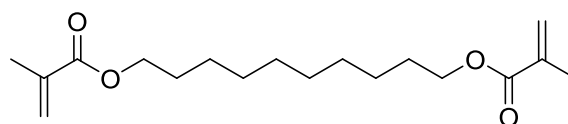
Ceramic inlays are usually dressed to size the cavity they have to fill and composite fillings are applied directly. The excellent mechanical properties of the composites are mostly resulting from the inorganic filler material (grinded glass, micro disperse SiO₂ or hybrid materials). The adhesion however is provided by an organic methacrylate matrix.⁷ This is what the ceramics and the composites have in common. This methacrylate matrix usually consists of bisphenol A – diglycidylmethacrylate (bis-GMA), urethanedimethacrylate (UDMA) and 1,10-decanedioldimethacrylate (D₃MA).



Bis-GMA



UDMA



D₃MA

Via radical polymerization of these difunctional compounds a 3-dimensional network is formed. Choice of monomers defines the reactivity, viscosity and shrinkage of the system. There is less but still some influence on mechanical properties and swelling of the hardened materials.

To achieve good adhesion of the hydrophobic dental composites onto the mainly hydrophilic, inorganic tooth substance first a so called primer layer (Figure 3) is applied to the tooth.

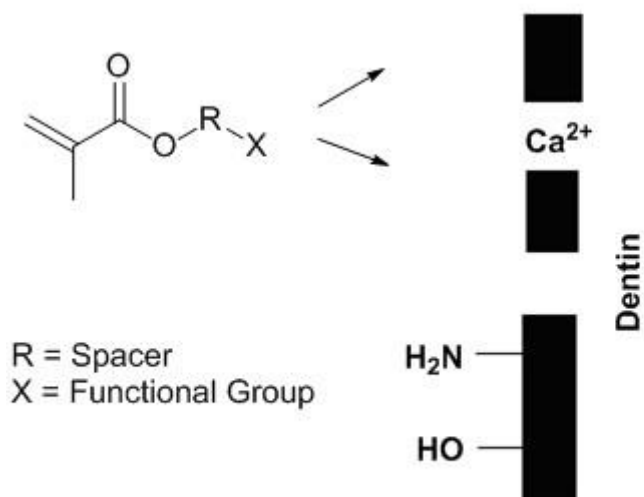
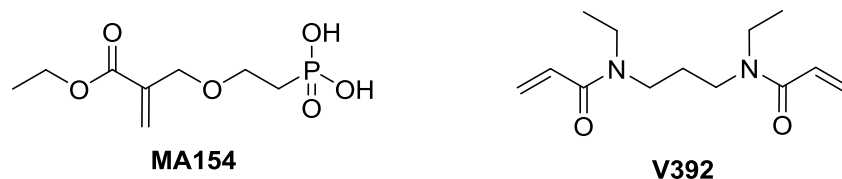


Figure 3. Primer with two functional groups

This primer contains two functional groups: A methacrylate group (connection with the hydrophobic matrix) and a reactive moiety that connects to the dentin. The collagen in the dentin has hydroxyls (-OH), carboxyls (-COOH), amines (-NH₂), amides (-CONH₂) and calcium ions (Ca²⁺). Therefore reactive moieties in the primer monomers can be carboxylic acids, acid chlorides, carboxylic acid anhydrides, isocyanates, aldehydes and ketones.

The newest development are self edging adhesives.⁸ A modern primer mixture of this type is a water-based two component system (MA154 and V392).⁹



Of course, also other acidic monomers with carboxylic acid or phosphonic acid groups can be used but MA154 shows best hydrolytic stability in acidic environments. V392 as crosslinker is an excellent addition to this compound not only because of its high stability against hydrolysis but also because of its very good biocompatibility.

For the polymerization of the organic monomer matrix of the dental composites as well as for the polymerization of the primer mixtures an initiator system is necessary. In dentistry photoinitiation is the technique of choice because initiation via light is easy to handle, cheap and offers excellent control over the start and propagation of

the polymerization reaction. Photoinitiators absorb light to form reactive species that initiate polymerization, therefore transforming physical light energy into chemical energy. To get a better understanding of this principle it is necessary to understand the quantum physics behind this phenomenon.¹⁰

If organic compounds contain heteroatoms, electronic states with a free electron pair (non-bonding states, n-states) occur that are not involved in bonds. Free, non-bonding electrons of an atom or molecule occupy these n-orbitals.

Electronic transitions can only occur from occupied to unoccupied states (Figure 4). The highest occupied molecular orbital in the ground state is called HOMO. The lowest unoccupied molecular orbital is called LUMO. Together, the HOMOs and LUMOs define many molecular properties.

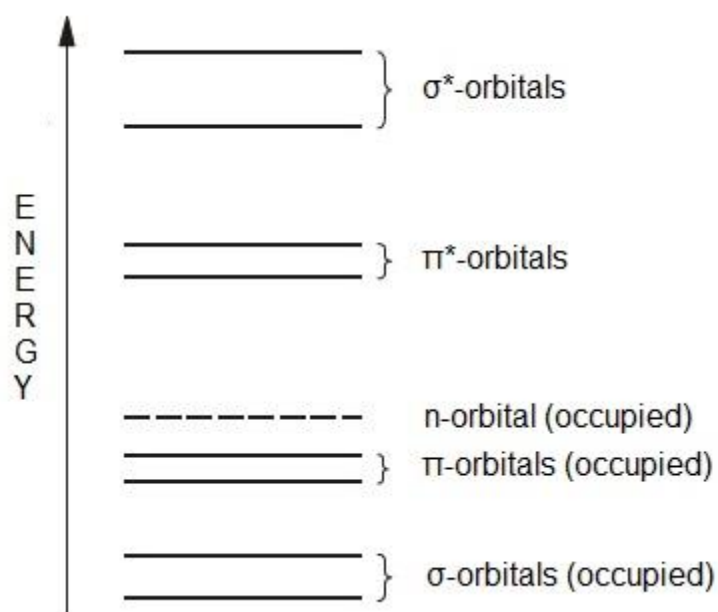


Figure 4. Simplified molecular orbital scheme for organic molecules

The part of the molecule that has UV-VIS-irradiation absorbing π - and n-electrons is called chromophore. It consists of minimum two conjugated double bonds or a mesomeric system, containing heteroatoms with free electron pairs. If the wavelength λ of the absorption lies between 400 nm and 800 nm, the compound is colored in the complementary color of the absorbed light. Electron excitation via radiation absorption causes the electrons to transit from occupied orbitals in unoccupied orbitals thus transforming the compound from a ground state to an excited state. Several transitions are possible (Figure 5).

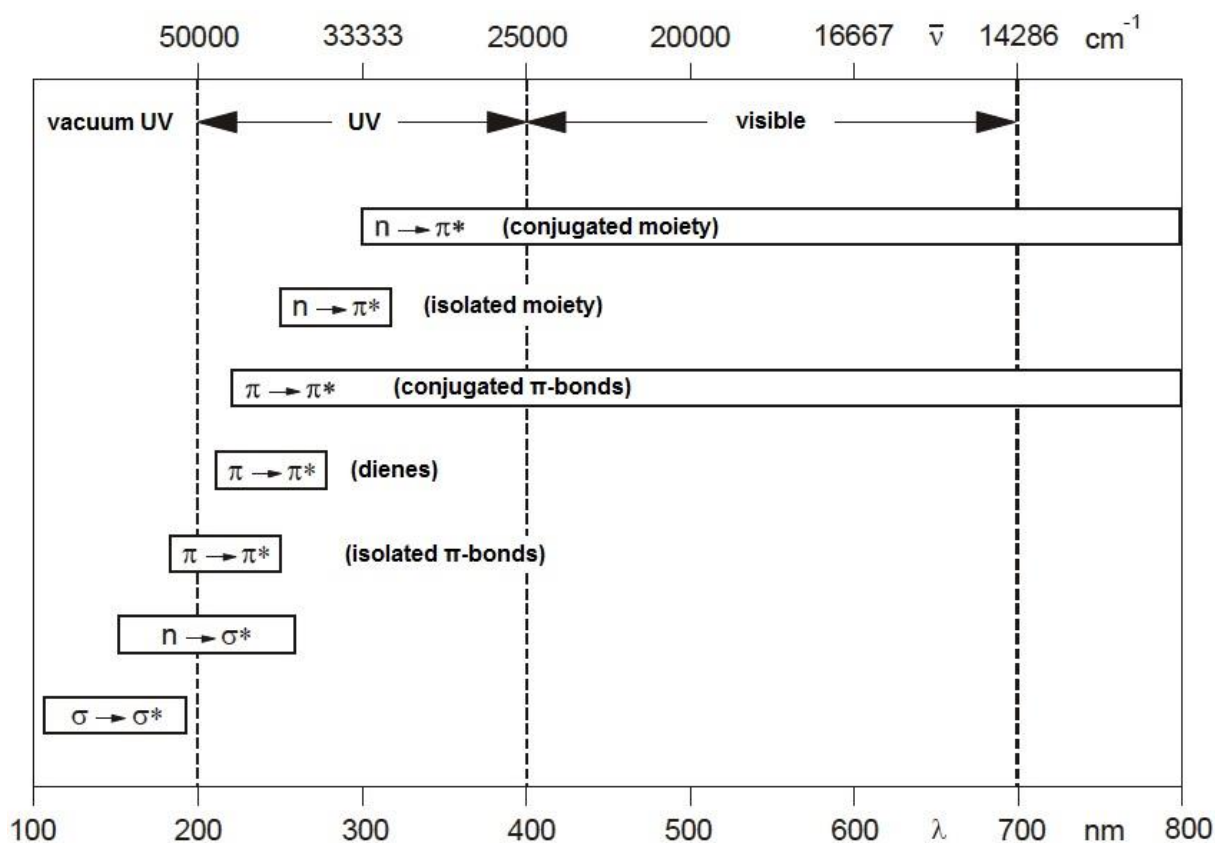


Figure 5. Areas of absorption for different transitions

- $n \rightarrow \pi^*$ -transitions are only possible if free electrons are available, which occupy in most cases the HOMO. These transitions require the least energy.
- $\pi \rightarrow \pi^*$ -transitions can occur whenever π -electrons are part of a bond. If a molecule contains no free electron pairs then the $\pi \rightarrow \pi^*$ -transitions are the ones with the least transitional energy from HOMO to LUMO.
- $n \rightarrow \sigma^*$ -transitions can be found in saturated molecules with heteroatoms that possess free electron pairs.
- $\sigma \rightarrow \sigma^*$ -transitions occur especially in saturated hydrocarbons.
- $\sigma \rightarrow \pi^*$ -transitions require a lot of energy and are usually hidden under the $\pi \rightarrow \pi^*$ - and $\sigma \rightarrow \sigma^*$ -transitions.

With the basics being understood the transformation of physical light energy into chemical energy via a photoinitiator can be explained.^{11,12} A photoinitiator starts a polymerization chain reaction by forming active radicals. This process takes three steps.¹³ First the transformation of the initiator to the excited state occurs either by direct light absorption or by energy transfer from a photochemically excited sensitizer. In the second step radicals are formed by electron transfer, H-abstraction from an H-donor or by photofragmentation resulting from α - or β -cleavage. The last step is the

reaction of the formed radicals with the monomer, initiating the polymerization chain reaction. For the formation of the excited state the main emission bands of the light source need to overlap as completely as possible with the absorption bands of the initiator. The photoinitiator needs chromophores for the energy uptake, mostly conjugated systems with C=O or C=N double bonds that allow $\pi-\pi^*$ - and $n-\pi^*$ -transitions (Table 1).

Table 1. Chromophores and the wavelength of their transitions

Chromophore	λ_{\max} (nm)	λ_{\max} (nm)
	$\pi-\pi^*$	$n-\pi^*$
C=C	170	-
C=O	166	280
C=N	190	300
N=N	-	350
C=S	-	500

First an electron pair that is in a singlet ground state (S_0) transfers through absorption of radiation ($h\nu$) to an excited singlet state (S_1 or S_2) (Figure 6).

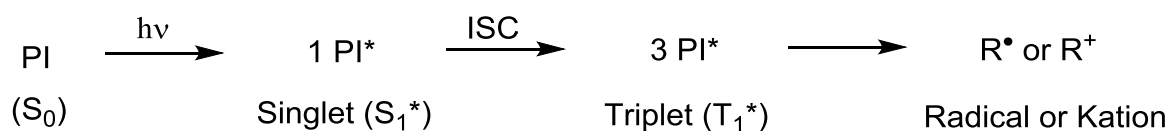


Figure 6. Radical/kation formation from a photoinitiator

These short term states ($<10^{-8}$ s) can't initiate photochemical reactions but their energy can be released by fluorescence or non-radiative deactivation. In case S_2 is occupied, internal conversion can transfer the energy within 10^{-12} s from the higher excited states to singlet state S_1 . From this state emission or internal conversion can cause energy loss and a drop back to the ground state S_0 . If intersystem crossing takes place the triplet states T can be formed (Figure 7).

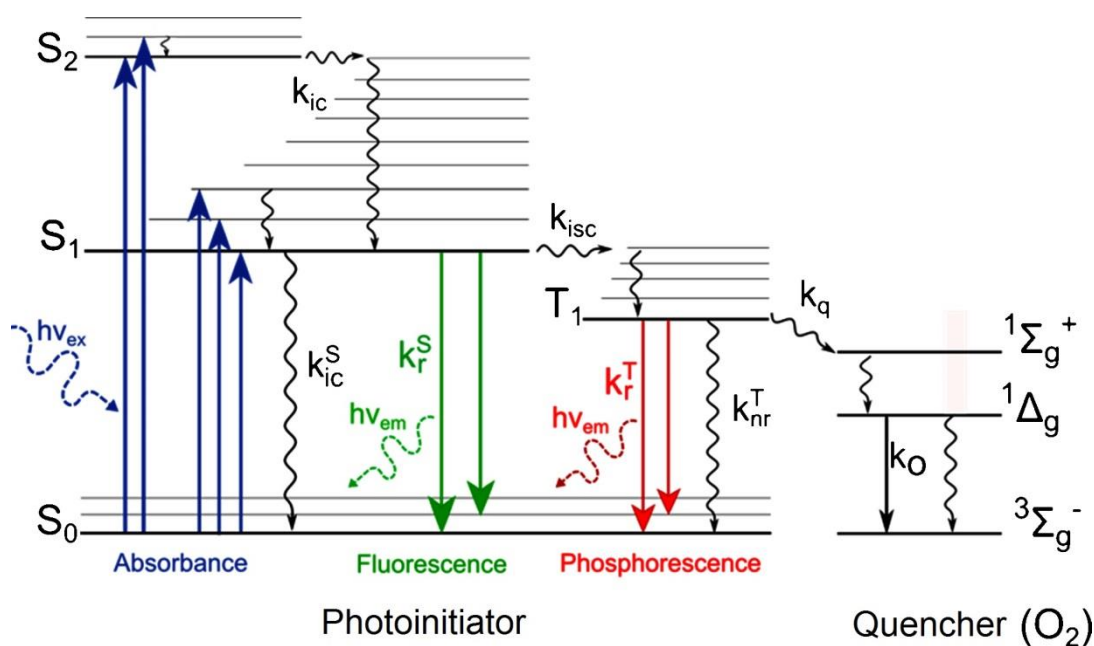


Figure 7. Jablonski diagram¹⁴

The triplet states show a much longer life time (10^{-6} s). Based on these states radicals can form but this radical formation competes with non-radiative deactivation, phosphorescence or bimolecular quenching (e.g. with O_2). The radicals appear after photofragmentation and depending on their stability these radicals can cleave again, recombine or initiate a polymerization chain reaction.

When it comes to radical formation by photoinitiators two different types exist (Figure 8). The monomolecular compounds (Norrish type I) produce radicals by α - or β -cleavage, while the bimolecular compounds (Norrish type II) need an additional coinitiator for radical production.¹²

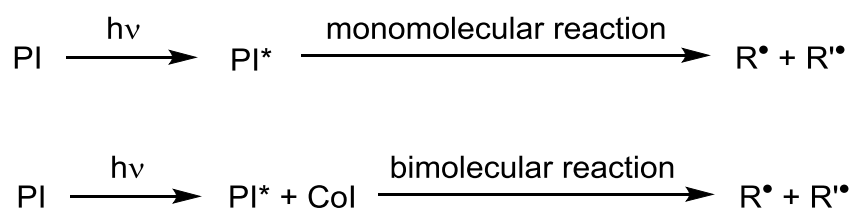
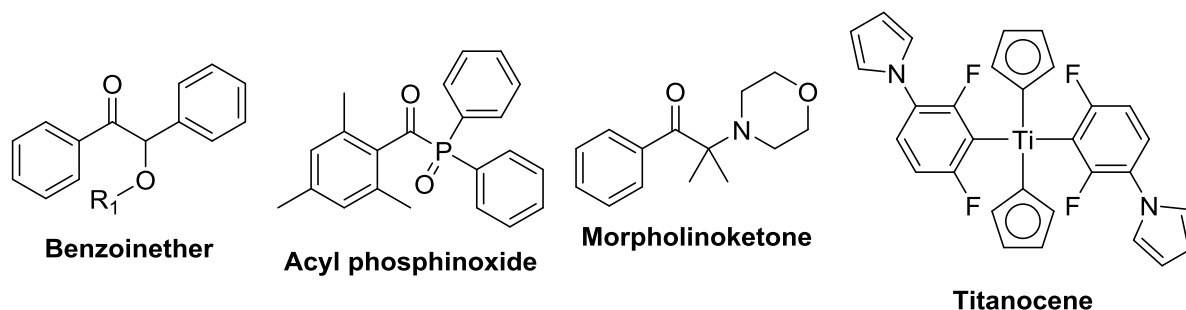


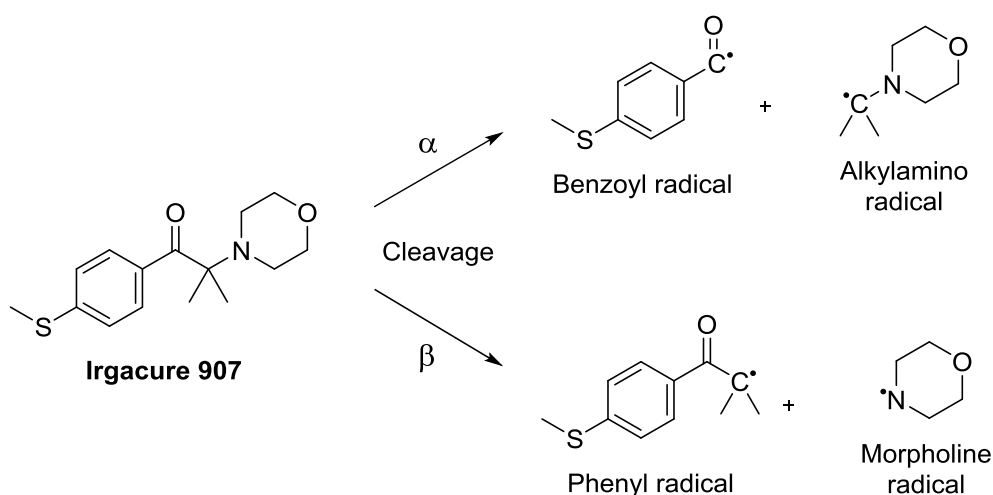
Figure 8. Norrish type I and Norrish type II photoinitiators

α -cleavage in Norrish type I initiators occurs mostly directly next to a carbonyl moiety resulting in an arylcarbonyl radical that starts polymerization. The most common type I photoinitiators are based on aromatic carbonyls. The carbonyl moiety is in this case the chromophore. Via α -cleavage benzoyl radicals are generated, which react very efficiently with unsaturated compounds. The high reactivity of these benzoyl radicals

towards C=C double bonds and in some cases (acyl phosphineoxides) a photobleaching effect due to decomposition of the initiator are the biggest advantages of type I photoinitiators. Important examples of type I photoinitiators¹⁵ are: Benzoinether, acylphosphine oxides, morpholinoketones and titanocenes.



The alkylaminoacetophenone based photoinitiator Irgacure 907 undergoes mostly α -cleavage but also β -cleavage of the weaker C-N-bond occurs as side reaction:



Norrish type II systems work according to a different mechanism. Radicals can be formed by hydrogen transfer to the energetically excited ketone. Also photoinduced electron/proton-transfer is possible. The excited compound (sensitizer) functions as electron donor and a so called coinitiator as electron acceptor. Switched roles are also possible (Figure 9).

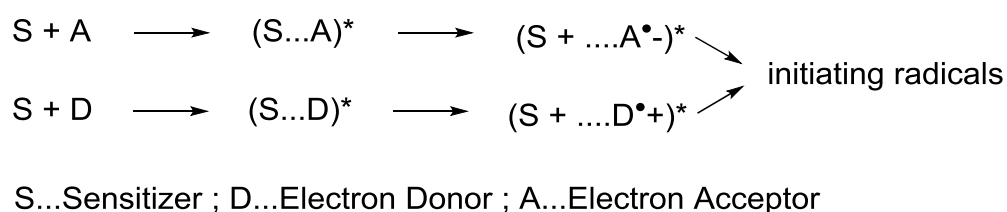
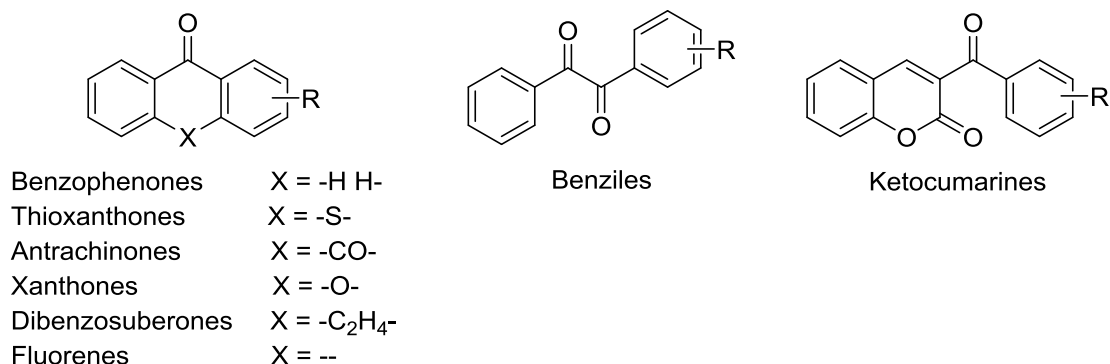
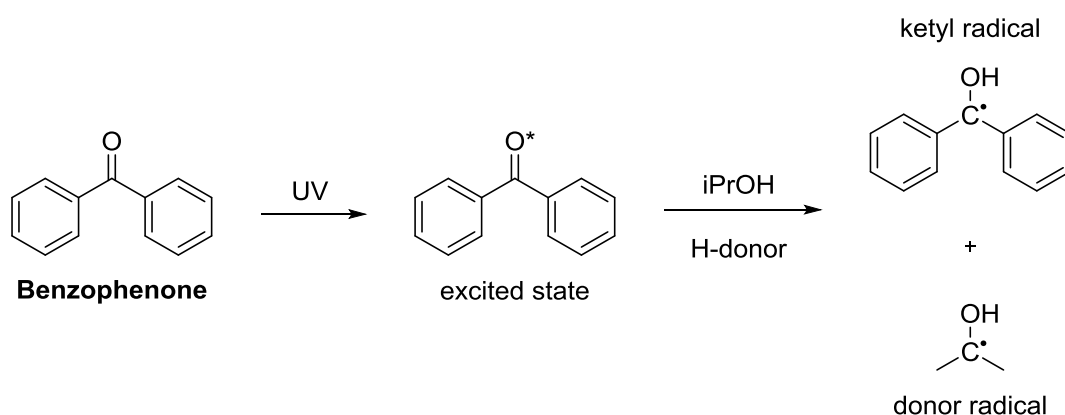


Figure 9. Norrish type II radical formation

Important type II photoinitiators are:¹⁵ Benzophenones, thioxanthenes, anthraquinones, xanthenes, dibenzosuberones, fluorenones, benziles and ketocoumarines.

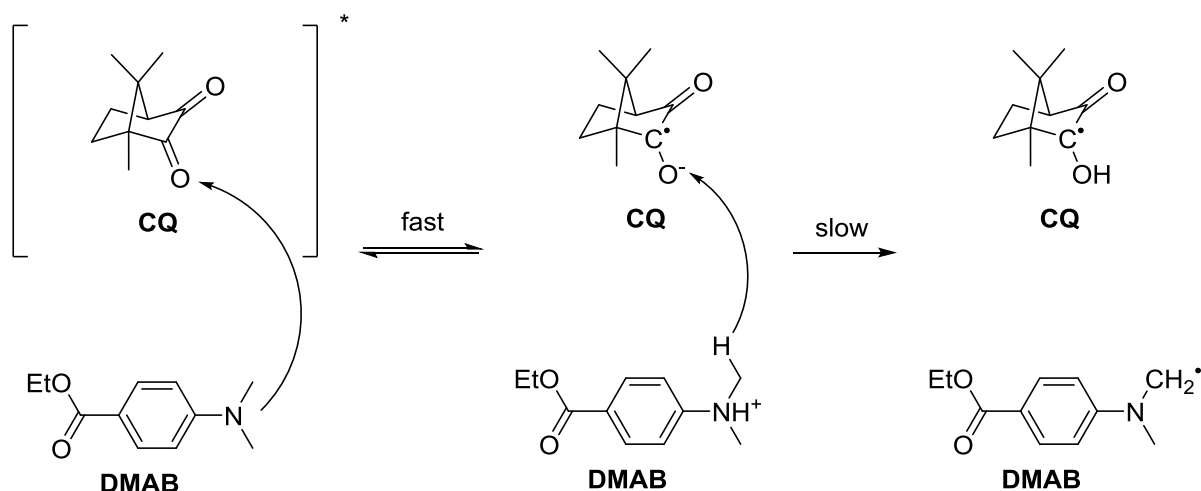


A concrete example of a type II reaction with an H-abstraction mechanism is the photoinitiation with benzophenone:



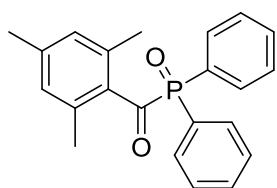
In the metastable excited triplet-state the photoinitiator can react with the proton donor resulting in a ketyl radical with lower reactivity and a highly reactive donor radical. This reaction competes with a possible transition from triplet to ground state via phosphorescence.

Due to absorption in the visible light area and low toxicity of camphorquinone¹⁶ (**CQ**) this type II photoinitiator is mainly used and state of the art in dental adhesives. Visible light initiation is important because UV-light can be problematic for applications involving living cells.^{17,18} **CQ** systems also show a photobleaching effect. This effect is necessary to yield tooth colored materials after polymerization. As a coinitiator for **CQ** N,N-dimethylaminobenzoic acid (**DMAB**) is used. Initiation of polymerization happens via bimolecular reaction according to a type II mechanism where as a result the highly reactive amine radical initiates polymerization:

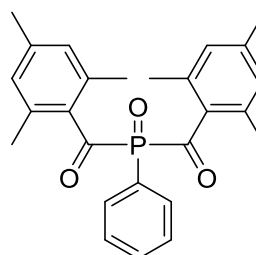


After radical formation the **CQ** radical can either dimerize or abstract hydrogen from other compounds. The reactivity of the radical is usually not high enough to initiate polymerization. As can be seen from the mechanism the electron transfer is very fast, while the hydrogen abstraction is a slow process. This can lead to a back reaction before the radical formation happens. In addition to that the reactivity is even further reduced by the bimolecularity of the system where for a reaction to occur the two compounds have to “meet” first. Herein the surrounding medium has a big influence, e.g. if water is present a solvent cage can lead to a great reduction in reactivity.¹⁹

To overcome this problem type I photoinitiators based on acylphosphine oxides were introduced for dental applications.²⁰ In general, this type of photoinitiator has been commercially very successful in the last decade.¹⁶ Bisacylphosphine oxides (BAPO derivatives) show in comparison to monoacylphosphine oxides (MAPO derivatives) a higher reactivity. The reason for that is the formation of four radicals instead of two via photocleavage and a bathochromic redshifted absorption maximum, overlapping better with the emission spectrum of the halogen dental lamps. Typical, commercially available acylphosphine oxides are:



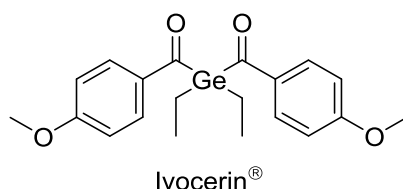
2,4,6,-Trimethylbenzoyl diphenylphosphine oxide = Speurecure TPO[®] = **MAPO**



Bis-(2,4,6-trimethylbenzoyl)-phenylphosphine oxide = Irgacure 819[®] = **BAPO**

A free d-orbital on the phosphorus heteroatom overlaps with the π^* -orbital of the carbonyl group thus reducing the orbital energy leading to a bathochromic redshift of the absorption maximum. Lower energy of the $n\rightarrow\pi^*$ transition of course requires longer wavelengths. The methyl-groups attached to the aromatic system are necessary to sterically hinder nucleophilic attacks on the carbonyl group(s). Otherwise the compounds would not be stable against hydrolysis and decompose after storage in reactive formulations. **MAPO** and **BAPO** show perfect photobleaching because the chromophore is destroyed by the photocleavage process. This makes them very effective in curing thick layers or layers with a high degree of pigments or filler like they are used in dentistry.¹⁶ Many acylphosphine oxides can be used only in very low concentrations in self edging adhesives because the systems are water-based but the initiators show very low water-solubility. To improve the water-solubility of acylphosphine oxides recently oligoethylenglycole monomethylether moieties were added, which worked very well with older and now outdated halogen lamps.²⁰

To increase the bathochromic red shift even further and achieve better overlap with state of the art LED dental lamps the phosphorus heteroatom can be exchanged to a germanium heteroatom.²¹



Ivocerin® (Ivoclar Vivadent) is the newest development in the sector of photoinitiators for dental applications. The $n\rightarrow\pi^*$ transition has a maximum of already 418 nm making the compound's absorption spectrum overlap very well with the emission spectrum of the dental lamps (Figure 10).

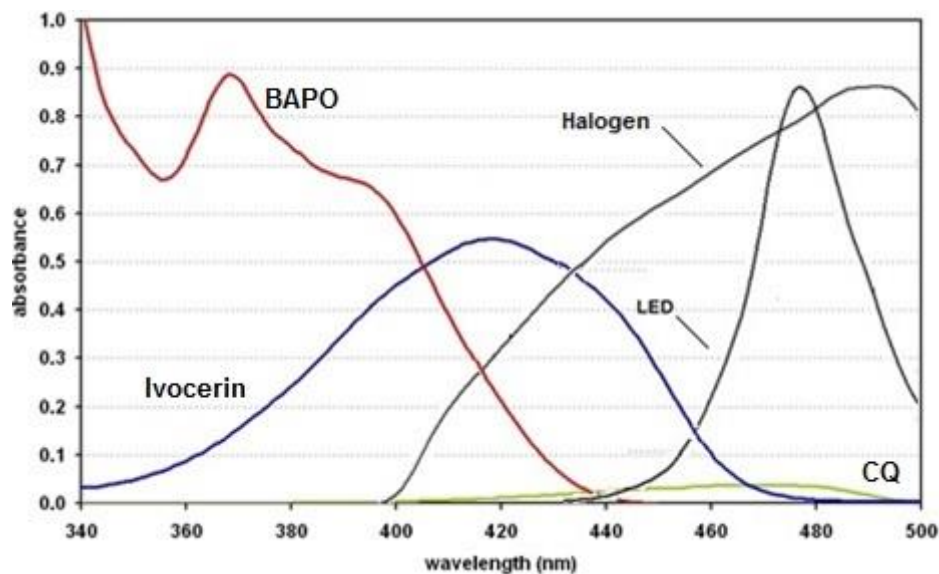


Figure 10. Absorption spectra of commercially used photoinitiators (red: BAPO; blue: Ivocerin; green: CQ) vs. emission spectra of state of the art dental lamps (LED and halogen).

Additionally Ivocerin forms benzoyl radicals and a germanium radical leading to higher reactivity of this photoinitiator compared to **BAPO**, where the reactivity of the phosphorus radical is comparably low. The only disadvantages lie in the low water solubility making it difficult to use Ivocerin for primer mixtures and particularly in the high price of germanium compounds in general giving Ivocerin bad cost effectiveness.

Objective

Goal of the work was to develop and test a new generation of photoinitiators for dental materials. Two problems should be addressed: First and mainly the problem of insufficient curing depth, which can be solved with using red-shifted photoinitiating systems. The other problem is the polymerization of primer mixtures, which means the photoinitiators have to be able to polymerize a methacrylate-based aqueous acidic system. In both cases the following criteria should be met as completely as possible:

- High reactivity
- Absorption between 400 and 500 nm
- Good solubility in the used monomer mixtures
- Stability against oxidation and hydrolysis at ambient conditions
- Storage stability in the monomer mixtures
- No or very low toxicity
- Sufficient photobleaching
- Low price

The usually used **CQ/DMAB** system shows very low reactivity and low solubility especially in primer mixtures. The absorption bands of **BAPO** on the other hand overlap very poorly with the emission bands of state of the art LED dental lamps. Ivocerin has limits concerning price but also solubility in aqueous formulations.

Preliminary studies led to bisphosphylketones as promising first concept but also tellurium as heteroatom next to a carbonyl group was an interesting approach. Also different and new concepts except the heteroatom-carbonyl approach were goals of this work. Metal complexes similar to already known titanocenes or new diketones as part of Norrish type II systems. For the problem with primer mixtures specifically water-soluble photoinitiators based on acylphosphine oxides all were ideas how these new initiator systems could look like.

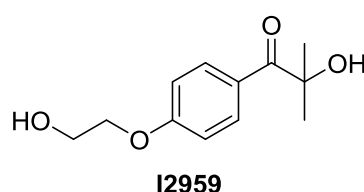
The characterization of the newly discovered compounds should be done by UV-VIS, photoreactivity by photo-DSC, storage stability in neutral, acidic and alkaline solutions, toxicity by in-vitro cell tests and mechanistic studies with a photoreactor.

Results and Discussion

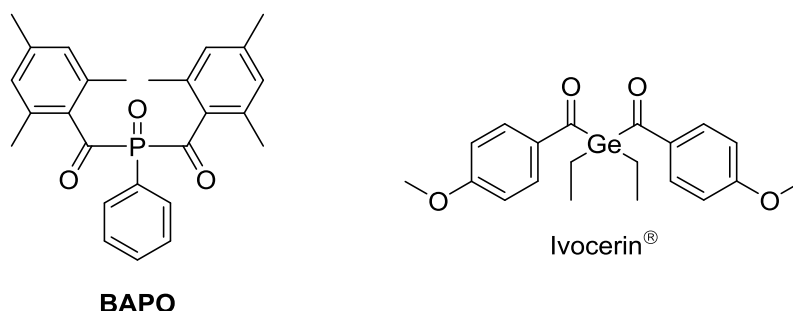
1. Bisphosphylketones

1.1. State of the Art

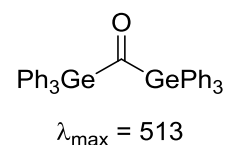
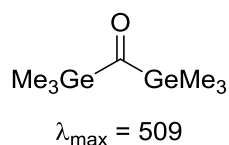
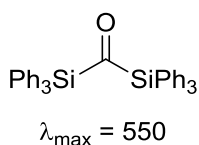
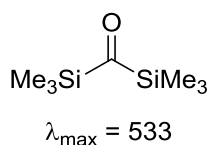
Classical photoinitiators like Irgacure 2959 (**I2959**) have the maximum of their $n\rightarrow\pi^*$ -transition at ~330 nm.



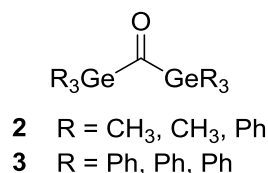
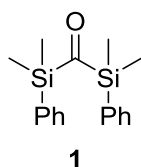
In recent days mono- and bisacylphosphinoxides were developed as photoinitiators. In these structures the overlap of a free d-orbital in the phosphorus heteroatom with the π^* -orbital of the neighboring carbonyl group reduces the energy required for the $n\rightarrow\pi^*$ -transition. This transition is responsible for the photocleavage reaction and therefore the initiation of a radical polymerization. If the P-atom is exchanged to Ge (~408 nm), Si (~404 nm) or Sn (~435 nm) an even higher shift can be achieved but some of these compounds are too instable for a use as photoinitiator. Symmetrical molecules like bisacylphosphine oxides (**BAPO**) or comparable germanium compounds (Ivocerin) prove that a further bathochromic redshift of 10 nm is possible by introducing a second carbonyl group.



Introducing two heteroatoms instead of two carbonyl groups like in disilyl- or digermyl ketones leads to another remarkable shift of the $n\rightarrow\pi^*$ -transition to values well above 500 nm.^{22,23}

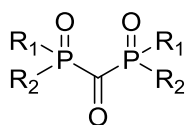


In preliminary experiments at our institute²⁴ the syntheses of a Si-compound and a Ge-compound were attempted.



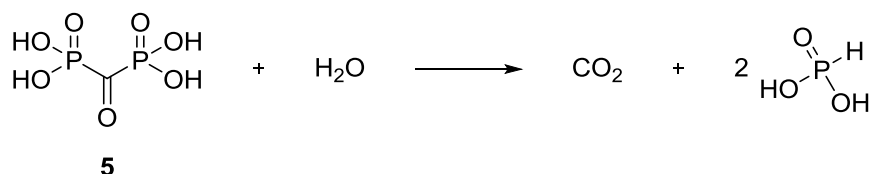
The Si-compound **1** was successfully synthesized and showed an absorption maximum at 541 nm. However, due to oxygen sensitivity a test of the initiator efficiency was impossible. The synthesis of the similar Ge-compound **2** failed during these experiments but Allonas et al. published the synthesis of the related compound bis(triphenylgermyl)ketone **3**.²⁵ The formation of germyl radicals and photopolymerization of a monomer film under visible light conditions were proven in this work.

Carbonyl bisphosphonates (examples **4-10**) can be expected to show the same properties as the digermyl- and disilyl ketones.



- 4** R₁, R₂ = -OH
5 R₁, R₂ = -ONa
6 R₁ = -O-iPr, R₂ = -Ph
7 R₁, R₂ = -O-iPr
8 R₁, R₂ = -Ph
9 R₁, R₂ = -O-Et
10 R₁, R₂ = -O-Me

Only two groups were working with this type of compound and there are only a very limited number of publications available. They are for example providing information about the free acid **4**. McKenna et al. describe its Na-salt **5** as a pale yellow powder.²⁶ On the other hand, Quimby et al. describe the acid **4** as only stable in solution and both acid **4** and salt **5** as generally instable, especially under acidic but also under basic conditions, characterize it only in solution and use it in-situ for other reactions.²⁷ The main decomposition pathway is given in the publication:



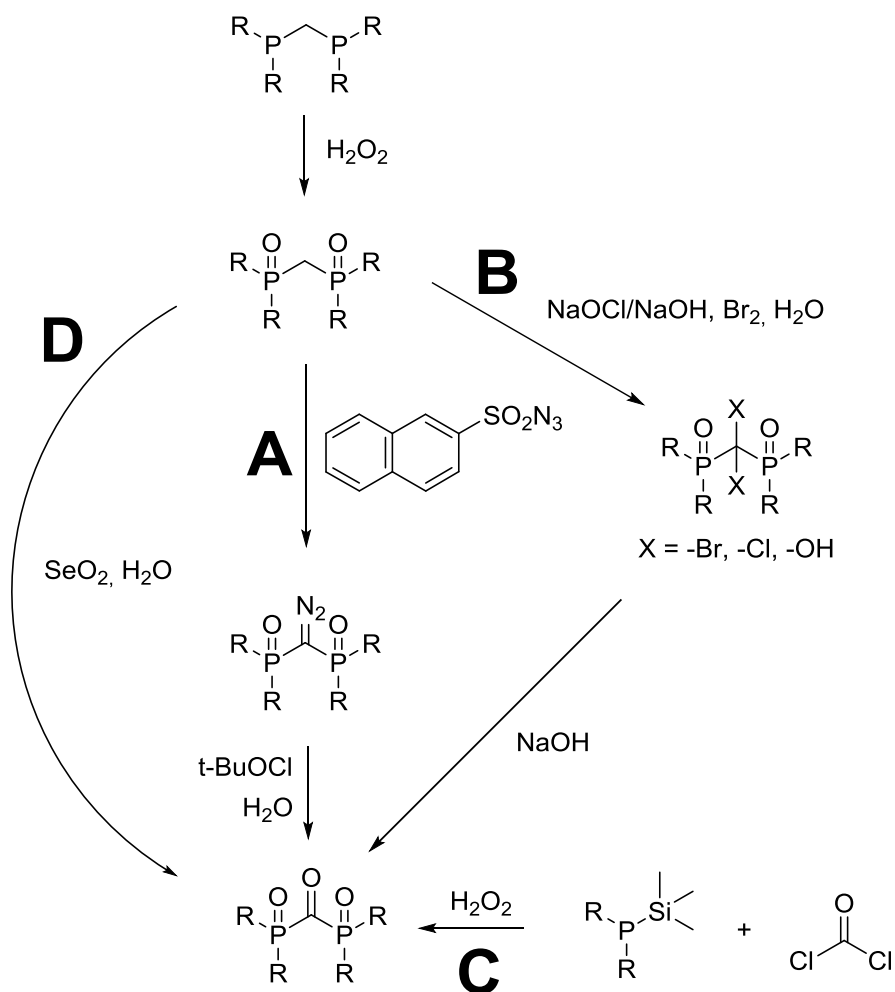
This contradicts the synthetic pathway used by McKenna et al., who claims the use of concentrated HCl and NaOH on reflux to yield the sodium salt **5** of the free acid **4** in isolated form.²⁶ Other publications concerning the compounds **7** and **9** are also from McKenna et al.²⁸⁻³⁰ Herein synthetic pathways are partly described but characterization is not complete (only one ³¹P-NMR given)³¹ because most of the desired compounds were only observed during reactions in-situ like carbonylbis(diethoxyphosphine oxide) **9**³¹ or the free acid **4** and its sodium salt **5**.²⁷ It was not clear if those compounds could be isolated or are even stable enough for isolation and further characterization. Mostly they are just mentioned as side products or intermediates for HIV or anti-cancer drugs. So the synthetic pathways should be tested and in case pure and stable bisphosphylketones could be isolated also new compounds could be prepared and characterized.

1.2. Syntheses

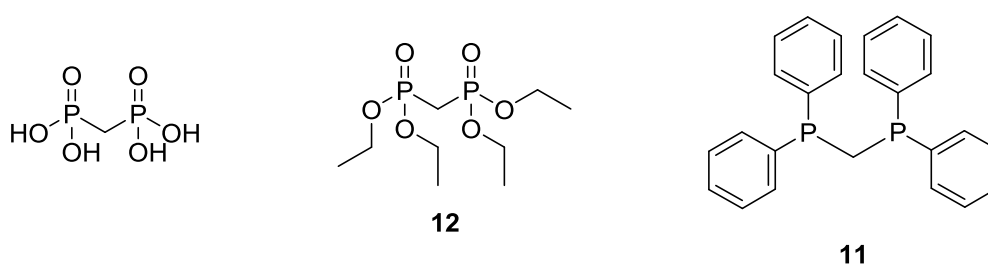
The first goal was now to check the synthetic pathways McKenna and Quimby et al described. The syntheses pathways **A** and **B** (Scheme 1) are mentioned in their publications for different bisphosphylketones. **B** can be used for the free acid **4** and sodium salt **5** respectively: R = -OH and R = -ONa.^{26,27} These bisphosphylketones are described to be stable in solution. Pathway **A** is used for the alkoxy compounds: R = -OMe **10**, -OEt **9**, -OiPr **7**.^{28,29,31} These bisphosphylketones are used as in-situ intermediates. For both pathways, **A** and **B** the starting material has two methylene bridged phosphorus atoms. This bridge is halogenated and hydrolyzed (**B**), in-situ hydrolyzed (**B**), or diazotized and subsequently hydrolyzed (**A**) to get the product, usually in solution. Synthesis **C** by Becker et al³² is used to prepare the non-oxidized form of the aromatic bisphosphylketone **8** (no P=O bond). By subsequent oxidation with H₂O₂ it can be tried to yield the desired product **8**.

The direct oxidation of the methylene group according to **D** is not described for a phosphorus compound but this synthetic pathway can be used to oxidize a methylene bridge with negative partial charge like it was for example shown in camphor.³³ Here 10-bromocamphor was oxidized to 10-bromocamphoroquinone.

Scheme 1. Potential syntheses pathways for bisphosphylketones



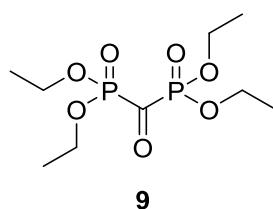
As potential starting materials basically three compounds were commercially available:



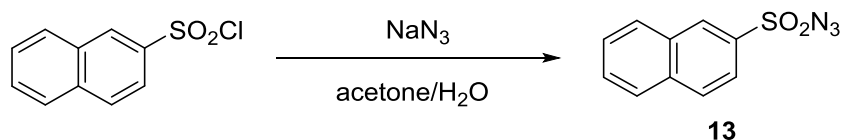
The free acid **4** and the sodium salt **5** of the bisphosphylketones are already described only stable in solution at certain pH values (slightly acidic for the acid, slightly alkaline for the salt).²⁷ Additionally a full characterization was not made for the obvious reason of stability issues. Even the starting material is already sensitive towards bases, which contradicts the synthetic pathways necessary.³⁴ For these reasons the synthetic pathways were checked with methylenebis(diethoxyphosphine oxide) **17**, which was also used in literature^{29,30,32} as in-situ reagent for the synthesis of an anti-HIV drug. Furthermore another option is to get an isolatable and stable compound with methylenebis(diphenylphosphine) **10**.

1.2.1. Synthesis of Carbonylbis(diethoxyphosphine oxide) **9** (pathway A)

The synthesis of a carbonylbis(diphosphine oxide) according pathway A (Scheme 1) via diazotation and subsequent hydrolysis is completely described in literature for carbonylbis(diethoxyphosphine oxide) **9** as intermediate in solution.³¹ So it was tried to reproduce literature and potentially even isolate the final product **9**.



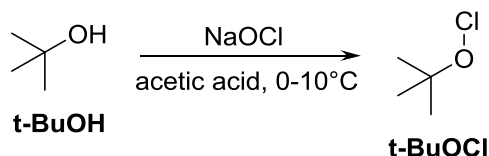
First the diazotizing agent 2-naphthalenesulfonyl azide **13** needed to be synthesized according to literature.³⁵



As starting material the commercially available 2-naphthalenesulfonyl chloride was used. 1 eq. of it was dissolved in acetone. 1 eq. of NaN_3 dissolved in water was added and the mixture was stirred at ambient temperatures for 2 h. Water was added to achieve an acetone:water ratio of 1:1. The product was found in the brown, organic phase, which was dried (Na_2SO_4) and the solvent evaporated.

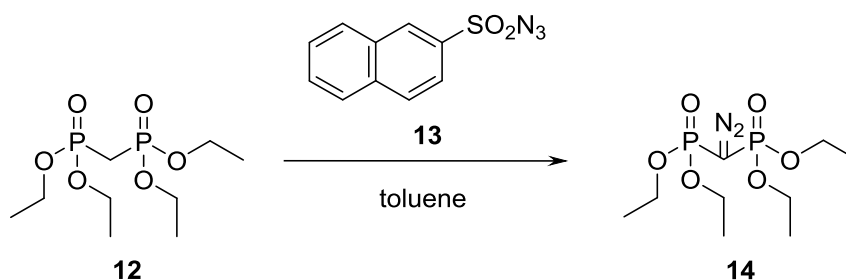
Recrystallization of the brown precipitate from PE gave the product as yellowish powder in 47% yield. Formation and purity were checked via melting point.

The synthesis of the hydrolyzing agent t-BuOCl can also be found in literature.^{36,37}



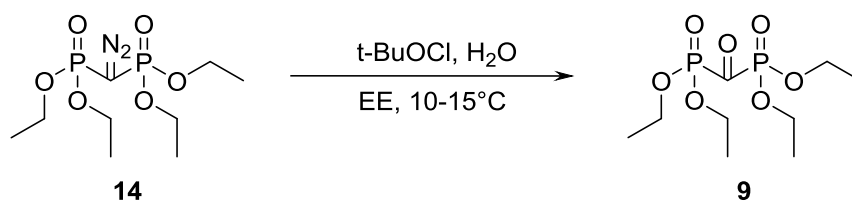
Under light protection aqueous NaOCl (7.5%, 1 eq.) was cooled below 10°C. 1 eq. of t-BuOH mixed with 1 eq. acetic acid was added and vigorously stirred for 3 min. Subsequently the phases were allowed to separate and the yellowish organic phase was washed with aqueous Na₂CO₃ (10%) solution and brine. After filtration the t-BuOCl was obtained as colorless liquid in a yield of 33% and stored at 5°C in a brown glass bottle over CaCl₂.

Afterwards the commercially available methylenebis(diethoxyphosphine oxide) **12** could be reacted with the diazotizing agent **13** according to literature.³⁵



For this synthesis KOtBu (1.2 eq.) was dissolved in toluene and cooled to 0°C. 1 eq. of methylenebis(diethoxyphosphine oxide) **12** also dissolved in toluene was added dropwise while the temperature was kept below 5°C. After 15 min 2-naphthalenesulfonyl azide **13** dissolved in toluene was added dropwise, while the temperature was again kept below 5°C. After 2 h reaction time the mixture was filtered and the solvent evaporated. The residue was distilled to get product **14** as yellow liquid in 52% yield. Product formation and purity were confirmed via GC-MS-, ¹H-NMR- and ³¹P-NMR-analysis.

The last step was the synthesis of carbonylbis(diethoxyphosphine oxide) **9**.³¹

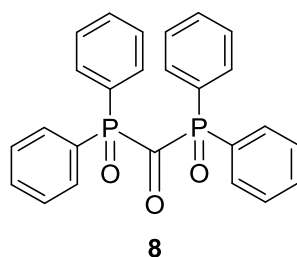


Therefore 4 eq. of water were dissolved in EE. 1 eq. diazomethylenebis(diethoxyphosphine oxide) **14** was added and the mixture was cooled to 10-15°C. 1.5 eq. of t-BuOCl were added and strong gas formation (N₂) occurred. The color of the reaction mixture changed to strong yellow. Subsequently 4 eq. of chlorotrimethylsilane were added. One time this was done after gas formation stopped (2-5 min.) and another time the reaction mixture was stirred for 0.5 h before it was quenched with chlorotrimethylsilane. The second case resulted in reduced yield. After solvent evaporation a yellow liquid was obtained that contained below 10% product calculated by ¹H-NMR. ATR-IR- and CC-MS-analysis also showed product formation but further purification via distillation or column chromatography led to complete decomposition of the product **9**, noticeable by decolorization of the liquid raw product and disappearance of the product peak in the GC-MS-chromatogram. The product **9** could not even be stored under argon atmosphere. After two days it completely decomposed. All this in good accordance with literature, where the product is used in-situ for follow-up reactions.³¹

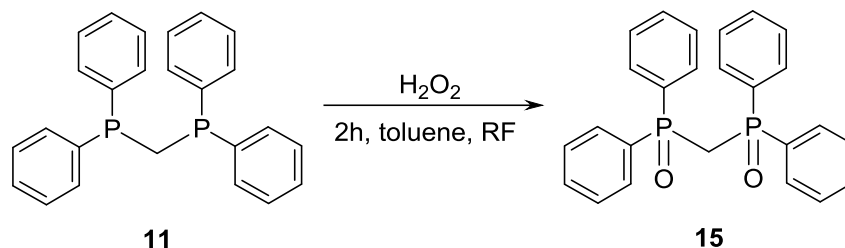
1.2.2. Synthesis of carbonylbis(diphenylphosphine oxide) **8**

1.2.2.1. Synthesis via Diazotation and Hydrolysis (Pathway A)

Since the reaction pathway worked before, it was tried to use a different substituent on the P-atoms to prepare an isolatable and stable product. The goal was to use the already tested synthesis pathway to yield carbonylbis(diphenylphosphine oxide) **8**.

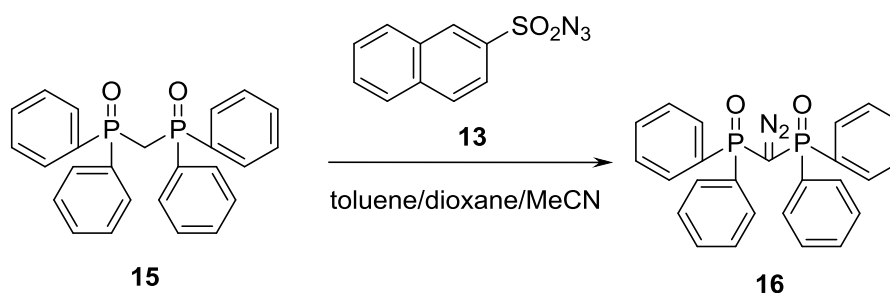


Methylenebis(diphenylphosphine) **11** is used as commercially available starting material. The required oxide **15** could be synthesized according to literature.³⁸



For that 1 eq. of the starting material **10** was dissolved in toluene 4 eq. of H_2O_2 (30%) were added dropwise and the reaction mixture was heated to reflux for 2 h. Afterwards the solvent was evaporated and the residue dissolved in chloroform. This solution was washed with saturated aqueous NaHCO_3 solution. Subsequent drying (Na_2SO_4) and solvent evaporation gave the raw product that could be purified via recrystallization from EE. Methylenebis(diphenylphosphine oxide) **15** was obtained as white powder in 83% yield and product formation was confirmed by $^1\text{H-NMR}$ -, $^{13}\text{C-NMR}$ - and melting point measurements.

In analogy to the synthesis of diazomethylenebis(diethoxyphosphine oxide) **14** that is described above, methylenebis(diphenylphosphine oxide) **15** had to be diazotized first, too.



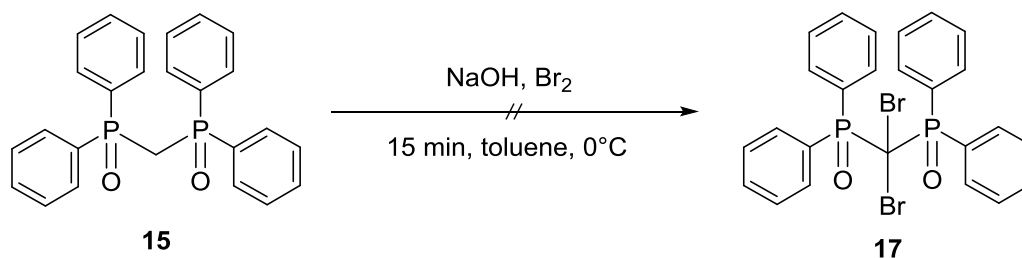
A slurry of 1.2 eq. KOtBu in toluene was cooled to 0°C . Another slurry of 1 eq. Methylenebis(diphenylphosphine oxide) **15** in toluene was added dropwise over a period of 10 min, while the temperature was kept at 5°C . After stirring for 15 min, 1 eq. 2-naphthalenesulfonyl azide **13** dissolved in toluene was added dropwise over a period of 10 min while the temperature was kept below 10°C . The mixture was stirred for 30 min at $5\text{-}10^\circ\text{C}$. Afterwards it was allowed to warm to ambient temperatures and stirred for 2 h. Subsequently the reaction slurry was filtrated and the solvent evaporated. The filtrate and the residue after evaporation showed the exact same

thin layer chromatogram, so both fractions were mixed and an ATR-IR was made where no diazo peak that could be found. The reaction was repeated with another solvent where all starting materials show good solubility. Dioxane shows the desired solubility but crystallizes at 10°C, so MeCN was used instead of toluene. This led to possible product formation. A diazo peak was visible in the ATR-IR at $\sim 2100\text{ cm}^{-1}$ for the raw product. Purification was tried via recrystallization from EE or EE/PE mixtures. Column chromatography with EE:MeOH = 10:1 was also tried but the product could not be isolated. Additionally it was estimated by TLC that the reaction yield was very low with $\sim 10\%$ and at least two side products appeared during the reaction that could not be separated from what was assumed to be the final product **16**.

So for the synthesis of the desired bisphosphylketone carbonylbis(diphenylphosphine oxide) **8** another pathway had to be found.

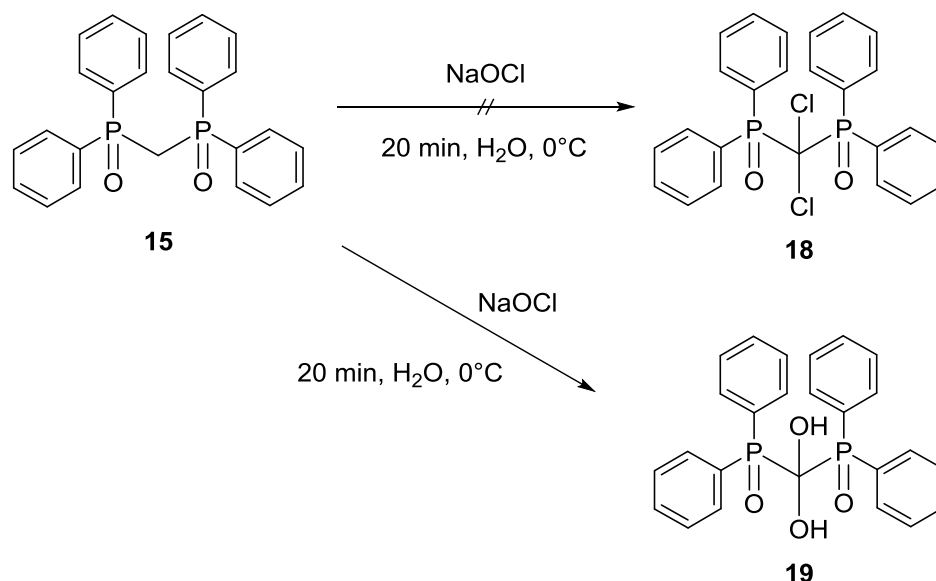
1.2.2.2. Synthesis via Halogenation and Hydrolysis (Pathway B)

Quimby et al describe the synthesis of bisphosphylketones in free acid or in sodium form from a dihalogenated ($-\text{Br}$ or $-\text{Cl}$) species.²⁷ McKenna et al describe the same synthesis only with a dichlorinated species.²⁶ It has to be noted again that those compounds were not fully characterized because of stability issues or stability only in solution at certain pH levels. Nevertheless, the reaction pathway was tried for diphenylphosphine oxides with the target of obtaining stable and isolatable products. The syntheses of the brominated or chlorinated bisphosphylketones with $-\text{OMe}$ -, $-\text{OEt}$ - or $-\text{OiPr}$ -moieties attached to the phosphorus atoms can be found in literature.³⁰ According to these reaction pathways it was tried to brominate or chlorinate methylenebis(diphenylphosphine oxide) **15**. The bromination should work as following:

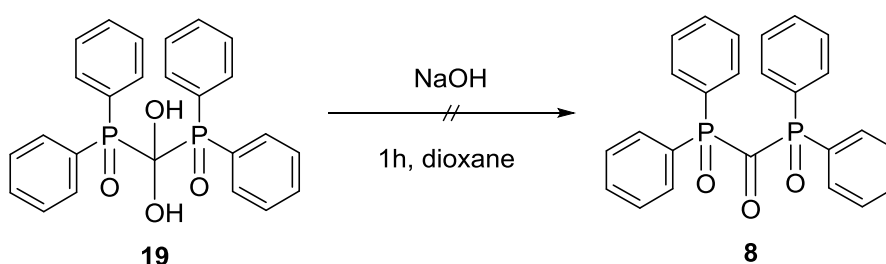


For that 9 eq. of aqueous NaOH (25%) were cooled to 0°C and 4.7 eq. of bromine were added dropwise. 1 eq. of methylenebis(diphenylphosphine oxide) **15** dissolved in a minimum amount of toluene was added and stirred vigorously for 10 min at 0°C. Choice of toluene as a solvent instead of CCl₄ as in literature was made because toluene dissolves the starting material and dissolves at least a little in water. Afterwards the mixture was stirred for additional 5 min at ambient temperatures. The phases were allowed to separate and the appearing precipitate was dissolved by addition of water. Extraction with chloroform, drying with Na₂SO₄ and subsequent evaporation of the solvent gave the raw product as brownish solid. ¹H-NMR measurements showed disappearance of some aromatic signals but appearance of multiplet signals at lower ppm values that could not be assigned, speaking for a decomposition of the starting material probably due to the strong alkaline conditions.

The synthesis of a dichlorinated bisphosphylketone is described in the same paper.³⁰ Herein a bisphosphylketone with –OMe groups on both phosphorus atoms is chlorinated. According to this reaction pathway the chlorination of methylenebis(diphenylphosphine oxide) **15** was tried.



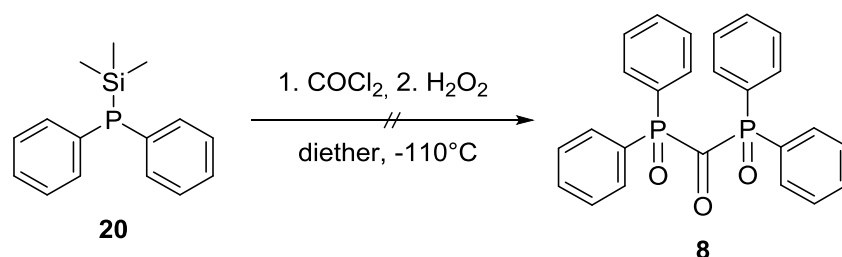
Therefore 3.25 eq. of NaOCl solution (15%) were mixed with 2.5 eq. NaCl and cooled to 0°C. 1 eq. of methylenebis(diphenylphosphine oxide) **15** dissolved in THF (dioxane was also tried in another attempt) was added dropwise and the reaction mixture was stirred for 20 min. Extraction with chloroform, drying with Na₂SO₄ and solvent evaporation gave a white powder with a yield of 29%. ¹H-NMR and ¹³C-NMR did not show product formation but in the ¹H-NMR a peak at 6.15 ppm appeared that disappeared with addition of D₂O. Unfortunately, GC-MS data could not be obtained and ATR-IR did not lead to further conclusions. However, Quimby et al describe a similar mechanism for the free acid.²⁷ During the halogenation reaction the dihydroxy compound appeared according to this publication as an intermediate, only stable in solution. Furthermore it is claimed that the dihydroxy compound can be reacted to the ketone by addition of NaOH. So in case the dihydroxy compound **19** really was obtained it should be possible to react it with NaOH to yield the final product carbonylbis(diphenylphosphine oxide) **8**.



The powder that was assumed to be 1 eq. dihydroxymethylenebis(diphenylphosphine oxide) **19** was dissolved in dioxane and in different experiments 8 eq. NaOH in different concentrations was added (30%, 20%, 10%) and the mixture was heated to reflux for 1h. Heating is according to literature necessary for the reaction to occur.^{26,27} After cooling to ambient temperatures highly viscous, brownish oil precipitated that could be dissolved only in DMSO. ¹H-NMR analysis showed only acid peaks and multiplets in the lower (4-2) ppm area, which concludes to decomposition of the product probably due to the strong basic environment. Repetition of the experiment at different temperatures (ambient and 50°C) did not lead to another outcome.

1.2.2.3. Synthesis with Phosgene (Pathway C)

In literature a synthesis for the non-oxidized form of the bisphosphylketones is described.³² Carbonylbis(diphenylphosphine) is described in this paper, which is basically carbonylbis(diphenylphosphine oxide) **8** without (P=O) bonds. Subsequent reaction with H₂O₂ or just with air should yield the desired carbonylbis(diphenylphosphine oxide) **8**.



In a first step 1 eq. of Phosgene (20% in toluene) was dissolved in more toluene and at -95°C under argon atmosphere 1.05 eq. diphenyl(trimethylsilyl)phosphane **20** dissolved in toluene were added. After a short period of time (10 min) a yellowish precipitate started to appear. After 45 min when no fresh precipitate appeared anymore it was filtered on a Schlenk-frit and washed with more toluene. ¹H-NMR of the precipitate showed very acidic peaks above 6 ppm that could not be assigned. HPLC analysis showed the formation of 5 different substances, all of them only absorbing light in the UV region. Additionally ¹³C-NMR did not show a carbonyl peak. Since in literature diethyl ether is used as a solvent, a second experiment was performed where a toluene:ether (1/18 v/v) mixture was used but the same results were obtained.

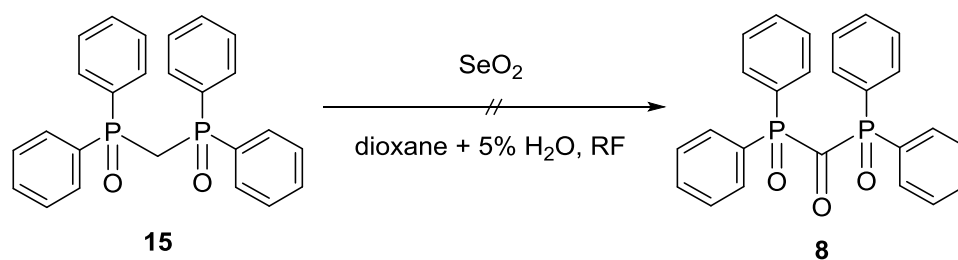
Since the non-oxidized form was already not stable and results from literature could not be reproduced the subsequent addition of H₂O₂ was of course unnecessary.

1.2.2.4. Synthesis via Direct Oxidation (Pathway D)

After the previous experiments it could already be assumed that the desired carbonylbis(diphenylphosphine oxide) **8** is unstable and cannot be isolated.

Nevertheless, a direct oxidation of the methylene bridge was tried, since this was a fresh and new approach that could be conducted in one step and was potentially milder than other approaches with strong bases or acids.

The oxidation should be done with SeO_2 .³³ This way is not in literature for the oxidation of a bisphosphyl compound but for the oxidation of camphor. According to literature the reaction works only with freshly sublimated SeO_2 and best in dioxane with 5% water.



So 1.3 eq. of freshly sublimated SeO_2 and 1 eq. methylenebis(diphenylphosphine oxide) **15** were dissolved in dioxane with 5% water and heated to reflux. During the reaction black precipitate formed, indicating an oxidation reaction. After 4.5 h the starting material had almost completely reacted according to TLC. After cooling to ambient temperature the black and insoluble precipitate was filtered off and the solvent was evaporated. The raw product was only soluble in DMSO and $^1\text{H-NMR}$ showed decomposition to a phosphoric acid. This led to the conclusion that not the methylene bridge but the phosphorus was oxidized leading to decomposition of the compound.

1.3. Characterization and Interpretation

The following figures show the $^{31}\text{P-NMR}$ - and $^1\text{H-NMR}$ -spectra of carbonylbis(diethoxyphosphine oxide) **9** and the starting materials from every synthetic stage (Figure 11 and Figure 12).

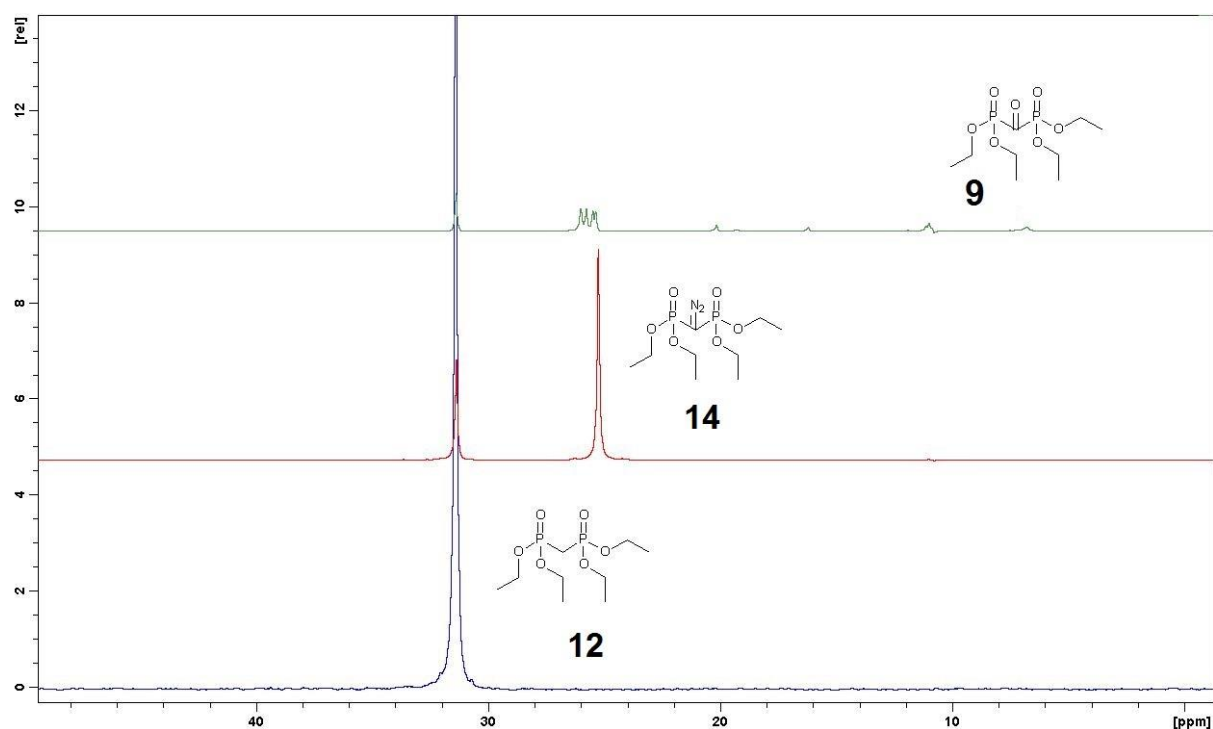


Figure 11. ^{31}P -NMR-spectrum of carbonylbis(diethoxyphosphine oxide) **9** and the starting materials from the previous synthetic stages

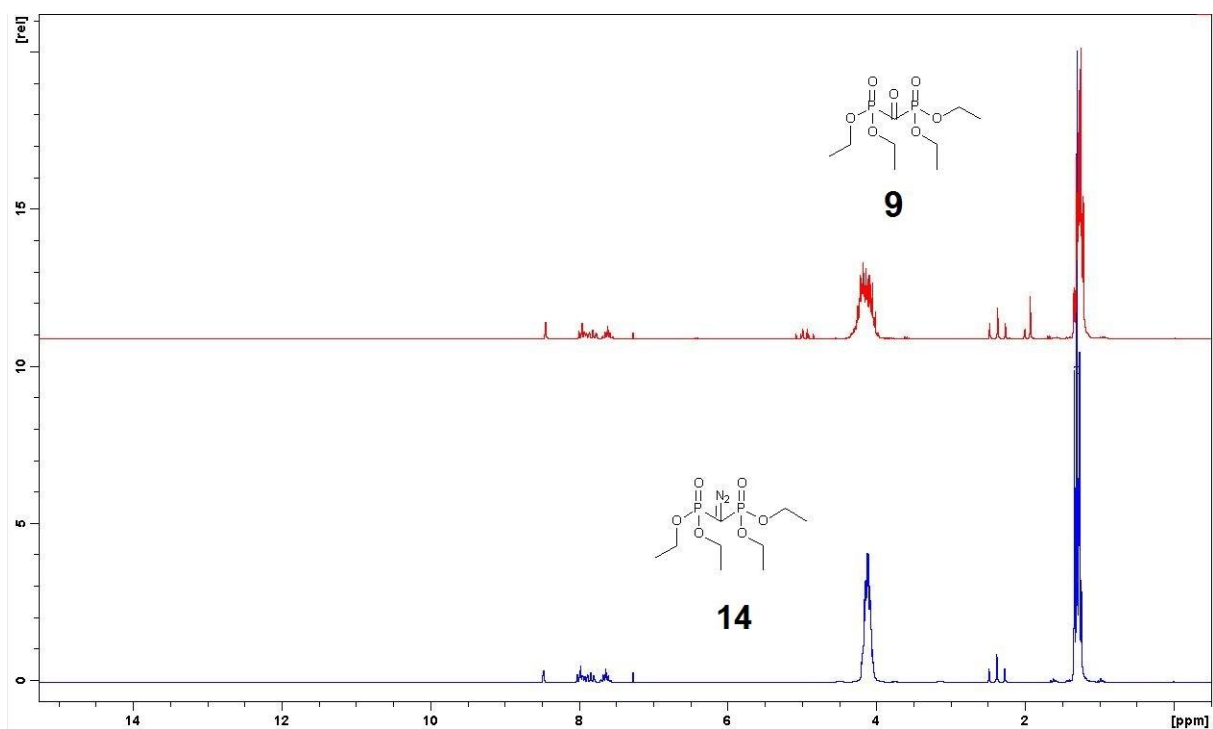
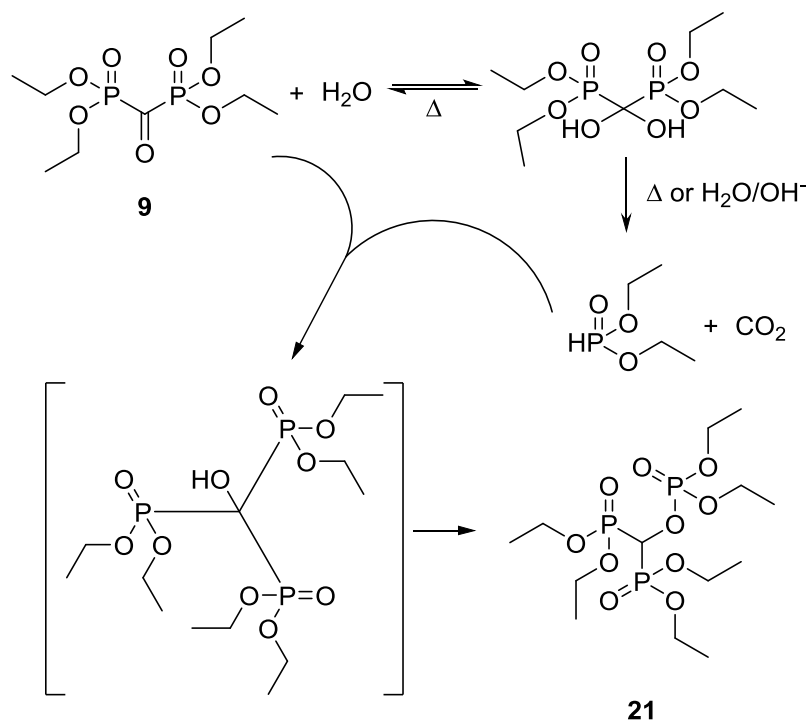


Figure 12. ^1H -NMR-spectrum of carbonylbis(diethoxyphosphine oxide) **9** and the starting materials from the previous synthetic stage

In the ^{31}P -NMR-spectrum starting material can still be seen in the spectrum of the diazo compound **14**. Integration of the peak at 2.38 ppm in the ^1H -NMR-spectrum gives a concentration of 10%, which should be no problem for the last step of the

synthesis. Also some diazotizing reagent **13** is still visible, which explains the aromatic peaks from 8.49-7.29 ppm but it is only traces and there is no expectable influence on the synthesis of the final product **9**. Since further purification was not possible a purity of approximately 90% was acceptable.

The ^{31}P -NMR-spectrum of the final bisphosphylketone product **9** clearly shows several peaks that could not be assigned, which indicates the formation of a variety of compounds. Only the peak at 6.84 ppm belongs to carbonylbis(diethoxyphosphine oxide) **9** according to literature.³¹ The other compounds can be explained by hydrolysis or rearrangements leading to the final decomposition of the product, which is also described in literature for bisphosphylketones:³¹



Following this scheme the carbonyl peak should be characteristic for product formation. Indeed, in the ATR-IR-spectrum a carbonyl peak could be found and it was also shown that the diazo peak of the starting material **14** disappears almost completely (Figure 13):

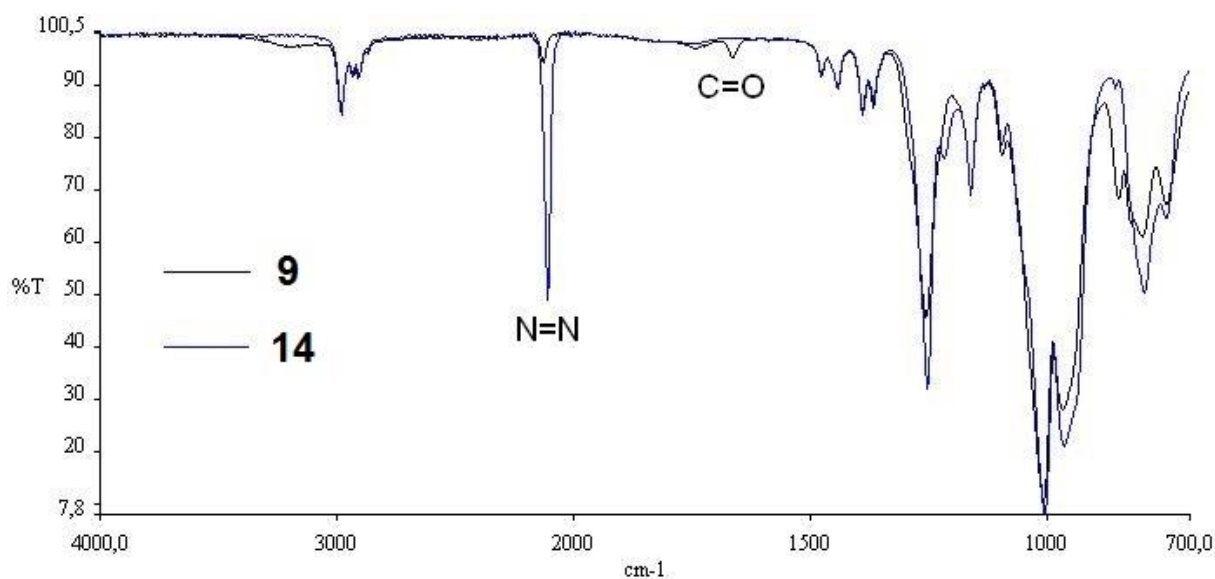


Figure 13. ATR-IR-spectrum of carbonylbis(diethoxyphosphine oxide) **9** and the starting materials from the previous synthetic stage

Finally, a GC-MS (Figure 14) was measured to prove the suggested pathway of decomposition for bisphosphylketone **9**.

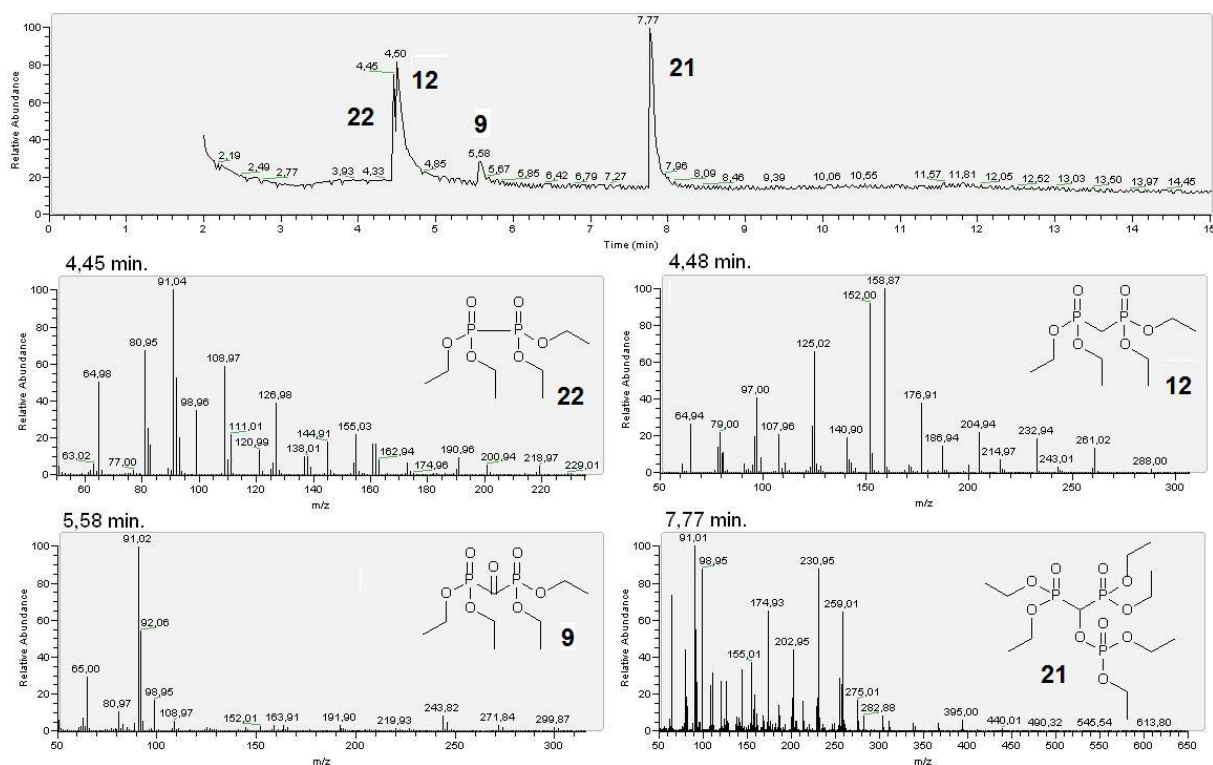


Figure 14. GC-MS of the raw product yielded from the synthesis of carbonylbis(diethoxyphosphine oxide) **9**

With this chromatogram it is clear that the final product **9** appeared during synthesis but decomposes due to its instability to the rearrangement product **21**. As already mentioned, also in literature the bisphosphylketones like **9** are used only in-situ to

react immediately with other reagents.^{28,29,31} To find out more about the possibility of getting a stable bisphosphylketone and also why carbonylbis(diphenylphosphine oxide) **8** could not be obtained some theoretical calculations were done by Dr. Markus Griesser (TU Graz/TU Vienna). An electrostatic potential of optimized structures was done with the B3LYP/6-31G(d) method and ESP according to Merz-Sing-Kollman, implemented in Gaussian09 (Figure 15). The result showed a very strong positive charge on both phosphorus atoms, which is probably responsible for the instability of the compounds.

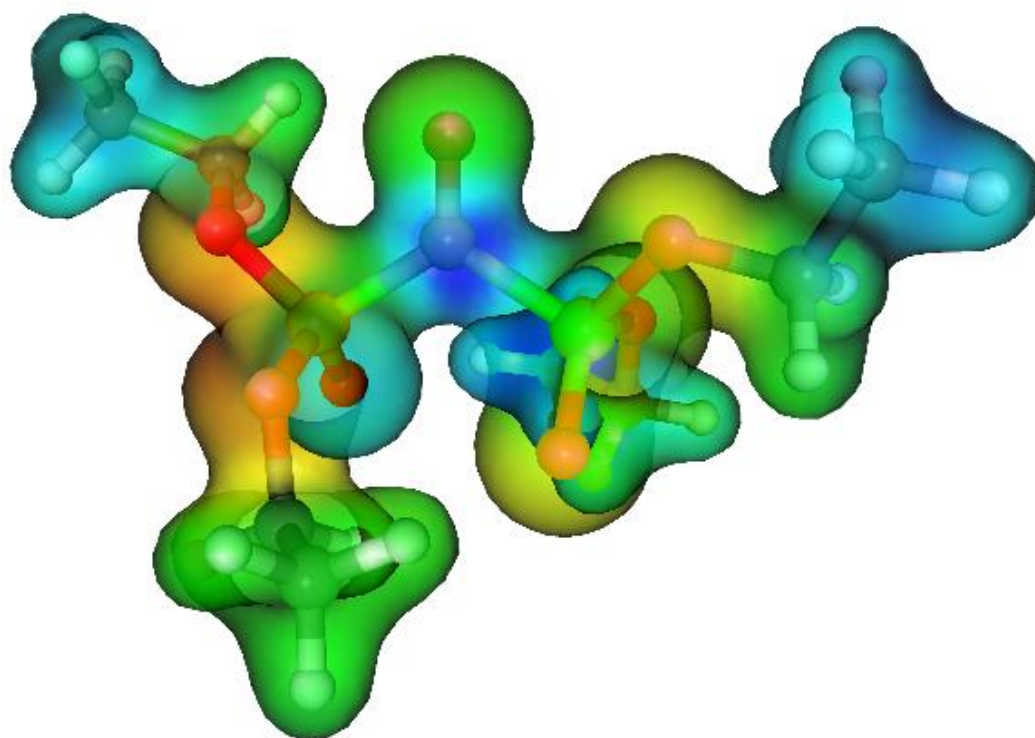


Figure 15. Calculated electrostatic potential for the final product **9** (blue: positive charge, red: negative charge)

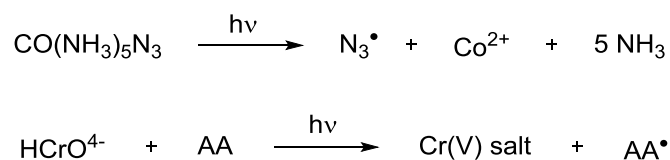
Since $-O-Et$ -moieties on the phosphorus like in the final product carbonylbis(diethoxyphosphine oxide) **9** already show a very strong +I- and +M-effect it is clear why the compound with phenyl groups carbonylbis(diphenylphosphine oxide) **8** could not be synthesized at all. Most likely a reduction of the positive charge on the phosphorus will not be possible in a magnitude that makes this type of compound stable enough for an application as photoinitiator. Literature suggests that the stability of different phosphyl ketones can be prolonged from 20 min to only 4 d³⁹ by introducing stronger electron donating moieties. Of course these are only similar and not the same compounds but it can be expected that the bisphosphyl ketones

show even less stability. So this would not be sufficient for a practical use. For this reason the concept of bisphosphylketones was no longer pursued.

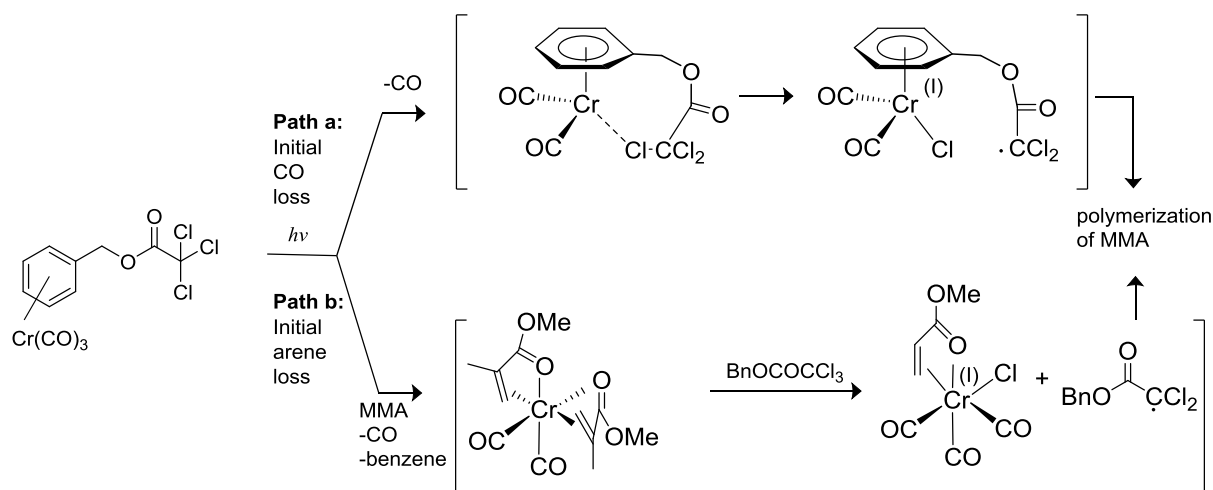
2. Zirconium Complexes

2.1. State of the Art

Metal-based compounds have been described quite a while ago as photoinitiators.⁴⁰ These compounds can be metal salts and metallic salt complexes or in fewer cases organometallic compounds and complexes. The first case of metal salts or metallic salt complexes is less interesting for dentistry, since these compounds and also their photoproducts are strongly colored and heavy metal ions would remain in the tooth fillings. Two examples for this class of compounds are azidopentaamine cobalt (III), which gives an initiating azide radical upon irradiation and chromic acid which produces together with acrylamide (AA) an initiating radical:⁴¹

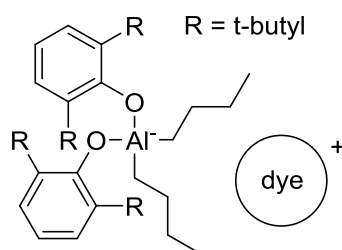


More interesting for the application in dentistry are the organometallic compounds and complexes. A partial occupation of metal d-orbitals leads to colored compounds, which therefore can potentially initiate upon visible light irradiation. Additionally, this absorption in the visible light area can theoretically be tuned by manipulating or changing the nature of the metal bound ligands. Only a handful of metal complexes were actually used as radical photoinitiators. These compounds were based on titanium,^{40,42,43} chromium^{42,44} or aluminum.⁴² Tricarbonyl chromium complexes of phenalkyl trichloroacetates can react as type I photoinitiators:⁴⁴



For dentistry this compound is not interesting of course, since colored photoproducts appear.

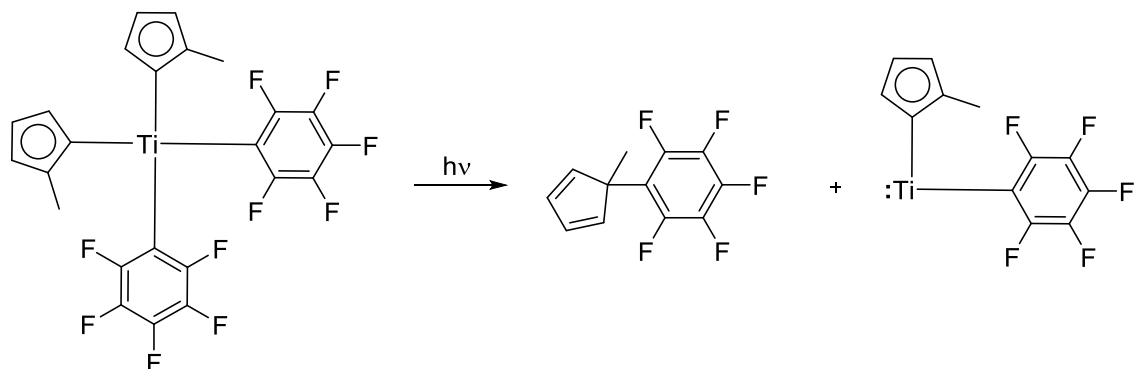
Aluminum on the other hand has a lot of colorless salts and complexes. Photoinitiators based on aluminum have already been developed:⁴⁵



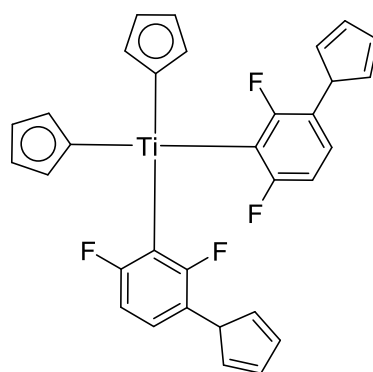
The problem with these complexes is that they cannot react according to a type I mechanism. The excitation is presumably based on electron transfer from the dye to the central Al-atom. While the exact mechanism is still not fully explored, it is known that C₄H₉-radicals are formed, which initiate polymerization. The aluminum complexes itself are colorless but the dye has to be colored in the complementary excitation wavelength for an electron transfer to happen. This excludes a photobleaching effect since the dye will still be present in the same color after curing the formulations. Therefore the aluminum complexes are no possible candidates for an application in dentistry.

Titanium based initiators suffer too from a lack of photobleaching. However, they were already used for dental applications⁴⁶ because they show absorption up to 520 nm.⁴³ The structural features of titanocene photoinitiators are always very similar. Four ligands, two of them fluorinated are bound to a central titanium atom.^{42,43} Fluorinated ligands are mandatory for the stability of the structure. After years of

trying to find a stable titanium complex the first titanium based photoinitiator was described including the initiation mechanism:⁴⁰



During the photocleavage reaction an electron transfer occurs from the ligand to the central atom leading to formation of two ligand radicals which combine. The polymerization was assumed to be started by the titanium diradical. However, newer studies suggest that also the ligand radicals might start polymerization to a certain degree but mostly the titanium radical is responsible for initiation.⁴³ Without the –I- and –M-effect of fluorine the electron transfer could occur even without excitation by radiation. Even after 25 years of research no other way was found to stabilize the titanocenes (only commercial product: Irgacure 784).⁴²



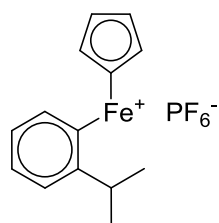
Irgacure 784

Except problems with stability and insufficient photobleaching also the reactivity of the titanium complexes is greatly reduced in aqueous environments. For these reasons the titanocenes could not penetrate the market for dental photoinitiators.

Nevertheless, the low number of patented compounds in this field makes research in this direction very appealing. Publications on several interesting candidates can be found in literature. Complexes absorbing in the visible light area, showing structural

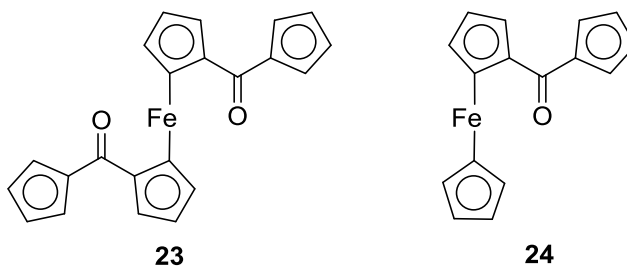
features that are already known from other photoinitiating compounds are usually based on zirconium,^{43,47} iron^{48,49} or ruthenium.^{48,50}

With ferrocenes it was already possible to produce a commercial product. Irgacure 261 is in fact no radical photoinitiator but upon irradiation it forms a lewis acid that can be used to cure epoxy resins.⁴⁴



Irgacure 261

For dentistry only radical photoinitiators are interesting, of course. Imaginable complexes could have for example benzophenone groups:⁴⁸



23

24

The ferrocenes **23** and **24** indeed show absorption maxima around 500 nm (Figure 16):

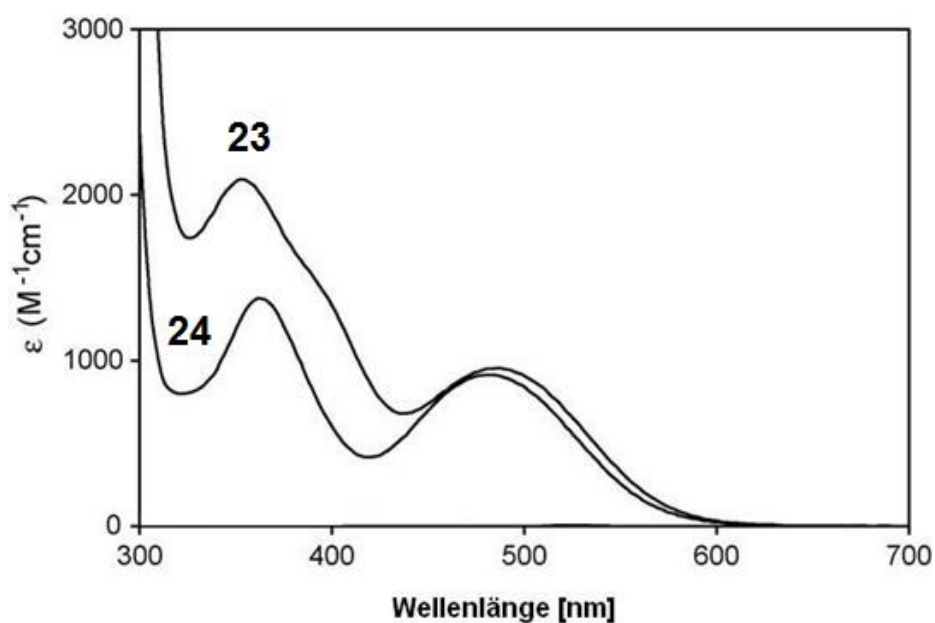
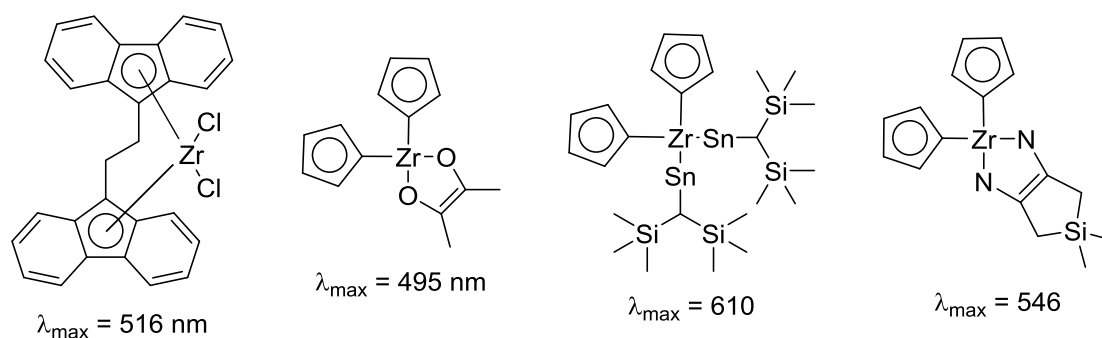


Figure 16. Absorption spectrum of the iron complexes 21 and 22⁴⁸

Unfortunately, ferrocenes have one big drawback. After potential photocleavage, iron salts are formed, which are usually strongly colored. This contradicts with a required photobleaching effect. The exact same behavior can be expected from the ruthenium complexes.⁴⁸

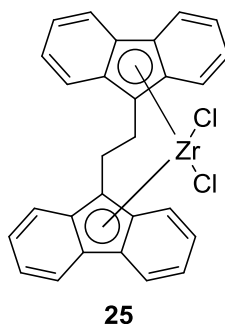
This chain of thoughts led in combination with what was already known from literature to the following conclusion: An organometallic compound, suitable for dental applications should be built as organometallic complex, single component, with initiation via cleavage and the salts of the central atom have to be colorless. Zirconium complexes show all of these features. Even though most of them are described as instable or are stored under argon after synthesis, they can be produced also in a relatively stable form if the right ligands are chosen. They show absorption in the visible light area, good photobleaching and recently published zirconium based photoinitiators possessed high reactivity.^{43,47,51} Cp₂ZrCl₂ shows for example very good properties.⁵² It is stable under air and even seems to compensate oxygen inhibition during polymerization to a certain degree. Furthermore it was more reactive than the state of the art initiator 2,2-dimethoxy-2-phenylacetophenone in a diacrylate system. The only problem with this complex is that it absorbs only in the UV area. Several other complexes are described in literature with absorption maxima between 425 nm and 750 nm.^{51,53-57} Of course most of these complexes were not investigated for an application as photoinitiator, nor was light sensitivity described. Additionally, most of the more complex structures were described only under argon atmosphere. The following scheme should just give an idea about the potential redshifts that are achievable with the use of zirconium complexes, which in case of photocleavage would form colorless salts:



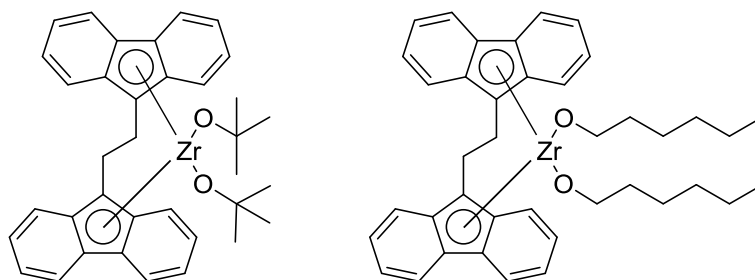
2.2. Syntheses

As already mentioned before the field of existing zirconium complexes is wide and the hunt for a zirconium based photoinitiator has only just begun. Within the limits of this work it was chosen to orientate oneself closely to literature and try to reproduce one of the more promising complexes for the application as photoinitiator. Since Cp_2ZrCl_2 showed good results but only initiates under UV irradiation it was tried to find a compound that absorbs in the visible light area but with similar structural features to guarantee stability and photoinitiation. The zirconium dichloride complexes in general seemed to be the most stable according to literature. Almost all other zirconium based complexes needed to be stored or were only characterized under argon atmosphere (examples given above).^{51,53-57} However, the zirconium dichlorides that can be found in literature are only red-shifted if the organic ligands are bridged.^{43,47,51} The reason for this was not closely investigated yet but a possible explanation might be that the bridge forces the ligands into a certain angle. This leads to absorption maxima in the visible light area in contrast to for example Cp_2ZrCl_2 , which has freely rotatable ligands.

(Ethylenbis(9-fluorenyl))zirconiumdichloride **25** is described in literature as stable under air and shows an absorption maximum at 516 nm. For these two reasons it was selected as a first model compound for synthesis, characterization and first tests concerning this barely explored class of compounds.

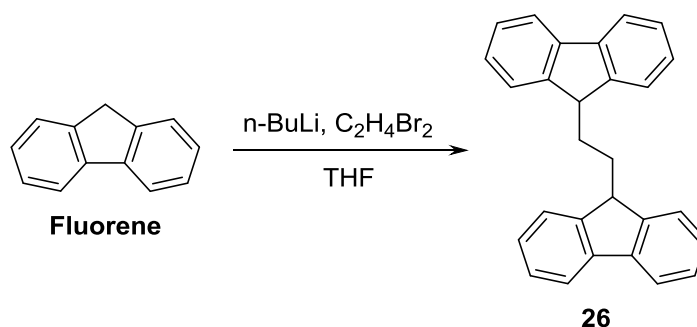


In case of solubility issues in the used methacrylic monomer formulations it was also considered to modify the structure:



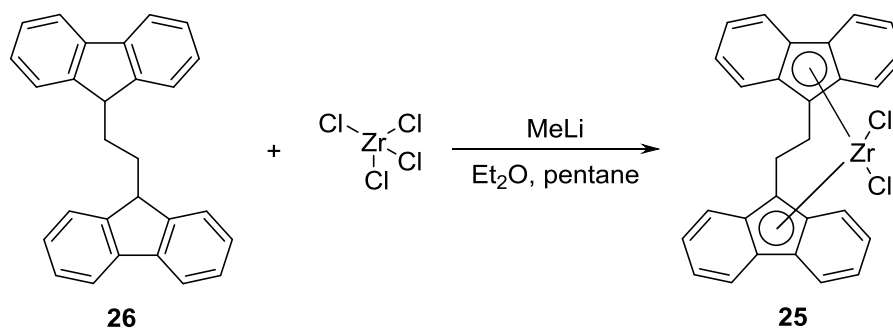
Of course this might have influence on the stability of the complexes since as already mentioned the zirconium dichlorides are the most stable, which can be explained by high dissociation energy of the two attached chlorine atoms. For this reason it would also not be possible to just exchange the chlorine with for example t-BuOH in one step but other synthetic approaches that were not described in literature yet would be necessary.

Nevertheless, model compound **25** was synthesized according to literature^{58,59} as a first step in this project. First the fluorenyl ligand needed to be synthesized:



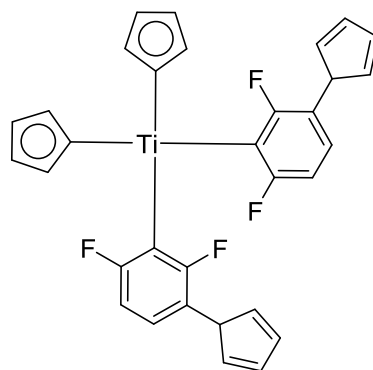
Therefore 1 eq. of fluorene was deprotonated with 1 eq. n-BuLi in THF and the resulting organolithium reagent was reacted with 1 eq. 1,2-dibromoethane at 0°C. After stirring for 21 h, the reaction mixture was quenched with aqueous NH₄Cl. A work-up in literature was not given. Therein just washing with pentane was used to yield the product. However, this did not lead to a pure product so as a work-up the white powder was recrystallized from ethanol to yield 48.6% of 90% pure bis(9-fluorenyl)ethane **26** according to ¹H-NMR-analysis. Higher purity could not be achieved with this synthetic method but is also not necessary because the starting material and possible side products can't form stable zirconium complexes.⁶⁰

With the ligand at hand the complex **25** could be synthesized.⁵⁹



After deprotonation of 1 eq. of the ligand **26** with MeLi, the resulting lithium organyl was reacted with 1 eq. of ZrCl₄ in diethyl ether. According to literature after 30 min. the solvent can be evaporated and the red residue extracted with dichloromethane to yield the pure product. Analysis was done only via elemental analysis. However, it was found that with this method no pure product could be obtained. After extraction with dichloromethane a white solid, which was assumed to be clustered zirconium chloride could be filtered off but side products, ZrCl₄ and the ligand starting material still remained in the raw product. After several retries and optimization experiments where recrystallization in different solvents and different temperatures were tried, Soxleth-extraction was found to be the most effective method of purification. With diethyl ether side products and starting materials could be removed and the residue was dissolved in dichloromethane. Filtration of this solution gave (ethylenbis(9-fluorenyl))zirconiumdichloride **25** in 54.8% yield as a red powder. Product formation was confirmed via ¹H-NMR-analysis. ¹³C-NMR analysis was also tried but coupling of the Zr central atom with the carbon atoms gave a bad signal/noise ratio so that no clear peaks could be obtained.

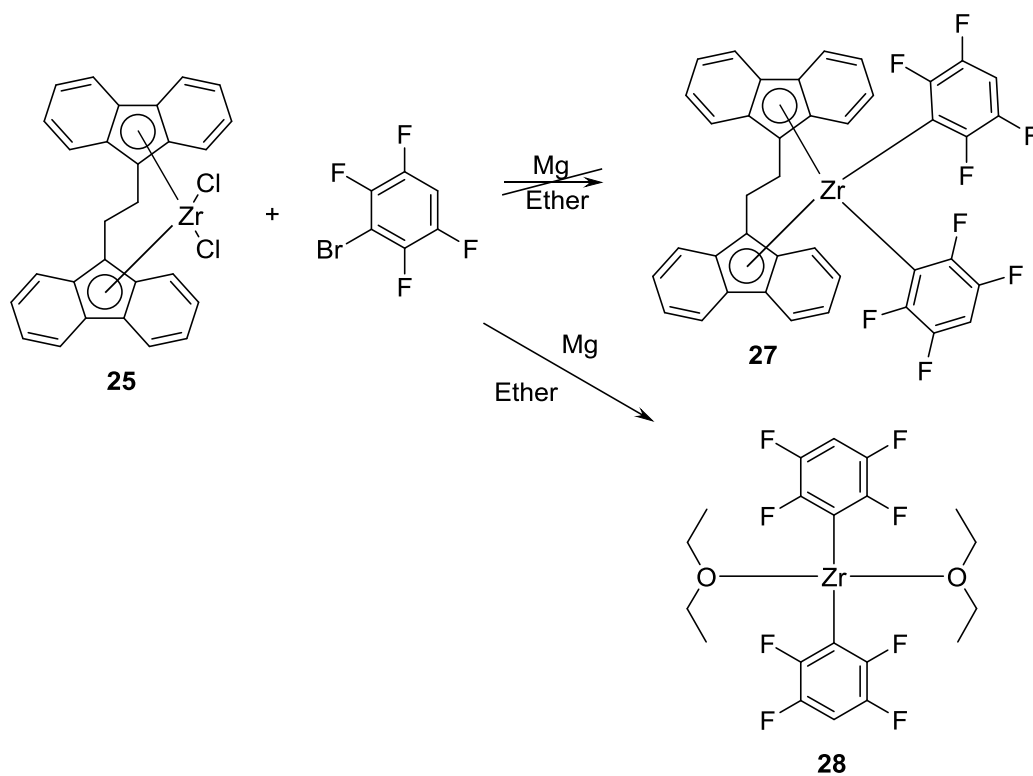
The product **25** was stable in organic solvents (diethyl ether, dichloromethane, MeCN) but not in methacrylate based monomer mixtures (mixture A: UDMA, D₃MA, bis-GMA). So it was tried to stabilize the zirconium complexes the same way as the titanium complexes were stabilized: By removing the chlorine and introducing fluorinated aromatic moieties to achieve a similar electronic state as in Irgacure 784.⁴²



Irgacure 784

Titanium and zirconium are both group 4 elements and have a similar orbital configuration. The idea was to have two aromatic hydrocarbon systems and two fluorinated hydrocarbons to stabilize the zirconium complexes the same way it was done for the titanium complexes.

In literature zirconium complexes with fluorinated aromatic systems are either synthesized with aryllithium⁶¹ or with a Grignard reagent⁶² from Cp_2ZrCl_2 and the chlorinated or brominated fluoro-aromatic species. For (ethylenbis(9-fluorenyl))zirconiumdichloride **25**, which already tends to be instable the softer synthetic route with a Grignard reagent was chosen:



In first experiments a fully fluorinated aromatic system was chosen but here it turned out to be impossible to analyze since the fully fluorinated system could not be detected via $^1\text{H-NMR}$. So in the end the reaction was done with a tetrafluorobenzene: A Grignard reagent was synthesized from 2.2 eq. bromotetrafluorobenzene and 4 eq. magnesium in diethyl ether. During a 6 h reaction time the reaction mixture changed its color from colorless to yellow and brown in the end. The ongoing reaction could be monitored by consumption of the magnesium in the reaction mixture. The resulting Grignard-reagent was reacted in-situ with 1 eq. (ethylenbis(9-fluorenyl))zirconiumdichloride **25** at -78°C under argon atmosphere in toluene. After stirring for 24 h at ambient temperatures the solvent was evaporated and completely substituted with toluene. Pentane was added until pentane/toluene = 1:1 v/v was obtained and the mixture was filtered. This procedure was repeated two times. Subsequent $^1\text{H-NMR}$ -analysis of the orange, powdery product did not show the formation of the desired (ethylenbis(9-fluorenyl))zirconiumtetrafluorobenzene **27** but the fluorenyl ligand was completely cleaved off and substituted by tetrafluorobenzene. The chlorine was most likely substituted by diether resulting in the undesired product **28**. Another possibility is that chlorine was not substituted but diethyl ether just coordinated additionally to the zirconium. This is however less likely since zirconium favors four ligand complexes. A closer investigation of the product with which photoinitiation was not possible was not done.

2.3. Characterization and Interpretation

To test the photoinitiator properties of (ethylenbis(9-fluorenyl))zirconiumdichloride **25** it was dissolved in mixture A (UDMA, D_3MA , bis-GMA, 1:1:1 molar) with a concentration of 1%. The deeply red photoinitiator ($\lambda_{\text{max}} = 516 \text{ nm}$) decolorized immediately in the monomer mixture and initiation with visible light was not possible. The stability of complex **25** under atmospheric conditions and in solution (dichloromethane, diethyl ether, MeCN) but its decolorization in methacrylate based monomer mixtures indicates a cleavage of the fluorenyl ligand only in the monomer. Indeed, zirconium is known to coordinate with monomer double bonds.^{63,64} In the first publication from Stoebenau et al zirconium cyclopentadienyl complexes are reacted

with various alkenes and alkynes. Also “alkene flipping” is described, which means continuous ligand exchange occurs in presence of more than one alkene. The second one by Mulhaupt et al describes Ziegler-Natta polymerization, where the ability of zirconium complexes to coordinate with monomer double bonds is used to catalyze a polymerization reaction. Probably during these coordination reactions the fluorenyl ligand is cleaved off and therefore the absorption maximum shifts to the UV area. In the end the formulation could be polymerized in a UV-oven (Figure 17).

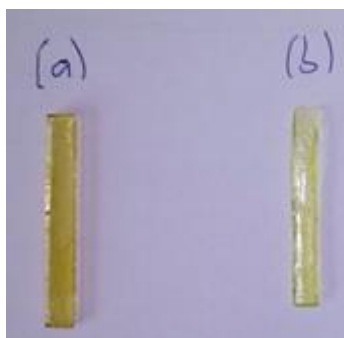


Figure 17. Mixture A with 1% PI, polymerized under broad band UV light; (a) CQ+DMAB as a reference, (b) (ethylenbis(9-fluorenyl))zirconiumdichloride **23**

As can be seen, the polymerization of mixture A is not as complete with (ethylenbis(9-fluorenyl))zirconiumdichloride **25** as it is with the state of the art **CQ/DMAB** system but a polymerization reaction clearly occurs. It was tried to isolate a potential newly formed complex from a mixture of complex **25** with MMA but evaporation of MMA just gave a white, partly insoluble precipitate. The soluble part consisted of the ligand **26**, the insoluble was assumed to be clustered zirconium chloride. It was now tried to polymerize mixture A also with pure ligand **26** in the UV-oven but no polymerization reaction could be observed. All this led to the conclusion that a new compound is formed in the monomer that is responsible for initiation under UV light but it is only stable in monomer solution.

After all it can be said that photoinitiation works but the visible light initiation necessary for dental applications was not reachable with zirconocenes at this point. Only the bridged ligands showed similar structural features as known photoinitiators from literature and at the same time visible light absorption. Bis(9-fluorenyl)ethane **26** was described in literature^{43,47,51} as most stable bridged ligand since it can be stored under air. Other ligands like for example indanes showed no absorption in the visible light area and other bridge lengths led to stability only under argon atmosphere.

So since the model reaction already did not work the way it was intended and no direct follow-up compounds were under consideration, the focus of the work was shifted to other projects.

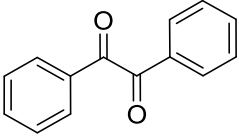
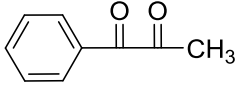
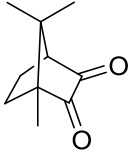
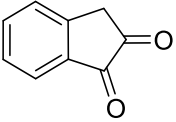
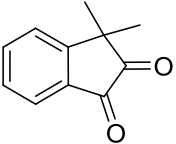
3. Diketone Systems

3.1. State of the Art

An aliphatic ketone alone has an $n-\pi^*$ transition at approximately 320 nm.⁶⁵ By addition of a second keto-group the absorption maximum can be shifted to longer wavelengths depending on the angle between the two carbonyl groups. For years the Norrish type II diketone photoinitiator system **CQ/DMAB** has been state of the art for dental applications. As a long wavelength photoinitiator it shows an absorption maximum at 468 nm. Compared to a pure aliphatic ketone this is a shift of about 130 nm.

However, as already mentioned this system suffers from low reactivity and it might be advantageous to shift the absorption maximum from 468 nm to higher wavelengths to allow penetration of light into deeper layers. It is known from literature that the maximum of the $n-\pi^*$ transition of a diketone system can be shifted by changing the angle between the two carbonyl groups. This correlation is shown in the table below (Table 2).

Table 2. Angle between carbonyl groups and absorption maxima of different diketone systems⁶⁶⁻⁶⁸

Compound	Angle [°]	λ_{\max} n— π^* [nm]	Range [nm]
	120	390	450
 PPD	100	400	490
 CQ	20	468	510
 29	0	484	530
 30	0	500	550

A single benzoyl chromophore that is frequently applied in Norrish type I systems has the maximum of its n— π^* transition at 320 nm. Moreover, it is known that the empty d-orbitals of a hetero atom next to a carbonyl group reduce the required energy for an n— π^* transition thus leading to a bathochromic red-shift. This effect has been proven for acylphosphinoylides, where the empty d-orbitals of a P-atom shift the absorption maximum from 320 nm to 385 nm. If these two effects (the diketone and the heteroatom effect) are combined, a new class of compounds with a high potential for an application as photoinitiator might be obtained (Figure 18).

Shift of the n- π^* -transition

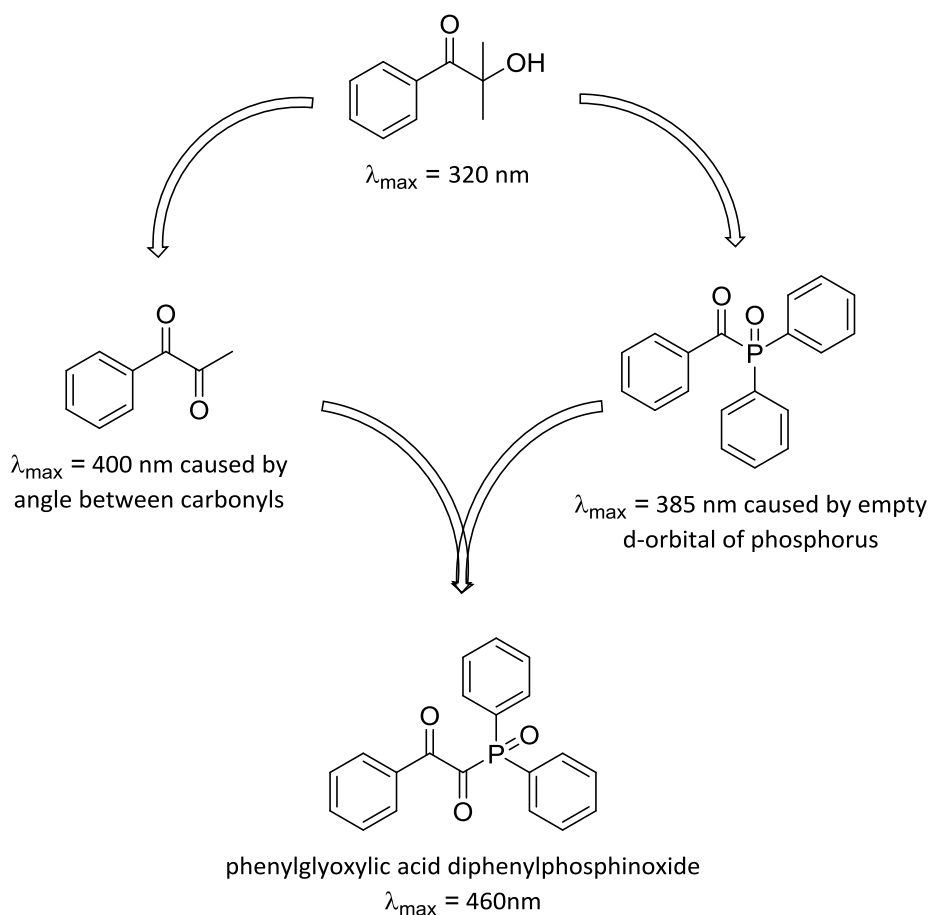
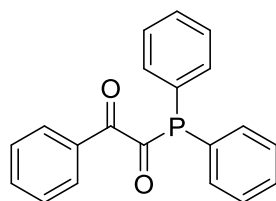


Figure 18. Scheme, showing the concept for the new class of diketone photoinitiators⁶⁵

A first compound phenylglyoxylic acid diphenylphosphine has already been synthesized in preliminary experiments at our institute.⁶⁹

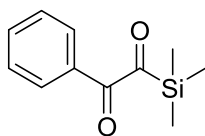


Phenylglyoxylic acid diphenylphosphine

$\lambda_{\max} = 460 \text{ nm}$

The compound showed promising results, regarding its absorption maximum, but wasn't stable enough for polymerization experiments.

The synthesis for a Si-based compound **31** with an absorption maximum at 518 nm can be found in literature. It is described as reddish-purple liquid and shows high light sensitivity.⁷⁰



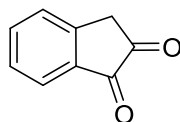
31, $\lambda_{\text{max}} = 518 \text{ nm}$

The drawback of this compound is the instability, which is a common problem among Si-compounds. However, it should be possible to adapt the described synthesis based on a multi-step reaction of chlorotrimethylsilicium with phenylacetylene for a Ge-based structure, leading to a stable compound. With Ivocerin it has already been confirmed that acylgermanes are more stable than the analogous Si-based molecules, which are highly sensitive towards hydrolysis and oxidation.

In literature it is not described if these diketone systems would work as a Norrish type I or type II initiator. A Norrish type I initiator would react through cleavage of the compound between heteroatom and carbonyl, which would be possible in case of a conjugated system. A type II reaction will work similarly to the **CQ/DMAB** system through hydrogen transfer and therefore also require a coinitiator.

3.2. Preliminary Experiments

Preliminary tests were made to decide, whether diketone systems in ring form or in linear form should be synthesized for a first characterization. For these tests an indanedione was chosen, since 1,2-indanedione **28** shows an absorption maximum at 484 nm ($\epsilon \sim 30 \text{ l mol}^{-1} \text{ cm}^{-1}$), which is more red-shifted than **CQ** ($\lambda_{\text{max}} = 468 \text{ nm}$, $\epsilon \sim 44 \text{ l mol}^{-1} \text{ cm}^{-1}$).



29

1,2-Indandione **29** is commercially available and was also therefore chosen as a first testing compound. In Photo-DSC measurements (Figure 19; mixture A, 1 wt% PI concentration, 400-500 nm irradiation) with **DMAB** as coinitiator and Ivocerin and

CQ/DMAB as references a very low reactivity of the indanedione system was observed.

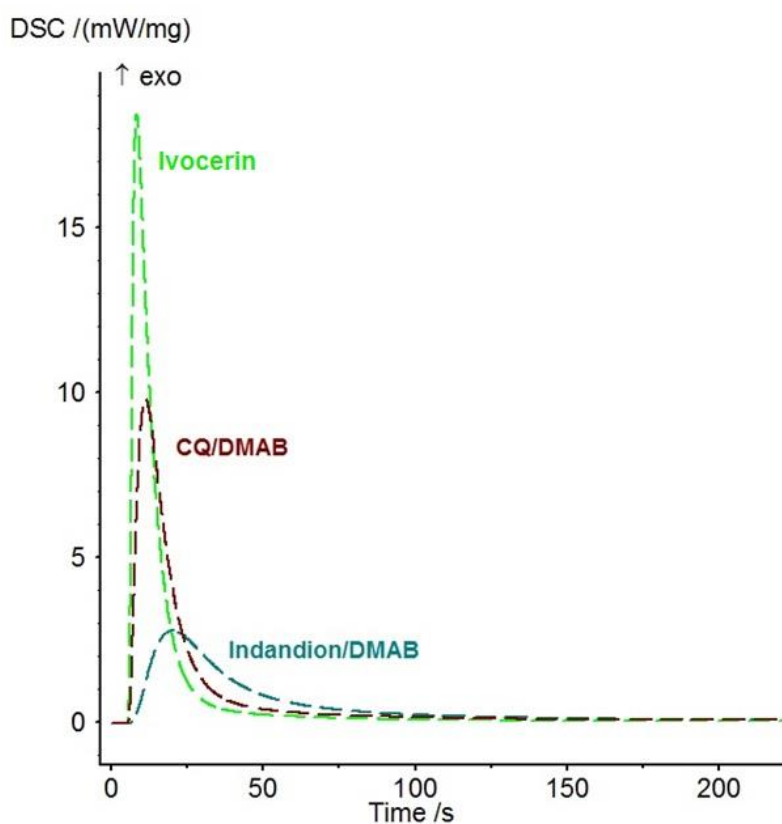


Figure 19. Photo-DSC measurements of 1,2-indandione **29** with references (mixture A, 1 wt% PI concentration, 400-500 nm irradiation)

This can be explained with the fluorescence of indanedione. The strong fluorescence of indanedione **29** (Figure 20) is already mentioned in literature.⁷¹ Quantitative fluorescence quantum yields are not given but it is commercially available because it is used in forensics to make fingerprints visible.

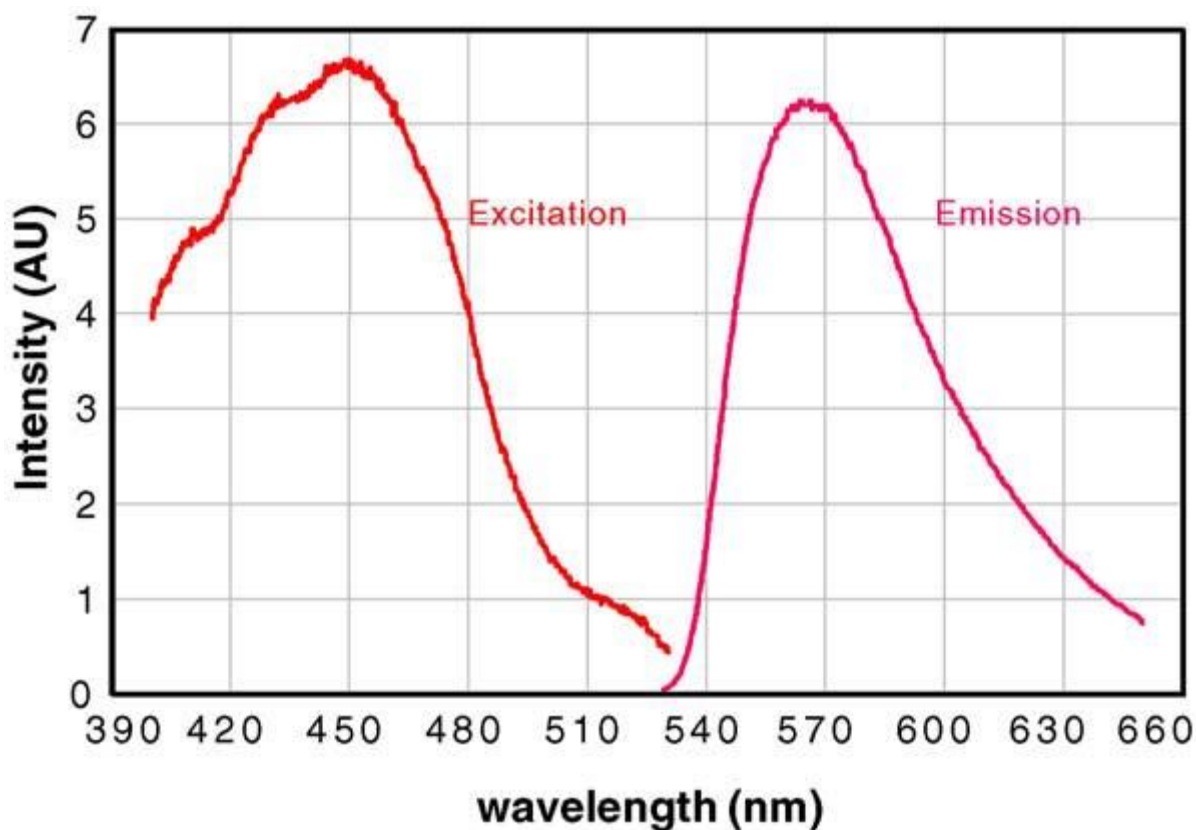
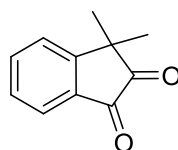


Figure 20. Absorption and emission spectrum of 1,2-indanedione 28⁷¹

The fluorescence hinders the compound from going in the excited triplet state, which is necessary for a photoreaction and the most likely reason for this fluorescence is the aromatic system, which forces the two ketones in a low angle, causing the high bathochromic red-shift.

The compound dimethylindanedione **30** is also known from literature and shows an even higher bathochromic shift (500 nm).⁶⁶



30

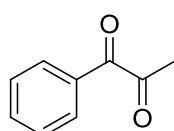
However, it is not commercially available and was not synthesized since also here typical fluorescence can be expected.

So the conducted experiments led to the conclusion that for a start and proof of concept linear diketone systems should be preferred. Phenylpropanedione (**PPD**) was for a long time a state of the art photoinitiator in dentistry and is therefore already

well described regarding its photoinitiator properties. The goal was now to get a compound with similar structural features and compare it to **PPD** as state of the art compound. More experimental data regarding **PPD** can therefore be found below.

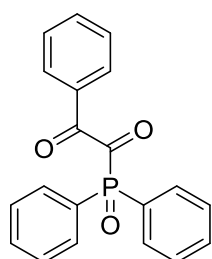
3.3. Syntheses

After the preliminary tests it was concluded that a good start for the diketone photoinitiator project would be to synthesize structures that are based on the already known and widely used **PPD**.

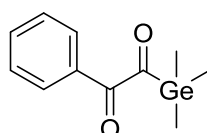


PPD

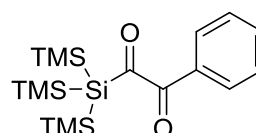
This has not only the advantage of structural features that are known literature and known to show photoinitiator properties but also **PPD** is in fact the most basic structure one could think of when it comes to a diketone photoinitiator system. A logical first step was now to substitute the methyl group neighboring the carbonyl with a heteroatom. P, Ge and Si were chosen as possible candidates as it was before also done for the cleavable type I systems (i.e. **MAPO** or Ivocerin). The most basic structures were chosen as first target compounds:



32



33

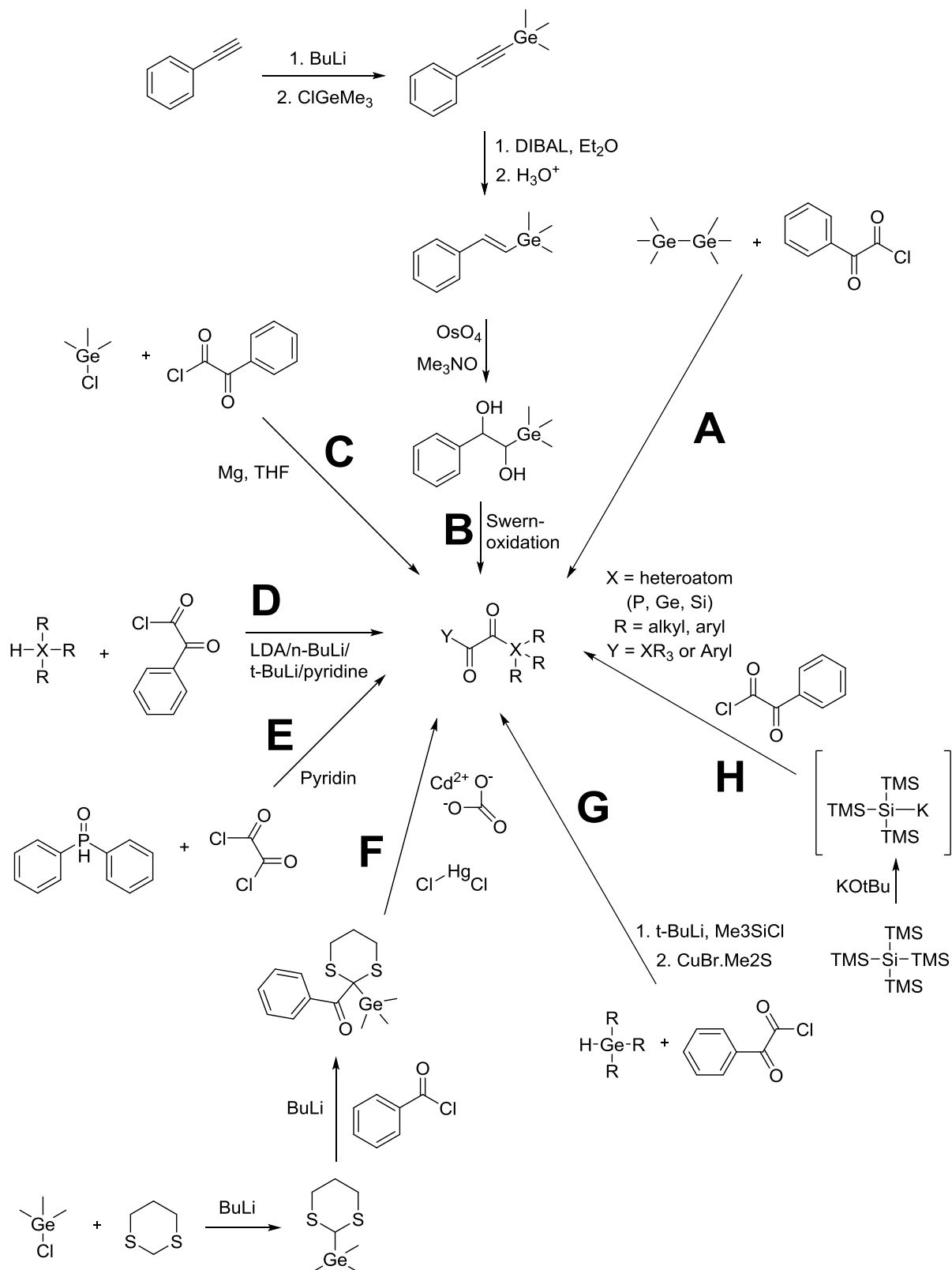


34

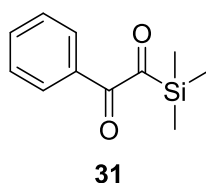
A syntheses scheme (Scheme 2) was made that was based on syntheses that were described in literature for similar structures (more information on that can be found directly at the synthesis) or in the case of germanium (especially pathway B) were described for silicium compounds. It was assumed that silicium and germanium could

behave similar during syntheses because both are group 14 elements and have therefore similar orbital configurations.

Scheme 2. Potential syntheses pathways for diketones



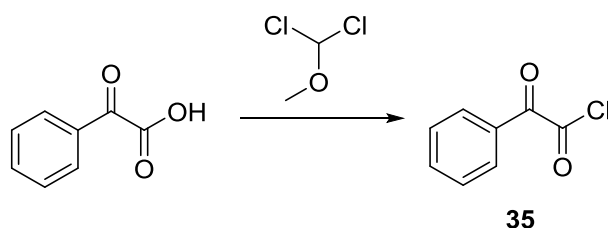
A simpler silicium diketone **31** is described in literature.⁷⁰



However, as already described above, in the same publication stability issues are mentioned. So the idea was to use germanium instead of silicium or stabilize the silicium with introducing TMS groups.

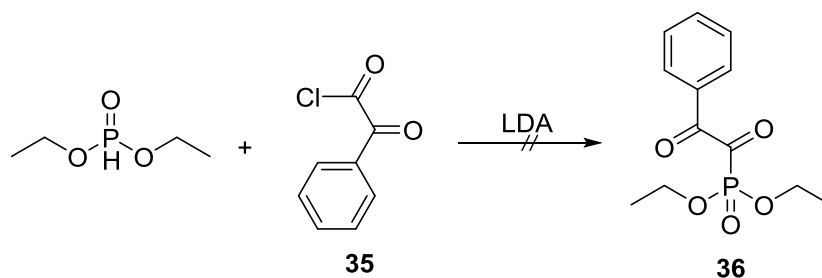
3.3.1. Synthesis of Phenylglyoxylic Diethylphosphite **36** and Phenylglyoxylic Diphenylphosphine Oxide **32** (Pathway D)

The acidity of phosphine hydrides was assumed to be high enough for an organolithium reaction pathway. This pathway has the advantage of a very simple and direct approach and was therefore tried first. The starting materials are either commercially available (diethylphosphite) or were synthesized according to literature (phenylglyoxylic acid chloride **35**):⁷²

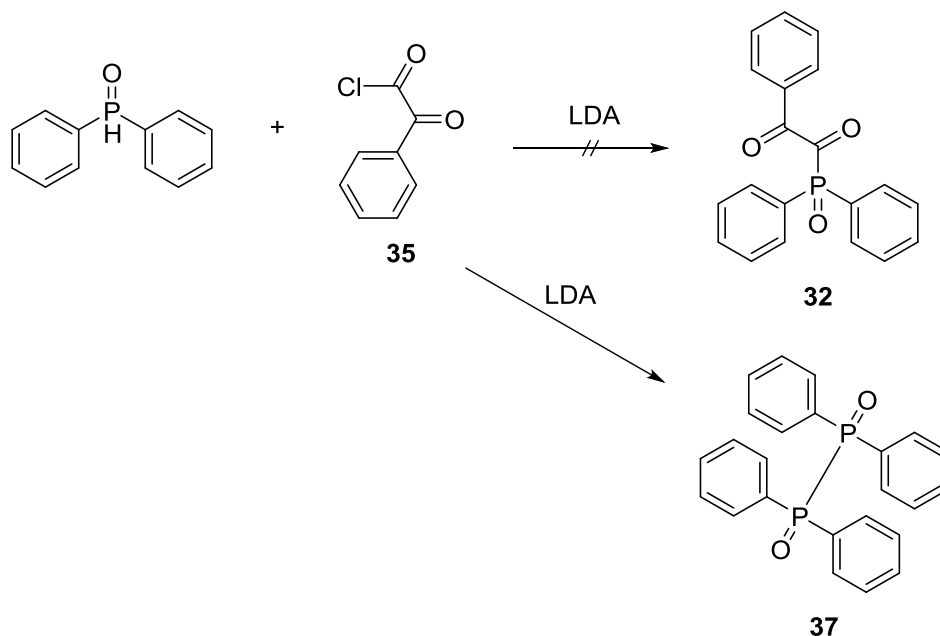


For this synthesis 1.5 eq. of Dichloromethoxymethane were added to 1 eq. of phenylglyoxylic acid under argon atmosphere. The reaction mixture was stirred for 1 h at 50°C. Work-up via Kugelrohr distillation gave the pure product **35** as yellow liquid with 38% yield.

Now the organolithium reaction could be tried.



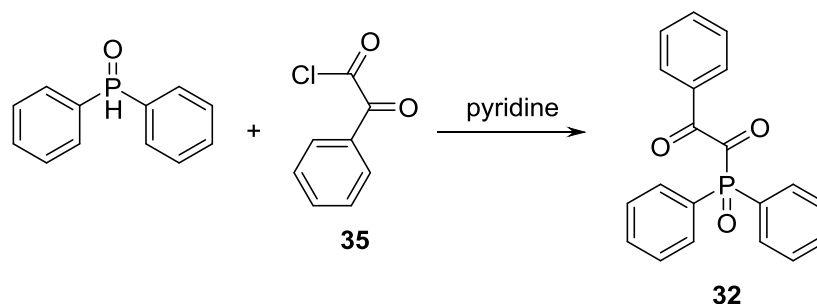
For this reaction 2.2 eq. of LDA in THF were added at -30°C over a period of 90 min to a solution of 1.1 eq. phenylglyoxylic acid chloride **35** and 1 eq. diethylphosphite in THF. After stirring the mixture at -30°C for 2 h toluene was added and the reaction quenched with water. During quenching the red reaction mixture decolorized completely. A product **36** formation could not be proven via GC-MS. Samples taken during the reaction before quenching and of the organic phase after quenching showed no product. Just in case phenylglyoxylic diethylphosphite **36** formed during the reaction but was not stable enough to be isolated and characterized another phosphorus reagent was tried too. From **MAPO** synthesis it is known that aryl substituents provide theoretically better stability to the system. So the synthesis was tried again with diphenylphosphine oxide.



In analogy to the synthesis conducted before 2.2 eq. of LDA in THF were added at -30°C over a period of 90 min to a solution of 1.1 eq. phenylglyoxylic acid chloride **35** and 1 eq. diphenylphosphine oxide in THF. After stirring the mixture at -30°C for 2 h, toluene was added and the reaction quenched with water. This time the reaction

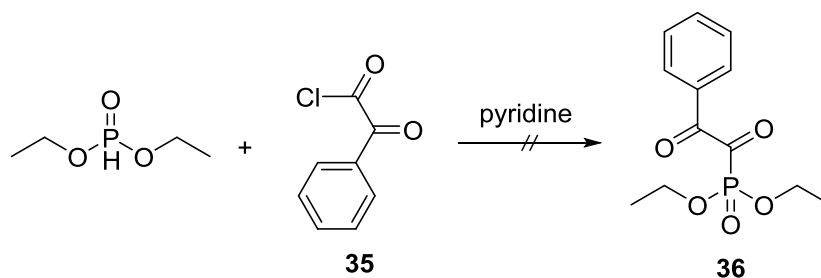
mixture changed its color to orange/yellow. After evaporation of the solvent a yellow precipitate was obtained. GC-MS and HPLC analysis showed starting materials (but phenylglyoxylic acid chloride in free acid form) and the dimer **37**. In good accordance with the germanium hydrides a dimerization reaction had occurred and instead of the product phenylglyoxylic diphenylphosphine oxide **32** the dimer **37** was obtained. Since the desired product could not be detected no further purification or characterization was done.

To avoid the dimerization reaction a reactive species had to be created from the acid chloride and not from the heteroatom hydride. Since the hydrogen in diphenylphosphine oxide is rather acidic a variation of the Einhorn-acylation⁷³ was tried where the alcohol was substituted with the phosphine oxide:



For that 1.1 eq. of phenylglyoxylic acid chloride **35** and 5 eq. of pyridine were dissolved in toluene and stirred for 10 min. at ambient temperature to get activated pyridinium salts. This solution was added to 1 eq. diphenylphosphine oxide. The reaction mixture turned red immediately. After 2 h stirring at ambient temperature it was washed with water and the solvent evaporated. The red/purple residue was purified via flash chromatography to obtain product **32** with 62.3% yield as red needles with a purity >90%. The impurities were mostly starting material diphenylphosphine oxide and to a small part the dimer of the starting material, visible in ³¹P-NMR measurements. These two substances could not be removed but were also no problem for subsequent characterization methods since they are not photoactive or absorb in the visible light region.

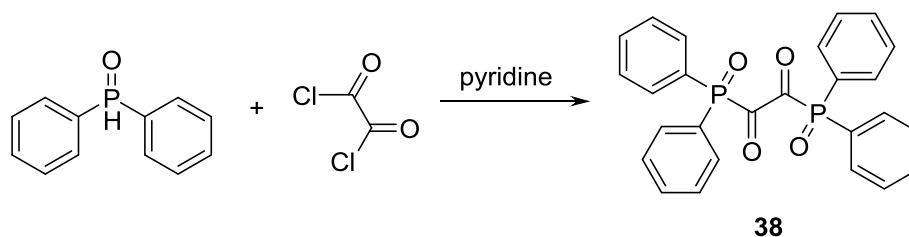
Since this reaction pathway worked very well for diphenylphosphine oxide it was repeated for diethylphosphite in the exact same way with the exact same equivalents of starting materials as described above:



Unfortunately, again no product **36** was obtained. TLC and GC-MS analysis showed a large variety of peaks. Some could be assigned to phosphorus dimers or transesterification products; others could not be assigned at all. This led to the conclusion that product **36** cannot be obtained in this way or might even not be stable at all.

3.3.2. Synthesis of Oxalylbis(diphenylphosphine) Oxide **38** (Pathway E)

To find out more about the influence of the benzoyl chromophore in the diketone systems, a system without benzoyl moiety was synthesized according to the already established Einhorn-like method:⁷³



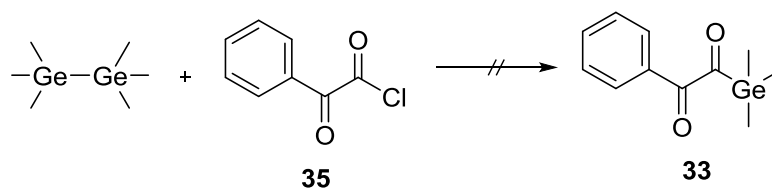
Under argon atmosphere a solution of 0.9 eq. of oxalylchloride and 10 eq. pyridine in dichloromethane was made and stirred for 10 min. at ambient temperature. This solution was added to 1 eq. diphenylphosphine oxide in dichloromethane. After stirring for 2 h at ambient temperature the reaction mixture was washed with water. The organic phase contained the product **38**, which was purified via flash chromatography to obtain the red product as red solid with 35.8% yield in a purity >80%. The impurities were mostly starting material diphenylphosphine oxide and to a small part the dimer of the starting material, visible in ³¹P-NMR measurements. These two substances could not be removed but were also no problem for

subsequent characterization methods since they are not photoactive or absorb in the visible light region.

3.3.3. Synthesis of Phenylglyoxylic Tri(m)ethylgermanium **33** and **39**

3.3.3.1. Synthesis with Pd-Catalyst (Pathway A)

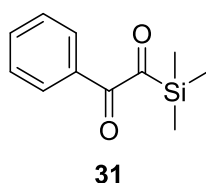
After two phosphorus diketones were successfully synthesized the focus was shifted to the germanium diketones. Pathway A (Scheme 2) was tried first, since this reaction pathway already worked for an Ivocerin derivate in a former work.²¹ It was described in literature only for digermanes and acid chlorides to yield benzoyl germanium compounds.⁷² That means the synthetic pathway described in literature was modified in a way that instead of benzoyl chlorides, phenylglyoxylic acid chloride **35** was used. It was synthesized according to a published procedure as also described above.⁷⁴



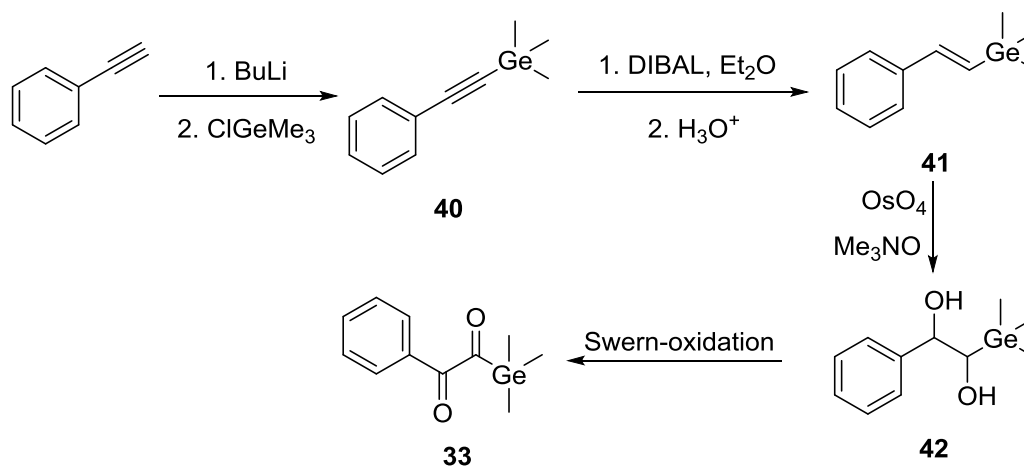
Subsequently, 1 eq. of hexamethyldigermane was reacted with 0.9 eq. of the acid chloride **35** at 110°C in the presence of 0.05 eq. allylpalladium(II)chlorid and 0.09 eq. triethylphosphite as catalyst. GC-MS measurements of the raw product did not show product formation but the presence of benzoylgermanes and other not closer defined benzoyl compounds. The Pd catalyst probably caused a decarbonylation reaction like it is also described in literature.⁷⁵ Hence, the same reaction was tried at lower temperatures (65°C) to avoid decarbonylation but at these temperatures no reaction occurred at all. This was visible in no formation of elemental Pd and no product formation according to GC-MS measurements.

3.3.3.2. Synthesis in Analogy to Phenylglyoxylic Trimethylsilicium 31 (pathway B)

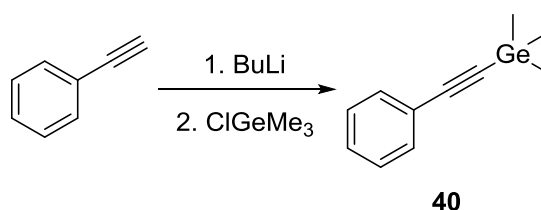
As already mentioned above Page et al describe the synthesis of the hydrolytically instable phenylglyoxylic trimethylsilicium **31**:⁷⁰



Since this is a common problem in silicium containing structures the idea was to substitute silicium with germanium. A higher stability could be expected like it is the case for Ivocerin compared to Si-benzoyls, which decompose under air because of their instability towards oxygen and moisture. It was tried to use the same synthetic pathway that works for silicium as germanium is also a group 14 element, which has a similar orbital configuration:

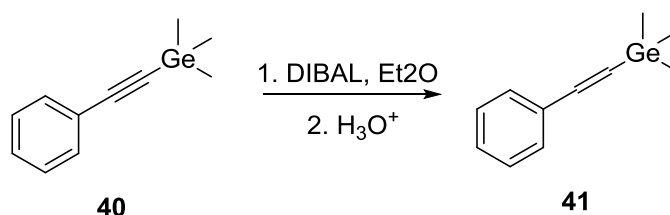


In a first step 2-phenyl-1-trimethylgermyl-2-ethyne **40** had to be synthesized from phenylacetylene and trimethylgermaniumchloride in an organolithium reaction:



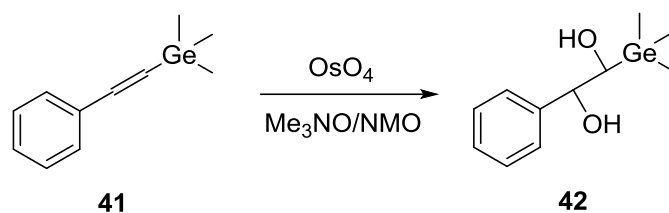
2-phenyl-1-trimethylgermylethine **40** is already known to literature⁷⁶ where it is made in a hydralumination reaction. Since it was tried to use the pathway of the Si compound **31** for germanium, the synthesis was done in this way. To a solution of 1 eq. phenyl ethyne in THF under an argon atmosphere at -78 °C a solution of 1.2 eq. butyl-lithium in hexane was added and the mixture was stirred at -78 °C for two hours. 1.2 eq. of trimethyl chlorogermane were added, and the reaction mixture was stirred at ambient temperatures for one hour. Quenching with saturated ammonium chloride solution and extraction with dichloromethane gave the raw product, which was purified via Kugelrohr distillation to get pure product in a yield of 51.6% as colorless oil.

In the next step the triple bond of the obtained product **40** was reduced with DIBAL (diisobutylaluminiumhydride) to yield Z-2-phenyl-1-trimethylgermylethene **41**. Also compound **41** is known to literature⁷⁷ and was prepared from germanium hydride and a corresponding bromine compound in an organolithium reaction. However, according to pathway B the next step in the reaction was as following:



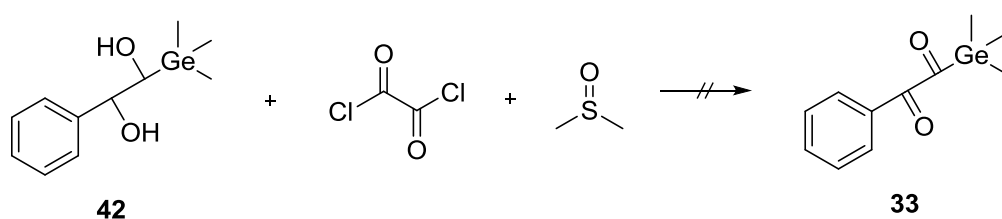
Therefore 1 eq. of 2-phenyl-1-trimethylgermylethine **40** and 1.5 eq. N-methylmorpholine dissolved in diethyl ether were mixed with 1.5 eq. diisobutyl aluminium hydride at ambient temperatures overnight. After quenching with 10% HCl and extraction with diethyl ether the raw product was purified via Kugelrohr distillation to obtain product **41** with >90% purity as colorless oil in a yield of 52%. The 10% starting material **40** in the purified product **41** were not possible to separate during work-up.

However, since the triple bond of the starting material **40** cannot be oxidized in the next step no further action was taken and the synthesis of the third step anti-2-hydroxy-2-phenyl-1-trimethylgermylethanol **42** was conducted:



It was tried to oxidize the double bond in the starting material Z-2-phenyl-1-trimethylgermylethene **41** with an $\text{OsO}_4/\text{Me}_3\text{NO}$ redox system. Unfortunately, the yield was very low. After some tries the best synthesis with a yield of ~3% was found: 1 eq. of Z-2-Phenyl-1-trimethylgermylethene was dissolved in tert-butanol, water and pyridine. 1.4 eq. Trimethylamine N-oxide dihydrate and freshly sublimated 0.02 eq. of osmium tetroxide were added to the solution. The resulting mixture was boiled under reflux under an argon atmosphere for twelve hours. The reaction mixture turned black during the reaction, indicating the formation of OsO_2 . Aqueous sodium bisulphite was subsequently used for quenching and extraction with dichloromethane in a continuous extractor gave the raw product, which contained <5% product **33** that was obtained in a total yield of ~3% estimated by GC-MS analysis. Due to the low amount of product and/or also potential instability it could not be isolated for further characterization. Distillation (Kugelrohr), recrystallization (CH_2Cl_2 , MeOH) and chromatography experiments with different solvents (CH_2Cl_2 , MeOH) and stationary phases (Florisil, SiO_2 , AlO_3) respectively always led to complete product decomposition, which means it was not detectable with GC-MS anymore. So it was tried to achieve a higher yield and therefore make the product isolation easier by repeating the synthesis once again but with NMO instead of Me_3NO as reoxidizing agent. NMO is the standard reoxidizing agent for oxidations with OsO_4 , which is a standard method in organic synthesis.⁷⁸ However, this led to no product formation at all.

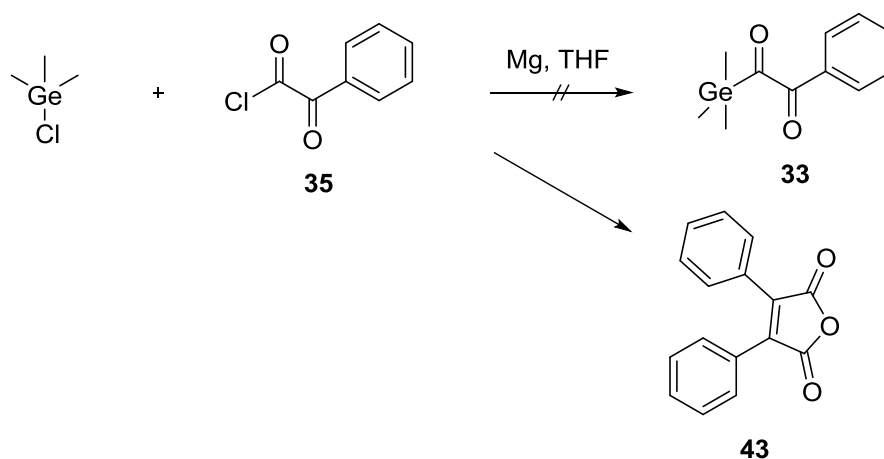
Since the few percent product could not be separated from the raw product the whole mixture was used for the last step of the synthesis looking for an easier separation after the last step:



A Swern-oxidation was carried out to oxidize anti-2-hydroxy-2-phenyl-1-trimethylgermylethanol **42** to phenylglyoxylic trimethylgermanium **33**. 4.4 eq. of oxaly chloride were dissolved in dichloromethane and at -60°C 4.4 eq. of DMSO was added. Afterwards 1 eq. of raw anti-2-hydroxy-2-phenyl-1-trimethylgermylethanol **42** was added and the mixture stirred for 30 min at -60°C. At this point a GC-MS of the reaction mixture showed no product formation. After addition of 2.9 eq. of trimethylamine the reaction mixture was warmed to ambient temperatures over a period of 45 min. Quenching with water and extraction with dichloromethane gave a residue wherein no product **33** could be found via GC-MS- or ¹H-NMR-analysis.

3.3.3.3. Synthesis via Grignard Reaction (Pathway C)

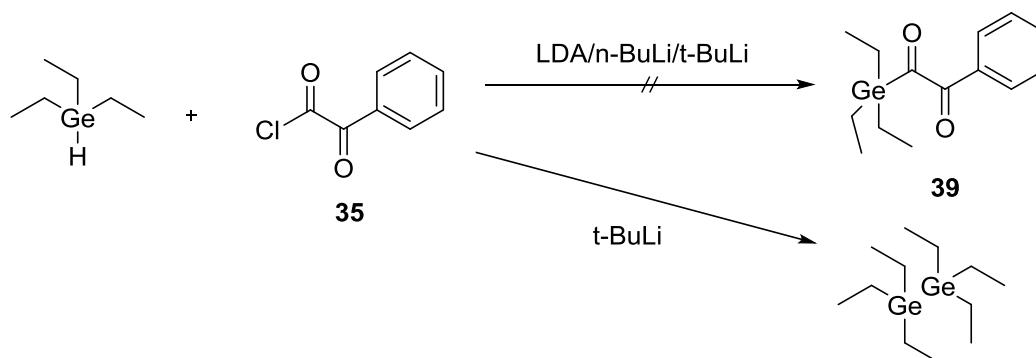
Another idea to get phenylglyoxylic trimethylgermanium **33** was a Grignard-type reaction. A Grignard reaction is a standard reaction in organic synthesis and Grignard reagents are usually of the type R₃CMgCl or R₃CMgBr. These Grignard reagents can be reacted with for example acid chlorides leading to the formation of MgCl₂ and ketones. In literature germanium Grignard reagents are described.⁷⁹ Herein it is also mentioned that the germanium Grignard reagents tend to react with themselves forming germanium dimers. For this reason they can only be used in-situ in a way that the germanium Grignard reagent is formed and immediately consumed by a reaction partner. This synthesis with phenylglyoxylic acid chloride is not described in literature but from a retrosynthetic point of view this pathway showed some potential, so it was tried out.



For this synthesis 1 eq. of Mg powder in THF was heated to reflux. 1 eq. of trimethylgermanium chloride and 3 eq. of phenylglyoxylic acid chloride dissolved together in THF were added. After 1 h the reaction mixture had turned red. It was stirred for 2 more hours, then the reaction was stopped and the solvent evaporated. The residue was partly soluble in Et₂O and the rest was soluble in CH₂Cl₂. After evaporation of the solvents the Et₂O fraction was obtained as orange solid and the CH₂Cl₂ fraction was an intensively red liquid. Both fractions were analyzed by TLC, GC-MS and ¹H-NMR. TLC and GC-MS showed a variety of not closer investigated peaks but ¹H-NMR showed no trimethyl germanium peak. At this point it was already clear that product **33** was not formed. Closer investigation showed as main peak on TLC and in GC-MS the undesired product **43**, which means the magnesium led to a reduction of the acid chloride. Since this product was unwanted it was not isolated or closer investigated.

3.3.3.4. Synthesis via Organolithium Reaction (Pathway D)

Alternative organometallic reactions to potentially obtain diketone germanium are organolithium reactions.⁷⁹ In this literature not only the germanium Grignard reagents were described but also reactions of germanium hydrides with organolithium reagents to yield the germanium lithium compounds, which can subsequently be reacted with for example acid chlorides to yield ketones like it was also already tried for the corresponding phosphorus compounds.

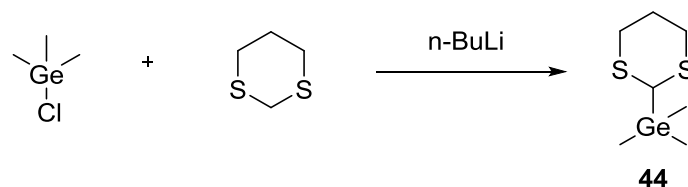


However, triethylgermanium hydride could not be deprotonated with LDA (lithium diisopropylamide) nor with n-BuLi (n-butyl lithium): 1.1 eq. of organolithium reagent

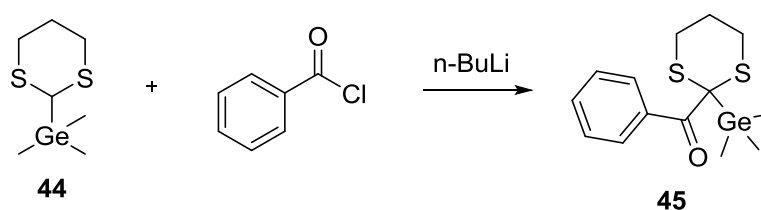
were added to 1 eq. of trimethylgermanium hydride in THF at -78°C and one time at 0°C . Subsequently 1.2 eq. of phenylglyoxylic acid chloride **35** were added. Toluene was added and the reaction was quenched with water. GC-MS of the organic phase showed only the starting materials or phenylglyoxylic acid respectively. As a result 0.9 eq. of *t*-BuLi as a stronger base were used but in this case the deprotonation reaction led to formation of hexaethyldigermene instead of the desired product. In GC-MS, TLC and HPLC analysis a variety of not closer investigated peaks could be found but the biggest one was according to GC-MS hexaethyldigermene. Since the desired product **39** could not be found, no further purification or characterization was done.

3.3.3.5. Synthesis via Seebach Umpolung (Pathway F)

A multistep Seebach diketone synthesis was also tried out.^{80,81} In the first step a Seebach reagent was made:

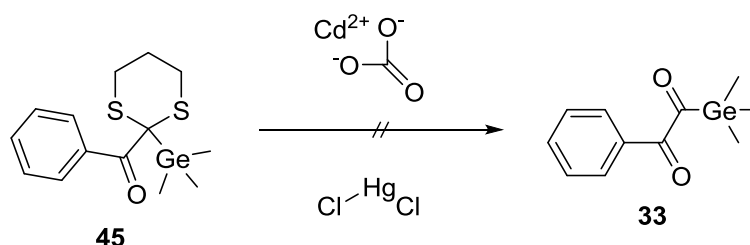


For synthesizing the Seebach reagent 0.95 eq. of 1,3-dithiane were deprotonated with 1 eq. *n*-BuLi in THF at -10°C and subsequently reacted with 1 eq. trimethylgermanium chloride at 0°C . Quenching with 2% HCl, extraction with diethyl ether and Kugelrohr distillation gave the product **44** with 37.5% yield as a colorless liquid. Afterwards this reagent **44** was deprotonated again with *n*-BuLi and reacted with benzoyl chloride:



For that 1 eq. of (1,3-dithian-2-yl)trimethylgermane **44** in THF at -15°C was reacted with 1 eq. of *n*-BuLi. This mixture was added to 0.95 eq. of benzoyl chloride in THF. After stirring for 3 h water was added and the resulting solution extracted with diethyl ether. Kugelrohr distillation of the raw product gave the product **45** with 23.1% yield.

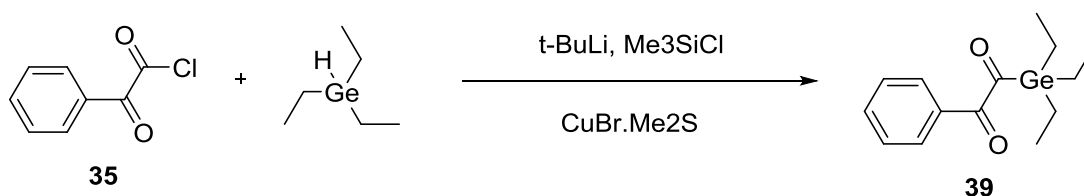
In the last step the dithiane protective group needs to be removed. There are several procedures available but the most efficient is usually stirring with CdCO_3 and HgCl_2 at elevated temperatures.⁸⁰ In case of a successful synthesis and since the photoinitiator is meant for biomedical applications these very toxic reagents could be substituted with CaCO_3 and I_2 but for this model reaction the most efficient way was used.



A slurry of 1 eq. phenyl(2-(trimethylgermyl)-1,3-dithian-2-yl)methanone **45**, 5 eq. of HgCl_2 and 5 eq. of CdCO_3 in THF and water was stirred for 8 h. No change in color of the reaction mixture occurred and GC-MS showed no product formation. So the reaction mixture was heated to reflux overnight. After 16 h still no change in color occurred and GC-MS analysis still showed no product formation. Additionally the starting material could not be detected anymore but a variety of peaks showing decomposition products were obtained. So at lower temperatures no reaction occurred at all within 8 hours and at reflux the starting material decomposed within 16 hours. This is in good accordance with literature, where a potential hydrolysis reaction of germanium and silicium dithianes is described.⁸¹ These observations in combination with what was known from literature led to the conclusion that another synthetic route will be necessary.

3.3.3.6. Synthesis with a Copper Intermediate (Pathway G)

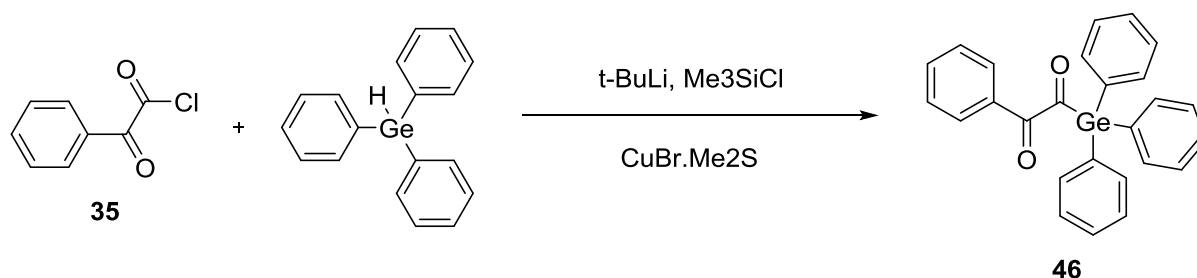
Piers and Lemieux describe another synthesis pathway where trimethylgermanium hydride was reacted with different acid chlorides via an intermediate copper reagent to yield a germanium ketone.⁸² The synthesis was modified because with the use of triethylgermanium hydride a liquid starting material can be used instead of the gaseous trimethylgermanium hydride. Additionally phenylglyoxylic acid chloride **35** was used instead of non-aromatic acid chlorides for the obvious reason of trying to get a diketone.



To 1 eq. of triethylgermanium hydride in THF at -10°C was added 0.85 eq. $t\text{-BuLi}$. Afterwards this was added to 0.85 eq. $\text{CuBr}\cdot\text{Me}_2\text{S}$ in THF at -78°C . Stirring at -78°C for 1 h resulted in a deeply red liquid. 0.55 eq. Me_3SiCl were used for quenching. Afterwards a solution of 0.55 eq. phenylglyoxylic acid chloride **35** in THF was added and the mixture turned black. The solution was stirred for 1 h at -78°C and for 2 h at -30°C . As a work-up the reaction mixture was poured in aqueous $\text{NH}_4\text{Cl}\text{-NH}_4\text{OH}$ (pH 8-9) und diluted with diethyl ether. The aqueous phase was extracted with diethyl ether. The deeply red and liquid raw product was purified via column chromatography, which yielded pure product **39**. It was identified with $^1\text{H-NMR}$ and GC-MS. The yield was with 6.4% very low and therefore the synthesis very inefficient but enough of the product could be obtained for a first characterization. However, further characterization was difficult and not done because of the low yield, the high price of the starting materials and the relative instability of the product **39**. It already decomposed after 3-4 days under argon atmosphere at 5°C , visible by complete decolorization and disappearance of the product peak in GC-MS measurements.

3.3.4. Synthesis of Phenylglyoxylic Triphenylgermanium 46 (Pathway G)

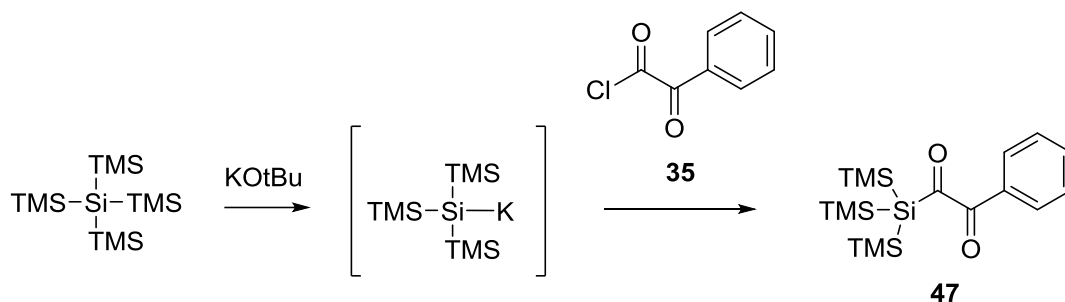
Since a pathway for the synthesis of germanium diketones was found, a second one with aryl moieties – phenylglyoxylic triphenylgermanium **46** – was synthesized in hope for a more stable product:



The synthesis was done in complete analogy to the synthesis described before for the triethylgermanium compound **39**. The yield was with 1.1% even lower than in the previous synthesis but still enough for some basic characterizations. Product formation was proven by $^1\text{H-NMR}$ analysis of the deeply red solid **46**, which was obtained after purification. Stability was even lower than for phenylglyoxylic triethylgermanium **39**. After 2 days under argon atmosphere at 5°C phenylglyoxylic triphenylgermanium **46** completely decomposed, visible by complete decolorization of the former deeply red solid and disappearance of the product peak in GC-MS measurements.

3.3.5. Synthesis of Phenylglyoxylic Trimethylsilyl Silicium 47 (Pathway H)

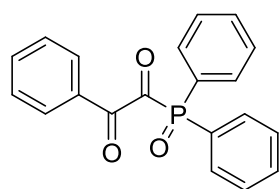
Since the silicium diketone compound **31** Page et al synthesized⁷⁰ was very instable another silicium compound with stability enhancing TMS (trimethylsilyl) moieties was synthesized according to literature:⁸³



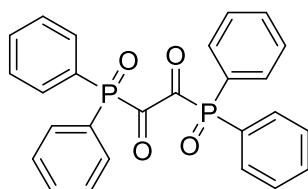
1 eq. of Tetrakis(trimethylsilyl)silan was dissolved with 1.05 eq. KOtBu in dimethoxyethane. The resulting solution was added to 1.05 eq. phenylglyoxylic acid chloride **35** in diethyl ether and cooled to -40°C . After complete addition the reaction mixture was allowed to warm to ambient temperature and stirred for another hour. Subsequently, HCl (3%) was added. The aqueous phase was extracted with diethyl ether. Column chromatography gave the pure product **47** in a yield of 33% as yellow oil. The stability of the product was even under argon atmosphere too low to conduct NMR measurements of over 15 min. The 40 min ^{29}Si -NMR and ^{13}C -NMR already show a variety of peaks. For this reason only ^1H -NMR spectra are given and for further characterization color and UV-VIS spectra were used respectively, which were obtained from freshly prepared Si-diketone **47**. A few hours old product **47** also showed bad and not interpretable results in ^1H -NMR measurements.

3.4. Characterization & Interpretation

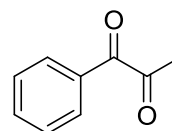
The first and most important characterizations for novel photoinitiators are UV-VIS- and photo-DSC-measurements to determine whether the absorption maximum is as desired in the visible light area or in the UV area and to determine the reactivity of the photoinitiator. Two phosphorus diketones, two germanium diketones and one silicium diketone were synthetically accessible. Those were compared to the reference **PPD** (phenylpropanedione):



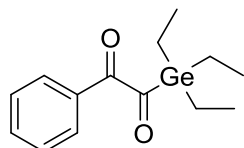
32



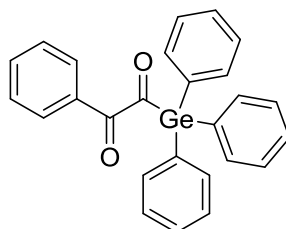
38



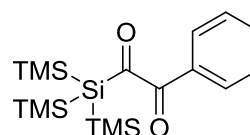
PPD



39



46



47

The germanium diketones **39** and **46** but especially the silicium diketone **47** needed to be freshly prepared for the following analysis to get reliable results. However, it should be kept in mind that the stability of these compounds is very low so even the results from the freshly prepared photoinitiators should be handled with care.

3.4.1. UV-VIS

UV-VIS-spectra were measured in dichloromethane with a concentration of 1×10^{-3} mol L⁻¹ (Figure 21, Figure 22 and Figure 23).

Phosphorus Diketones

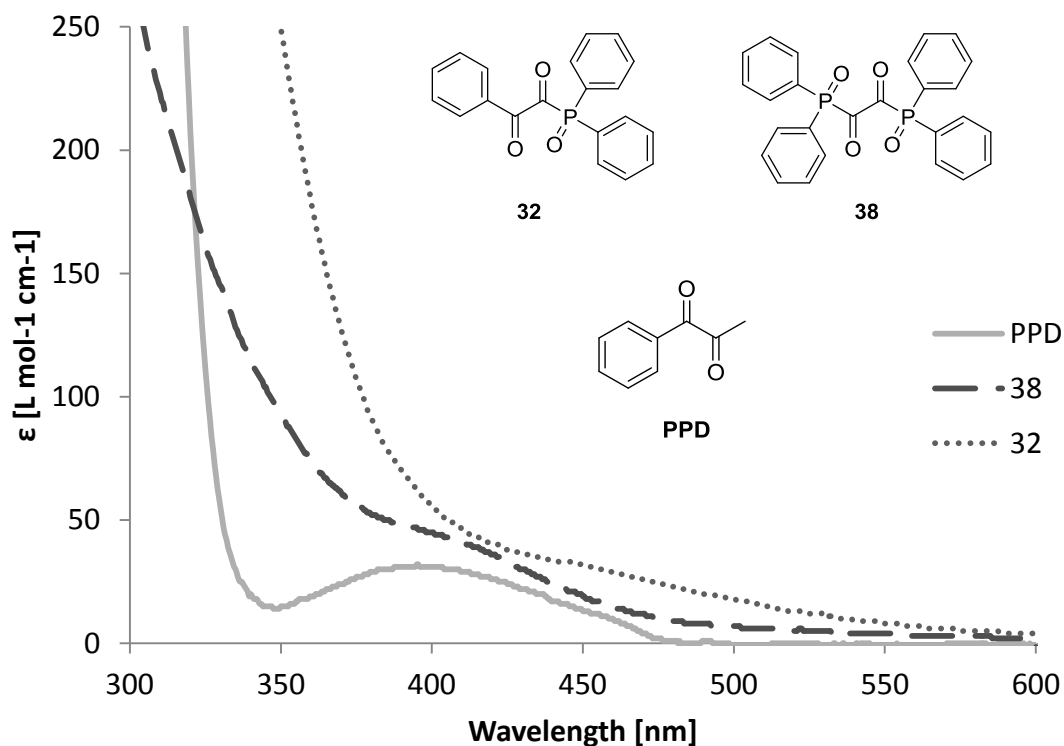


Figure 21. UV-VIS-spectra of the phosphorus diketones **32** and **38** with the reference **PPD** ($1 \times 10^{-3} \text{ mol L}^{-1}$ in CH_2Cl_2)

As can be seen from the UV-VIS spectrum of the phosphorus diketones (Figure 21) the concept of a bathochromic redshift via combining the redshift of two neighboring carbonyl groups with the redshift of d-orbital overlap works. Phenylglyoxylic diphenylphosphine oxide **32** ($\lambda_{\text{max}} = 450 \text{ nm}$) shows a redshift of approximately 50 nm compared to the reference **PPD**, which can be explained by the overlap of the empty phosphorus d-orbital with one carbonyl group.

The bisphosphine oxide compound **38** shows a lower absorption maximum of just 410 nm. The lack of the benzoyl chromophore most likely leads to this lower maximum. This is in good accordance with literature, where it is described that by introducing a benzoyl chromophore in an arbitrary structure a red-shift can be achieved.⁸⁴

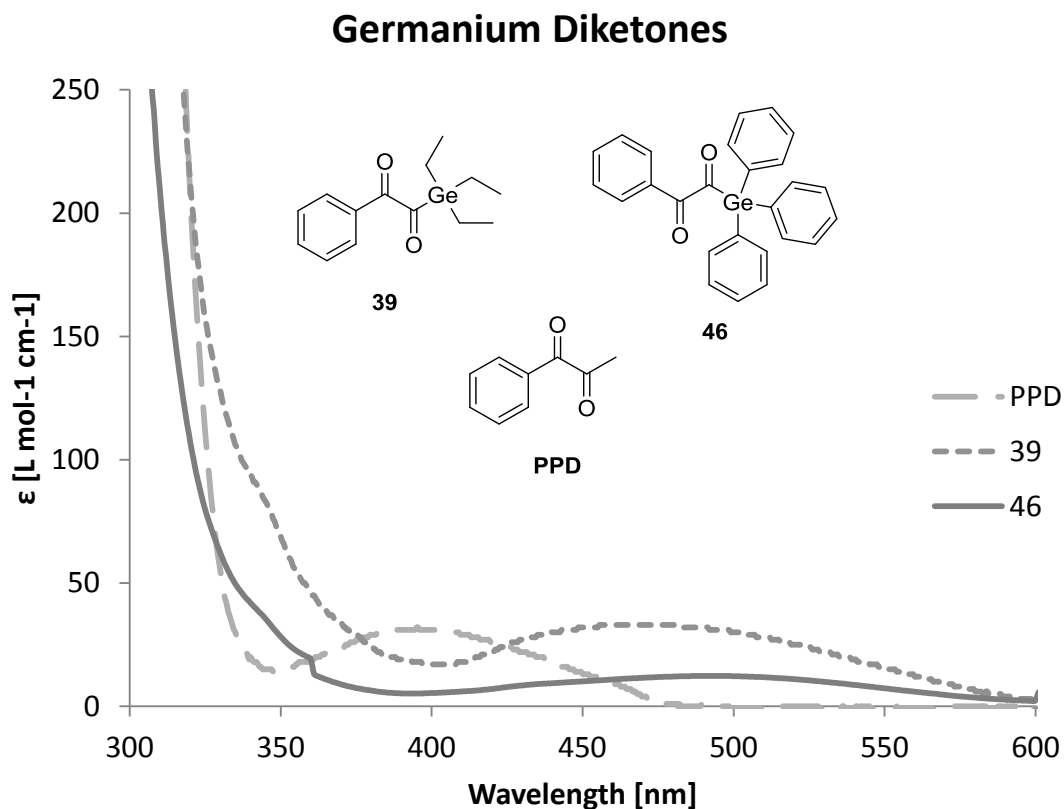


Figure 22. UV-VIS-spectra of the germanium diketones 39 and 46 with the reference PPD ($1 \times 10^{-3} \text{ mol L}^{-1}$ in CH_2Cl_2)

The germanium diketones (Figure 22) show an even higher absorption maximum than the phosphorus diketones (Figure 21). Phenylglyoxylic triethylgermanium has a λ_{max} of 470 nm, while phenylglyoxylic triphenylgermanium led to a higher redshift of 490 nm. The shift of 20 nm between the phosphorus compound **32** and the germanium diketone **39** fits with the difference between **BAPO** and Ivocerin. With introducing aryl groups in **46** a further shift of 20 nm occurs. Surprisingly, germanium diketone **39** shows the highest extinction coefficient even though no aryl groups are present at the germanium atom.

Silicium Diketones

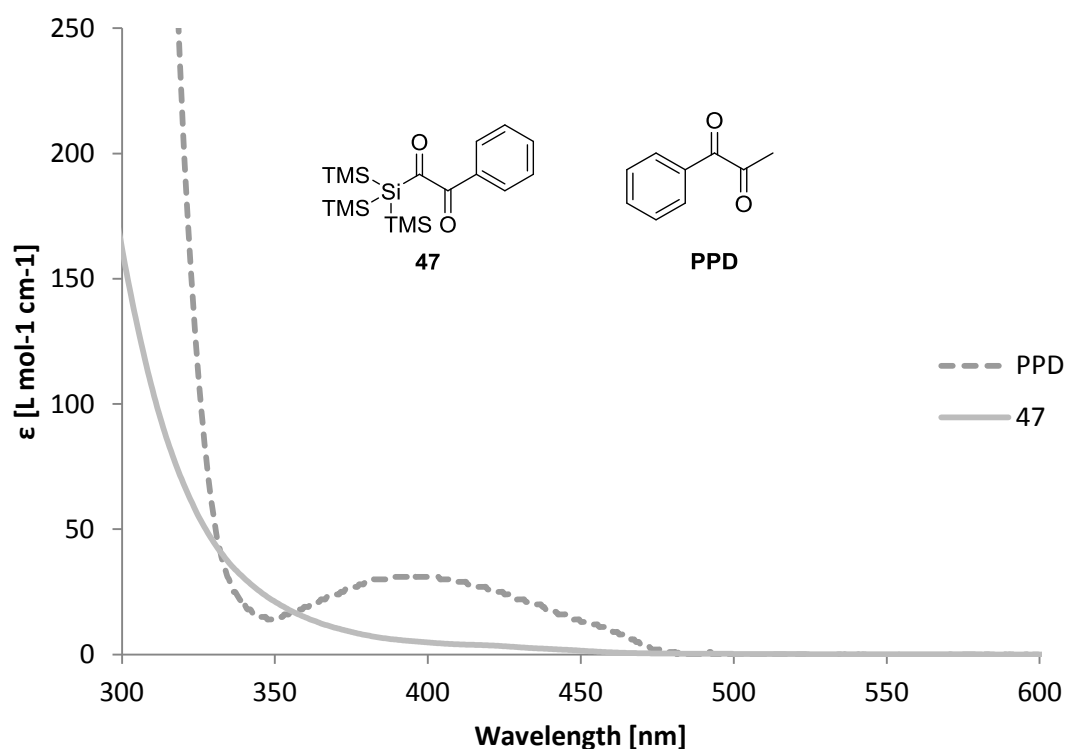
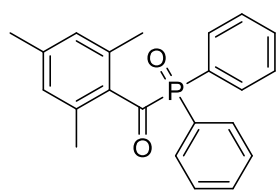
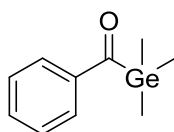


Figure 23. UV-VIS-spectra of the silicium diketone **47** with the reference PPD ($1 \times 10^{-3} \text{ mol L}^{-1}$ in CH_2Cl_2)

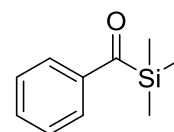
The silicium diketone **47** (Figure 23) shows the lowest absorption maximum of the newly described diketones ($\lambda_{\text{max}} = 420 \text{ nm}$). This comes as a surprise since it could be expected from already known acyl compounds²¹ that the silicium diketones would show an absorption maximum in the range of germanium diketones.



$\lambda_{\text{max}} = 394 \text{ nm}$



$\lambda_{\text{max}} = 412 \text{ nm}$



$\lambda_{\text{max}} = 416 \text{ nm}$

As already mentioned before, the silicium diketone is very unstable. So a possible explanation could also be that the results of the UV-VIS measurement got adulterated since the compound decomposed during or already before the measurements.

3.4.2. Photo-DSC

Photo-DSC measurements were carried out to determine the reactivity of the new diketone photoinitiators. Initiator concentration was 1 mol% in mixture B (UDMA:D₃MA = 1:1 m/m) with 1 equivalent **DMAB** as coinitiator. Mixture B was chosen because of its lower viscosity compared to mixture A and therefore better and easier solubility of the tested diketones. Range of irradiation was 400-500 nm since all compounds possess absorption maxima of their n—π*—transitions in this range. The results were as following (Figure 24):

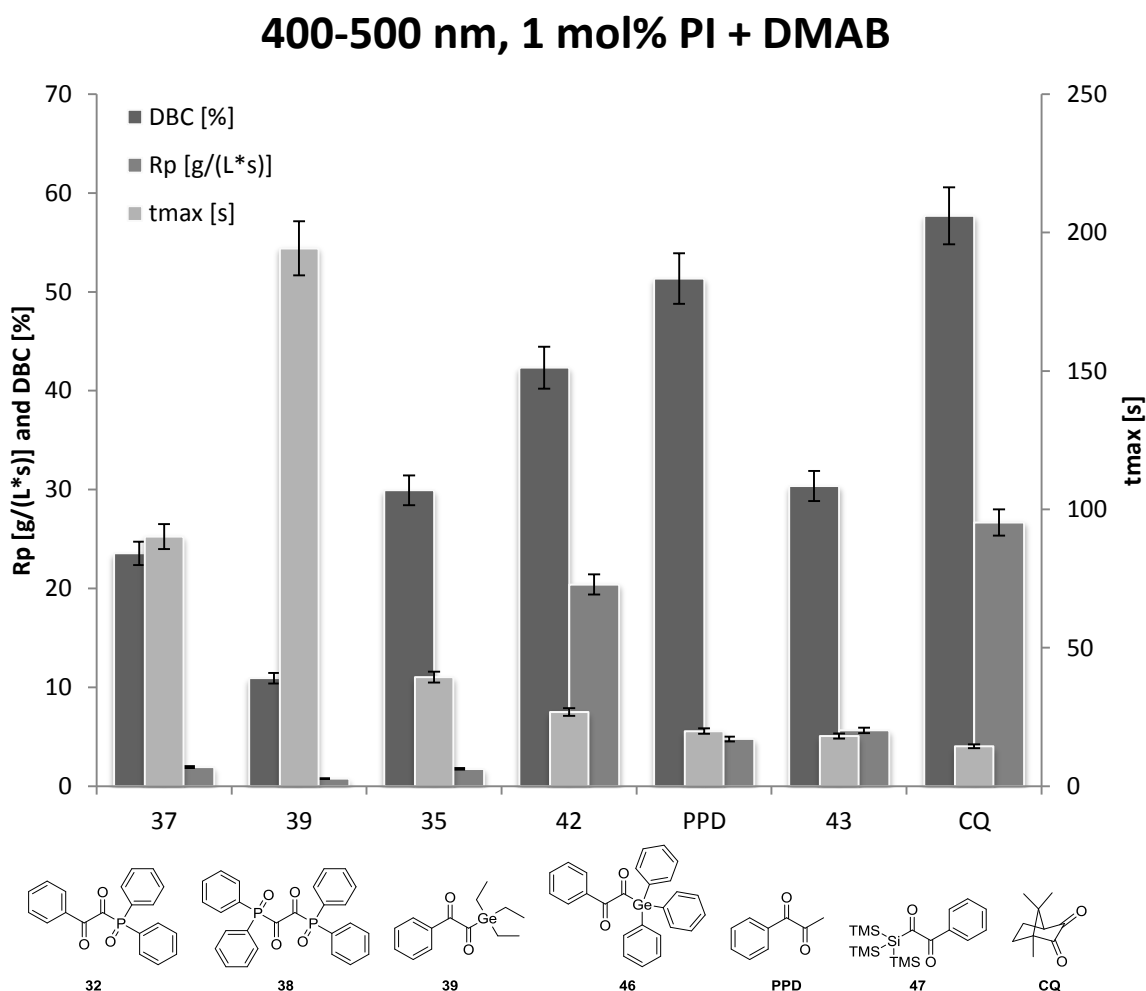


Figure 24. Photo-DSC results for the new diketone initiators (1 mol% in mixture B with equimolar DMAB and 400-500 nm irradiation)

As can be seen, the new diketone photoinitiators show reactivity worse than the reference **PPD**. The best of the new initiators is the phenylgermanium compound **46**

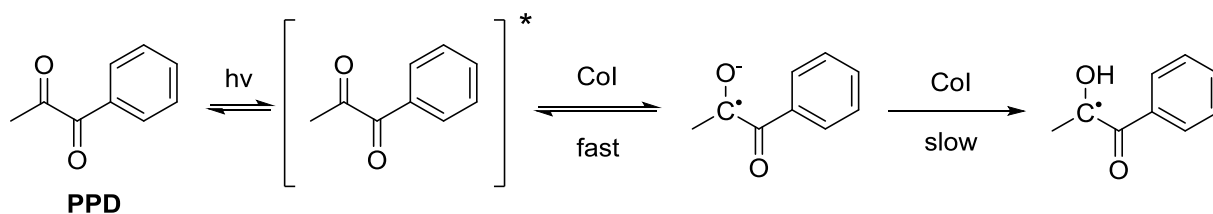
with a DBC (double bond conversion) of 42% and a t_{\max} (time until the maximum heat of polymerization is reached) of 26.8 s, which is almost as good as the reference. Only the rate of polymerization is with $20 \text{ g L}^{-1} \text{ s}^{-1}$ higher than the reference **PPD** but this has to be seen in a relation with the overall lower DBC. So germanium is actually a suitable heteroatom concerning reactivity and phenyl groups do not sterically hinder the initiation reaction. The germanium compounds lack of stability though and are therefore not applicable for a use as photoinitiators.

The bisphosphine oxide **38** was synthesized and characterized to find out more about the influence of the benzoyl chromophore in the other tested structures. The achievable reactivity is with a DBC of 10% and a t_{\max} of over 45 s extremely low. A benzoyl chromophore seems to be very important not only for a higher and more redshifted λ_{\max} but also for the reactivity of the system. Nevertheless is the reactivity of the phosphorus diketones (also for diphenylphosphine oxide **32**) much too low to be considered for an application as photoinitiator.

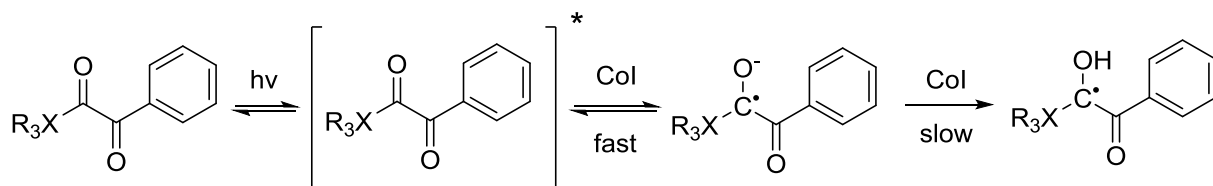
Silicium as a heteroatom turned out to be not suitable as well. Even though t_{\max} was for the silicium diketone **47** below the reference **PPD** the achievable DBC is with 30% very low. However, these results have to be once again handled with care since the silicium diketone was very instable. Of course the photo-DSC was measured with freshly prepared silicium compound **47** but decomposition reactions before or even during the measurements cannot be for sure excluded. Of course, also this instability is a K.O. criterion for an application as photoinitiator.

It was tried to find a reason for the unexpected low reactivity of the diketone systems compared to the reference **PPD**. Of course the following explanation only consists of theoretical thoughts since no further studies concerning the reaction mechanism were done. Even though this would be interesting, it was decided to focus on other projects since no revolutionary results could be expected from the diketone photoinitiators.

The reference **PPD**, which is much more reactive even though it has very similar structural features than the newly described diketones reacts under visible light irradiation as following.^{85,86}



The Mechanism adapted to the new diketones would look as following:



So the question can be reduced to why the substitution of the C-atom in **PPD** with a heteroatom like in the new diketones leads to a cut in reactivity of in some cases more than half. Three possible explanations are thinkable:

- The quantum yield for the transition from singlet ground state to triplet excited state is too low, leading to inefficient conversion of physical light energy to chemical energy and therefore inefficient initiation.
- Electron transfer from the coinitiator does not happen sufficiently since the new diketones already have electron rich heteroatoms and are therefore not enough electrophile.
- Back electron transfer to the coinitiator happens too fast because the C-radical is not stabilized enough by a neighboring heteroatom. This makes the H-transfer and subsequent active radical formation even less likely and reduces the reactivity.

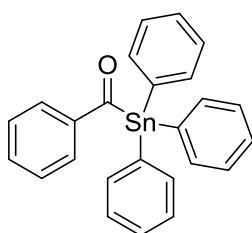
In the end the conclusion of the experiments with new diketone initiators can only be that the concept of achieving bathochromic redshift worked but the low reactivity remains a problem. It could not be solved by varying heteroatoms or substituents. The most likely reason is that the electron density in the system gets changed too much compared to the reference **PPD**.

4. Acyltellurides

4.1. State of the Art

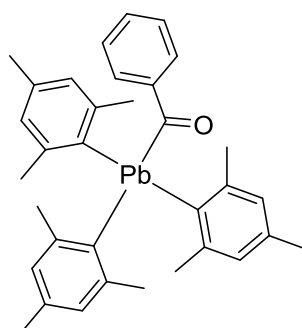
The initial idea for this part of the work was to introduce a new heteroatom next to a carbonyl group to achieve a red-shifted photoinitiator as it was already described before. Many acyl metal/metalloid compounds have been successfully synthesized and described in literature, but have not yet been tested as photoinitiators for radical polymerization.

According to Peddle,⁸⁷ an absorption maximum of 435 nm was detected for the $n-\pi^*$ transition in benzoyltriphenyl stannate.



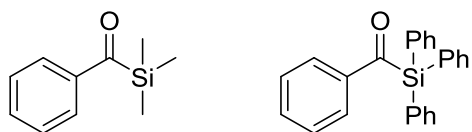
Generally, acyl stannanes are described as very sensitive to oxygen and moisture. Additionally, some of these compounds exhibit low thermal stability.⁸⁸

Acyl lead compounds are another class of these acyl metal structures. Generally, organolead derivatives are quite unstable, although the synthesis and successful characterization of benzoyltrimesityl lead led to a breakthrough.⁸⁹



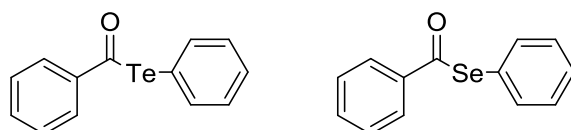
This compound is stable under air and the $n-\pi^*$ transition shows an absorption maximum at 448 nm.

Acyl silanes are also very interesting. The extraordinary absorption properties of this class of compounds were insistently discovered by Brook et al.⁸¹



Absorption maxima referring to the $n-\pi^*$ transitions are located far above 400 nm. In competition to the α -cleavage reaction, a siloxycarben could be formed reversibly. Generally acyl silanes, excluding benzoyltriphenyl silane, are not very stable, because even air moisture causes hydrolysis of these compounds.

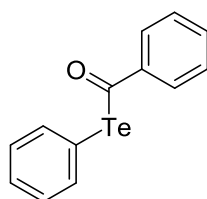
Photochemical studies on benzoylphenyl selenide and benzoylphenyl telluride showed, that these compounds formed radicals after irradiation (300 nm).⁹⁰ A full absorption spectrum of these compounds was not available.



Bond cleavage occurred always between the carbonyl-C and the selenium/tellurium atom leaving a benzoyl radical and a phenyl selenide/telluride radical behind. Since selenium compounds are known to be very toxic they are not very interesting for an application in dentistry. For this reason the acyl tellurides were first objects of closer investigation.

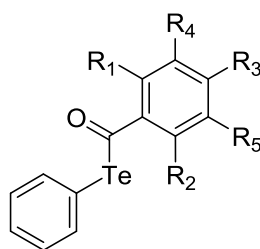
4.2. Syntheses

The goal of the conducted syntheses was to introduce a highly reactive benzoyl chromophore next to a tellurium heteroatom as in compound **BPT** to get a red-shifted photoinitiator, which is suitable for dental applications.



BPT

That means mainly high reactivity, stability, photobleaching and low toxicity. Stability or reactivity was not checked in literature so in case of issues with these properties the benzoyl chromophore can also be modified for example the same way it was done in the case of mono- and bisacylphosphine oxides, where mesityl instead of benzoyl was used to stabilize the compound. Since the goal was to screen potentially available acyl tellurides for the most reactive and stable ones a set of compounds should be synthesized with different moieties.

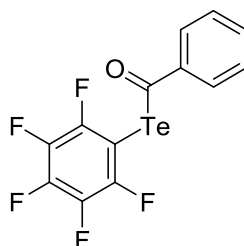


48 R₁₋₂ = O-CH₃, R₃₋₅ = H;

49 R₁₋₃ = CH₃, R₄₋₅ = H

50 R₁₋₅ = F

Fluorine gives a very strong electron withdrawing effect and can protect the carbonyl group from a nucleophilic attack via hydrophobic interactions. Methoxy groups can donate electrons and potentially increase the reactivity of the system. Methyl groups were, as already mentioned, used successfully in acylphosphine oxides for steric hindrance.



51

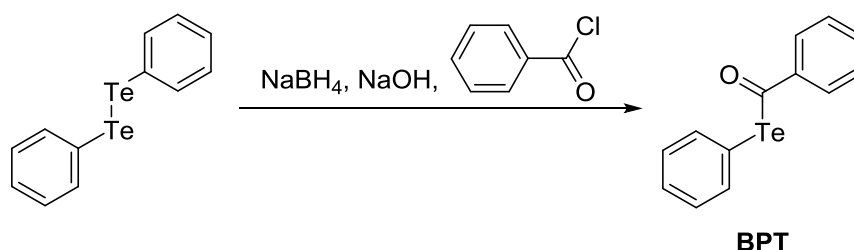
Additionally the aromatic ring at the side of the tellurium atom offers modification possibilities. The idea was to introduce also here electron donating or withdrawing

groups to check the effect on stability and/or reactivity. To test if a modification on this side of the compound is possible pentafluoro phenyltelluride **51** should be synthesized as a first compound.

4.2.1. Synthesis of benzoyl phenyltelluride BPT

4.2.1.1. Synthesis with a NaBH₄/NaOH Redox-System

The most basic structure benzoyl phenyltelluride **BPT** can be found in literature and was synthesized according to the given scheme.⁹¹

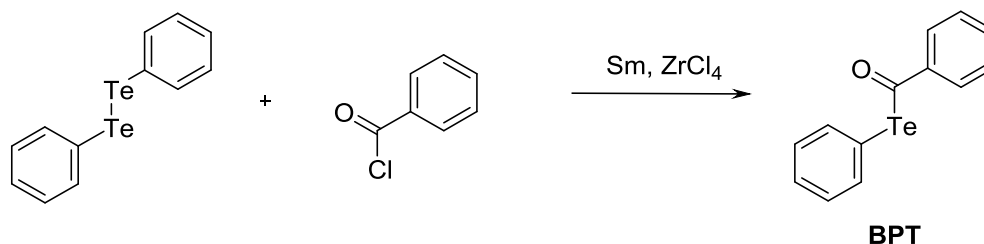


Herein 1 eq. of diphenyl ditelluride in toluene and ethanol (25/75 v/v) were heated to reflux. To this solution 0.8 eq. NaBH₄ dissolved in 1N NaOH was added. During the addition there appeared a strong formation of H₂ and the solution became colorless. Afterwards, 1.22 eq. of benzoyl chloride were added. Water was used to quench the reaction and the mixture was extracted with diethyl ether. The crude product was purified via liquid chromatography to yield pure **BPT** with 74% yield as yellow powder. However, stability was not perfect. Under atmospheric conditions at 5°C it started to decompose slowly within a few days, visible in a color change to black, indicating the formation of elemental tellurium.

Since benzoyl chloride is rather hydrolytically stable this synthetic pathway can be chosen even though it involves an aqueous and alkaline reduction system. The yield is very high nevertheless. For other acid chlorides with substituents on the aromatic system another synthetic route is necessary because it turned out, those acid chlorides are not hydrolytically stable enough. Mesityl chloride for example immediately decomposed in contact with water, visible in a strong exothermic reaction.

4.2.1.2. Synthesis with a Sm/ZrCl₄ Redox-System

For the more instable acid chlorides a different route is described in literature.⁹² Zhang et al found a very general route for a variety of telluroesters with for example methyl or methoxy groups, using diphenyl ditelluride and the corresponding acid chloride.

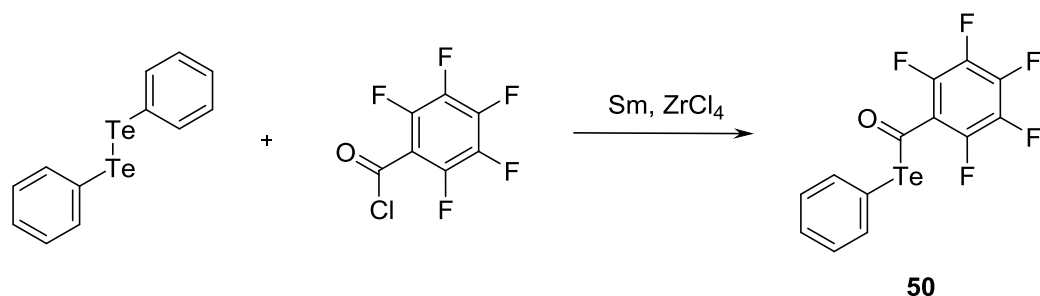


The feasibility of this method was tested with synthesizing benzoyl phenyltelluride **BPT**, which was already shown to be a quite stable and isolatable compound in the previous synthesis. The general reaction pathway for this synthesis and the ones conducted subsequently on the same pathway was as following: 1 eq. of Samarium, 1 eq. of diphenyl ditelluride and 0.2 eq. of zirconium tetrachloride were dissolved in THF. The mixture was stirred for 2 h at room temperature undergoing a change in color from red to brown, indicating the reduction of the bond between the two tellurium atoms. Then, 1.5 eq. of acid chloride (benzoyl chloride in case of **BPT**) were added to the mixture rapidly. The reaction mixture was stirred for 1 h at ambient temperatures, followed by the evaporation of the solvent applying vacuum. Dichloromethane was added to the gray/black precipitate and stirred for 30 min to dissolve the product. After filtration, the solvent was evaporated giving the crude product, which was purified using liquid chromatography. Yield for **BPT** was 22%.

4.2.2. Synthesis of Pentafluorobenzoyl Phenyltelluride 50

After the synthesis pathway was checked, first the fluorine moieties were introduced because the idea was to stabilize **BPT** with the hydrophobic interactions caused by the electron withdrawing effect of fluorine moieties. With that it was hoped to prevent

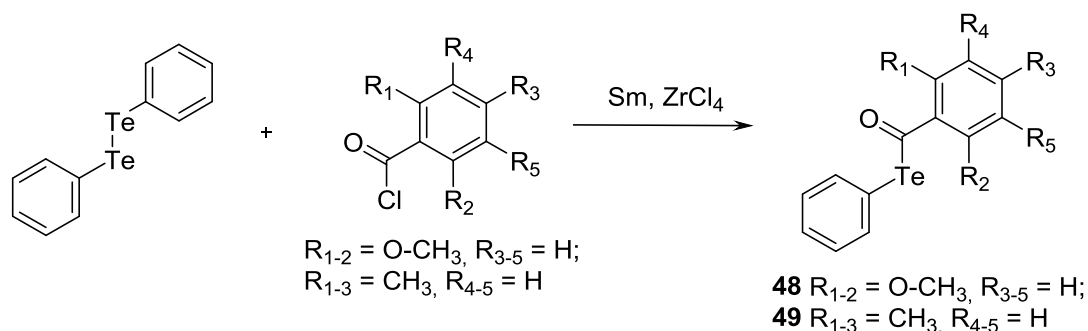
a nucleophilic attack on the carbonyl C. The general procedure described above and in literature was used.⁹²



The synthesis gave the product **50** in a yield of 49%. Unfortunately also this compound, like **BPT**, was not completely stable under air (stability for 2-3 h) but under argon it could be stored for ~1.5 weeks.

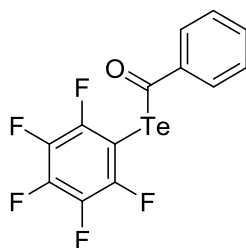
4.2.3. Synthesis of Mesityl and Dimethoxybenzoyl Phenyltelluride **48** and **49**

The synthesis was again conducted the same way as described above and in literature.⁹²



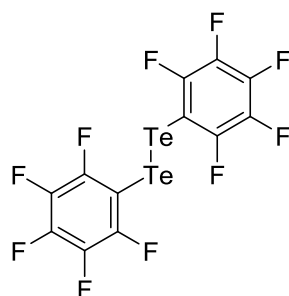
The Sm/ZrCl₄ reduction system works in water-free environments. Work-up however is conducted in a slightly acidic aqueous environment, which leads to immediate decomposition of the very instable mesityl- and dimethoxybenzoyl-compounds **48** and **49** indicated by a loss of color and black precipitate formation. Product formation in the reaction mixture could be shown via GC-MS analysis (molecule peak and typical fragments) but hence their instability they are not interesting for an application as photoinitiators and it was not tried to find other syntheses routes where they could have potentially been isolated.

4.2.4. Synthesis of Benzoyl Pentafluorophenyltelluride 51



51

To find out more about the substituent effect also on the aromatic ring that belongs to the Te atom the idea was to synthesize the fluorinated compound **51** as a first structure. It should be tried to use the same syntheses as before with a Sm/ZrCl₄ redox-system but with a different ditelluride **52**.

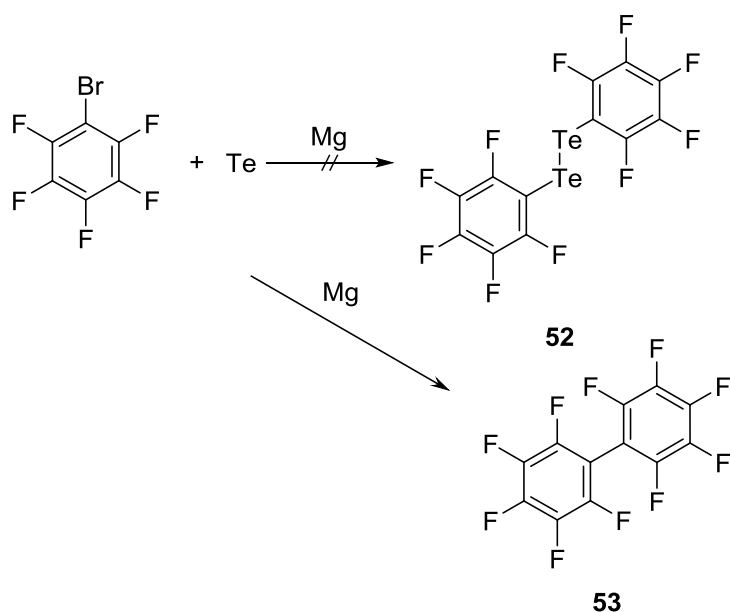


52

Since it is not commercially available, it had to be synthesized.

4.2.4.1. Grignard-Type Reaction

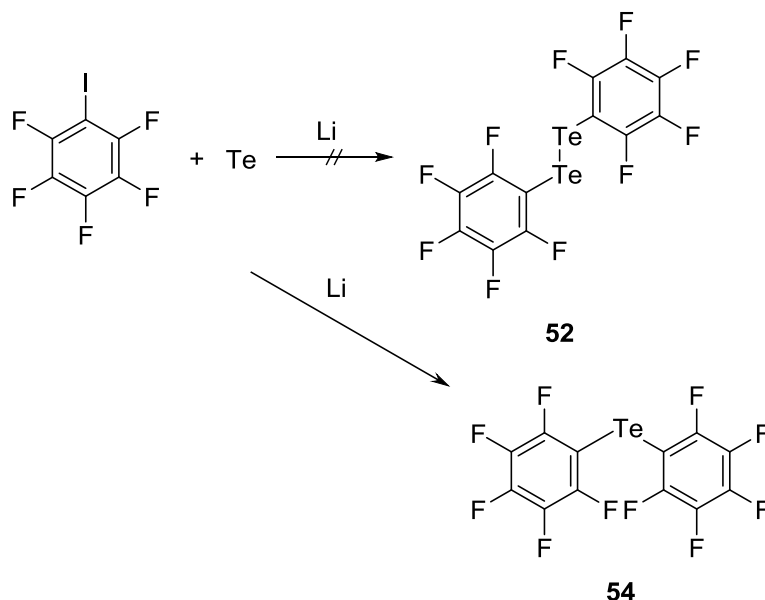
Literature provides for example a Grignard-type reaction of the corresponding bromides with elemental tellurium.⁹³ The fluoro-compound is directly described here so it was used as a first structure to check this pathway.



For synthesis 2.5 eq. of magnesium powder were added to THF. 1 eq. of bromopentafluoro benzene was added and after stirring for 3 h, 2 eq. of elemental tellurium were added. Afterwards the reaction mixture was quenched with water and filtered. The filtrate was extracted with diethyl ether. After evaporation of the solvent GC-MS measurements of the residue were done, which showed no product **52** formation but instead mostly potential side product **53** was formed. This was visible in the molecule peak and characteristic fragments and occurs when the Grignard-reagent reacts again with the starting material.⁷³ Since this side product was undesired it was not isolated, further characterized or quantified. Instead another synthetic pathway with the same goal was tried.

4.2.4.2. Organolithium Reaction

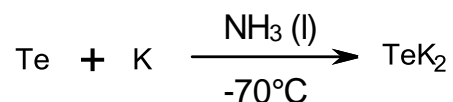
Another organometallic reaction that is described in literature uses elemental tellurium, lithium and the corresponding iodine.⁹⁴



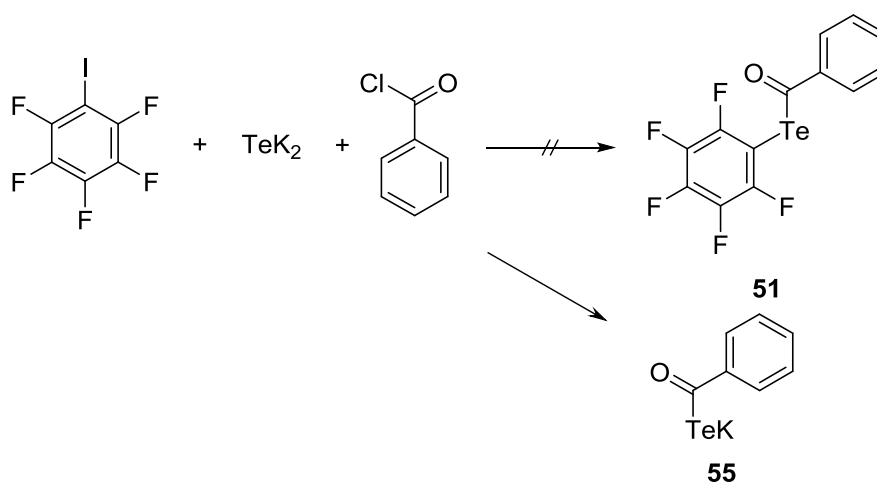
It was hoped that with the more reactive iodine and with the more reactive lithium a successful synthesis will be possible. Therefore 1 eq. iodopentafluoro benzene, 1 eq. elemental tellurium and 2 eq. of elemental lithium were dissolved in THF. The reaction mixture was stirred at ambient temperatures until the lithium was completely dissolved (18 h). Afterwards, it was quenched with saturated ammonium chloride. Extraction with diethyl ether and evaporation of a solvent gave a residue that was analyzed with GC-MS. The product **52** could be detected in traces via GC-MS in the reaction mixture (molecule peak and characteristic fragments visible) but a work-up was not conducted since almost exclusively the undesired monotelluride **54** was formed that could also be seen by the molecule peak and characteristic fragments. So another way was tried out.

4.2.4.3. Synthesis from TeK₂

After a substituted ditelluride could not be successfully synthesized with the pathways described above (Grignard and organolithium) another approach was chosen. In literature a route⁹⁵ is described that starts from potassium telluride, which was prepared according to known procedures:⁹⁶



In a Birch reduction with 1 eq. elemental tellurium and 1 eq. of elemental potassium TeK₂ was prepared. The potassium telluride was subsequently tried to be reacted with iodopentafluoro benzene and benzoyl chloride as it is described in literature for iodoalkanes and -alkenes:⁹⁵



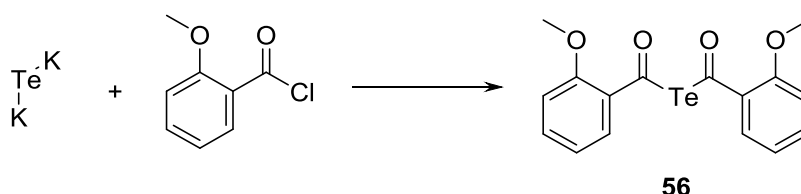
Therefore 1.5 eq of TeK₂ were added to MeCN. The slurry was cooled to 0°C and 1 eq. of benzoyl chloride was added. The color of the reaction mixture changed to black and it was stirred for 2h at 0°C. Afterwards the black precipitate was filtered and the solvent evaporated. To the resulting red oil 7 eq. of iodopentafluoro benzene were added and stirred overnight. Diethyl ether was added and after stirring for 15 min at ambient temperatures the precipitate was filtered off. A product in form of red oil was obtained. Subsequent GC-MS measurements showed unreacted potassium benzoyltellurate **55** (molecule peak and characteristic fragments). So it can be assumed that aromatic iodides are not reactive enough for this reaction pathway that did not lead to the desired product **51**, but instead the reaction stopped at the stage

of the theoretical intermediate potassium benzoyltellurate **55**. Further characterization or purification was not done because the desired product was not accessible via this pathway.

In general, it has to be said that the fluorinated aromatic bromine and iodine compounds seemed to be not reactive enough to form a substituted diphenyl ditelluride. Since no aromatic tellurium compounds with other substituents than fluorine could be found in literature the focus of the screening was switched to the bisacyl tellurides as another class of compounds. This was possible because TeK_2 as a starting material was now available.

4.2.5. Synthesis of Bis(2-methoxybenzoyl)telluride **56**

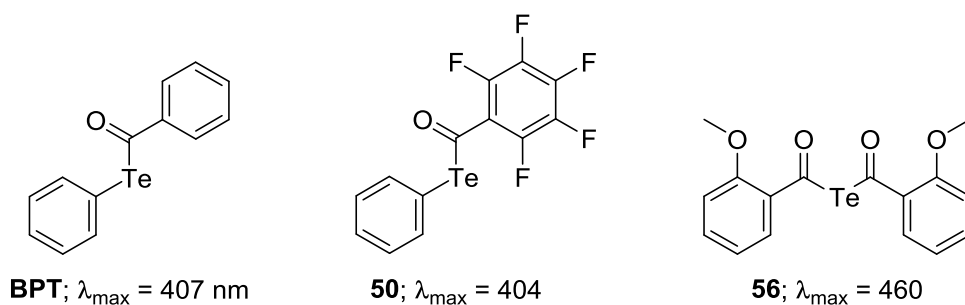
This new and fresh approach can be found in literature where the synthesis of bis(2-methoxybenzoyl)telluride **56** is described.⁹⁷ As a bisacyl compound it was synthesized to get a deeper insight in the properties of acyl tellurides. It was hoped to achieve higher stability or higher reactivity with them and of course it was tried to have a more complete screening.



Therefore 1 eq. of potassium telluride was added to acetonitrile and cooled to 0°C. Then, a cooled solution of 2.5 eq. 2-methoxybenzoyl chloride in acetonitrile was added slowly to the potassium telluride suspension. After that, the reaction mixture was stirred for 3 hours at 0°C. Acetonitrile was removed and diethyl ether was added, before stirring for another 45 min. The black precipitates were removed by filtration, giving a yellow filtrate. Diethyl ether was then largely removed, followed by washing with n-pentane. Vaporization of solvent residues gave the product bis(2-methoxybenzoyl)telluride **56** with 58% yield. The product was stable under argon atmosphere but decomposed under air within several hours and in solution under atmospheric conditions almost immediately.

4.3. Characterization

In the end benzoyl phenyltelluride **BPT**, its fluorinated derivate **50** and the bis-compound **56**⁹⁷ were synthetically accessible, isolatable and available for further characterization.



Since the bis(2-methoxybenzoyl)telluride **56** was not stable under air and insoluble and instable in methacrylic monomer mixtures no further studies were made with it. UV-VIS spectra were measured and Benzoyl phenyltelluride **BPT** showed an absorption maximum at 407 nm, was stable under air and showed good solubility in the monomer mixtures. Same goes for the fluorinated compound **50**, which showed less stability under air but still enough (stability for 2-3 h) for some preliminary tests. The absorption maximum could be found at 404 nm so photo-DSC measurements were done at 400-500 nm irradiation to determine the reactivity of the compounds (Figure 25 and Figure 26). Two separate measurements were done, so also the reproducibility of the photo-DSC measurements is clearly visible. Initiator concentration was 0.5 wt% in mixture A (UDMA:D₃MA:bis-GMA = 1:1:1 m/m). Irradiation intensity was 3 W/cm².

Pentafluorobenzoyl Phenyltelluride 50

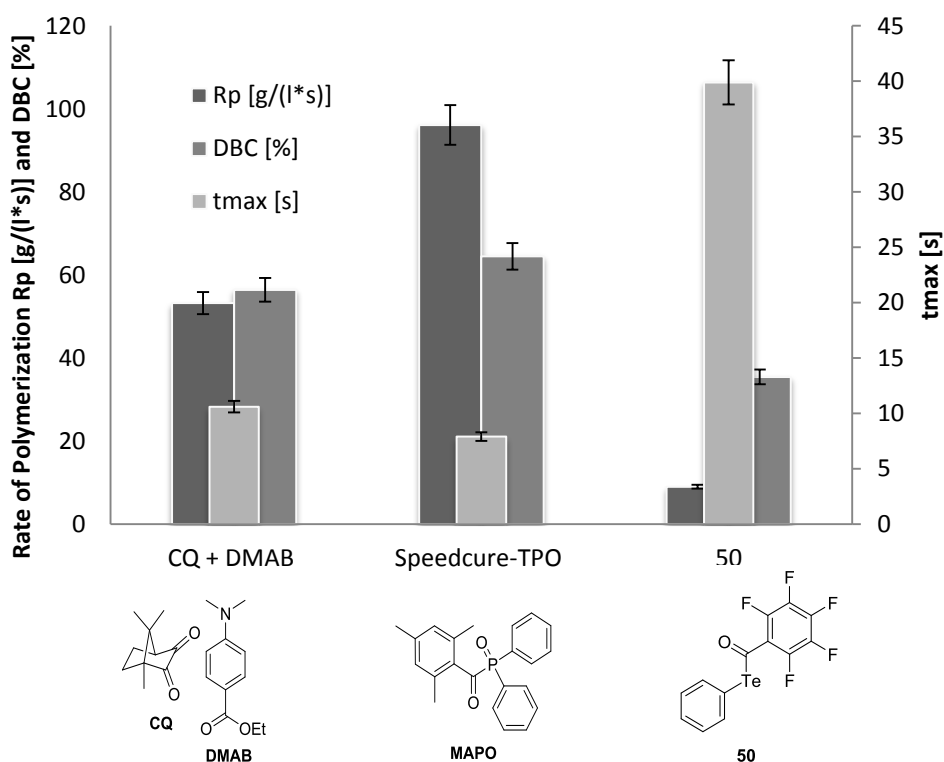


Figure 25. Photo-DSC results for pentafluorobenzoyl phenyltelluride 50 (0.5 wt% in mixture A and 400-500 nm irradiation)

Benzoyl Phenyltelluride BPT

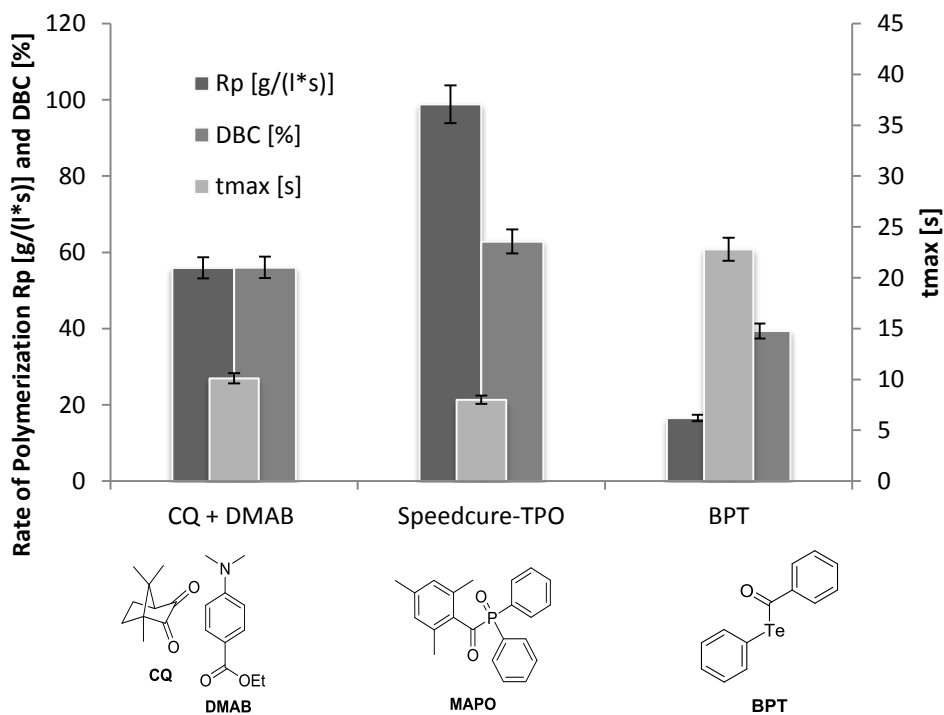
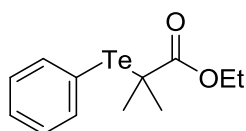


Figure 26. Photo-DSC results for benzoyl phenyltelluride BPT (0.5 wt% in mixture A and 400-500 nm irradiation)

Based on these preliminary results pentafluorobenzoyl phenyltelluride **50** was discarded as possible candidate for an application in dental materials. The reactivity is with a t_{\max} of 40 s much too low. Even though the DBC is with about 40% in a similar range for both compounds, the rate of polymerization for the fluorinated compound **50** is only approximately half of **BPT**. Furthermore the stability was not high enough. After only a few hours in the monomer formulations the compound started to visibly decompose.

In general the reactivity of both the fluorinated compound **50** and **BPT** were much lower than expected. This came as a surprise but literature research showed a very recently published paper from Nakamura,⁹⁸ where the organotellurium compound ethyl 2-phenyltellanyl-2-methylpropionate was used for controlled radical polymerization under visible light.



ethyl 2-phenyltellanyl-2-methylpropionate

This method called TERP (tellurium mediated controlled radical polymerization) was the explanation for the low reactivity since the control of the reaction leads to a loss of speed. In general this control was very interesting not only for dentistry but even more for other applications involving controlled living polymerization. For this reason some basic investigations were done to test the potential of **BPT** as a TERP reagent.⁹⁹

4.4. TERP – State of the Art

To understand TERP it is necessary to understand the basics of controlled radical polymerization. There are three classical ways to achieve controlled living radical polymerization (CRP): Atom transfer radical polymerization (ATRP), which reacts according to an atom transfer mechanism;¹⁰⁰ Nitroxide-mediated polymerization (NMP) with a dissociation-combination mechanism;¹⁰¹ and reversible addition fragmentation chain transfer (RAFT), which is based on degenerative transfer.¹⁰²

These methods are well known and in use for various applications, such as drug delivery systems, synthesis of complex polymer architectures (Figure 27) and others.¹⁰³⁻¹⁰⁵

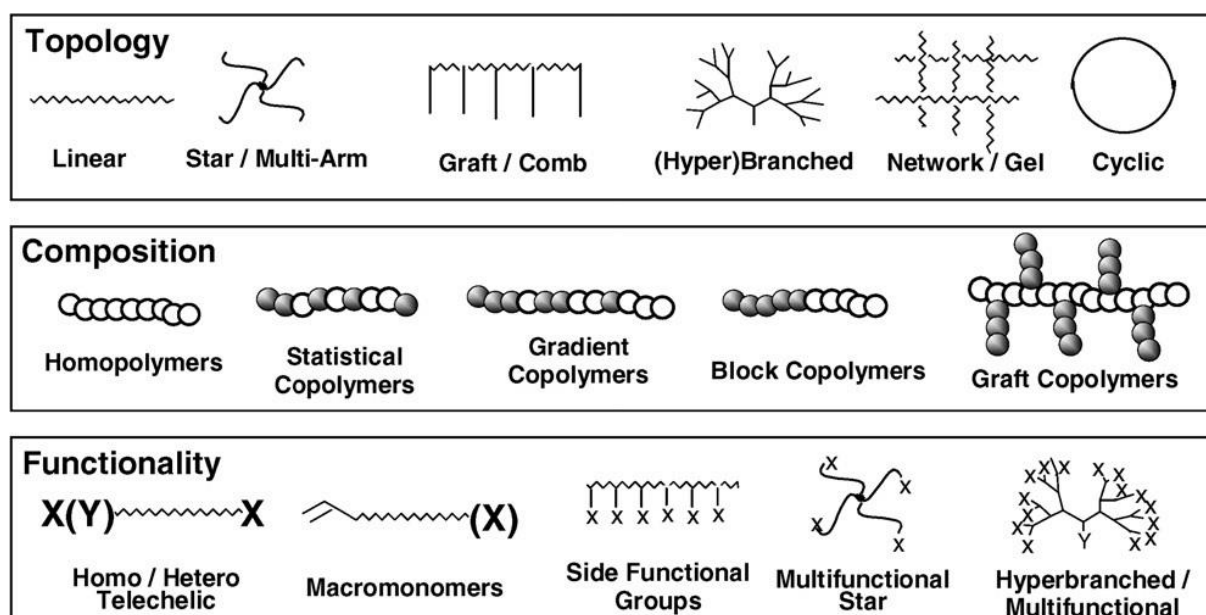
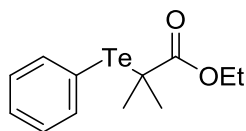


Figure 27. Complex polymer architectures that can be achieved with controlled radical polymerization.¹⁰⁶

To ensure a linear increase of the molecular weight with ongoing monomer double bond conversion and a narrow molecular weight distribution, the concentration of active radicals has to be kept low to avoid unwanted radical-radical recombination reactions. While control is the main advantage, the main disadvantage is reduced reactivity and as a result a long reaction time (usually several hours). Furthermore the classical living systems are usually thermally initiated, which provides less spatio and temporal control in comparison to photochemical systems. To provide better control, photoiniferters function as initiators that allow controlled living polymerization.^{107,108} These systems are capable of behaving as photoinitiator, transfer agent and polymerization control agent in one single compound and react based on a dissociation-combination mechanism. Applications for photoiniferters include synthesis of complex polymer structures (e.g. surface grafted polymers), photolithography, photografting and so on.¹⁰⁹⁻¹¹² Especially for applications where a narrow polydispersity is beneficial, photoiniferters should be considered. One disadvantage though is the higher polydispersity (PDI) obtained by the use of photoiniferters (1.5 for the best ones reported so far)¹¹³ in comparison to thermal control agents (1.1-1.4).¹⁰⁸

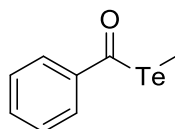
To date only a few compounds have been reported in literature, which show the ability to function as photoiniferters.^{107,114-118} Most of these compounds are based on a dithiocarbamate structure like for example benzyl dithiocarbamate **BDC**. These photoiniferters are only active in the UV-region, although many absorb up to 500-600 nm. This limits the use of photoiniferters to applications where UV-light isn't considered problematic, but even there, special light protection is usually required along with other problems that are to overcome.¹¹⁹

Recently new and alternative methods to achieve controlled radical polymerization were reported. Reversible chain transfer catalyzed polymerization and cobalt-mediated radical polymerization are only two of them.^{120,121} Important for this work is the organotellurium-mediated controlled radical polymerization (TERP).^{122,123} TERP has been established as a powerful method to achieve controlled radical polymerization, but most of the TERP-reagents still require additional thermal initiation and/or temperatures above room temperature. An exception is the photolabile TERP reagent (ethyl 2-phenyltellanyl-2-methylpropionate),¹²⁴ which allows reasonable molecular weight polymer with low polydispersity.



ethyl 2-phenyltellanyl-2-methylpropionate

The positive characteristics of the already mentioned organotellurium compound ethyl 2-phenyltellanyl-2-methylpropionate can be combined with the reactivity of a benzoyl chromophore. It is worth mentioning that a similar compound (benzoyl methyltelluride) has already been described in literature as a thermal TERP-reagent.



benzoyl methyltelluride

It is claimed in literature without giving specific values that this compound showed poor control abilities because of the high C-Te-bond dissociation energy, which should be lower in the case of an aryl substituent on the Te atom.¹²⁵

4.5. Characterization of BPT as TERP Reagent

Benzoyl phenyltelluride **BPT**, which was the most stable and therefore most interesting compound, was now characterized in detail. It was compared to the most relevant photoiniferter from literature benzyl dithiocarbamate (**BDC**).^{107,114-116} The comparison to a photoiniferter makes more sense than the comparison to other TERP reagents, since TERP reagents behave very similar to photoiniferters when they are used as photoinitiator instead of thermal initiator.¹²⁴ This applies especially to the mechanism. While in thermally initiated TERP a degenerative transfer mechanism is exclusively responsible for the control abilities, in photoinduced TERP a dissociation-combination is assumed to play also an important role, although degenerative transfer still occurs as a competing reaction.¹²⁶ This is also the case for photoiniferters even though the degenerative transfer is less important. The ability of **BPT** to control the polymerization was confirmed by steady state polymerization experiments, which include measurements of the polydispersity and the combination of molecular weight and double bond conversion, respectively. While rate constants for reactions of dithiocarbamyl radicals were reported in literature,⁴² no constants for photo-induced reactions of TERP reagents have been reported yet. Therefore the comparison of control abilities was done on the basis of achievable PDIs. A polymerization mechanism based on literature was proposed, Photo-DSC and UV-VIS measurements are provided for comparison with other photoinitiating systems (Figure 28).

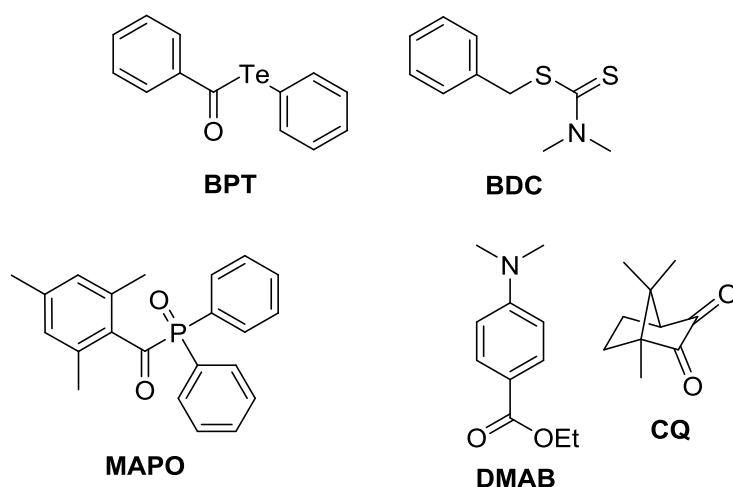


Figure 28. Compared photoinitiating and polymerization control systems

4.5.1. UV-VIS

The UV-VIS spectrum (Figure 29) of the tellurium compound **BPT** is compared to the spectrum of the dithiocarbamate **BDC** and a classical Type I (**MAPO**) and Type II (**CQ**) photoinitiator.

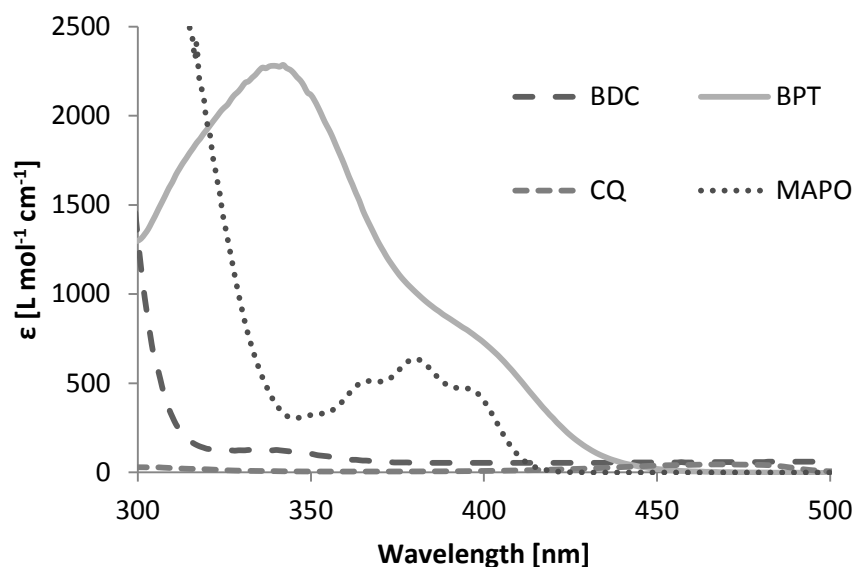


Figure 29. UV-VIS-absorption spectra of the photoiniferters/photoinitiators **BDC**, **BPT**, **MAPO** and **CQ** ($1 \times 10^{-3} \text{ mol L}^{-1}$ for **BDC**, **BPT** and **MAPO** and $1 \times 10^{-2} \text{ mol L}^{-1}$ for **CQ** in CH_2Cl_2)

The telluride **BPT** has a maximum of 339 nm in the absorption spectrum, which most likely marks the $n\text{--}\sigma^*$ transition of the compound. This was already shown in literature for telluriumorganic compounds by using time-dependent DFT calculations.¹²⁴ In this band a significant shoulder appears at 407 nm that tails out until 473 nm, which can be assigned to the $n\text{--}\pi^*$ transition of the carbonyl moiety. This is in good accordance with other Ar-CO-X systems like acylphosphine oxides (e.g. **MAPO**, $\lambda = 380 \text{ nm}$) and acyl germanium compounds (e.g. benzoyl trimethylgermane, $\lambda = 412 \text{ nm}$).²¹ The strong shift of the $n\text{--}\pi^*$ transition compared to the classical benzoyl chromophore ($n\text{--}\pi^* \sim 350\text{-}360 \text{ nm}$) can be explained by the overlap of the d-orbitals of P, Ge or Te with the π^* -orbital of the C=O group thus reducing the necessary energy for the $n\text{--}\pi^*$ transition.

BDC on the other hand has its maximum absorption (belonging to the $n\text{--}\pi^*$ transition of the carbamate moiety) at 335 nm.^{127,128} Due to the high conjugation of this functional group the peak tails out far into the visible region even above 500 nm.

The extinction coefficient is $50 \text{ L mol}^{-1} \text{ cm}^{-1}$, which is very low but still in the same range of **CQ**.

The classical Type II photoinitiator **CQ** has its absorption maximum at 468 nm. The long wavelength of the $n-\pi^*$ transition can be explained by the angle between the two carbonyl groups.⁶⁶

The quantitative results can be found in Table 3.

Table 3. UV-VIS data^a for the compared CRP-reagents/photoinitiators

	λ_{max} [nm] ^a	ϵ [$\text{L mol}^{-1} \text{ cm}^{-1}$] ^a
BDC	335	126
BPT	407^b	595
MAPO	380	636
CQ	468	44

Footnote: 1. ^a $1 \times 10^{-3} \text{ mol L}^{-1}$ for BDC, BPT and MAPO and $1 \times 10^{-2} \text{ mol L}^{-1}$ for CQ in CH_2Cl_2 . ^bAbsorption at the shoulder of the UV-VIS-spectrum determined by peak deconvolution, marking the $n-\pi^*$ transition of the carbonyl group

4.5.2. Controlled Living Radical Photopolymerization

The living character of a polymerization can be proven with studies of the polymerization kinetics.¹²⁹ If the polymerization occurs according to a living mechanism, the molecular weight increases in a linear relationship with the double bond conversion (DBC) of the monomer. Also the PDI should be significantly below 1.5, since the control agent should theoretically provide a homogenous chain length. In case of a free radical polymerization the overall number-average molecular weight (M_n) will decrease before the gel point is reached. Moreover, due to termination and unwanted transfer reactions the PDI will usually be above 1.5.

The living character of the reference **BDC** for a polymerization carried out with UV light has already been shown in literature.¹¹³ The typical PDI for that compound as photoiniferter for the bulk polymerization of MMA is around 1.7-1.8 over 50%

conversion. In that paper also a linear correlation between increasing molecular weight and double bond conversion has been proven.

In the present study, the experiments for the determination of the polymerization kinetics were carried out in a photoreactor with a 400-500 nm light source and four different classes of monomers (St, BMA, BA, NAM) to find out which monomer types can be polymerized in a controlled way with **BPT**. The molar concentration of photoiniferter/TERP-reagent in the monomer varies between 1:100 and 1:500 (0.3-2.2 wt%) and was adjusted to the reactivity of the monomer. For both the reference **BDC** and the tellurium compound **BPT** M_n vs. DBC plots from data of $^1\text{H-NMR}$ -spectroscopy and GPC measurements were made. Additionally the PDIs of the synthesized polymers were measured.

Generally, styrene photoinitiation with both **BDC** and **BPT** was ineffective since styrene is more likely to quench the initiator than to propagate under these conditions. By comparison, benzoyl tellurides have been previously shown to moderate styrene propagation under thermal initiation conditions (Yamago 2002).⁹⁸ The methacrylate BMA could be polymerized with both BDC and BPT, but not in a living radical polymerization and the rate for the reference **BDC** was very low (Figure 30).

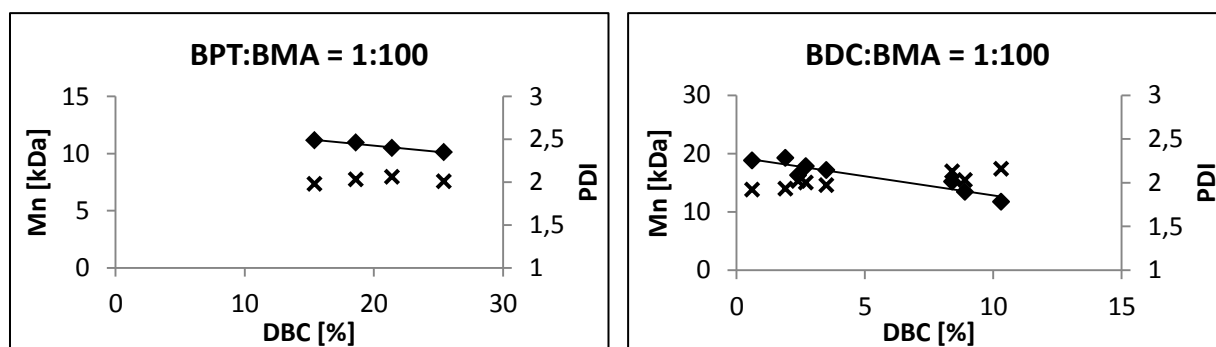


Figure 30. Number-average molecular weight M_n (diamonds) and PDI (crosses) vs. double bond conversion (DBC) plots for BDC and BPT with BMA in bulk determined with photoreactor experiments.

This is in good accordance with literature, which highlights the important role of dimethyl ditelluride for the controlled TERP polymerization of methacrylates.¹³⁰ The monomers BA and NAM both met the criteria for a living radical polymerization with **BPT** (Figure 31).

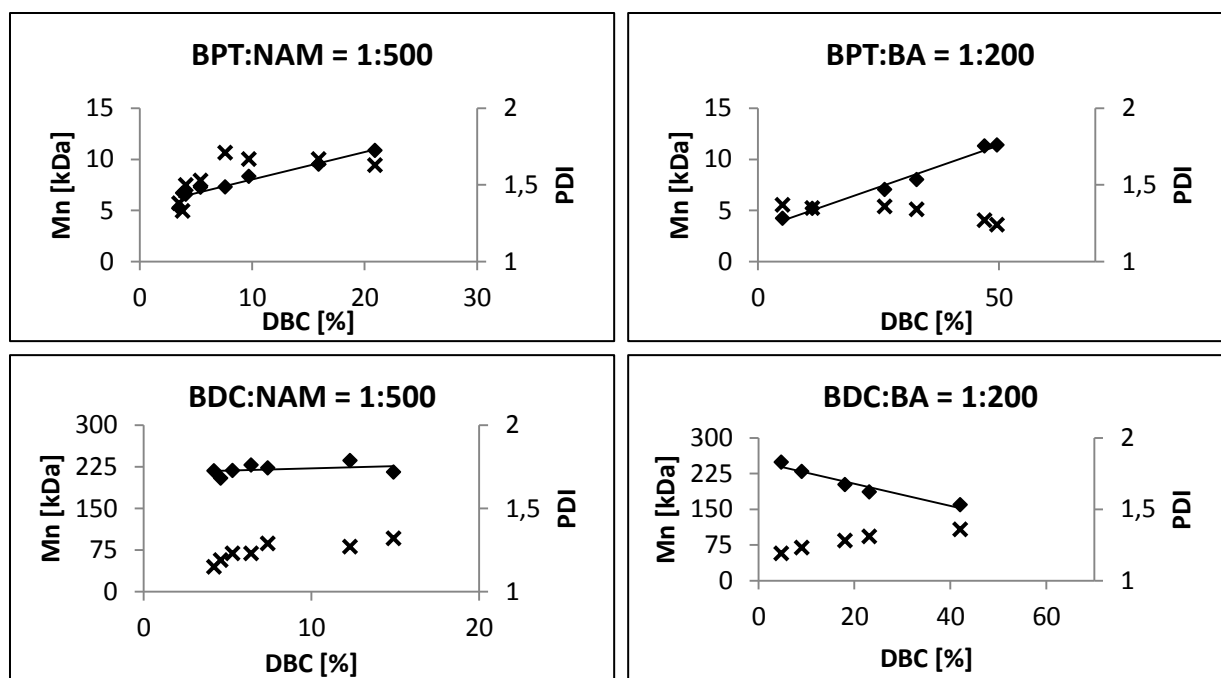


Figure 31. Number-average molecular weight M_n (diamonds) and PDI (crosses) vs. double bond conversion (DBC) plots for BDC and BPT with BA and NAM in bulk determined with photoreactor experiments.

It has to be noted, that NAM was only polymerized to a DBC of $\sim 20\%$ with both photoiniferters due to its high viscosity, which made it impossible to take samples from the photoreactor at higher DBCs.

The increase of the PDI for NAM with **BPT** in the beginning can be explained by termination reactions, which still appear in this early phase of the polymerization.

At conversions as low as 4%, M_n has values around 4-5 kDa for both BA and NAM polymerized with the tellurium compound **BPT**. M_n increases linearly with DBC to values around 11 kDa. The deviation of the best-fit line from the origin is due to radical recombination reactions, which still appear in the early stage of the reaction.¹¹⁸ This causes an initial steep increase in molecular weight as the initiator is consumed followed by a less steep but linear propagation phase. All this is in good accordance with other photoiniferter studies found in literature.¹¹³ The PDIs are significantly below 1.5 and are as low as 1.2 for BA over 50% DBC and 1.3 for NAM over 50% DBC (PDI over 50% DBC for **BDC** according to literature: 1.7-1.8).¹¹³ This fact is especially remarkable, since the best photoiniferter system so far (benzyl 9H-carbazole-9-carbodithioate), can only reach a PDI of 1.5 over 40% conversion.¹¹³

In contrast to **BPT**, the reference **BDC** was not suitable for living polymerization under visible light for any tested monomer. Even though the PDIs were below 2 for BA and NAM, M_n does not increase linearly for either monomer.

4.5.3. Photo-DSC

For comparing the reactivity of photoinitiators Photo-DSC is versatile method. The reactivity of the telluride **BPT** was compared with the reactivity of the reference dithiocarbamate **BDC**. The comparison was done only for acrylamides, since the reactivity of butylacrylate was too low to produce significant and accurate results with photo-DSC. In general, the reactivity of photoiniferters is lower than the reactivity of photoinitiators, which can be explained by the reaction mechanism. While photoinitiators produce radicals, which directly induce radical chain growth, the use of photoiniferters leads to the formation of so called dormant species during the polymerization reaction. These species have to be reactivated by light, which leads to a significant decline in the reaction rate. Of course this is a generalization and it also has to be mentioned that other effects like quantum yields of the compounds play an important role as well. Nevertheless, classical photoinitiator systems, which initiate in the visible light range (**MAPO** and **CQ/DMAB**) were measured (Table 4 and Figure 32) too, to compare the controlled radical polymerization reagents among commercially used photochemical polymerization systems.

Table 4. Results of the photo-DSC measurement with CRP-reagent/photoinitiator in NAM with a molar ratio of 1:500 each.

	$R_p [10^{-3} \text{ mol L}^{-1} \text{ s}^{-1}]$	DBC [%]	$t_{\text{max}} [\text{s}]$	$t_{95\%} [\text{s}]$
BDC	15.9	40	53.5	257
BPT	14.0	29	33.0	180
MAPO	665.2	89	8.0	22
CQ/	281.0	80	14.1	34
DMAB				

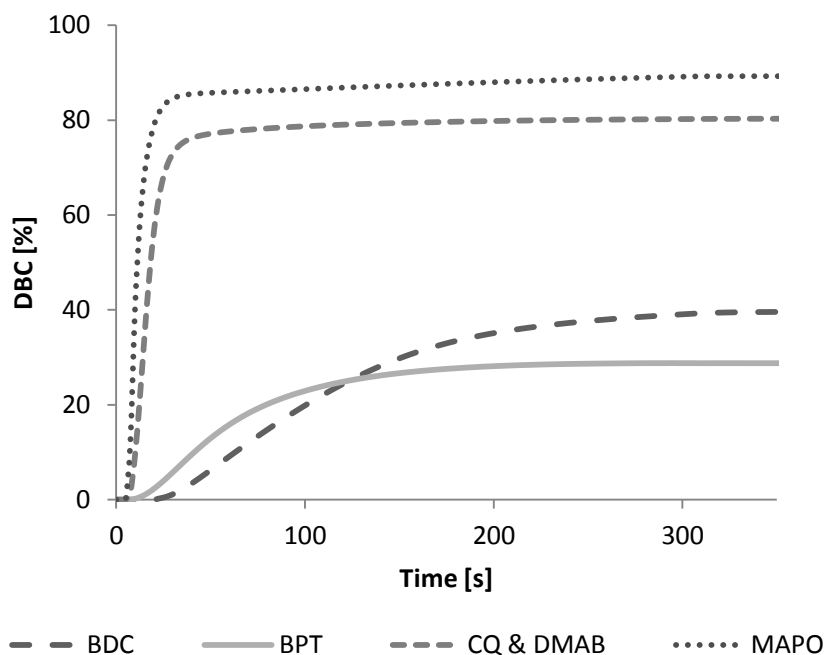


Figure 32. Double bond conversion DBC [%] vs. time [s] for BDC and BPT and for the photoinitiator systems MAPO and CQ/DMAB in NAM with a molar ratio of 1:500 each (0.3, 0.4, 0.5 and 0.5 wt%, respectively).

As expected, the reactivity (expressed by R_p , t_{max} and $t_{95\%}$) and the DBC of the classical free radical photoinitiator systems **MAPO** and **CQ/DMAB** are significantly higher than the values for the controlled polymerization reagents. The photoiniferter **BDC** and **BPT** are both in a similar range of reactivity. The rate of polymerization R_p is approximately the same ($14.0 \times 10^{-3} \text{ mol L}^{-1} \text{ s}^{-1}$ for **BPT** and $15.9 \times 10^{-3} \text{ mol L}^{-1} \text{ s}^{-1}$ for **BDC**), but the time till the maximum heat of polymerization t_{max} is reached and the time till 95% of the polymerization reaction is completed $t_{95\%}$, are significantly lower for **BPT**. The reason for that might be the formation of a highly reactive benzoyl radical in the case of **BPT** (which is also the main difference to the photoinducible TERP reagent ethyl 2-phenyltellanyl-2-methylpropionate), instead of a benzyl radical as for **BDC**,^{108,113} which makes the initiation step very efficient (Figure 34 and Figure 35, Line 2). The DBC is, with around 30% for **BPT** and around 40% for **BDC** for both systems, relatively low. The higher DBC for the reference **BDC** can be explained by the non-controlled polymerization mechanism.

Higher DBC (over 50%) for **BPT** can be achieved by longer polymerization times as it could be seen in the kinetic studies. A higher light intensity leads of course to faster polymerization and higher concentration of TERP reagent leads to slower polymerization as can be seen below (Figure 33). This figure should give an idea about

the tuning possibilities one has, with changing light intensity and TERP-reagent concentration.

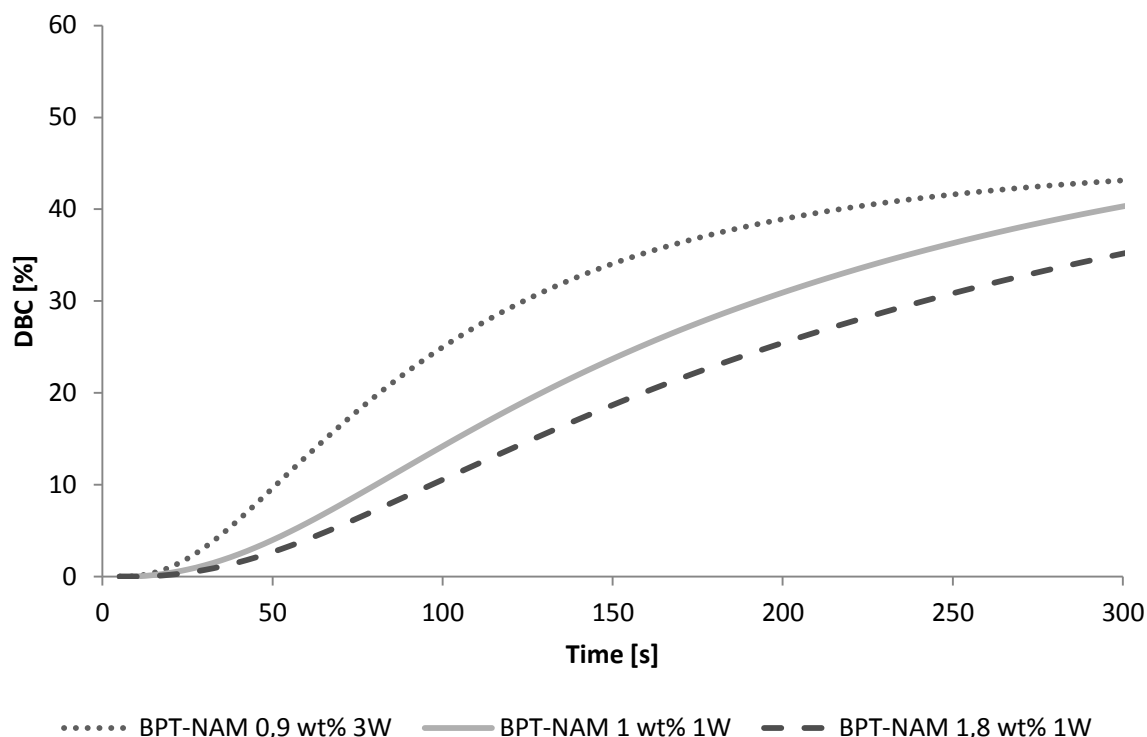


Figure 33. Double bond conversion DBC [%] vs. time [s] for BPT in NAM determined with photo-DSC experiments. Graph is showing different concentrations and irradiation intensities.

The reason for the slower polymerization with higher concentration is more transfer reactions, which is described much more detailed in the mechanistic part below. However, the concentrations used for the comparison with other photoinitiating systems were chosen, to get comparable results for every system and also to be consistent with the concentrations used in the kinetic studies.

Generally, the fact that the reference **BDC** is slightly less reactive doesn't come as a surprise. Literature already suggests that **BDC** would need UV-light for reinitiation¹⁰⁸ (Figure 34, Line 3) or at least UV-light would make this reinitiation much more efficient.¹¹³

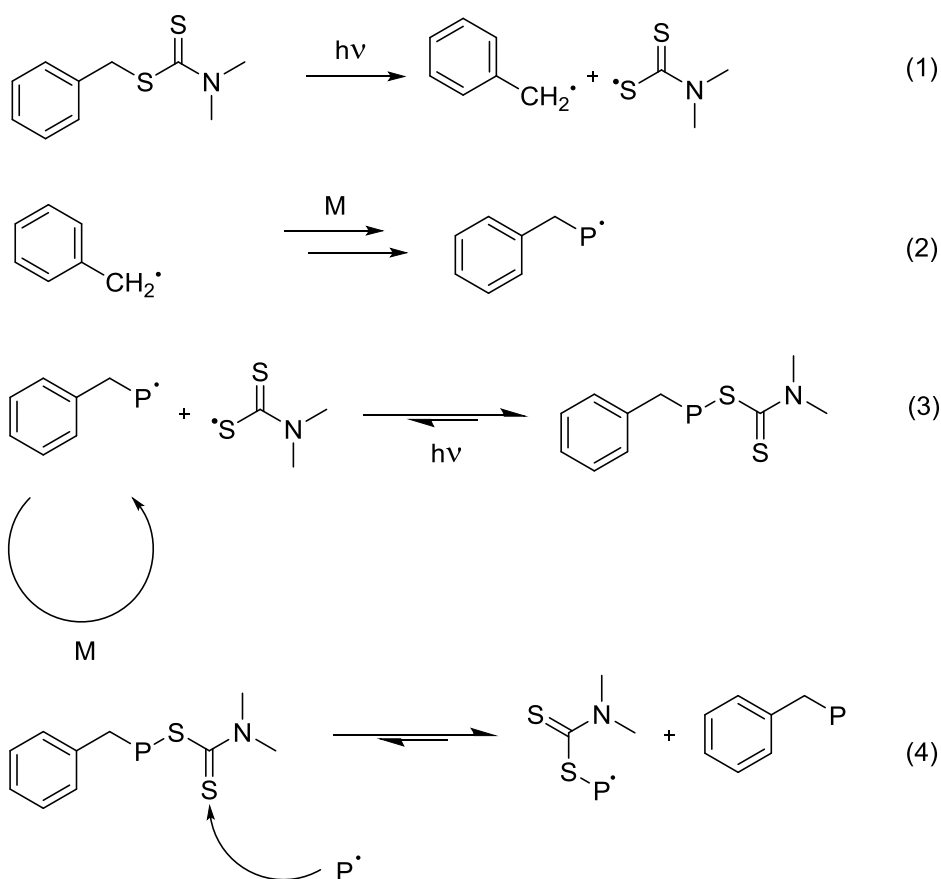


Figure 34. Mechanism for the living radical polymerization with BDC as photoiniferter.¹⁰⁸

Poor visible light efficiency of **BDC** is explained by poor overlap with the $n-\pi^*$ transition, which has its maximum in the UV region. As thus requires UV-light for efficient cleavage of the C-S-bond between polymer and chain transfer agent. It can be assumed that the absorption in the visible light region for the reagent **BDC** is similar to the resulting dormant species. Therefore cleavage can take place but is very inefficient, which results in no control of the polymerization. In contrast, it can be expected from the dormant species of our **BPT** to still efficiently cleave in the visible light area, which is in good accordance with literature, where the TERP reaction is described to propagate with visible light irradiation.¹²⁴ It is also worth mentioning that a degenerative transfer mechanism may compete with the described mechanism (Figure 34, Line 4), therefore reducing the reactivity of **BDC**, but for the control of polymerization the dissociation-combination mechanism plays the main role.¹¹³

The tellurium compound **BPT** reacts via a similar mechanism which is already proposed in literature for another telluroorganic compound.¹²⁴ The adapted mechanism for the specific photoiniferter is shown below (Figure 35).

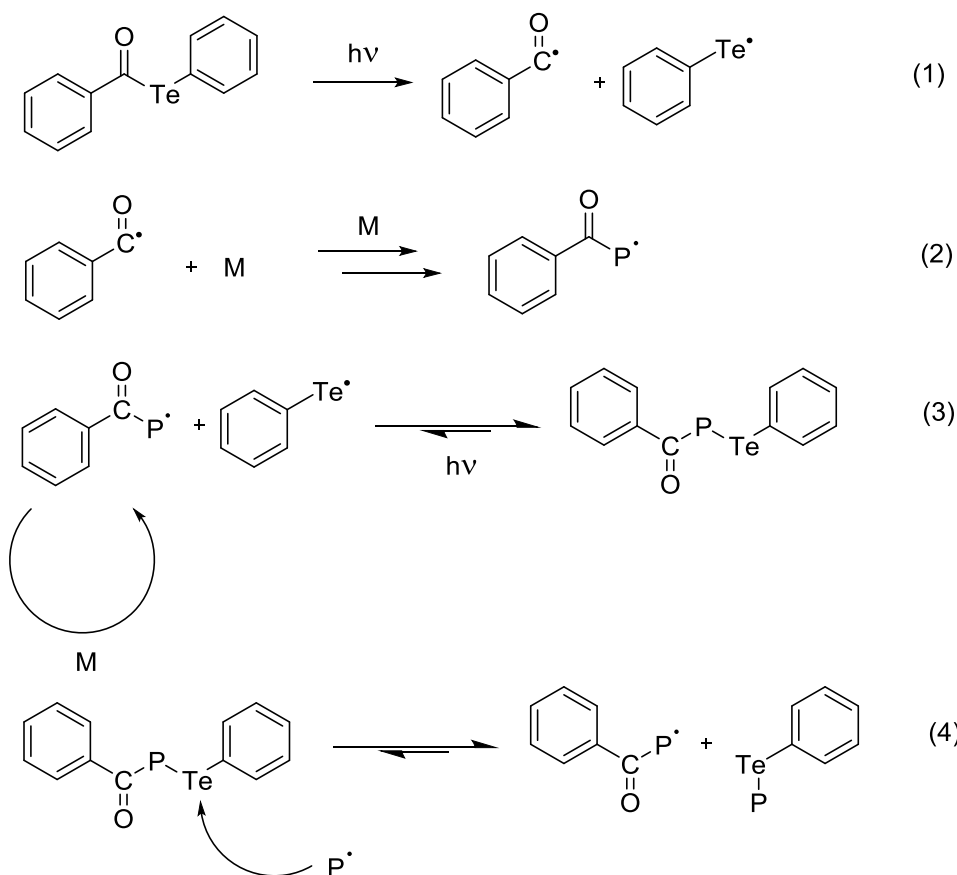
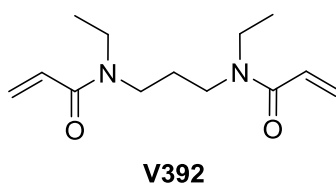


Figure 35. Proposed living radical polymerization mechanism with BPT as TERP-reagent.¹²⁴

The cleavage of the C-Te-bond (Figure 35, Line 3) requires less energy (absorption above 400 nm) and is therefore still efficient under the influence of visible light, which was already shown in literature for tellurium controlled living radical polymerizations (TERP).^{98,123} It has to be noted that also here degenerative transfer (Figure 35, Line 4) may compete with the dissociation-combination mechanism (Figure 35, Line 3) and may even be very important for polymerization control. However, while degenerative transfer is the major mechanism for thermally initiated TERP, for photoinduced TERP the dissociation-combination also plays a major role.^{124,126}

In conclusion it can be said that **BPT** is a very interesting TERP reagent but for dental applications it is not widely usable because it does not polymerize methacrylic monomers in a living way. However, for special applications, like for example the polymerization of the dental primer **V392** it has some potential.



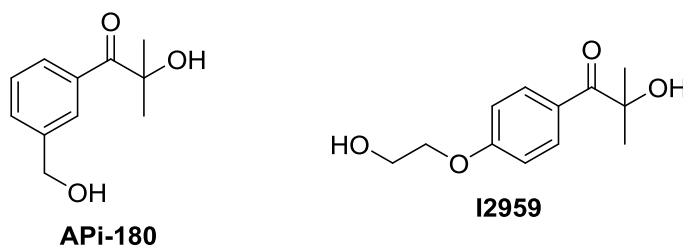
This would be an interesting topic for future investigations.

5. Water-Soluble Photoinitiators

5.1. State of the Art

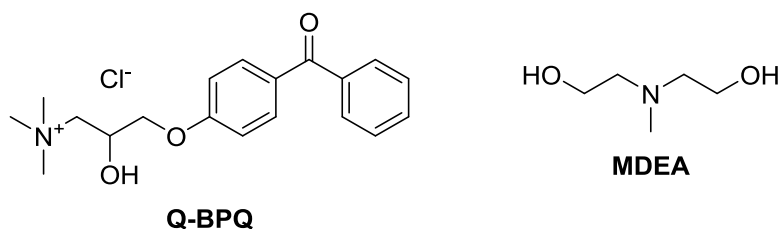
Water soluble photoinitiators¹³¹ are not only required for dental primer mixtures but for various applications, such as industrial inkjet printing,¹³² hydrogel production,¹³³ cell encapsulation for biological applications,¹³⁴ liquid crystal monomer production,¹³⁵ 3D-printing technologies¹³⁶ and many others.¹³⁷⁻¹³⁹ Given that fact, it is hard to understand why the commercially available variety and performance of water soluble photoinitiators (PIs) is much lower as for the organo-soluble initiators.

Currently, almost exclusively 2-hydroxy-1-[4-(2-hydroxyethoxy)phenyl]-2-methyl-1-propanone (Irgacure 2959®) is used when water solubility is required¹⁴⁰⁻¹⁴² since years of research have not yet led to a breakthrough in establishing well suitable water-borne photoinitiators.^{19,143,144} The advantages of Irgacure 2959 (**I2959**) are high reactivity because of a Norrish Type I cleavage process and good biocompatibility. However, one major drawback is low water-solubility. This can become a problem especially for applications where a higher photoinitiator concentration (over 0.5 wt%) is required. To overcome this problem the structure of **I2959** was recently modified.¹⁴⁵ 2-Hydroxy-1-[3-(hydroxymethyl)phenyl]-2-methyl-1-propanone (**APi-180**®) offers much better solubility in water but, like **I2959**, only cleaves under irradiation with UV-light, which can be undesired for applications involving living cells like it is the case in dentistry.^{17,18}



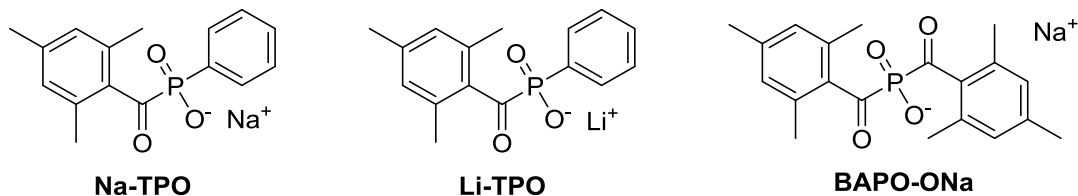
Furthermore there is a variety of Norrish type II photoinitiators, which are used for water-based monomer formulations. Naphthalimid¹⁴⁶ and thioxanthone¹⁴⁷ derivatives

were reported recently, whereas benzophenone¹⁴⁸ type initiators, like 3-(4-benzoylphenoxy)-2-hydroxy-*N,N,N*-trimethyl-1-propanaminium-chloride (Quantacure BPQ; **Q-BPQ**) have been on the market for quite a while. As a coinitiator usually methyldiethanolamine (**MDEA**) is used.



Even though these photoinitiators show usually good solubility and biocompatibility they suffer from lower reactivity. This can be explained by the Norrish type II initiation mechanism. The cleavage of a type I system is much faster, than the electron and/or proton transfer of a type II system. Additionally type II systems are usually two component systems, wherein a solvent cage hinders the two components from a fast reaction.¹⁹ This is also the case for **CQ/DMAB**, which is still used in dental primer mixtures even though it shows very low solubility in the formulations but it is the only available system, which absorbs in the visible light region.

A new development is the discovery of monoacylphosphineoxide (**MAPO**) and bisacylphosphineoxide (**BAPO**) salts and especially the discovery of their good photoinitiation properties. The **BAPO** salt **BAPO-ONa**^{149,150} was only recently published, while the **MAPO** salts **Na-TPO**¹⁵¹ and **Li-TPO**¹⁵² are already known for some years but their properties and application in aqueous media has not been fully explored yet.

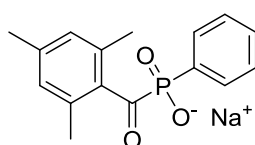


In fact, there are currently only a very limited number of publications were available, where **BAPO** and **MAPO** salts were used for photopolymerization.^{149,150,152-154}

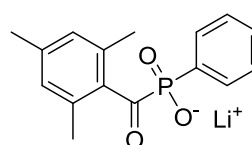
Both the **MAPO** and **BAPO** salts show very promising results, especially in comparison to state of the art photoinitiators (**I2959**, **APi-180** and **Q-BPQ**).

5.2. Syntheses

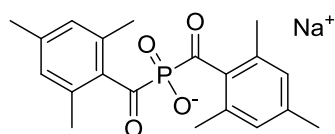
The goal was to synthesize the sodium and lithium salts of **MAPO** and **BAPO** and explore their potential for the use in water-based monomer formulations. Literature provides syntheses pathways for the desired compounds.¹⁴⁹⁻¹⁵² Additionally it was tried to modify Ivocerin to increase its water-solubility by adding –OH-groups as it was done for **APi-180**¹⁴⁵ and subsequently also diethanolamine-groups^{157,158} to the molecule. The target compounds are summarized below.



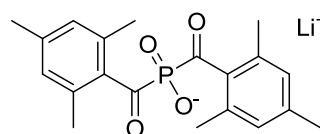
Na-TPO



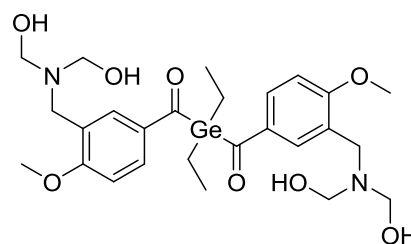
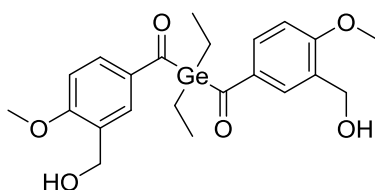
Li-TPO



BAPO-ONa



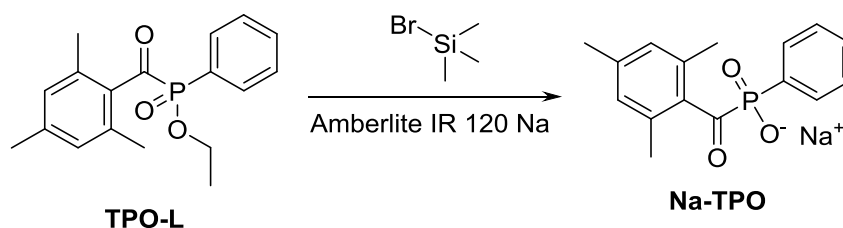
BAPO-OLi



5.2.1. Syntheses of the MAPO-Salts Na-TPO and Li-TPO

5.2.1.1. Synthesis of Na-TPO with an Ion-Exchange Resin

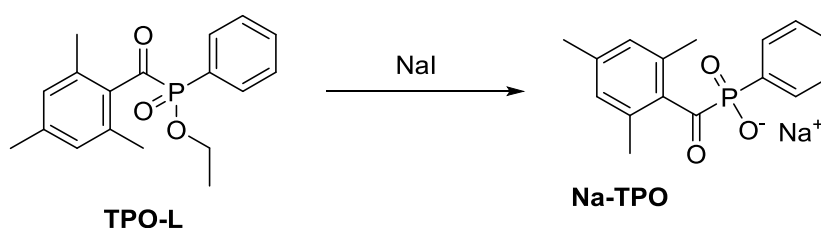
A synthesis from literature was chosen to get the **MAPO** salt **Na-TPO**.¹⁵⁵ This route has the advantage of using commercially available **TPO-L** as starting material. Via ion exchange reaction sodium is introduced in the structure.



For this synthesis 1 eq. of **TPO-L** was dissolved in MeCN and 2.15 eq. of bromotrimethylsilane were added. After 4 h at 60°C, MeOH/H₂O was added. After removal of the solvent a white solid was obtained, which was assumed to be the free acid. H₂O and Amberlite IR 120 Na were added. After the reaction was finished, visible in complete solution of the former white precipitate (~2.5 h), the product was dissolved in MeOH and filtered. Removal of the solvent gave the product **Na-TPO** with 56% yield.

5.2.1.2. Synthesis of Na-TPO from NaI

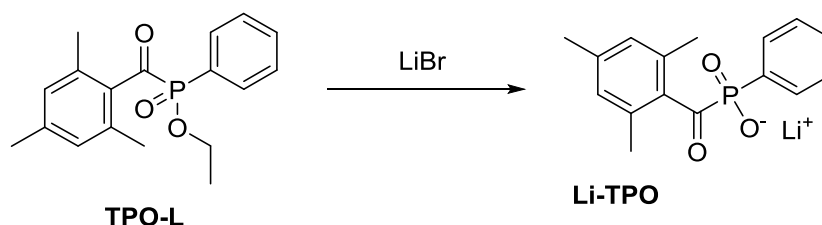
There is also a very similar pathway described in literature where alkali salts are stirred with **TPO-L** in ethylmethylketone and the desired product precipitates.^{153,156,157} In hope of an easier synthesis with better yield this method was tried too.



It was tried first for **Na-TPO**. Therefore 1 eq. of **TPO-L** was dissolved in ethylmethylketone and 1.1 eq. of NaI were added. The solution was heated to 65°C and stirred for 24 h. The resulting precipitate was filtered off and washed with ethylmethylketone and PE. After drying in high vacuum the product was recrystallized from diethylether to yield the product **Na-TPO** as yellowish powder in almost quantitative yields.

5.2.1.3. Synthesis of Li-TPO from LiBr

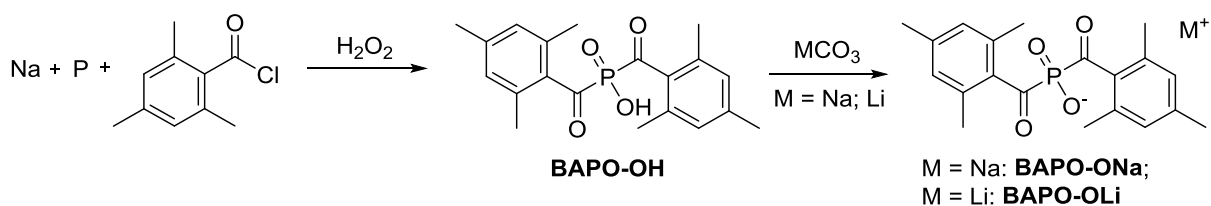
The same synthetic pathway as for **Na-TPO** was now also used for **Li-TPO**.^{153,156,157}



Here 1 eq. of **TPO-L** was dissolved in ethylmethylketone and 4 eq. of LiBr were added. The solution was heated to 65°C and stirred for 24 h. The resulting precipitate was filtered off and washed with ethylmethylketone and PE. After drying in high vacuum the product was recrystallized from diethylether to yield the product **Li-TPO** as white powder in almost quantitative yields.

5.2.2. Syntheses of the BAPO-Salts Na-BAPO and Li-BAPO

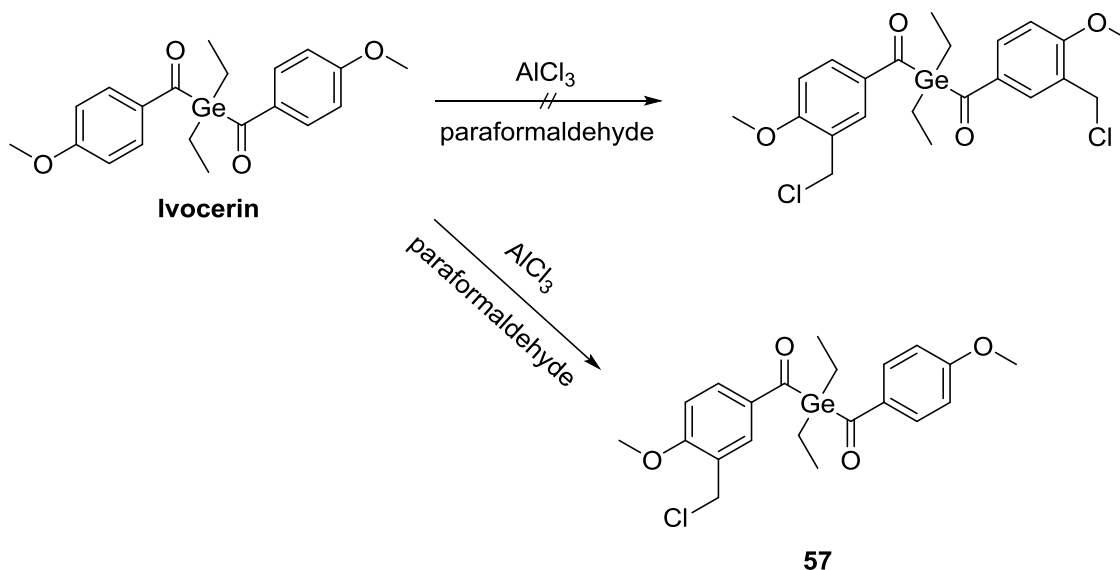
In contrast to the **MAPO** salts where **TPO-L** could be used as commercially available starting material, the **BAPO** salts had to be made from scratch. This was done by cooperation partners from ETH Zurich, namely Jieping Wang.^{131,150}



5.2.3. Modification of Ivocerin

5.2.3.1. Synthesis of ((3-(Chloromethyl)-4-methoxybenzoyl)-diethylgermyl)-(4-ethoxyphenyl)methanone **57**

The modification of Ivocerin was planned according to a modified synthesis from literature.¹⁴⁵ Herein the synthesis of **APi-180** is described, where basically CH_2OH groups are introduced in the structure of Darocur 1173. In a first step chloromethyl moieties had to be introduced:

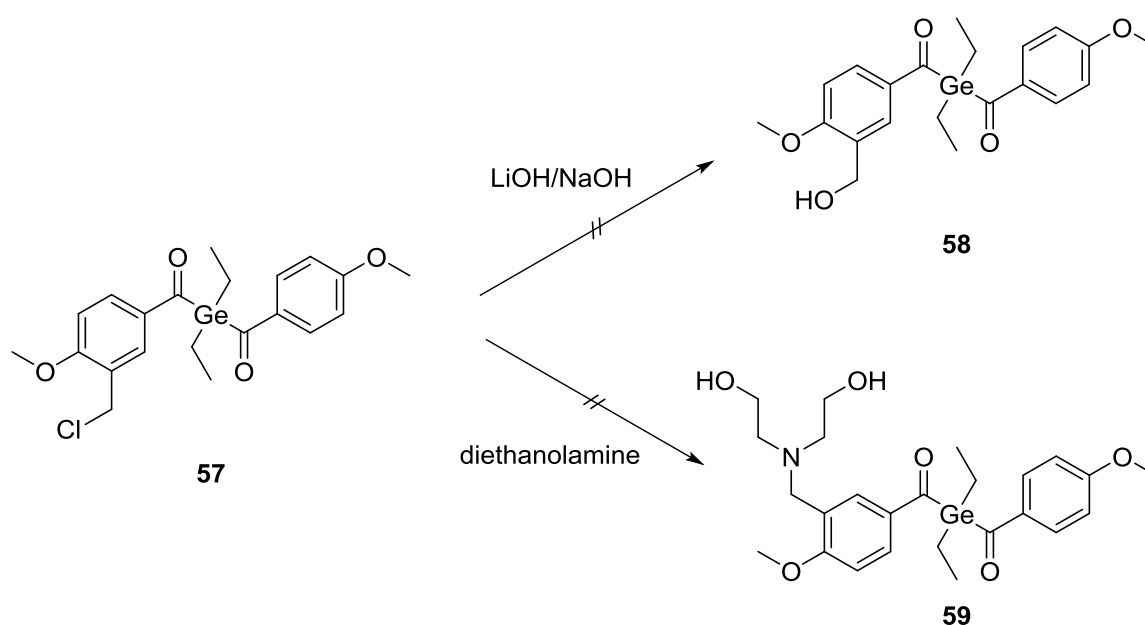


Therefore, under argon 1 eq. of Ivocerin and 6 eq. of AlCl_3 were dissolved in CHCl_3 and cooled to 4°C . 12 eq. of Paraformaldehyde were added slowly and the mixture was stirred overnight (16 h) at ambient temperatures. Subsequently, water was added and the organic phase was separated. The red, jelly precipitate was dissolved in EE and washed with water too. The combined organic phase was dried and the solvents removed. The yellow, liquid residue was purified via column chromatography, which gave the monosubstituted product **57**. Unfortunately, a

double substitution did not work because after introducing only one chloromethyl group product **60** already precipitated from the reaction mixture. Nevertheless, after work-up the monosubstituted product **57** could be obtained as yellow oil with a yield of 64%.

5.2.3.2. Attempted Introduction of –OH- and diethanolamino-groups

Since for a proof of concept (model reaction) also a monosubstituted compound is enough the next steps of the syntheses were conducted.



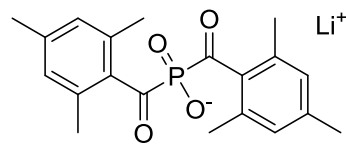
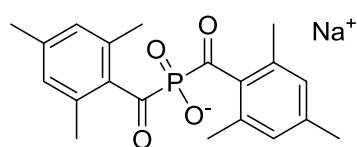
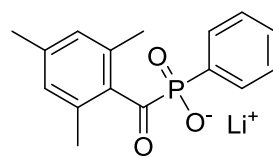
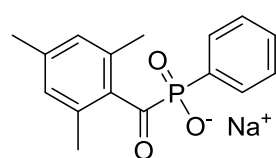
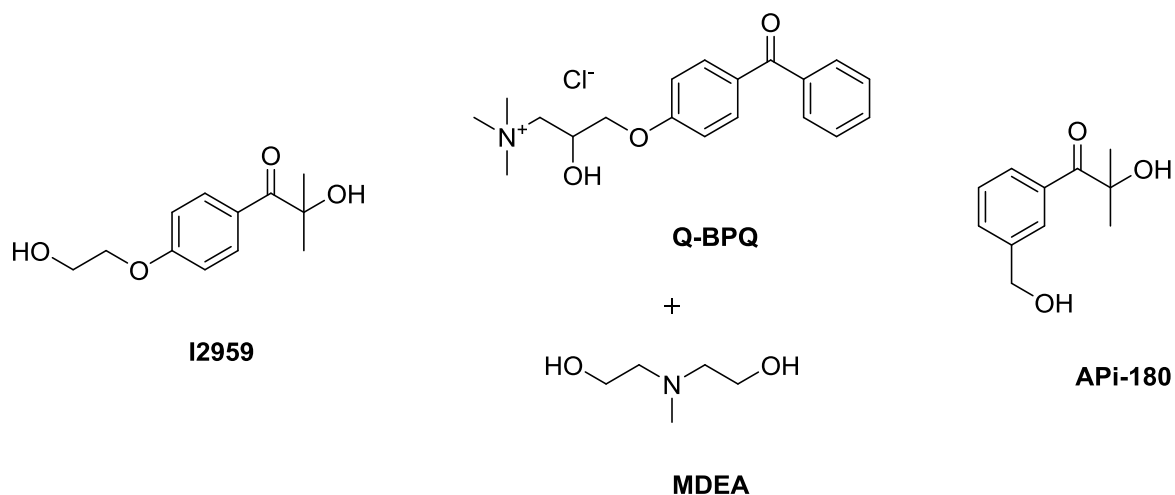
First it was tried to introduce –OH-groups.¹⁴⁵ Under argon atmosphere and at 40°C 1 eq. of the Ivocerin derivate **57** was mixed with 1.2 eq. 0.5 N LiOH solution and stirred overnight. TLC and GC-MS during reaction showed no product formation but only the starting materials. So to half of the reaction mixture 1.2 eq. 1 N NaOH was added as it is also described in literature.¹⁴⁵ The other half was heated to reflux for 24 h. Both cases led to decolorization and on TLC plates no product **58** but also no starting materials could be found anymore.

A similar case was the attempted reaction with diethanolamine.^{158,159} 1 eq. of the Ivocerin derivate **57** was dissolved in MeCN and added to a mixture of 1 eq. diethanolamine and 0.7 eq. Na₂CO₃ in MeCN. The resulting slurry was stirred for 1 h

at ambient temperatures and heated afterwards to reflux since at ambient temperatures no reaction occurred. After 6 h at reflux the starting material had to a small part decomposed according to TLC but mostly no reaction had occurred. A small amount of water was added to dissolve the Na_2CO_3 fully and the mixture was continued to stir overnight. After 24 h TLC showed complete decomposition of the starting material but no product **59** formation. The reaction mixture was completely decolorized.

5.3. Characterization

Since the modification of Ivocerin was not successful only the **MAPO** and **BAPO** salts were further characterized.¹³¹ They were compared to the state of the art water-soluble photoinitiators **I2959**, **APi-180** and also **Q-BPQ**, to offer better comparability between different initiating systems.



The photoinitiators were compared concerning their solubility in water, storage stability, UV-VIS-spectra, cytotoxicity and reactivity.

5.3.1. Solubility

The solubility in water is of course the most important characteristic of a photoinitiator for applicability in water-based formulations. The solubility of the **MAPO** and **BAPO** salts and of the references can be seen below (Figure 36).

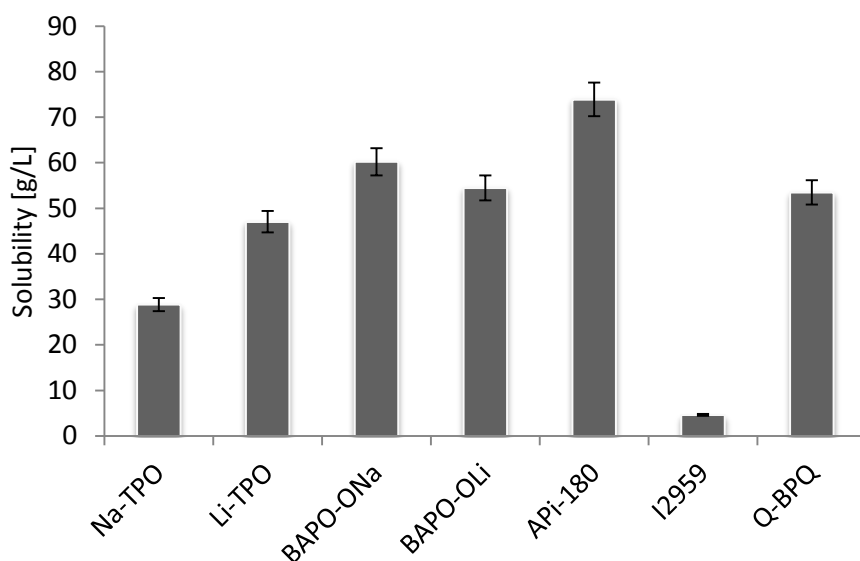


Figure 36. Solubility of MAPO and BAPO salts and references in deionized water.

The **MAPO** and **BAPO** PIs have an excellent solubility in water that ranges from 29 g L⁻¹ for **Na-TPO** to 60 g L⁻¹ for **BAPO-ONa**. Only **APi-180** (74 g L⁻¹) as a modified **I2959** offers water solubility in a similar range. The state of the art photoinitiator **I2959** suffers from very low solubility (5 g L⁻¹). The solubility of the reference **Q-BPQ** (54 g L⁻¹) is also quite good and comparable to the **MAPO** and **BAPO** salts. The quantitative results are summarized in Table 5.

Table 5. Comparison of the solubility data of the described MAPO and BAPO salts with state of the art photoinitiators as an overview.

	Solubility [g/L]
Na-TPO	29
Li-TPO	47
BAPO-ONa	60
BAPO-OLi	54
APi-180	74
I2959	5
Q-BPQ + MDEA	54 ^a

Footnote: 2. ^aValue for BPQ only

5.3.2. UV-VIS

Below, the UV-VIS spectra of the MAPO and BAPO salts (Figure 37) are compared to the references (Figure 38).

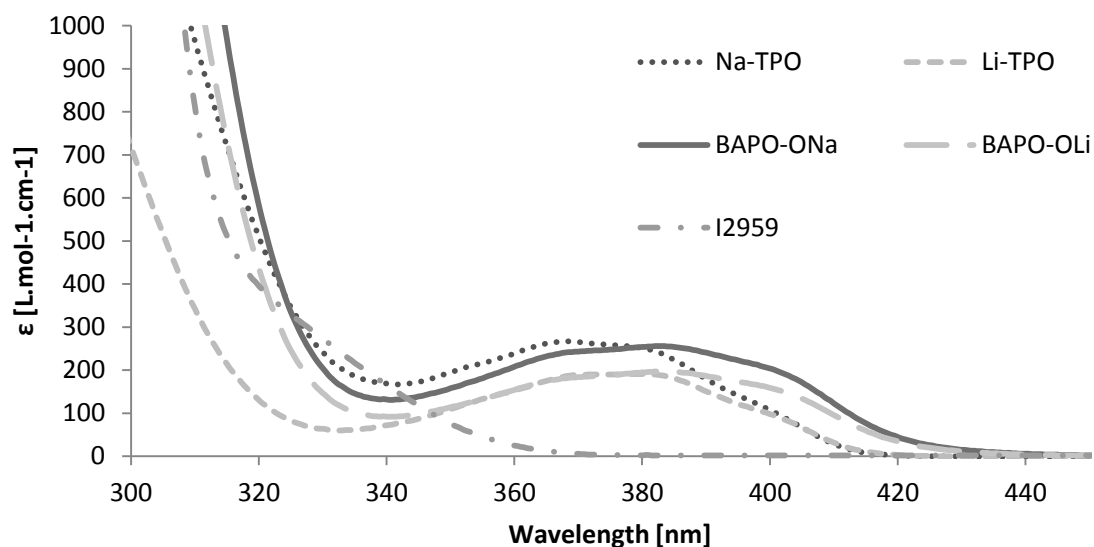


Figure 37. UV-VIS-spectra of the tested photoinitiators. The concentration was $10^{-3} \text{ mol L}^{-1}$ in methanol.

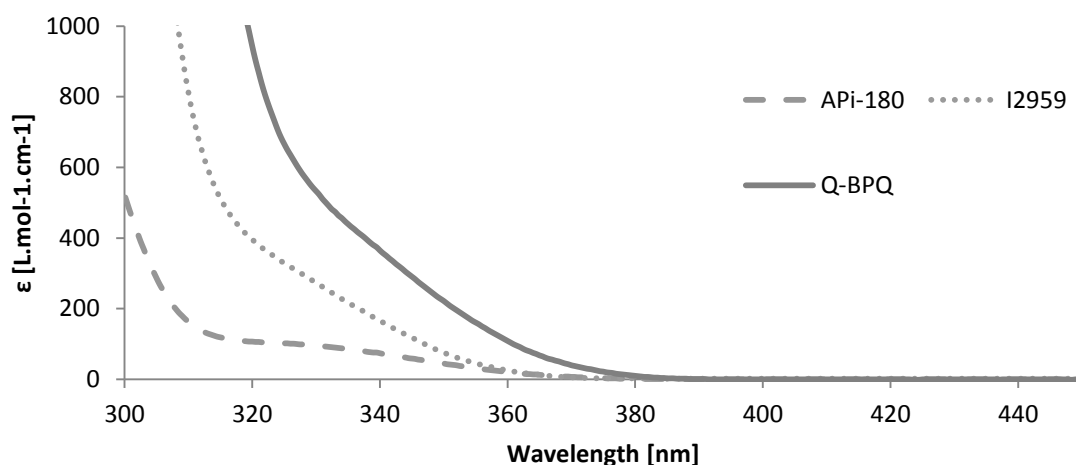


Figure 38. UV-VIS-spectra of the tested photoinitiators. The concentration was $10^{-3} \text{ mol L}^{-1}$ in methanol.

As expected, the references **API-180**, **I2959** and **Q-BPQ** only absorb in the UV-region and have their maxima of the $n \rightarrow \pi^*$ transitions between 328 and 347 nm. The **MAPO** and **BAPO** salts have strong absorption bands well above 400 nm. The maxima below 340 nm in the absorption spectra mark the $\pi \rightarrow \pi^*$ transitions of the compounds. For the **MAPO** salts the maximum of the $n \rightarrow \pi^*$ transition of the

carbonyl moiety is at 380.5 nm and for the **BAPO** salts it is at 383.5 nm. This is in good accordance with other Ar-CO-X systems like monoacylphosphine oxides (e.g. **MAPO**, $\lambda = 380$ nm) and acyl germanium compounds (e.g. benzoyl trimethylgermane, $\lambda = 412$ nm).²¹ The strong shift of the $n-\pi^*$ transition compared to the classical benzoyl chromophore ($n-\pi^* \sim 350-360$ nm) can be explained by the overlap of the d-orbitals of P or Ge with the π^* -orbital of the C=O group thus reducing the necessary energy for the $n-\pi^*$ transition. The slight red-shift for the **BAPO** salts compared to the **MAPO** salts can be explained by the presence of a second benzoyl chromophore. All data is summarized in Table 6.

Table 6. Comparison of the UV-VIS spectra of the described MAPO and BAPO salts with state of the art photoinitiators as an overview.

	UV-VIS	
	λ_{\max} [nm]	ϵ [L mol ⁻¹ cm ⁻¹]
Na-TPO	380.5	250
Li-TPO	380.5	191
BAPO-ONa	383.5	256
BAPO-OLi	383.5	197
APi-180	329.5 ^c	97
I2959	328.0 ^c	296
Q-BPQ + MDEA	347.0 ^{b,c}	262 ^b

Footnote: 3. ^bValue for BPQ only. ^cAbsorption at the shoulder of the UV-VIS-spectrum determined by peak deconvolution, marking the $n-\pi^*$ transition of the compound.

5.3.3. Storage Stability

Storage stability is crucial for industrial applications in general and for dental materials in particular to sell ready to use light curable mixtures of monomer, additives and photoinitiator. Very often the monomer mixtures are not neutral but show acidic or basic behavior because of impurities from the production process or

functional groups on the monomer. Therefore the storage stability not only in neutral solvents (MeCN/H₂O = 50/50 v/v) but also in acidic (MeCN/H₂O = 50/50 v/v + H₃PO₄, pH = 2) and basic (MeCN/H₂O = 50/50 v/v + NaOH, pH = 11) environments was tested. After storing the photoinitiator samples in solution for 20 days none of them showed any degradation in a neutral environment. However, there was some degradation detectable for acidic but especially for basic environments (Figure 39).

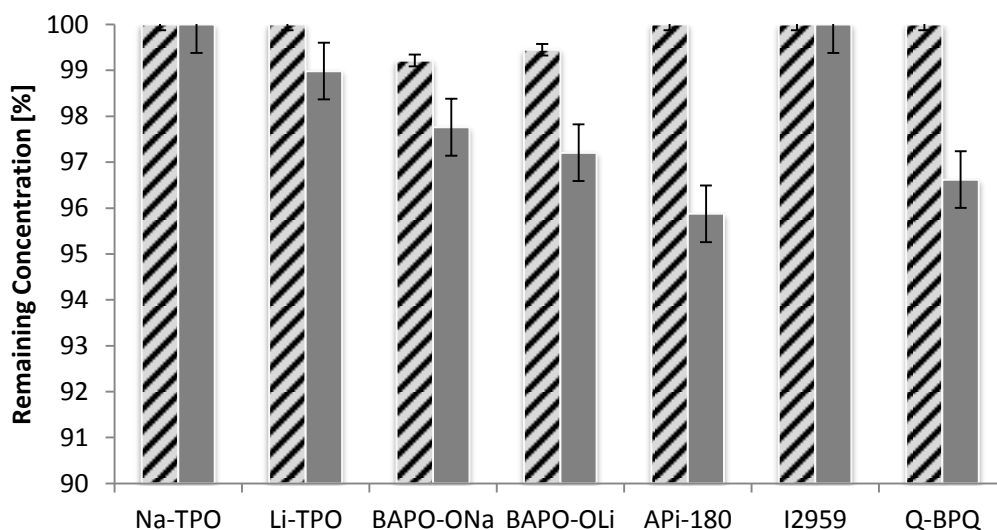


Figure 39. Remaining concentration of tested photoinitiators after storage in solution (MeCN/H₂O = 50/50 v/v) (10^{-3} mol L⁻¹) for 20 days. Solid: + NaOH (pH = 11); dashed: + H₃PO₄ (pH = 2)

Most likely a nucleophilic attack on the benzoyl chromophore is favored under alkaline conditions. This degradation behavior was detected via UV/VIS measurements. Especially the **MAPO** and **BAPO** salts lose their functionality if a cleavage reaction occurs between heteroatom and carbonyl group. For this reason the relative decline of the extinction coefficient of the chromophore was used for calculating the residual (functional) compound after storage. For the references **API-180**, **I2959** and **Q-BPQ** this method of evaluation is more problematic since it shows only the disappearance of the chromophore. Here it is theoretically thinkable that the chromophore still is detectable even after the molecule reacted with another moiety and potentially even decomposed, since the benzoyl chromophore is not particularly far red-shifted for example in **I2959**. Nevertheless, since the references are industrial products good storage stability is already known and to have a consistent method, evaluation was done in the same way. However, the values measured for the references have to be seen within the limits of the method.

As a conclusion, both the **MAPO** and **BAPO** salts show quite good storage stability in neutral, acidic and basic environments. The remaining concentration after storage is in any case at least 96%, usually over 99%. This makes the PIs easy to use and a variety of industrial applications possible.

5.3.4. Cytotoxicity and Cell Encapsulation

Cytocompatibility is a very important factor for the applicability of water-soluble PIs. For biological applications, like cell encapsulation it is absolutely mandatory. Also for other applications like industrial inkjet printing it can be very important when it comes to printing on food packaging.

A number that describes the cytotoxicity of a compound very well is the LC_{50} (lethal concentration, 50%), which is the concentration required to kill half of the members of a tested population after a specified test duration. In our case this means 50% of the cell culture (fibroblast cells L929) still showed metabolic activity after incubation for 24 h together with an LC_{50} concentration of the photoinitiator (Figure 40). All the subsequent tests and characterization concerning cytotoxicity and cell encapsulation were done by a cooperation partner from TU Wien, namely Marica Markovic.

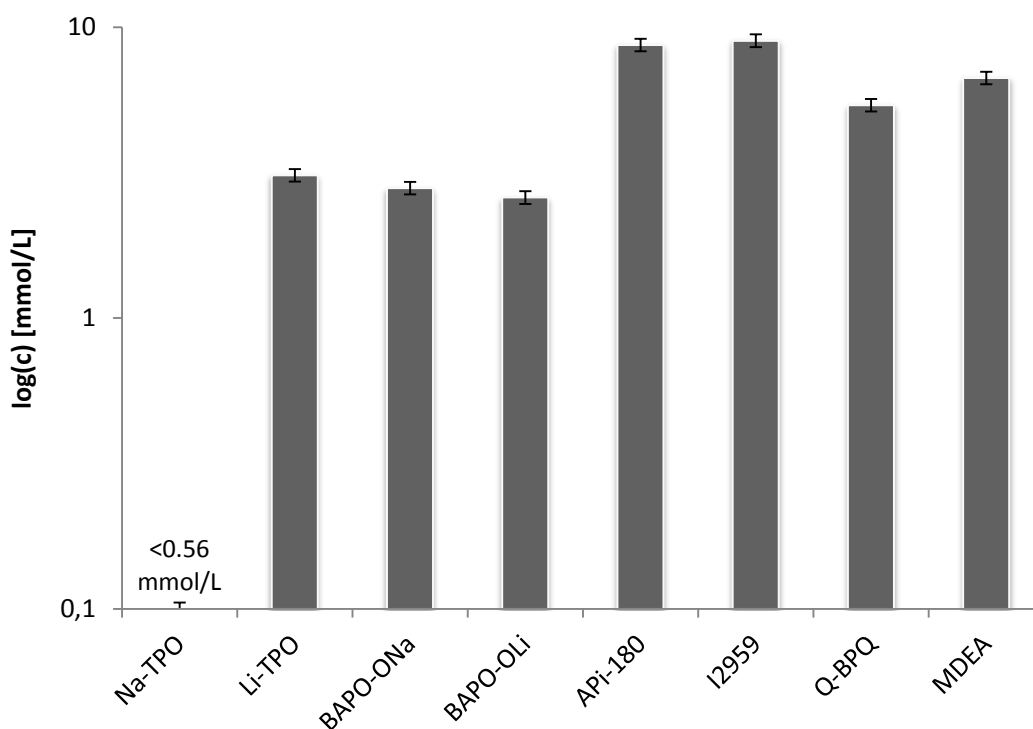


Figure 40. LC₅₀ of the tested photoinitiators.

As can be seen (Figure 40) the biocompatibility of the **MAPO** and **BAPO** photoinitiators is in a similar range as the state of the art PIs. Only **Na-TPO** has a very low biocompatibility (LC₅₀ < 0.56 mmol L⁻¹). However, the cytotoxicity of **Li-TPO** (LC₅₀ = 3.1 mmol L⁻¹), **BAPO-ONa** (LC₅₀ = 2.8 mmol L⁻¹) and **BAPO-OLi** (LC₅₀ = 2.6 mmol L⁻¹) is very low. This can also be seen very clearly from the quantitative results in the following table (Table 7):

Table 7. Comparison of the toxicity data of the described MAPO and BAPO salts with state of the art photoinitiators as an overview.

	Toxicity
	LC ₅₀ [mmol/L]
Na-TPO	<0.56
Li-TPO	3.1
BAPO-ONa	2.8
BAPO-OLi	2.6
API-180	8.7

I2959	9.0
Q-BPQ + MDEA	5.4 ^a

Footnote: 4. ^aValue for BPQ only.

These good results are making it possible to use the **MAPO** and **BAPO** salts even for biological applications, such as cell encapsulation. To show this cell viability and distribution within a 10 % GelMod (methacrylamide-modified gelatin)¹⁶⁰ pellet was monitored for 36 days using laser scanning microscopy. The figure below (Figure 41) shows confocal images of stained MC3T3-E1 on day 9 pellet showing that the cells formed small clusters. This could be due to proliferation of the cells. They also preserved round morphology from the beginning of encapsulation until the last monitored time point. After approximately 2 weeks, the cell number in the pellets started to drop.

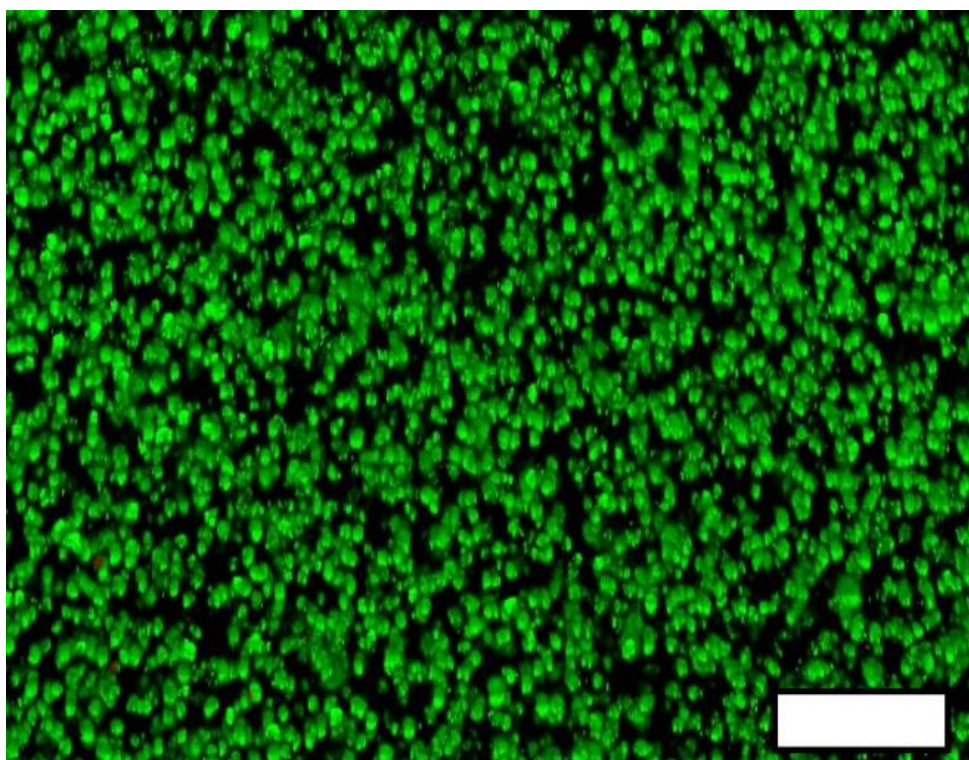


Figure 41. Distribution of MC3T3-E1 in 10 % GelMOD pellet with 0,6 mM Li-TPO 56 9 days after structuring. Living cells were stained green with calcein and dead red cells stained with propidium iodide were not found. Cells formed small clusters and had a round morphology. Scale bar represents 200 μ m.

5.3.5. Photo-DSC

The reactivity of the tested photoinitiators was characterized via photo-DSC experiments. As a monomer N-acryloylmorpholine (NAM) 40 wt% in water was used. NAM was used because of its excellent miscibility with water, good biocompatibility,^{161,162} high monomer reactivity and the ability to form polymer hydrogels.

All photoinitiators were tested with a 320-500 nm light source. As can be seen from the UV-VIS-spectrum (Figure 37) the **MAPO** and **BAPO** salts also have strong absorption bands in the visible light spectrum. Therefore they were additionally tested with a 400-500 nm light source to determine the reactivity under visible light irradiation, which is especially important for an application in dentistry.

There are several numbers that characterize the reactivity of a photoinitiator/monomer system. The time until the maximum heat of polymerization is reached, t_{\max} [s] as well as the time until 95% of the polymerization is complete, $t_{95\%}$ [s] should both be as low as possible for high reactivity. The monomer double bond conversion DBC [%] is another indicator. A higher percentage means higher reactivity. Furthermore the rate of polymerization R_p [mmol L⁻¹ s⁻¹] is a possibility to compare the reactivity. Besides these quantitative numbers (Table 8) the reactivity can also be compared in a qualitative way by plotting the DBC during the polymerization against the time (Figure 42, Figure 43 and Figure 44).

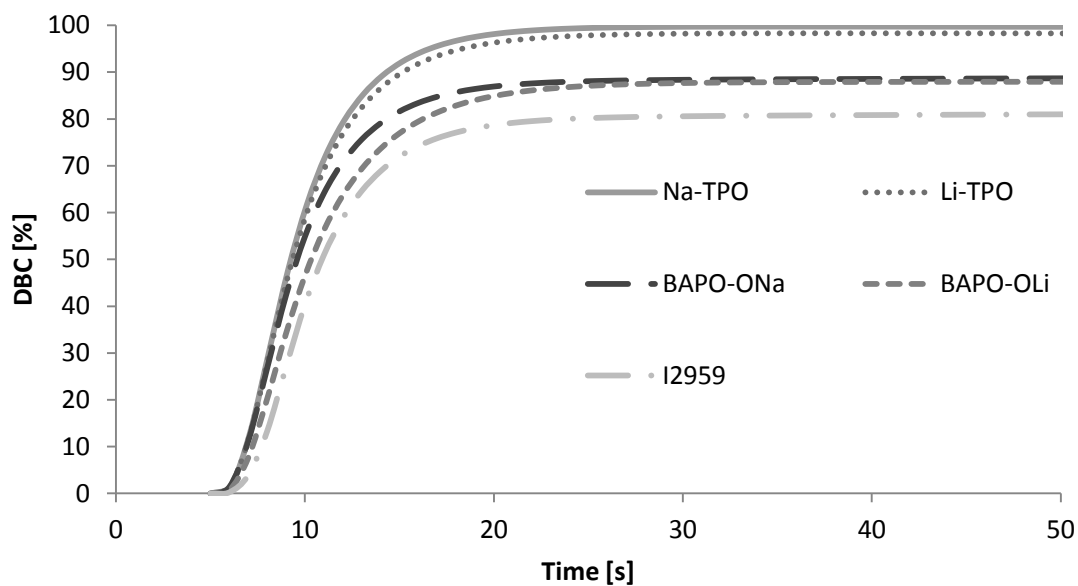


Figure 42. Double bond conversion (DBC) vs. time for the tested photoinitiators in a concentration of 1 mol% in NAM + H₂O (40/60 w/w). Irradiation wavelength was 320-500 nm with an irradiation intensity of 1 W cm⁻².

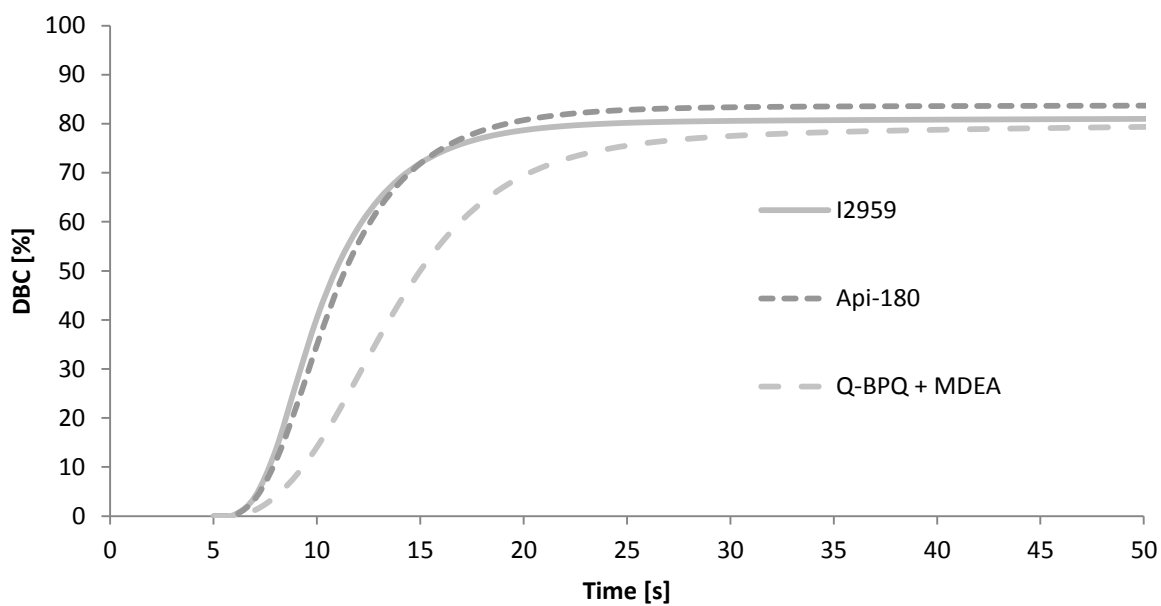


Figure 43. Double bond conversion (DBC) vs. time for the tested photoinitiators in a concentration of 1 mol% in NAM + H₂O (40/60 w/w). Irradiation wavelength was 320-500 nm with an irradiation intensity of 1 W cm⁻².

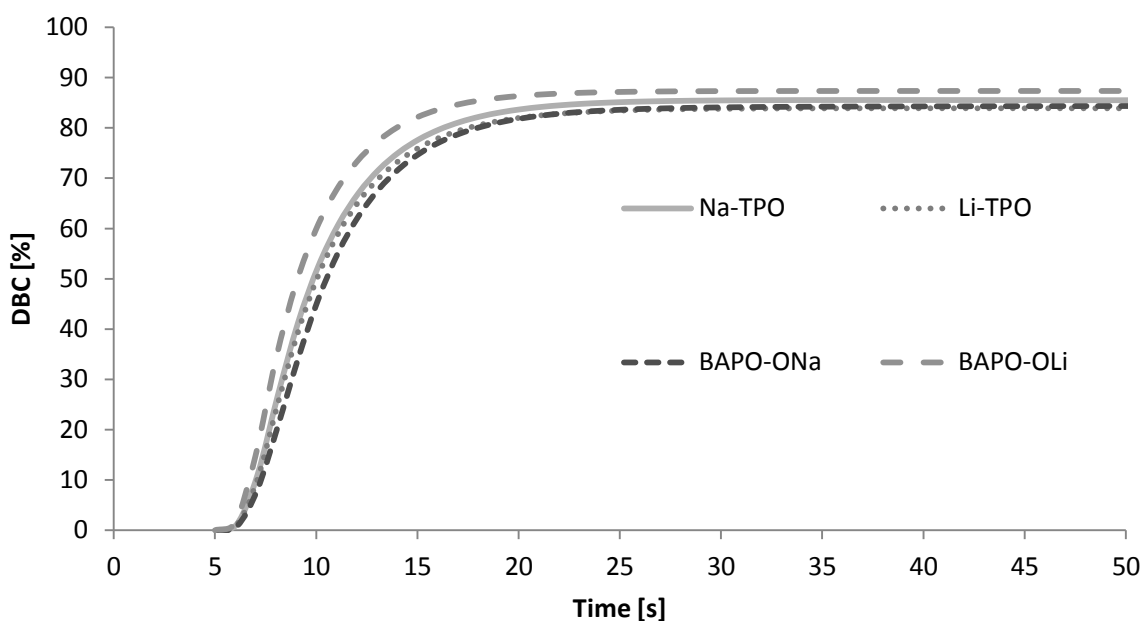


Figure 44. Double bond conversion (DBC) vs. time for the MAPO and BAPO salts in a concentration of 1 mol% in NAM + H₂O (40/60 w/w). Irradiation wavelength was 400-500 nm with an irradiation intensity of 1 W cm⁻¹.

The **MAPO** and **BAPO** salts clearly show higher reactivity than the references. With UV irradiation (320-500 nm) the **MAPO** salts **Na-TPO 55** and **Li-TPO 56** show best reactivity. The polymerization is very fast with rates of polymerization over 660 mmol L⁻¹ s⁻¹ and double bond conversions of over 97% are achievable. The **BAPO** salts **BAPO-ONa 57** and **BAPO-OLi 59** also show good reactivity with double bond conversions almost at 90%. The references **APi-180**, **I2959** and **Q-BPQ** only show DBCs around 80%. As expected, **Q-BPQ** shows the lowest reactivity because of its bimolecular Norrish type II initiation mechanism.

For visible light irradiation (400-500 nm), both the **MAPO** and **BAPO** salts show very good reactivity with double bond conversions around 85%. Only **BAPO-OLi 59** displays outstanding performance with a rate of polymerization of 750 mmol L⁻¹ s⁻¹.

The photo-DSC data can be summarized as following: The MAPO salts **Na-TPO 55** and **Li-TPO 56** show best reactivity for UV-irradiation and for visible light irradiation **BAPO-OLi 59** is the photoinitiator of choice.

The data from photo-DSC measurements can be found in the following table (Table 8):

Table 8. Comparison of the reactivity of the described MAPO and BAPO salts with state of the art photoinitiators as an overview.

Photo-DSC				
	t_{\max} [s] ^a	R_p [mmol L ⁻¹ s ⁻¹] ^a	DBC [%] ^a	$t_{95\%}$ [s] ^a
Na-TPO	8.0 (7.8)	690 (620)	99.1 (84.9)	16.2 (16.9)
Li-TPO	8.0 (7.9)	670 (590)	97.7 (83.7)	16.9 (17.2)
BAPO-ONa	7.9 (8.3)	620 (520)	89.8 (84.9)	17.9 (18.5)
BAPO-OLi	8.3 (7.3)	540 (750)	88.1 (87.6)	18.6 (15.9)
APi-180	9.5	480	84.4	21.2
I2959	8.8	540	82.2	19.5
Q-BPQ + MDEA	12.1	290	81.4	30.1

Footnote: 5. ^aValues for 320-500 nm irradiation and in brackets () values for 400-500 nm irradiation.

Experimental

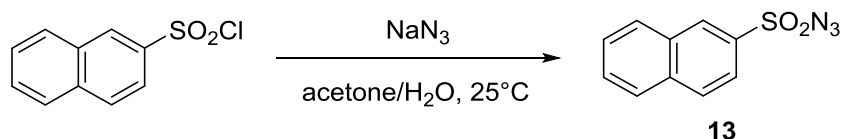
If not mentioned otherwise all syntheses were performed in an orange light lab, which provided light protection from wavelengths below 520 nm. Additionally inert atmospheres were used (typically argon) by application of basic Schlenk line techniques.

1. Bisphosphylketones

1.2. Syntheses

1.2.1. Carbonylbis(diethoxyphosphine oxide) **9**

1.2.1.1. 2-Naphthalenesulfonyl Azide **13**

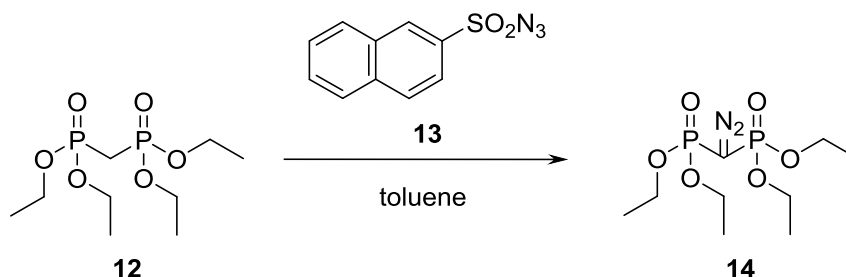


The diazotizing agent 2-naphthalenesulfonyl azide **13** was synthesized according to literature.³⁵ 2-Naphthalenesulfonyl chloride (4.03 g, 17.8 mmol, 1 eq.) was dissolved in acetone (24 mL). An aqueous (4 mL) solution of NaN₃ (1.16 g, 17.8 mmol, 1 eq.) was added over a period of 2 h at ambient temperature. Subsequent addition of 20 mL of water led to phase separation. The lower, brown organic phase contained the product and was separated, the solvent evaporated and the residue recrystallized from PE (53 mL g⁻¹) to yield the product **13**.

Yield: 2.0 g, 47%, yellowish powder

T_m = 44.6-45.8 °C; Lit³⁰.: 44-45 °C

1.2.1.2. Diazomethylenebis(diethoxyphosphine oxide) **14**



Methylenebis(diethoxyphosphine oxide) **12** could be reacted with the diazotizing agent **13** according to literature.³⁵ Potassium tert-butoxide (0.43 g, 3.9 mmol, 1.2 eq.) was mixed with toluene (33 mL) and cooled to 0°C. Methylenebis(diethoxyphosphine oxide) **12** (0.94 g, 3.2 mmol, 1 eq.) was dissolved in toluene (6 mL) and added dropwise over a period of 10 min., while the temperature was kept below 5°C. After stirring for 15 min. 2-naphthalenesulfonyl azide **13** (0.76 g, 3.2 mmol, 1 eq.) in toluene (6 mL) was added dropwise, while the temperature was kept below 5°C again. After 2 h at 25°C the reaction mixture was filtered and the solvent evaporated. As a work-up the residue was distilled via Kugelrohr distillation (120°C, 0.36 mbar).

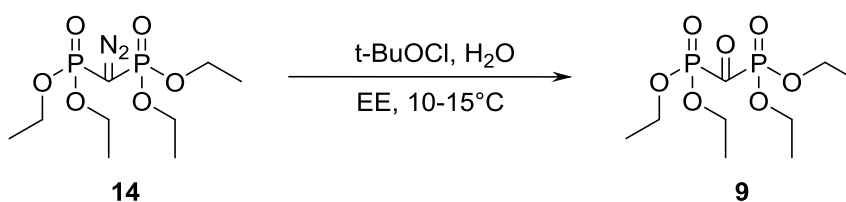
Yield: 0.52 g, 52%, yellow liquid

$^1\text{H-NMR}$ (CDCl_3): δ [ppm] = 1.30 (m, 3 H), 4.12 (m, 2H)

$^{13}\text{C-NMR}$ (CDCl_3): δ [ppm] = 25.2 (CH_3), 62.8 (CH_2)

T_{bp} = 120°C, 0.36 mbar ; Lit³⁵: 94-95°C, 0.010 torr

1.2.1.3. Carbonylbis(diethoxyphosphine oxide) **9**



Hydrolysis of Diazomethylenebis(diethoxyphosphine oxide) **14** led to the formation of carbonylbis(diethoxyphosphine oxide) **9**.³¹ Therefore water (0.17 mL, 9.3 mmol, 4 eq.) was dissolved in EE (46 mL). Diazomethylenebis(diethoxyphosphine oxide) **14** (0.73 g, 2.3 mmol, 1 eq.) was added and the mixture was cooled to 10-15°C. t-BuOCl (0.39 mL, 3.5 mmol, 1.5 eq.) in EE (23 mL) was added, which led to strong N₂ formation and a change in color to strong yellow. Chlorotrimethyl silane (1.18 mL, 9.3 mmol, 4 eq.) was added and after stirring for 5 min the solvent was evaporated. Further purification led in any case to product decomposition.

Yield: ~3 mg, ~5% (calculated from ¹H-NMR), yellow liquid

¹H-NMR (CDCl₃): δ [ppm] = 1.26 (m, 3 H), 4.15 (m, 2H)

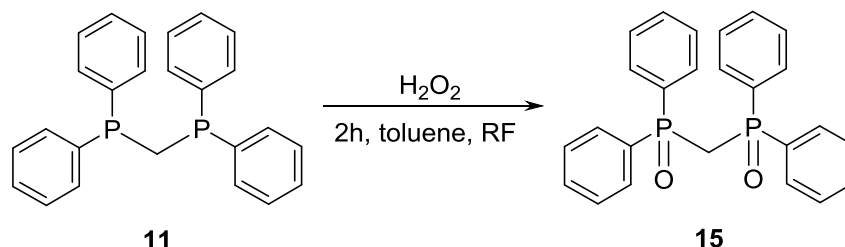
³¹P-NMR (CDCl₃): δ [ppm] = 6.84

GC-MS (EI, CH₂Cl₂): m/z: 299.87 (M), 271.84 (M - Et), 243.82 (M - (Et)₂), 219.93 (M - (Et)₃), 191.90 (M - (Et)₄), 163.91 (COPO(OEt)₂), 108.97 (COPO(O)₂), 92.06 (PCOP), 91.02 (POOEt), 65.00 (POO)

IR (ATR) [cm⁻¹]: 1666.25 ν(C=O)

1.2.2. Carbonylbis(diphenylphosphine oxide) **8**

1.2.2.1. Methylenebis(diphenylphosphine oxide) **15**



The synthesis according to literature³⁸ was modified to avoid the formation of acetoneperoxide. Methylenebis(diphenylphosphine) **11** (4.17 g, 10.8 mmol, 1 eq.) was dissolved in toluene (55 mL) and H₂O₂ (30%, 4.34 mL, 43.4 mmol, 4 eq.) was added dropwise. After heating 2 h at reflux the solvent was evaporated and the residue dissolved in chloroform (10 mL). The resulting solution was washed with

aqueous NaHCO₃ (30 mL) and water (30 mL). The organic phase was dried with Na₂SO₄ and the solvent again evaporated. Purification was done via recrystallization from ethyl acetate (34 mL g⁻¹), which gave the product methylenebis(diphenylphosphine oxide) **15** as a white powder.

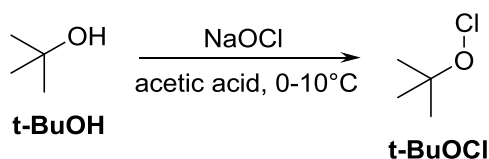
Yield: 3.7g, 83%, white powder

¹H-NMR (CDCl₃): δ [ppm] = 3.49 (t, 2 H), 7.15-7.41 (m, 12H), 7.66 (t, 8H)

¹³C-NMR (CDCl₃): δ [ppm] = 34.6 (CH₂), 128.47 (Ar-CH), 131.01 (Ar-CH), 131.85 (Ar-CH), 132.41 (Ar-CH)

T_m = 185-186 °C; Lit³⁸: 186-186.5 °C

1.2.2.2. t-BuOCl



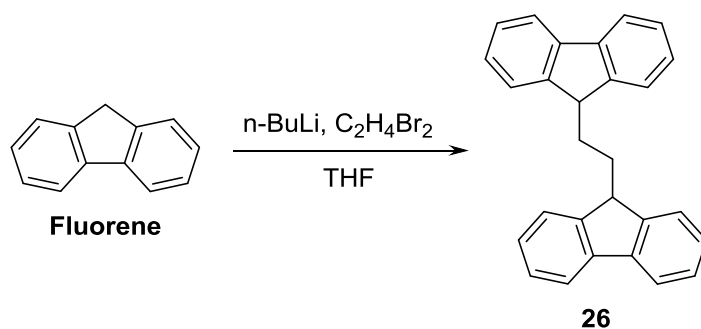
The synthesis of t-BuOCl can be found in literature.^{36,37} NaOCl (15%, 114 mL, 276 mmol, 1 eq.) was added to water (114 mL). The solution was cooled to 10°C. t-BuOH (26 mL) mixed with acetic acid (16 mL) was added and vigorously stirred for 3 min. Subsequently the phases were separated and the yellow organic phase was washed with an aqueous solution of Na₂CO₃ (10 wt%) (100 mL) and brine (100 mL) respectively. After drying with CaCl₂ and filtration the product t-BuOCl was stored in a brown glass flask over CaCl₂ at 6°C. The liquid was characterized by its pungent smell and look (colorless, in contrast to the yellow starting material NaOCl). Further characterization was not possible due to stability issues.

Yield: 9.9 g, 33%, colorless liquid

2. Zirconium Complexes

2.2. Syntheses

2.2.1. Bis(9-fluorenyl)ethane **26**



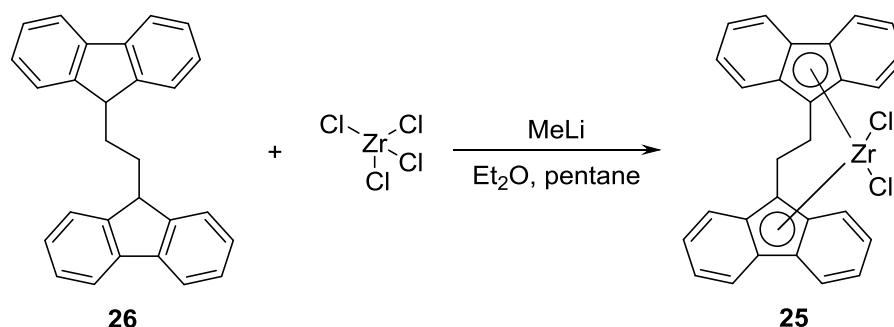
The synthesis was performed with slight modifications in regards to literature.^{58,59} Fluorene (13.9 g, 83.7 mmol, 1 eq.) was dissolved in THF (98 mL) and cooled to 0°C. n-BuLi (2.5M in hexane, 33.5 mL, 83.7 mmol, 1 eq.) was added dropwise and the reaction mixture was allowed to warm to ambient temperature. After stirring for 5 h the mixture was again cooled to 0°C and 1,2-dibromoethane (3.6 mL, 41.8 mmol, 1 eq.) was added dropwise. Subsequently the reaction mixture was again allowed to warm to ambient temperature and stirred overnight (16 h). Quenching with aqueous NH₄Cl (70 mL) led to phase separation. The organic phase was separated and dichloromethane (~100 mL) was added until all precipitate was dissolved. Washing with water and evaporating the solvent gave a residue, which could be recrystallized from ethanol (~100 mL g⁻¹) to yield the product **26** with 90% purity. Since starting materials and side products can complex with ZrCl₄ further purification was not necessary.⁶⁰

Yield: 14.6 g, 48.6%, white powder

¹H-NMR (CDCl₃): δ [ppm] = 1.75 (m, 4H), 3.85 (broad s, 2H), 7.1-7.5 (m, 12H), 7.73-7.77 (d, 4H)

T_m = 207-208 °C; Lit¹⁶³: 207.5 °C

2.2.2. (Ethylenebis(9-fluorenyl))zirconiumdichloride **25**



The synthesis is described in literature but the work-up had to be adapted to yield pure product **25**.⁵⁹ Bis(9-fluorenyl)ethane **26** (1.33 g, 3.7 mmol, 1 eq.) was added to diethyl ether (55 mL) and cooled to 0°C. MeLi (1.6 M, 4.6 mL, 7.4 mmol, 1 eq.) was added dropwise and afterwards the reaction mixture was allowed to warm to ambient temperature. After gas formation stopped (~1 h) stirring was continued for 19.5 h. The resulting slurry was again cooled to 0°C and added to a slurry of ZrCl₄ (0.86 g, 3.7 mmol, 1 eq.) in pentane (37 mL). Afterwards the reaction mixture was allowed to warm to room temperature and stirred for 2 h. The resulting red precipitate was filtered off and dried in high vacuum. Starting materials and side products were removed by washing this red solid in a Soxhlet-extractor for 20 h with diethyl ether (200 mL). After drying again in high vacuum the red solid was dissolved in dichloromethane (200 mL g⁻¹) and filtered, whereby a white solid could be removed, which is most likely clustered zirconium chloride. The red filtrate was once again dried in high vacuum, which gave the product **25**.

Yield: 1.05 g, 54.8%, deeply red powder

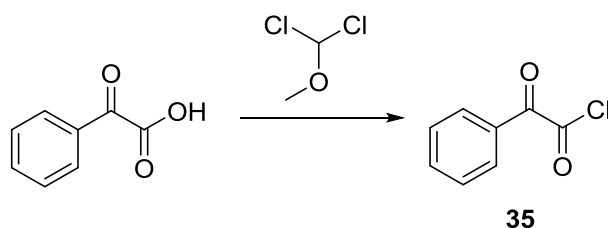
¹H-NMR (CDCl₃): δ [ppm] = 4.41 (s, 4H), 7.04-7.27 (sext, 8H), 7.61-7.80 (q, 8H)

3. Diketone Systems

3.3. Syntheses

3.3.1. Synthesis of Phenylglyoxylic Diethylphosphite 36 and Phenylglyoxylic Diphenylphosphine Oxide 32 (Pathway D)

3.3.1.1. Phenylglyoxylic Acid Chloride 35



Phenylglyoxylic acid chloride was prepared according to known procedures.⁷⁴ Dichloromethoxymethane (5.11 g, 44.5 mmol, 1.5 eq.) was added to phenylglyoxylic acid (4.45 g, 30 mmol, 1 eq.) under argon atmosphere. The reaction mixture was stirred for 1 h at 50°C. Work-up via Kugelrohr distillation gave the pure product **35**.

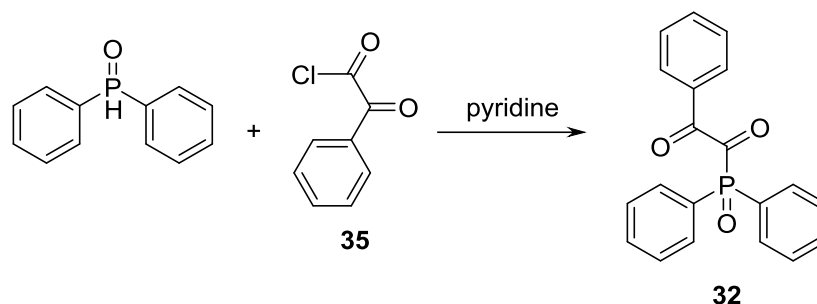
Yield: 1.9 g, 38 %, yellow liquid

¹H-NMR (CDCl₃): δ [ppm] = 7.5 (m, 3H), 7.7 (m, 2H)

¹³C-NMR (CDCl₃): δ [ppm] = 181.29 (CO-Ar), 166.88 (CO-Cl), 136.15 (Ar-CH), 131.76 (Ar-CH), 130.68 (Ar-CH), 129.51 (Ar-CH)

T_{bp} = 87°C, 10 torr; Lit⁷⁴.: 80°C, 3 torr

3.3.1.2. Phenylglyoxylic Diphenylphosphine Oxide **32**



In a Einhorn-type acylation reaction⁷³ phenylglyoxylic acid chloride **35** (1.66 g, 9.9 mmol, 1.1 eq.) and pyridine (3.62 mL, 44.9 mmol, 5 eq.) were dissolved in toluene (15 mL) and stirred for 10 min. at ambient temperature. This solution was added to diphenylphosphine oxide (1.81 g, 9.0 mmol, 1 eq.) in toluene (15 mL). The reaction mixture turned red immediately and aluminum foil was used to protect it from light. After 2 h stirring at ambient temperature it was washed with water, the organic phase dried with sodium sulfate and the solvent evaporated. The red/purple residue was dissolved in EE and filtered over silica gel. Subsequent removal of the solvent gave the red product **32** in a purity >90%.

Yield: 1.87 g, 62.3%, red needles

GC-MS (CH₂Cl₂, EI): m/z: 335.04 (M), 201.09 (POAr₂), 118.06, 105.15 (ArCO), 90.17 (ArC), 77.07 (Ar)

HR-MS (MeOH, ESI⁻): m/z: 201.07619 (Ph₂PO⁻)

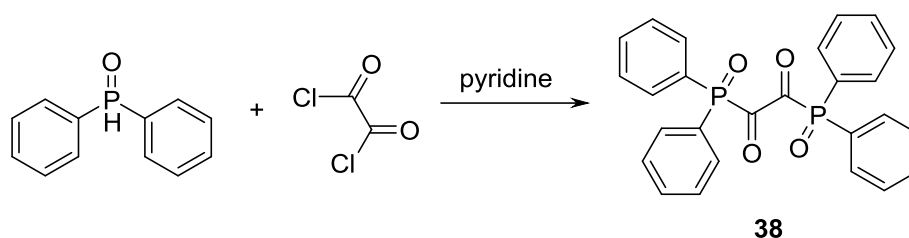
¹H-NMR (CD₂Cl₂): δ [ppm] = 7.89-7.10 (m, 15H)

¹³C-NMR-CPD (CD₂Cl₂): δ [ppm] = 193.0 (PCO), 192.2 (ArCO), 136.3 (CAr), 134.2 (CAr), 133.0 (CAr), 132.0 (CAr), 129.8 (CAr), 129.0 (CAr), 128.9 (CAr), 128.7 (CAr)

³¹P-NMR (CD₂Cl₂): δ [ppm] = 32.7

T_m = 49-52 °C

3.3.2. Synthesis of Oxalylbis(diphenylphosphine Oxide) **38**



The already established Einhorn-acylation was also used to synthesize the bis substituted product **38**. Under argon atmosphere a solution of oxalylchloride (0.51 mL, 11.7 mmol, 0.9 eq.) and pyridine (5.28 mL, 65.4 mmol, 10 eq.) in dichloromethane (15 mL) was made and stirred for 10 min. at ambient temperature. This solution was added to diphenylphosphine oxide (2.65 g, 13.1 mmol, 1 eq.) in dichloromethane (15 mL). After stirring for 2 h at ambient temperature the reaction mixture was washed with water and the aqueous phase was separated. The organic phase was dried with sodium sulfate and the solvent removed. The residue was dissolved in EE and filtered over silica gel. Subsequent elution with methanol and removal of the solvent gave the red product **38** in a purity >80%.

Yield: 2.15 g, 35.8%, red solid

LC-MS (MeOH, DUII): m/z: 459.1 (M)

HR-MS (MeOH, ESI⁻): m/z: 201.07617 (Ph₂PO⁻)

¹H-NMR (CD₂Cl₂): δ [ppm] = 8.19-6.56 (m, 20H)

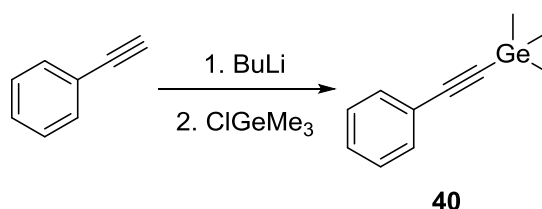
¹³C-NMR-CPD (CD₂Cl₂): δ [ppm] = 132.5 (CAr), 130.6 (CAr), 128.9 (CAr), 127.7 (CAr)

³¹P-NMR (CD₂Cl₂): δ [ppm] = 20.6

T_m = 43-45 °C

3.3.3. Synthesis of Phenylglyoxylic Tri(m)ethylgermanium 33 and 39

3.3.3.2.1. 2-Phenyl-1-trimethylgermylethine 40



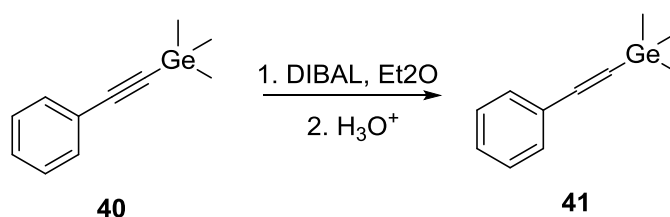
This synthesis and the following steps were a modification of the synthesis for a corresponding silicon compound.⁷⁰ To a solution of phenyl ethyne (2.05 g, 20.1 mmol, 1 eq.) in anhydrous tetrahydrofuran (15 mL) under an argon atmosphere at -78 °C a solution of butyl-lithium in hexane (2.5M, 9.65 mL, 24.1 mmol, 1.2 eq.) was added and the mixture was stirred at -78 °C for two hours. Trimethyl chlorogermane (2.98 mL, 24.1 mmol, 1.2 eq.) was added, and the reaction mixture was allowed to reach room temperature over a period of one hour. The solution was poured into saturated ammonium chloride solution (20 mL) and extracted with dichloromethane (3 x 20 mL). The combined organic layers were washed with water (20 mL) and brine (20 mL), and dried over sodium sulphate. Evaporation of the solvent, followed by bulb-to-bulb distillation (Kugelrohr) gave the product **40**.

Yield: 2.27 g, 51.6%, colorless liquid

¹H-NMR (CDCl₃): δ [ppm] = 0.32 (s, 9H), 7.11-7.20 (m, 3H), 7.29-7.39 (m, 2H)

T_{bp} = 87°C, 1.5 torr; Lit⁷⁶: 70 °C, 1.5 torr

3.3.3.2.2. Z-2-Phenyl-1-trimethylgermylethene 41



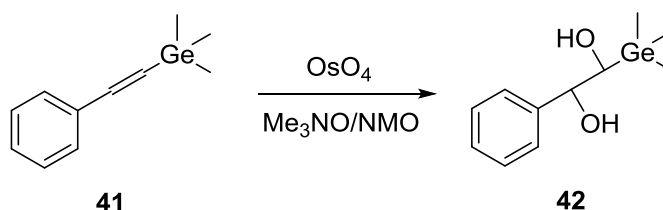
To a stirred solution of 2-phenyl-1-trimethylgermylethine **40** (1.59 g, 7.2 mmol, 1 eq.) and N-methylmorpholine (1.19 mL, 11 mmol, 1.5 eq.) in anhydrous ether (8 mL) at room temperature, was added dropwise a diisobutyl aluminium hydride solution in heptane (1M, 10.9 mL, 11 mmol, 1.5 eq.). The solution was stirred overnight at room temperature under an argon atmosphere. The mixture was then poured into a separating funnel containing cold 10% hydrochloric acid and ice. The layers were separated, and the aqueous layer was extracted with ether. The combined organic extracts were washed with water and brine, and dried over magnesium sulphate. Evaporation of the solvent followed by bulb-to-bulb distillation of the residue (Kugelrohr) gave the product **41** with >90% purity.

Yield: 0.83 g, 52%, colorless liquid

$^1\text{H-NMR}$ (CDCl_3): δ [ppm] = 0.31 (s, 9H), 6.11 (d, 1H), 7.33-7.44 (m, 5H) 7.49 (d, 1H)

T_{bp} = 60-62°C, 0.5 torr; Lit¹⁶⁴: 83 °C, 4 torr

3.3.3.2.3. Anti-2-hydroxy-2-phenyl-1-trimethylgermylethanol **42**

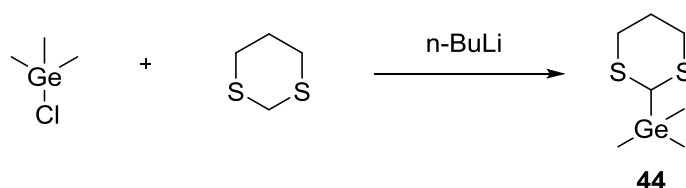


Z-2-Phenyl-1-trimethylgermylethene (0.39 g, 1.8 mmol, 1 eq.) was added to a solution of tert-butanol (3.9 mL), water (0.8 mL), and pyridine (0.16 mL). Trimethylamine N-oxide dihydrate (0.27 g, 2.5 mmol, 1.4 eq.) and osmium tetroxide (9 mg, 0.035 mmol, 0.02 eq.) were added to the solution and the mixture boiled under reflux under an argon atmosphere for twelve hours. Work-up: Aqueous sodium bisulphite (20 mL) was added and the solvent removed under reduced pressure. The residue was added to saturated aqueous ammonium chloride (100 mL) and extracted with dichloromethane (20 mL) in a continuous extractor. The organic layer was dried with sodium sulphate. Evaporation of the solvent gave 256 mg of the raw product, which contained estimated <5% product **42**.

Yield: ~14 mg, ~3%, estimated by GC-MS

GC-MS (EI, CH₂Cl₂): m/z: 253.09 (M), 219.83 (M – (OH)₂), 204.95, 175.00 (M – Ar), 147.00 (OHCHGe(CH₃)₃), 115.08, 88.99 (ArCH)

3.3.3.5.1. (1,3-Dithian-2-yl)trimethylgermane 44



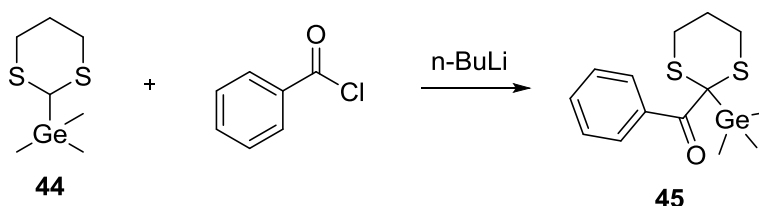
To 1,3-dithian (0.72 g, 6 mmol, 0.95 eq.) in dry THF (30 mL) was added n-BuLi (2.53 mL, 6 mmol, 1 eq.) under argon atmosphere at -10°C within 11 min. The resulting slurry was warmed to 0°C and trimethylgermanium chloride (0.78 mL, 6 mmol, 1 eq.) in THF (19 mL) was added dropwise within 30 min. Subsequently, the reaction mixture was stirred at 0°C for 3 h. Afterwards, the solution was concentrated and HCl (2%) was added. Extraction with diethyl ether and Kugelrohr distillation gave the product **44**.

Yield: 533 mg, 37.5%, colorless liquid

¹H-NMR (CDCl₃): δ [ppm] = 3.80 (d, 1H), 2.79 (m, 4H), 2.06 (m, 2H), 0.28 (s, 9H)

T_{bp} = 60°C, 0.5 torr; Lit¹⁶⁵: 99 °C, 3 torr

3.3.3.5.2. Phenyl(2-(trimethylgermyl)-1,3-dithian-2-yl)methanone 45



(1,3-Dithian-2-yl)trimethylgermane **44** (0.56 g, 2 mmol, 1 eq.) was dissolved in dry THF (11 mL) and cooled to -15°C. n-BuLi (0.95 mL, 2 mmol, 1 eq.) was added dropwise within 11 min. The reaction mixture was warmed to 0°C and added to a 0°C solution of benzoyl chloride (0.26 mL, 2 mmol, 0.95 eq.) in THF (7 mL). After stirring for 3 h water was added and the resulting solution extracted with diethyl ether. The combined organic phase was washed with water and brine, dried with sodium sulfate and the solvent evaporated. Kugelrohr distillation gave the product **45**.

Yield: 158 mg, 23.1%, colorless liquid

GC-MS (CH₂Cl₂, EI): m/z: 339.37 (M), 237.41 (M – ArCO), 133.34 (Dithian + Me)

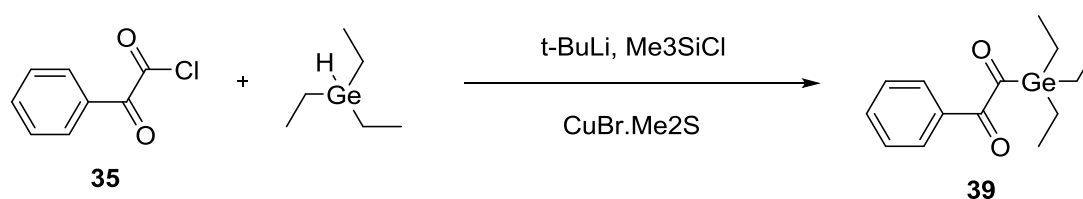
HR-MS (MeOH, ESI⁺): m/z: 341.15607 (M)

¹H-NMR (CD₂Cl₂): δ [ppm] = 7.89-7.10 (m, 15H)

¹³C-NMR-CPD (CD₂Cl₂): δ [ppm] = 192.7 (CO), 134.8 (CAr), 133.4 (CAr), 128.8 (CAr), 31.3 (SCS), 27.2 (SCH₂), 25.3 (CH₂), 0.05 (CH₃)

T_{bp} = 160°C, 0.1 mbar

3.3.3.6. Phenylglyoxylic Triethylgermanium **39**



To a solution of triethylgermanium hydride (0.47 g, 3.4 mmol, 1 eq.) in dry THF (1 mL) at -10°C under argon atmosphere was added t-BuLi (1.71 mL, 2.9 mmol, 0.85 eq.) within 3 min. After stirring the mixture for 5 min. it was added to vigorously stirred slurry of CuBr.Me₂S (0.60 g, 2.9 mmol, 0.85 eq.) in THF (15 mL) at -78°C. Stirring at -78°C for 1 h resulted in a deeply red liquid. Me₃SiCl (0.24 mL, 1.9 mmol, 0.55 eq.) was added to the reaction mixture, which was then stirred for 5 min. Afterwards a solution of phenylglyoxylic acid chloride **35** (0.32 g, 1.9 mmol, 0.55 eq.) in THF (1

mL) was added and the mixture turned black. The flask was wrapped in aluminum foil and the solution stirred for 1 h at -78°C and for 2 h at -30°C.

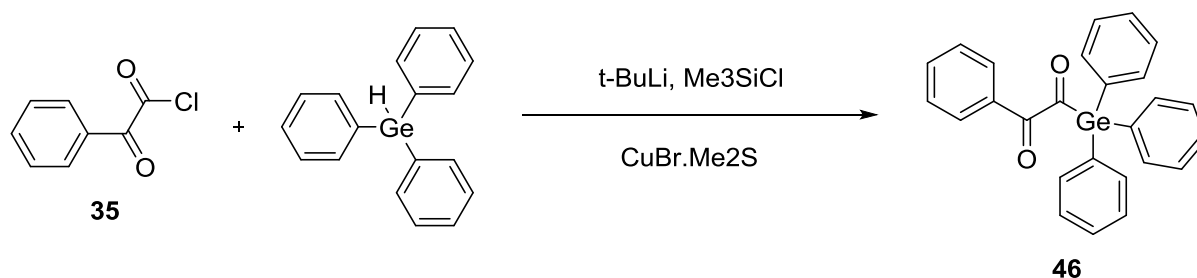
As a work-up the reaction mixture was poured in aqueous NH₄Cl-NH₄OH (pH 8-9, 18 mL) und diluted with diethyl ether (18 mL). The heterogeneous mixture was vigorously stirred until the aqueous phase was deeply blue and no color change was visible anymore (~15 min.). Afterwards the phases were separated and the aqueous phase was extracted with diethyl ether. The combined organic phase was washed with water and then with brine, dried with sodium sulfate and the solvent evaporated. The deeply red and liquid raw product was purified via column chromatography (PE:EE = 50:1), which yielded pure product **39**. Low product yield and stability issues even under argon atmosphere made further characterization impossible.

Yield: 64 mg, 6.4%, deeply red liquid

GC-MS (CH₂Cl₂, EI): m/z: 324.20 (M + Et), 293.20 (M), 261.27 (M – Et), 235.29 (M – Et₂), 205.32 (M – Et₃), 177.27 (MeGeEt₃), 133.27 (ArCOCO), 103.21 (ArCO), 75.10 (Ar)

¹H-NMR (CD₂Cl₂): δ [ppm] = 7.95 (d, 2H), 7.66 (t, 1H), 7.51 (t, 2H), 1.08 (s, 15H)

3.3.4. Phenylglyoxylic Triphenylgermanium 46



To a solution of triphenylgermanium hydride (2.09 g, 6.9 mmol, 1 eq.) in dry THF (2.3 mL) at -10°C under argon atmosphere was added $t\text{-BuLi}$ (3.43 mL, 5.8 mmol, 0.85 eq.) within 3 min. After stirring the mixture for 5 min. it was added to vigorously stirred slurry of $\text{CuBr}\cdot\text{Me}_2\text{S}$ (1.20 g, 5.8 mmol, 0.85 eq.) in THF (30.1 mL) at -78°C. Stirring at -78°C for 1 h resulted in a deeply red liquid. Me_3SiCl (0.48 mL, 3.8 mmol, 0.55 eq.)

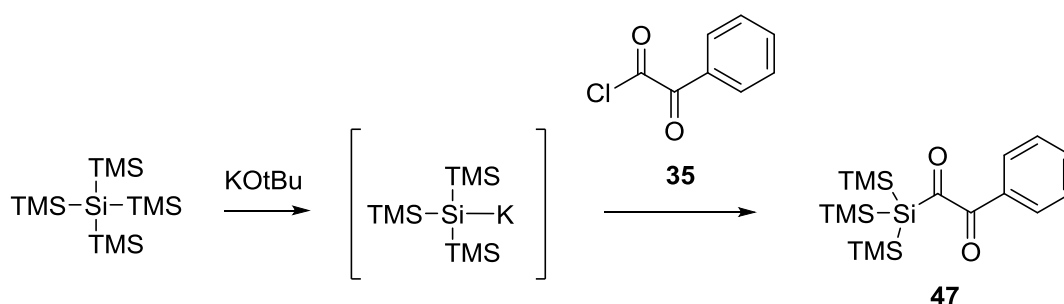
was added to the reaction mixture, which was then stirred for 5 min. Afterwards a solution of phenylglyoxylic acid chloride **35** (0.64 g, 3.8 mmol, 0.55 eq.) in THF (2.3 mL) was added and the mixture turned black. The flask was wrapped in aluminum foil and the solution stirred for 1 h at -78°C and for 2 h at -30°C.

As a work-up the reaction mixture was poured in aqueous NH₄Cl-NH₄OH (pH 8-9, 18 mL) und diluted with diethyl ether (18 mL). The heterogeneous mixture was vigorously stirred until the aqueous phase was deeply blue and no color change was visible anymore (~15 min.). Afterwards the phases were separated and the aqueous phase was extracted with diethyl ether. The combined organic phase was washed with water and then with brine, dried with sodium sulfate and the solvent evaporated. The deeply red and liquid raw product was purified via column chromatography (PE:EE = 50:1), which yielded pure product **46**. Yield of product and stability even under argon atmosphere were too low, to reasonably get ¹³C-NMR-spectra and characterization with GC-MS was not possible.

Yield: 33 mg, 1.1%, deeply red solid

¹H-NMR (CD₂Cl₂): δ [ppm] = 7.96 (d, 2H), 7.70-7.21 (m, 15H)

3.3.5. Synthesis of Phenylglyoxylic Trimethylsilyl Silicium **47**



Tetrakis(trimethylsilyl)silan (0.7 g, 2.2 mmol, 1 eq.) and KOtBu (0.26 g, 2.3 mmol, 1.05 eq.) were dissolved in dimethoxyethane (10 mL). The mixture was stirred for 2 h at ambient temperature. The resulting solution was added dropwise over a period of 40 min to phenylglyoxylic acid chloride **35** (0.39 g, 2.3 mmol, 1.05 eq.), which was dissolved in diethyl ether (5 mL) and cooled to -40°C. After complete addition the

reaction mixture was allowed to warm to ambient temperature and stirred for another hour. Subsequently, HCl (3%) was added resulting in a phase separation. The aqueous phase was extracted with diethyl ether and the combined organic phase was dried with sodium sulfate and the solvent removed. Column chromatography (DCM:PE = 1:1) gave the pure product **47**. Stability of the product was even under argon atmosphere too low to conduct NMR measurements of over 15 min. For this reason only $^1\text{H-NMR}$ spectra are given and for further characterization color and UV-VIS spectra were used respectively.

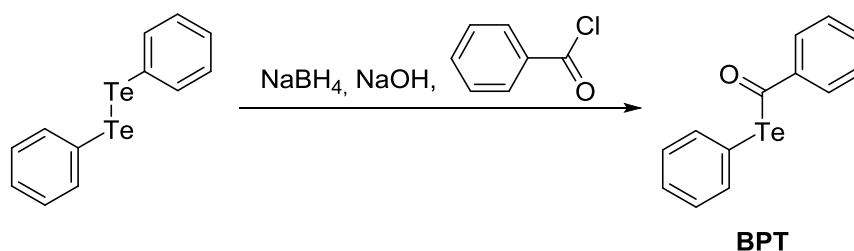
Yield: 276 mg, 33%, yellow oil

$^1\text{H-NMR}$ (CDCl_3): δ [ppm] = 7.93–6.76 (5H, m), 0.07 (27H, s)

4. Acytellurides

4.2. Syntheses

4.2.1. Benzoyl Phenyltelluride BPT



The following procedure is slightly modified from that of Gardner et al.⁹¹ Diphenyl ditelluride (1.32 g, 3.23 mmol, 1 eq.) was dissolved in a mixture of toluene and ethanol (5 mL, 25/75 v/v) and heated to reflux. To this solution NaBH_4 (0.20 g, 5.17 mmol, 0.8 eq.) dissolved in 1N NaOH (4.4 mL) was added dropwise. During the addition there appeared a strong formation of H_2 and the solution became colorless. Then benzoyl chloride (1.09 g, 0.89 mL, 7.75 mmol, 1.22 eq.) was added in one portion and the warm reaction mixture was stirred for another 5 min. Afterwards 25 mL of water were added and the resulting mixture was extracted with diethyl ether. The combined organic phase was dried over anhydrous NaSO_4 and after removal of

the solvent the crude product was purified via liquid chromatography (PE:Et₂O = 20:1, silica gel) to yield pure **BPT**.

Yield: 0.74 g, 74%, bright yellow powder

GC-MS (THF, EI): m/z: 311.96 (M), 282.00, 206.99, 154.10, 105.03, 77.06

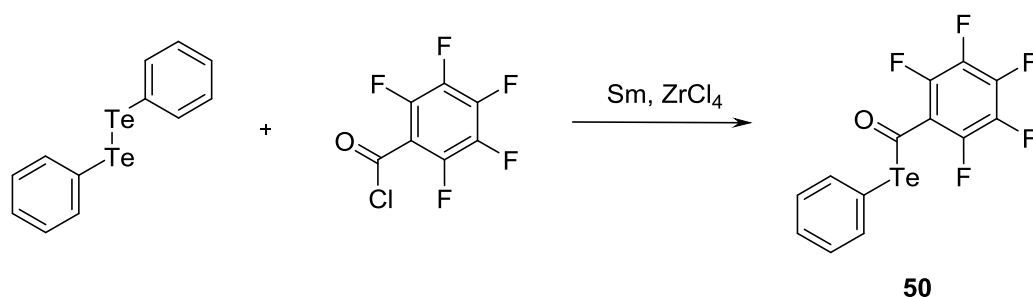
¹H-NMR (CD₂Cl₂): δ [ppm] = 7.75-7.49 (m, 5H), 7.48-7.20 (m, 5H)

¹³C-NMR (CDCl₃): δ [ppm] = 143.3 (Ar-C-CO), 141.1 (Ar-CH), 134.5 (Ar-CH), 129.9 (Ar-CH), 129.6 (Ar-CH), 129.3 (Ar-CH), 127.3 (Ar-CH), 125.7 (Ar-C-Te)

IR (ATR) [cm⁻¹]: 1663.47 ν(C=O)

T_m = 70-72°C; Lit⁹⁹: 70-72°C

4.2.2. Pentafluorobenzoyl Phenyltelluride **50**



Samarium (301 mg, 2.00 mmol, 1.0 eq.), diphenyl ditelluride (410 mg, 1.00 mmol, 1 eq.) and zirconium tetrachloride (93 mg, 0.40 mmol, 0.2 eq.) were weighed into the reaction vessel (Schlenk tube) using a Glove box and Schlenk tubes. Dry THF (20 mL) was added and the mixture was stirred for 2 h at room temperature undergoing a change in color from red to brown, indicating the reduction of the bond between the two tellurium atoms. Then, pentafluorobenzoyl chloride (692 mg, 3.00 mmol, 1.5 eq.) was added to the mixture rapidly using a syringe. The acid chloride was stored in a Schlenk tube under argon atmosphere to prevent hydrolysis and in the refrigerator due to its apparently low flash point (49.7°C). The reaction mixture was stirred for 1 h at ambient temperature, followed by the evaporation of the solvent applying vacuum. Dry dichloromethane (50 mL) was then added to the gray/black precipitate and stirred

for 30 min to dissolve the product. Afterwards, the precipitate was separated from the product solution using a funnel filter. The solvent was evaporated giving the crude product **50**, which was purified using liquid chromatography (PE:CH₂Cl₂ 10:1 + triethyl amine).

Yield: 392 mg, 49%, yellow solid

¹H-NMR (CD₂Cl₂): δ [ppm] = 7.73 (m, 2H), 7.30 (m, 3H)

¹³C-NMR-APT (CD₂Cl₂): δ [ppm] = 140.9 (Ar-C-CO), 140.5 (Ar-CH), 130.2 (Ar-CH), 130.1 (Ar-CH)

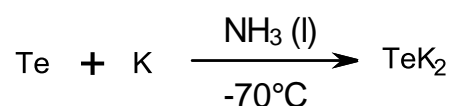
GC-MS (THF, EI): m/z: 401.90 (M), 206.93 (ArTe), 194.96 (ArF₅CO), 166.96 (ArF₅), 77.04 (Ar)

IR (ATR) [cm⁻¹]: 1673.32 ν(C=O)

R_f-value (PE:CH₂Cl₂ 10:1): 0.31

4.2.5. Synthesis of Bis(2-methoxybenzoyl)telluride **56**

4.2.5.1. TeK₂

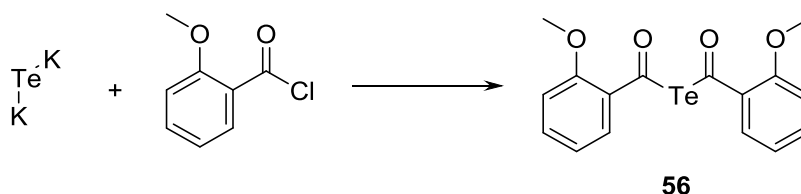


By using a Glove box providing argon atmosphere, elemental potassium (7.55 g, 194.37 mmol, 2.0 eq.) and tellurium powder (12.401 g, 97.18 mmol, 1.0 eq.) were weighed into a Schlenk tube. Then, gaseous ammonia was passed over a condenser into the mixture. For cooling to -70°C, an acetone/liquid N₂ mixture was used. After condensing ammonia (150 mL) into the reaction vessel, the mixture was intensively stirred for 6 hours at -70°C under argon. The color of the solution changed to purple, indicating the ionization of potassium. Afterwards, cooling was stopped and temperature was raised gradually to room temperature overnight forming potassium telluride. The majority of ammonia was evaporated at this point. To remove last

traces of NH_3 , the reaction vessel was put into a tube furnace giving the product TeK_2 .

Yield: 14 g, 70%, bright brown solid

4.2.5.2. Bis(2-methoxybenzoyl)telluride **56**



Potassium telluride (517 mg, 2.51 mmol, 1 eq.) was weighed into a Schlenk tube using a Glove box. Afterwards, dry acetonitrile (25 mL) was added under argon and the mixture was cooled to 0°C . Then, a cooled solution of 2-methoxybenzoyl chloride (0.84 mL, 6.3 mmol, 2.5 eq.) in acetonitrile (12 mL) was added slowly to the potassium telluride suspension under argon using a syringe. After that, the reaction mixture was stirred for 3 hours at 0°C . Acetonitrile was removed applying vacuum and diethyl ether (32 mL) was added, before stirring for another 45 min. The black precipitates were removed by filtration using a funnel filter, giving a yellow filtrate. Diethyl ether was then largely removed keeping 1 mL of the solution, followed by 3 washing steps each with 5 mL of dry n-pentane. After each step, the supernatant was removed with a pipette. Vaporization of solvent residues gave the product bis(2-methoxybenzoyl)telluride **56**.

Yield: 580 mg, 58%, yellow crystals

$^1\text{H-NMR}$ (CD_2Cl_2): δ [ppm] = 7.88 (d, 2H), 7.49 (t, 2H), 6.96 (m, 4H), 3.75 (s, 6H)

$^{13}\text{C-NMR-APT}$ (CD_2Cl_2): δ [ppm] = 160.5 (Ar-C-O), 135.7 (Ar-CH), 133.2 (Ar-CH), 120.7 (Ar-CH), 118.5 (Ar-CH), 112.6 (Ar-CH), 56.3 (CH_3)

IR (ATR) [cm^{-1}]: 1729.50 $\nu(\text{C}=\text{O})$

R_f -value (CH_2Cl_2): 0.70

4.5.2. Kinetic Studies

The photopolymerization of the four different monomers (BA, BMA, St, NAM) was carried out in a photoreactor. The reactor was filled to a height of approximately 25 mm with monomer formulation (monomer + BPT/BDC), which was degassed with argon. For irradiation an OmniCure 2000 (Lumen Dynamic) mercury lamp with a filter excluding all but 400-500 nm was used. The effective irradiation intensity was adjusted to the reactivity of the monomer (0.07 W cm^{-2} on the surface of the formulation for BA, BMA and St and 0.03 W cm^{-2} on the surface for NAM). For the more reactive monomers a lower effective irradiation intensity and photoiniferter/TERP-reagent to monomer molar ratio was chosen (BA: 1:200, BMA: 1:100, St: 1:100, NAM: 1:500), to make sure the polymerization would be slow enough to take samples. These samples were taken with a syringe over the side joint of the reactor. Typical sample size was 0.05 mL of which 10 mg was used for GPC analysis and the rest of approximately 40-50 mg was used for $^1\text{H-NMR}$ -spectroscopy.

For determination of the number-average molecular weight (M_n) and the polydispersity index (PDI) a Waters 717plus GPC with three columns (Styragel HR 0.5 THF, Styragel HR 3 THF and Styragel HR 4 THF) and a Waters 2410 refractive index detector was used. The eluent was THF with a flow rate of 1.0 mL min^{-1} and the temperature was set to 40°C . For calibration polystyrene standards were used which offer a molecular weight resolving range of 10^2 - 10^6 g/mol .

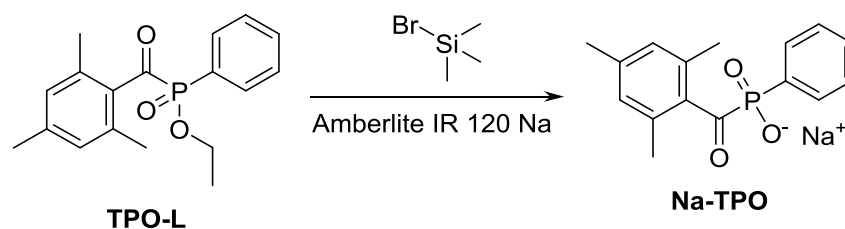
A Bruker AC-E-200 FT-NMR-spectrometer was used for the samples taken from the photoreactor, to determine the monomer double bond conversion. The solvent was deuterated chloroform (CDCl_3) with a degree of deuteration $\geq 99.8\% \text{ D}$. Out of these spectra the double bond conversion was calculated by comparing the integrals of the monomer specific double bonds to the combined integrals of the side chains of monomer and polymer.

5. Water-Soluble Photoinitiators

5.2. Syntheses

5.2.1. Syntheses of the MAPO-Salts Na-TPO and Li-TPO

5.2.1.1. Sodium Phenyl(2,4,6-trimethylbenzoyl)phosphine Oxide (Na-TPO) Synthesized with Ion Exchange Resin



This route is described completely in literature.¹⁵⁵ Trimethylbenzoylphenylphosphine acid ethylester (Lucirin® TPO-L, BASF AG; 1.02 g, 3.22 mmol, 1 eq.) was dissolved in MeCN (3 mL) and bromotrimethylsilane (1.06 g, 6.93 mmol, 2.15 eq.) was added. After 4 h at 60°C, MeOH/H₂O (32 mL, MeCN/H₂O = 95/5 v/v) was added. After removal of the solvent a white solid was obtained, which was assumed to be the free acid. H₂O (10 mL) and Amberlite IR 120 Na (5 g) were added. After the reaction was finished, visible in complete solution of the former white precipitate (~2.5 h), the product was dissolved in MeOH (40 mL) and filtered. Removal of the solvent and subsequent recrystallization from diethyl ether gave the product **Na-TPO** as yellowish powder.

Yield: 0.56 g, 56%, yellowish powder

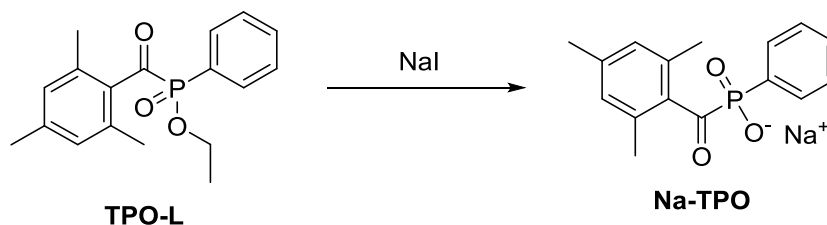
¹H-NMR (d₆-DMSO): δ [ppm] = 2.2 (s, 6 H), 2.25 (s, 3H), 6.6 (s, 2H), 7.3 (m, 3H), 7.6 (m, 2H)

¹³C-NMR-APT (CD₂Cl₂): δ [ppm] = 134.9 (Ar-C), 134.0 (Ar-C), 133.8 (Ar-C), 132.4 (Ar-C), 128.9 (Ar-C), 21.4 (CH₃), 19.9 (CH₃)

³¹P-NMR (d₆-DMSO): δ [ppm] = 10.8

T_m = 372.4°C

5.2.1.2. Sodium Phenyl(2,4,6-trimethylbenzoyl)phosphine Oxide (Na-TPO) Synthesized from NaI



The synthesis was done according to Noe et al.¹⁵¹ Trimethylbenzoylphenylphosphine acid ethylester (Lucirin® TPO-L, BASF AG; 1.02 g, 3.22 mmol, 1 eq.) were dissolved in ethylmethylketone (5 mL). NaI (0.53 g, 3.55 mmol, 1.1 eq.) was added and after 15 min. the homogenous solution was heated to 65°C and stirred for 24 h. The resulting yellow precipitate was filtered off and washed one time with 10 mL ethylmethylketone and two times with 10 mL PE. After drying in high vacuum the product was recrystallized from diethylether to yield the product **Na-TPO** as yellowish powder.

Yield: 0.85 g, 85%, yellowish powder

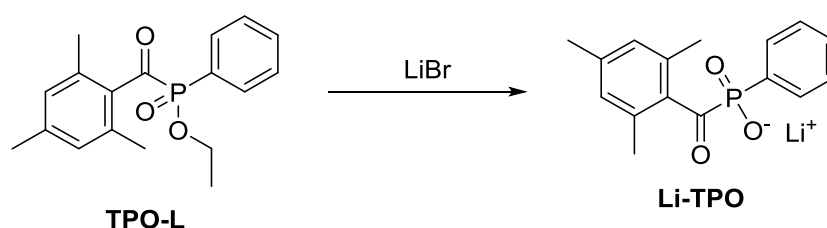
¹H-NMR (d₆-DMSO): δ [ppm] = 2.2 (s, 6 H), 2.25 (s, 3H), 6.6 (s, 2H), 7.3 (m, 3H), 7.6 (m, 2H)

¹³C-NMR-APT (CD₂Cl₂): δ [ppm] = 134.9 (Ar-C), 134.0 (Ar-C), 133.8 (Ar-C), 132.4 (Ar-C), 128.9 (Ar-C), 21.4 (CH₃), 19.9 (CH₃)

³¹P-NMR (d₆-DMSO): δ [ppm] = 10.8

T_m = 372.4°C

5.2.1.3. Lithium Phenyl(2,4,6-trimethylbenzoyl)phosphine Oxide (Li-TPO)



The synthesis was performed with slight changes compared to Majima et al.¹⁵² Trimethylbenzoylphenylphosphine acid ethylester (Lucirin® TPO-L, BASF AG; 10.75 g, 33.99 mmol, 1 eq.) were dissolved in ethylmethylketone (150 mL). LiBr (11.81 g, 135.96 mmol, 4 eq.) was added and after 15 min. the homogenous solution was heated to 65°C and stirred for 24 h. The resulting yellow precipitate was filtered off and washed one time with 10 mL ethylmethylketone and two times with 10 mL PE. After drying in high vacuum the product was recrystallized from diethylether to yield the product **Li-TPO** as white powder (9.9 g, 33.65 mmol).

Yield: 9.9 g, 99%, white powder

¹H-NMR (CD₃OD): δ [ppm] = 2.12 (s, 6H), 2.23 (s, 3H), 6.77 (s, 2H), 7.4 (m, 3H), 7.81 (t, 2H)

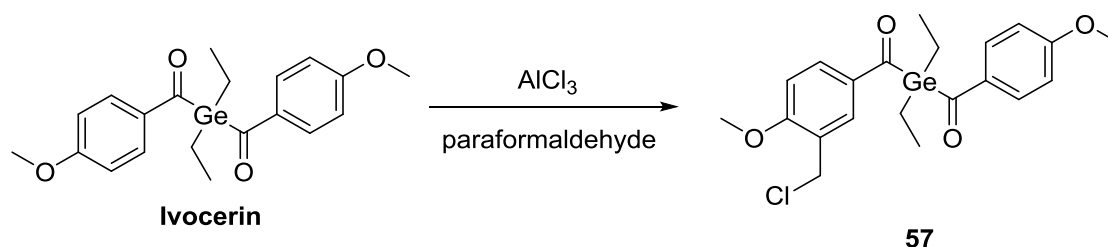
¹³C-NMR (CD₃OD): δ [ppm] = 21.3 (CH₃), 128.5 (Ar-C), 129.0 (Ar-C), 129.1 (Ar-C), 132.2 (Ar-C), 134.0 (Ar-C), 134.3 (Ar-C), 135.1 (Ar-C)

³¹P-NMR (d₆-DMSO): δ [ppm] = 11.1

T_m = 350.5 °C

5.2.3. Modification of Ivocerin

5.2.3.1. ((3-(Chloromethyl)-4-methoxybenzoyl)-diethylgermyl)-(4-methoxyphenyl)methanone **57**



Under argon Ivocerin (2.42 g, 6 mmol, 1 eq.) and AlCl₃ (4.82 g, 36 mmol, 6 eq.) were dissolved in CHCl₃ and cooled to 4°C. Paraformaldehyde (2.17 g, 72 mmol, 12 eq.) was added slowly and the mixture was stirred overnight (16 h) at ambient temperature. Subsequently water was added and the organic phase was separated.

The red, jelly precipitate was dissolved in EE and washed with water too. The combined organic phase was dried with sodium sulfate and the solvents removed. The yellow, liquid residue was separated via column chromatography (PE:EE = 4:1), which gave the monosubstituted product **57**.

Yield: 1.7 g, 64%, yellow oil

GC-MS (CH₂Cl₂, EI): m/z: 450.98 (M), 423.02 (M – Et), 393.91, 349.86, 315.77 (M – COArOMe), 287.73, 267.67 (M – COArOMeCH₂Cl), 259.64, 239.62, 211.57, 183.53 (COArOMeCH₂Cl), 135.45 (COArOMe), 91.41 (ArC), 77.28 (Ar)

HR-MS (MeOH, ESI⁺): m/z: 473.05283 (M + Na), 449.07227 (M)

¹H-NMR (CD₂Cl₂): δ [ppm] = 7.75 – 7.51 (m, 4H), 6.93 – 6.73 (m, 3H), 4.53 (s, 2H), 3.82 (s, 3H), 3.74 (s, 3H), 1.51 – 1.25 (m, 4H), 1.11 – 0.92 (m, 6H)

¹³C-NMR-CPD (CDCl₃): δ [ppm] = 163.9 (ArO), 161.4 (ArO), 134.8 (CAr), 130.8 (CAr), 130.5 (CAr), 114.1 (CAr), 110.5 (CAr), 55.7 (OCH₃), 41.0 (CH₂Cl), 9.0 (CH₃), 6.5 (GeCH₂)

R_f (SiO₂, PE:EE = 5:1): 0.43

5.3.1. Solubility

The solubility in deionized water was tested by preparing a saturated solution of photoinitiator at ambient temperature (25°C) and drying a defined volume (1 mL) of this solution after filtration through a syringe filter. The resulting precipitate was weighed and the residual water in the crystal structure of the dried compounds was measured with ¹H-NMR analysis. Via subtraction of the crystal water content the solubility in mg mL⁻¹ was obtained. For checking the reproducibility of this method it was tried two times, where the values in g/L deviated from the first measurement only in the first digit after the comma.

5.3.3. Storage Stability

The storage stability of the photoinitiators was tested in 3 different solvents. MeCN/H₂O = 50/50 v/v for stability in neutral solutions, MeCN/H₂O = 50/50 v/v with a few drops of H₃PO₄ (pH = 2) for stability in acidic solutions and MeCN/H₂O = 50/50 v/v with a few drops of concentrated NaOH (pH = 11) for stability in alkaline solutions. Each photoinitiator was dissolved in each solvent with a concentration of 1 x 10⁻³ mol L⁻¹ and at t = 0 d UV-VIS-spectra were measured. Afterwards the solutions were stored in the dark for 20 days at 40°C. At t = 20 d UV-VIS-spectra were measured again. The percentage of decline in absorbance at the maximum (or shoulder) of the n—π* transition (Table 5) is directly proportional to the percentage in concentration decline, therefore directly providing the remaining concentration of photoinitiator.

5.3.4. Cytotoxicity Studies

The mouse fibroblast cells L929 (Sigma) were used for cytotoxicity experiments. Among others this cell line is recommended for biological evaluation of medical devices as described in ISO10993 standard testing. The cells were cultured in Dulbecco's Modified Eagle's Medium (DMEM) with 4500 mg L⁻¹ glucose, L-glutamine and sodium bicarbonate, without sodium pyruvate (Sigma), supplemented with 10% fetal bovine serum (Sigma) and 1% of 10000 U mL⁻¹ Penicillin/Streptomycin (Lonza). 96 well plates were seeded with 5000 cells per well and incubated overnight for cells to attach in an incubator in a humid atmosphere with 5% carbon dioxide at 37°C. On the next day the medium was removed from the wells and freshly prepared solutions of different PIs in different concentrations (8.92 mM, 4.43 mM, 2.23 mM, 1.12 mM and 0.56 mM) were added to the cells residing in different wells. Due to the photosensitivity of the PIs, all subsequent cell and PIs handling were performed under red light.

The plates with cells and PI were wrapped with aluminum foil and incubated for 24h in an incubator. After 24h the medium was removed and all wells were washed with PBS.

To evaluate the viability of cells exposed to different photoinitiators PrestoBlue Cell Viability Reagent (Life Technologies) was used. The resazurin-based reagent PrestoBlue was diluted 1:10 with DMEM and 100 μ L were applied per well and incubated for 1 hour. This reagent transforms and turns red thus becoming highly fluorescent because of the reducing environment of viable cells. The fluorescence was measured with a plate reader (Synergy BioTek, excitation 560 nm, emission 590 nm). After correction for background fluorescence, the metabolic activity of the cells exposed to different concentrations of photoinitiators were compared to each other and to the positive control (non-stimulated cells, 5000 cells per well) and DMSO control (cells stimulated with 50% DMSO and 50 % medium for 1 hour to evaluate fluorescence signal of the wells containing dead cells). On every plate were five point standard curves (1000, 2000, 3000, 4000, 5000 cells per well). Wells with 5000 cells were chosen for positive control (showing the highest metabolic activity).

LC₅₀ of the different photoinitiators was determined by polynomial (second order) regression of the metabolic activity at different PI concentrations and then graphical evaluation of the resulting curve.

5.3.4. Cell Encapsulation

Cell encapsulation experiments were performed with mouse calvaria-derived preosteoblast cells (MC3T3-E1 Subclone 4 from ATCC-LGC Standards). MC3T3-E1 were expanded in Alpha Minimum Essential Medium (α MEM) with ribonucleases, deoxyribonucleases, 2 mM L-glutamine, without ascorbic acid (Gibco), supplemented with 10% fetal bovine serum (Sigma) and 1% of 10000 U mL⁻¹ Penicillin/Streptomycin (Lonza).

Methacrylamide-modified gelatin (Gel-MOD) with degree of substitution of 72 % was prepared in accordance to previously reported protocol.¹⁶⁰ Cells were encapsulated in 10 % Gel-MOD solution in α MEM containing 0.6 mM **Li-TPO 56** and a cell density of 10 million cells per mL. Gel pellets with encapsulated cells were produced using chambered coverslip molds (Sigma) resulting in pellets with 6 mm in diameter and 1 mm height subsequently exposed to UV light for 10 minutes (365 nm, 4 mW cm⁻²) in

order to cross-link the gel. After that, pellets were soaked in α -MEM and left in incubator. Samples were maintained during 36 days.

The LIVE/DEAD viability assay (Molecular Probes, Life technology) was used to assess cell viability according to manufacturer's instructions. The culture media was aspirated and the scaffolds and pellets were rinsed 3 times in sterile phosphate-buffered saline (PBS, Sigma). The staining solution with 0.2 μ M Calcein AM (live stain) and 0.6 μ M propidium iodide (dead stain) was added for 20 minutes at 37°C. Samples were washed 3 times with PBS and examined and imaged using laser scanning microscopy (LSM 700, Zeiss) with excitation/emission filter set at 488/530 nm to observe living cells (green) and 530/580 nm to detect dead (red) cells.

Materials, Equipment and Analysis

Chemicals and solvents:

If not mentioned otherwise the used chemicals were ordered from Sigma-Aldrich and TCI respectively. Solvents were taken from the TU internal distillation facility and if necessary further dried according to known procedures.¹⁶⁶

Melting points:

The melting points were measured with an OptiMelt – Automated Melting Point System. For that the samples had to be put in a one side open capillary (80 x 1.3 mm).

TLC:

Aluminum based TLC plates from Merck (silica gel 60 F₂₅₄) were used for thin layer chromatography.

GC-MS:

GC-MS measurements were carried out on a Thermo Fisher Scientific DSQ II employing a Fused Silica capillary column (30m x 0.25mm).

LC-MS:

LC-MS measurements were carried out on a Shimadzu LCMS-2020 MS Detektor with DUISI ionisation, Eluent was typically methanol:water = 90:10 or pure methanol at 30 °C and 0.5 ml/min.

HR-MS:

HR-MS were measured in cooperation with FH Tulln by Dr. Justyna Rechthaler. Measurements were conducted on an Exactive PLUSTM Massenspektrometer (Thermo Fisher Scientific) in ESI mode with a capillary temperature of 320°C. Typical sample concentration was 1 ppm in MeOH.

NMR:

The ¹H-NMR and ¹³C-NMR signals were measured on a BRUKER AC-E-200 FT-NMR. ³¹P-NMR signals were measured on a BRUKER AVANCE 200. Deuterated dichloromethane, chloroform and methanol were used in the highest degree of deuteration available at euriso-top.

IR:

All IR-spectra were measured on a Perkin Elmer Spectrum 65 FT-IR Spectrometer with a Specac MKII Golden Gate ATR system.

UV-VIS:

UV-VIS measurements were carried out on a Shimadzu UV-1800 Spectrophotometer using quartz cuvettes with 10 mm thickness. Samples were typically dissolved in CH₂Cl₂ or MeOH with a concentration of usually 1 x 10⁻³ mol L⁻¹ and measured in the dark if light protection was required.

Photo-DSC:

Photo-DSC analysis was done on a Netzsch DSC 204 F1 using an OmniCure 2000 (Lumen Dynamic) mercury lamp light source equipped with a built in 400-500 nm filter. The lamp was calibrated with an OmniCure R2000 radiometer to an effective irradiation intensity of 1.00 W cm⁻². The measurements were done with 10±1 mg of monomer formulation, which consisted of photoinitiator and monomer. As a result from the measurements, the time until the maximum heat of polymerization (t_{max}) is reached can be obtained directly. Also the time until 95% of the maximum double bond conversion (t_{95%}) can be directly acquired through integration of the resulting curves. However, the rate of polymerization (R_p) and the double bond conversion (DBC) of the monomer need to be calculated according to eq. 1 and 2:

$$R_p = \frac{\Delta H_{max} * \rho}{\Delta H_0 * M_w} \quad (1)$$

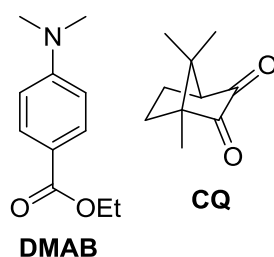
$$DBC = \frac{A}{\Delta H_0} * 100 \quad (2)$$

Herein ΔH_{max} is the maximum heat of polymerization, ΔH₀ (NAM: 460.58 J g⁻¹; mixture A: 240.4 J g⁻¹; mixture B: 299.54 J g⁻¹)^{167,168} is the theoretical heat of polymerization, ρ (NAM: 1.1 kg L⁻¹; mixture A: 1.1 kg L⁻¹; mixture B: 1.1 kg L⁻¹)^{167,168} is the density of the formulation, M_w the molecular weight and A the integrated area of the DSC-plot. All these numbers are referring to the monomer.

The maximum heat of polymerization for NAM ΔH₀ was determined by photo-DSC measurements of pure NAM polymerized with the photoinitiator **MAPO** (Speedcure TPO®) and subsequent ¹H-NMR measurements of the resulting polymer to correlate the double bond conversion after polymerization with the measured heat of polymerization in the photo-DSC.

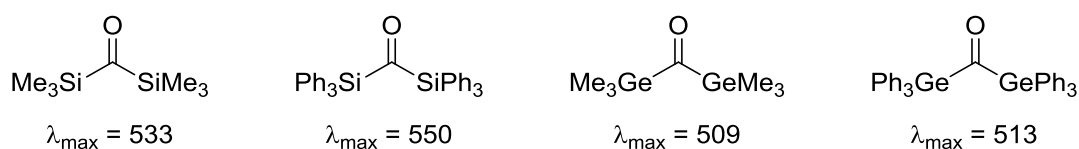
Summary

Modern composite materials, which are used in dentistry, consist of inorganic filler and an organic methacrylate matrix. To cure this matrix, photoinitiator systems are used. Currently, camphorquinone/dimethylamino benzoate (**CQ/DMAB**) is state of the art for this application.



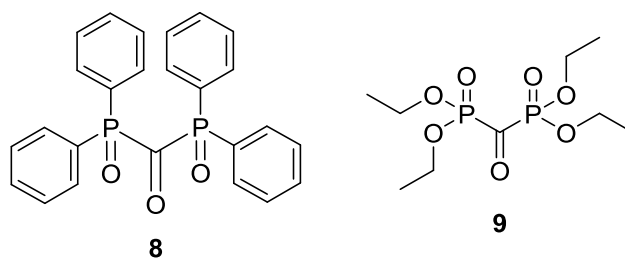
However, there are problems concerning reactivity due to the Norrish type II system, especially in water-based primer mixtures, which are used as a first layer directly on the tooth material. However, the main problem addressed in this work is the insufficient photobleaching of this type II system but also the low curing depth. For these reasons the goal of the work was to find new cleavable, one-component systems for visible light initiation to replace state of the art systems. These systems should be as red-shifted as possible to guarantee a deeper penetration depth of light.

The first project – the syntheses of the bisphosphylketones – was based on preliminary experiments with germanium and silicium containing compounds:^{24,25}



These compounds showed a strong bathochromic red-shift and were also assumed to initiate radical polymerization very efficiently, due to the formation of four active radicals. However, they did not show enough stability under atmospheric conditions to be considered as new dental photoinitiators.

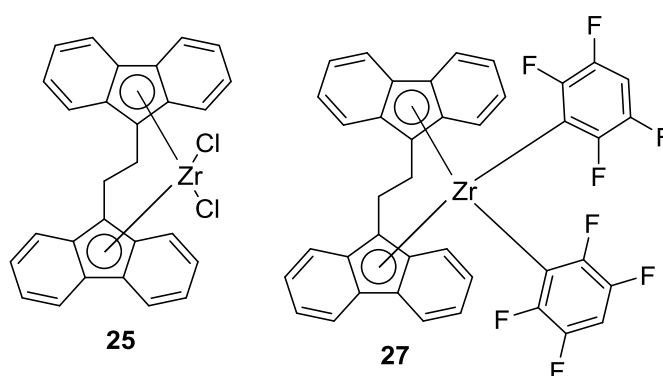
Syntheses and attempted syntheses of the corresponding bisphosphylketones **8** and **9** led to a similar conclusion.



This class of compounds indeed shows interesting properties and also the bathochromic red-shift could be shown. The major problem of course was the hydrolytic and thermal instability, leading to decomposition and rearrangement reactions already at low temperatures and atmospheric conditions. This was also described in literature³¹ and could be proven by GC-MS measurements.

In fact, only carbonylbis(diethoxyphosphine oxide) **9** could be synthesized but shown to exist only in the reaction mixture. Attempts to stabilize the compound further with different substituents on the phosphorus heteroatoms failed and subsequent theoretical calculations showed that a stabilization of the compound type will most likely not be possible.

The attention was shifted to metal based photoinitiators. Especially zirconium complexes offer interesting possibilities in this field because of a cleavage reaction during initiation and uncolored zirconium salts that are formed. Indeed, the zirconium complex **25** showed no stability problems under atmospheric conditions and in solution (dichloromethane, diether, MeCN).

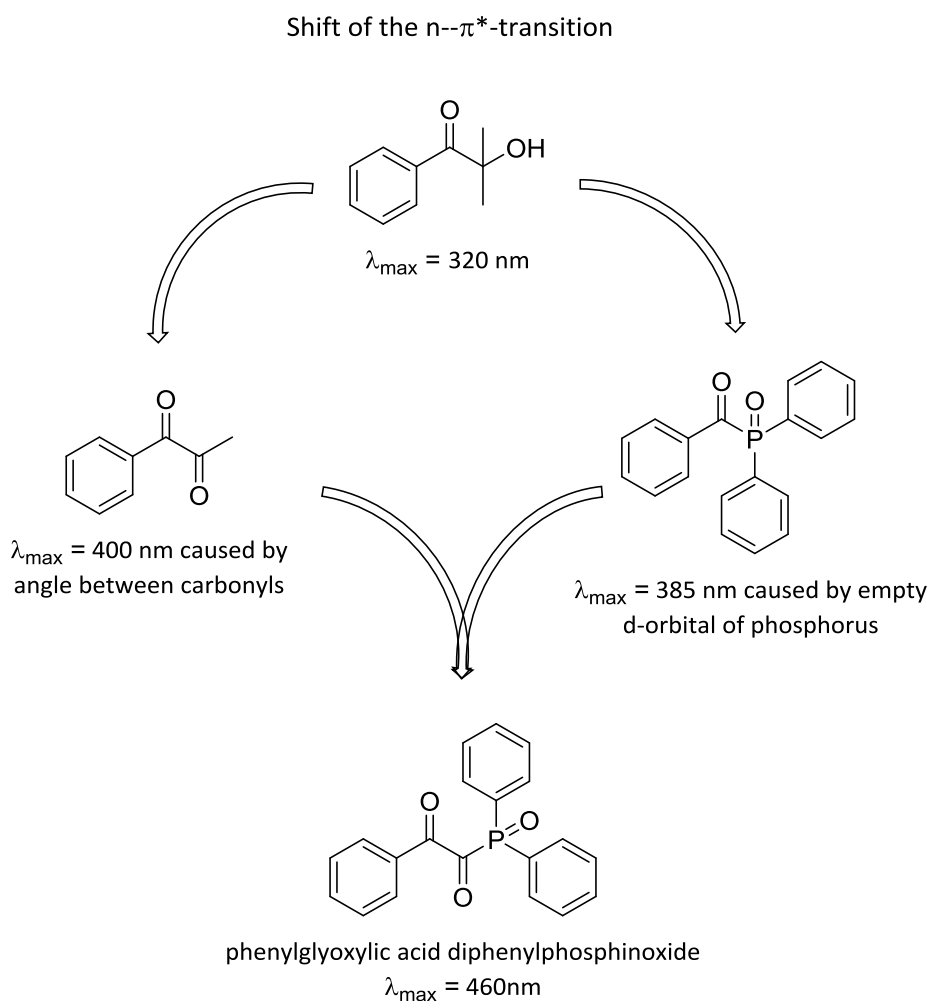


Nevertheless, it is not suitable for an application as long wavelength photoinitiator, since it reacted with monomer double bonds as it is described in literature for other zirconium complexes.^{63,63,64} This led to cleavage of the fluorenyl ligand and decolorization of the photoinitiator, meaning that the red-shift of the compound was

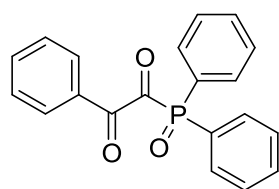
lost and only UV-polymerization was possible. It was tried to stabilize the complex also in methacrylic monomer mixtures as it was done for the commercially available titanocene Irgacure 784. In this compound fluorinated aromatic ligands were used to hinder the electron back donation from ligand to central atom already at ambient conditions.

This electron back donation was assumed to be the reason for the instability of the compound. Unfortunately, (ethylenbis(9-fluorenyl))zirconiumtetrafluorobenzene **27** was synthetically not accessible.

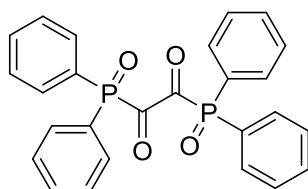
Another very interesting concept was the achievement of a bathochromic red-shift via combination of the empty d-orbital effect next to a carbonyl group with the effect that two neighboring carbonyl groups also lead to a red-shift:



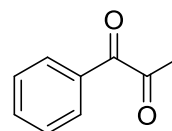
A whole set of compounds, also with different heteroatoms, was synthesized and characterized.



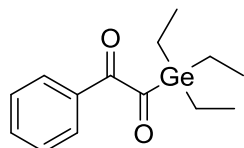
32



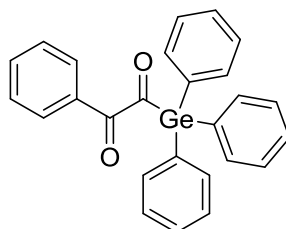
38



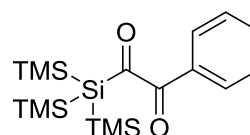
PPD



39



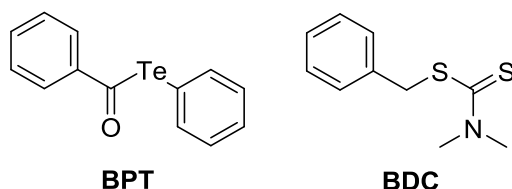
46



47

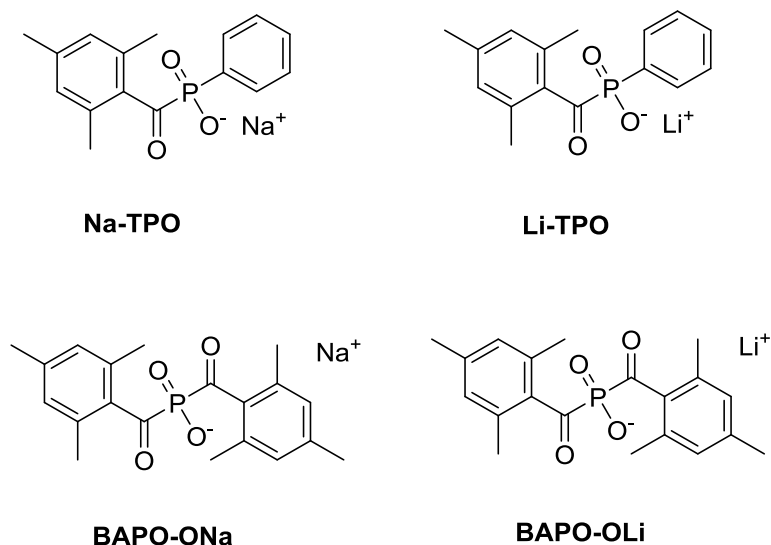
Even though the concept of the red-shift worked very well, the synthesized compounds did not show reactivity in a range, where an application as photoinitiator is reasonable. All tested compounds' reactivity was significantly below the reactivity of the reference **PPD** and therefore also much worse than the reactivity of the state of the art **CQ/DMAB** system.

Subsequently, the focus of the work was shifted to acyl tellurium compounds. It was hoped to achieve a bathochromic red-shift by introducing a tellurium heteroatom next to a carbonyl group of a benzoyl chromophore. However, reactivity of these systems turned out to be very low. Literature research gave an explanation for this phenomenon. Organotellurium compounds can be used for controlled living polymerization. For special applications but even more for non-dentistry related fields, photochemical polymerization control agents can be very beneficial. The concept of using acyltellurides as exclusively photoactivated TERP (tellurium mediated controlled radical polymerization) reagents worked very well. It could be shown that the telluroorganic compound **BPT** is a suitable polymerization control agent for acrylates and acrylamides, yielding polydispersities as low as 1.2-1.3. **BPT** leads to lower polydispersities than it was reported in literature for photoiniferters so far. The most important benefit of **BPT** though, can be found in the ability to carry out controlled radical polymerization at room temperature with a visible light (400-500 nm) radiation source. The reference **BDC** also has some potential, but needs UV light for its living radical polymerization mechanism.



Explanation can be given by the UV-VIS spectrum in general and the $n-\pi^*$ transition (335 nm for **BDC** and 407 nm for **BPT**) of the two compared compounds in particular. The subsequently formed tellurium dormant species was still active under visible light irradiation. The high reactivity of the tellurium compound **BPT**, compared to the reference **BDC** has been shown by photo-DSC experiments and can be attributed to the highly reactive benzoyl radical. In conclusion, **BPT** is highly suitable for photopolymerizations, where a narrow molecular weight distribution is mandatory and visible light is preferred. This is for example the case for debonding on demand applications in dentistry.¹⁶⁹

As already mentioned above, another project in this work was to find a photoinitiator system with improved water-solubility for primer mixtures. Especially in water-based primer mixtures the state of the art system **CQ/DMAB** has its limits. The MAPO and BAPO salts as water-borne photoinitiators not only show storage stability and biocompatibility in the same range as state of the art photoinitiators but exceed them by far in solubility and reactivity.



Furthermore it is possible to use the MAPO and BAPO salts as visible light initiators, which is a big advantage for applications involving living cells. However, the compared compounds differ in some properties from each other. **Na-TPO** and **Li-**

TPO are recommended for UV irradiation as they show best results for these irradiation wavelengths. Best biocompatibility can be achieved with **Li-TPO**. For visible light irradiation **BAPO-OLi** is the initiator of choice with an extraordinary high rate of polymerization. The biggest advantage of **BAPO-ONa** is the highest solubility for applications where very high PI concentrations are necessary. In conclusion, the goal to find and characterize well suited water-borne photoinitiators, which show better properties than state of the art photoinitiators was achieved. Therefore a variety of new possibilities for many applications also besides dentistry are imaginable.

Indices

1. Abbreviations

AA	Acryl amide
APi-180	2-Hydroxy-1-[3-(hydroxymethyl)phenyl]-2-methyl-1-propanone
ATRP	Atom transfer radical polymerization
BA	Butylacrylate
BAPO	Bisacylphosphine oxide
BDC	Benzyl dithiocarbamate
bis-GMA	Bisphenol A – diglycidylmethacrylate
BMA	Butylmethacrylate
BPT	Benzoyl phenyltelluride
BuLi	Butyl lithium
CQ	Camphorquinone
CRP	Controlled living radical polymerization
D ₃ MA	1,10-Decanedioldimethacrylate
DBC	Double bond conversion
DFT	Density functional theory
DMAB	N,N-Dimethylaminobenzoate
DSC	Differential scanning calorimetry
ESP	Equally spaced polynomial
GC-MS	Gas chromatography - mass spectrometry coupling
GPC	Gel permeation chromatography
HOMO	Highest occupied molecular orbital
I2959	2-Hydroxy-1-[4-(2-hydroxyethoxy)phenyl]-2-methyl-1-propanone
ISC	Intersystem crossing
KOtBu	Potassium tert-butoxide
LDA	Lithium diisopropylamide
LED	Light-emitting diode
Li-BAPO	Li salt of bisacylphosphine oxide
Li-TPO	Li salt of monoacylphosphine oxide
LUMO	Lowest unoccupied molecular orbital
MA154	Phosphonic ester acrylate for primer mixtures
MAPO	Monoacylphosphine oxide
MDEA	Methyldiethanolamine
Mixture A	UDMA, D ₃ MA, bis-GMA = 1:1:1 molar
Mixture B	UDMA, D ₃ MA = 1:1 molar
MMA	Methyl methacrylate
Na-BAPO	Na salt of bisacylphosphine oxide
NAM	N-Acryloylmorpholine

Na-TPO	Na salt of monoacylphosphine oxide
NMO	N-Methylmorpholine N-oxide
NMP	Nitroxide-mediated polymerization
NMR	Nuclear magnetic resonance spectroscopy
PDI	Polydispersity index
PPD	Phenylpropanedione
Q-BPQ	3-(4-benzoylphenoxy)-2-hydroxy- <i>N,N,N</i> -trimethyl-1-propanaminium-chloride
RAFT	Reversible addition fragmentation chain transfer
St	Styrene
t-BuOCl	tert-butyl-hypochlorite
TERP	Organotellurium-mediated controlled radical polymerization
TLC	Thin layer chromatography
TPO-L	2,4,6-Trimethylbenzoylphenylphosphinate
UDMA	Urethanedimethacrylate
UV-VIS	Ultraviolet and visible light
V392	Acrylamide based crosslinker for primer mixtures

2. Literature

- (1) Asgar, K. and Reichman, S. H., *Dental amalgam*. 1975, USA . p. 5 pp.
- (2) Greener, E. H., *Dental amalgams*. 1976, Engelhard Minerals and Chemicals Corp., USA . p. 6 pp.
- (3) Bates, M. N., *Mercury amalgam dental fillings: an epidemiologic assessment*. Int. J. Hyg. Environ. Health, 2006. **209**(4): p. 309-316.
- (4) Albert, P., Dermann, K. and Rentsch, H., *Amalgam and its alternatives*. Chem. Unserer Zeit, 2000. **34**(5): p. 300-305.
- (5) Blaus, B. 2014, Wikiversity Journal of Medicine: Blausen gallery 2014.
- (6) Schneider, L. F. J., Cavalcante, L. M. and Silikas, N., *Shrinkage Stresses Generated during Resin-Composite Applications: A Review*. Journal of Dental Biomechanics, 2010. **1**(1).
- (7) Moszner, N. and Salz, U., *New developments of polymeric dental composites*. Prog. Polym. Sci., 2001. **26**(4): p. 535-576.
- (8) Van Landuyt, K. L., Yoshida, Y., Hirata, I., Snauwaert, J., De Munck, J., Okazaki, M., Suzuki, K., Lambrechts, P. and Van Meerbeek, B., *Influence of the chemical structure of functional monomers on their adhesive performance*. J. Dent. Res., 2008. **87**(8): p. 757-761.
- (9) Salz, U., Zimmermann, J., Rheinberger, V., Landfester, K., Ziener, U. and Volz, M., *Microencapsulated photo-initiators and use for dental materials*. 2008, Ivoclar Vivadent AG, Liechtenstein . p. 33pp.
- (10) Fleming, I. U., *Molekülorbitale und Reaktionen organischer Verbindungen*. 2012: Wiley-VCH.
- (11) Gruber, P. H. and Knaus, D. S., *Chemische Technologie organischer Stoffe I*, Wien, T., Editor.

- (12) Gruber, H. F., *Photoinitiators for free radical polymerization*. Progress in Polymer Science (Oxford), 1992. **17**(6): p. 953 - 1044.
- (13) Rutsch, W., Dietliker, K. and Hall, R. G., *Mono- and di-acylphosphine oxides*, Ciba-Geigy, C., Editor. 1993.
- (14) Randy, *Jablonski Diagram*. 2015: For Diagrams.
- (15) Fouassier, J.-P., Rabek, J. F. and Editors, *Radiation Curing in Polymer Science Technology, Vol. 2: Photoinitiating Systems*. 1993: Elsevier. 717 pp.
- (16) Dietliker, K., *A Compilation of Photoinitiators Commercially Available for UV Today*. 2002: SITA Technology Limited.
- (17) Cadet, J., Sage, E. and Douki, T., *Ultraviolet radiation-mediated damage to cellular DNA*. Mutat. Res., Fundam. Mol. Mech. Mutagen., 2005. **571**(1-2): p. 3-17.
- (18) Kappes, U. P., Luo, D., Potter, M., Schulmeister, K. and Ruenger, T. M., *Short- and Long-Wave UV Light (UVB and UVA) Induce Similar Mutations in Human Skin Cells*. J. Invest. Dermatol., 2006. **126**(3): p. 667-675.
- (19) Ullrich, G., Burtscher, P., Salz, U., Moszner, N. and Liska, R., *Phenylglycine derivatives as coinitiators for the radical photopolymerization of acidic aqueous formulations*. J. Polym. Sci., Part A: Polym. Chem., 2005. **44**(1): p. 115-125.
- (20) Moszner, N., Rheinberger, V. M., Salz, U., Gruber, H., Liska, R., Ganster, B. and Ullrich, G., *Photopolymerizable dental materials with bisacylphosphine oxides as initiators*. 2007, Ivoclar Vivadent A.-G., Liechtenstein . p. 14 pp.
- (21) Ganster, B., Fischer, U. K., Moszner, N. and Liska, R., *New Photocleavable Structures. Diacylgermane-Based Photoinitiators for Visible Light Curing*. Macromolecules (Washington, DC, U. S.), 2008. **41**(7): p. 2394-2400.
- (22) Johannesen, R. and Benneche, T., *Synthesis of trimethylgermyl trimethylsilyl ketone and bis(trimethylgermyl) ketone*. Perkin 1, 2000(16): p. 2677-2679.
- (23) Wakasa, M., Mochida, K., Sakaguchi, Y., Nakamura, J. and Hayashi, H., *Fluorescence of silyl and germlyl ketones and their primary photochemical processes*. J. Phys. Chem., 1991. **95**(6): p. 2241-6.
- (24) Gugg, A., Diploma Thesis, TU Wien
- (25) Tehfe, M.-A., Blanchard, N., Fries, C., Lalevee, J., Allonas, X. and Fouassier, J. P., *Bis(germyl)ketones: Toward a New Class of Type I Photoinitiating Systems Sensitive Above 500 nm?* Macromol. Rapid Commun., 2010. **31**(5): p. 473-478.
- (26) Talanian, R. V., Brown, N. C., McKenna, C. E., Ye, T. G., Levy, J. N. and Wright, G. E., *Carbonyldiphosphonate, a selective inhibitor of mammalian DNA polymerase β* . Biochemistry, 1989. **28**(21): p. 8270-4.
- (27) Quimby, O. T., Prentice, J. B. and Nicholson, D. A., *Tetrasodium carbonyldiphosphonate. Synthesis, reactions, and spectral properties*. J. Org. Chem., 1967. **32**(12): p. 4111-14.
- (28) McKenna, C. E., Kashemirov, B. A. and Li, Z.-M., *Synthetic Approaches to Biologically Active Bisphosphonates and Phosphonocarboxylates*. Phosphorus, Sulfur and Silicon and the Related Elements, 1999. **144**: p. 313 - 316.
- (29) McKenna, C. E., Khare, A., Ju, J.-Y., Li, Z.-M., Duncan, G. and et al., *Synthesis and HIV-1 Reverse Transcriptase Inhibition Activity of Functionalized Pyrophosphate Analogues*. Phosphorus, Sulfur and Silicon and the Related Elements, 1993. **76**(1-4): p. 139 - 142.
- (30) McKenna, C. E., Khawli, L. A., Ahmad, W.-Y., Pham, P. and Bongartz, J.-P., *Synthesis of Alpha-Halogenated Methanediphosphonates*. Phosphorus and Sulfur and the Related Elements, 1988. **37**: p. 1 - 12.

- (31) McKenna, C. E. and Kashemirov, B. A., *Preparation and use of $\hat{I}\pm$ -keto bisphosphonates*. 2000. p. 28 pp.
- (32) Becker and Langer, *Darstellung von Kohlensäure-bis(diphenylphosphid)*. Angewandte Chemie, 1973. **85**: p. 910.
- (33) Herzog, D., *Funktionelle Photoinitiatoren und neue initiierende Strukturen für die radikalische Polymerisation*. Dissertation, 2003.
- (34) Sigma-Aldrich, *MSDS - Methylendiphosphonsäure*. 2015, Sigma-Aldrich.
- (35) Khare, A. B. and McKenna, C. E., *An Improved Synthesis of Tetraalkyl Diazomethylenediphosphonates and Alkyl Diazo(dialkoxyphosphoryl)acetates*. Synthesis, 1991(5): p. 405 - 406.
- (36) Du, H., Zhao, B. and Shi, Y., *Catalytic asymmetric allylic and homoallylic diamination of terminal olefins via Formal C-H Activation*. J. Am. Chem. Soc., 2008. **130**(27): p. 8590-8591.
- (37) Chen, D., Guo, T. and Guo, X., *Process for preparation of Nepafenac*. 2013. p. 6pp.
- (38) Tsvetkov, E. N., Bondarenko, N. A., Malakhova, I. G. and Kabachnik, M. I., *A Simple Synthesis and Some Synthetic Applications of Substituted Phosphide and Phosphinite Anions*. Synthesis, 1986(3): p. 198 - 208.
- (39) Sekine, M., Satoh, M., Yamagata, H. and Hata, T., *Acylphosphonates: phosphorus-carbon bond cleavage of dialkyl acylphosphonates by means of amines. Substituent and solvent effects for acylation of amines*. J. Org. Chem., 1980. **45**(21): p. 4162-7.
- (40) Cunningham, A. F., Jr. and Desobry, V., *Metal-based photoinitiators*. Radiat. Curing Polym. Sci. Technol., 1993. **2**: p. 323-73.
- (41) Billaud, C., Sarakha, M. and Bolte, M., *Kinetic study of azidopentaammine cobalt(III) complex as photoinitiator and termination agent of N-vinylpyrrolidone radical polymerization*. J. Polym. Sci., Part A: Polym. Chem., 2000. **38**(21): p. 3997-4005.
- (42) Fouassier, J.-P. and Lalevée, J., *Photoinitiators for Polymer Synthesis*. 2012.
- (43) Polo, E., Barbieri, A. and Traverso, O., *From zirconium to titanium: the effect of the metal in tert-butyl acrylate photoinitiated polymerization*. New J. Chem., 2004. **28**(5): p. 652-656.
- (44) Kundig, E. P., Xu, L.-H., Kondratenko, M., Cunningham, A. F., Jr. and Kunz, M., *Photoinitiation of acrylate polymerization with (arene)chromium complexes*. Eur. J. Inorg. Chem., 2007(18): p. 2934-2943.
- (45) Matsumo, H., Yamaguchi, Y., Yanagihara, N. and Yamamoto, H., EP 90, 1990. **119**: p. 767.
- (46) Davidenko, N., Garcia, O. and Sastre, R., *The efficiency of titanocene as photoinitiator in the polymerization of dental formulations*. J. Biomater. Sci., Polym. Ed., 2003. **14**(7): p. 733-746.
- (47) Polo, E., Barbieri, A. and Traverso, O., *The effect of phenyl substituents on the activity of some zirconocene photoinitiators*. Eur. J. Inorg. Chem., 2003(2): p. 324-330.
- (48) Yamaguchi, Y., Ding, W., Sanderson, C. T., Borden, M. L., Morgan, M. J. and Kutal, C., *Electronic structure, spectroscopy, and photochemistry of group 8 metallocenes*. Coord. Chem. Rev., 2007. **251**(3+4): p. 515-524.
- (49) Kutal, C., Yamaguchi, Y., Ding, W., Sanderson, C. T., Li, X., Gamble, G. and Amster, I. J., *Harvesting the fields of inorganic and organometallic photochemistry for new photoinitiators*. ACS Symp. Ser., 2003. **847**(Photoinitiated Polymerization): p. 332-350.

- (50) Fancy, D. A. and Kodadek, T., *Chemistry for the analysis of protein-protein interactions: rapid and efficient cross-linking triggered by long wavelength light*. Proc. Natl. Acad. Sci. U. S. A., 1999. **96**(11): p. 6020-6024.
- (51) Polo, E., Barbieri, A., Sostero, S. and Green, M. L. H., *Zirconocenes as photoinitiators for free-radical polymerization of acrylates*. Eur. J. Inorg. Chem., 2002(2): p. 405-409.
- (52) Versace, D.-L., Lalavée, J., Dalmas, F. and Fouassier, J. P., *Zirconocene Dichloride: an Efficient Cleavable Photoinitiator Allowing the in-situ Production of Zr Based Nanoparticles Under Air*. ACS Macro Letters, 2013.
- (53) Hiller, J., Thewalt, U., Polasek, M., Petrusova, L., Varga, V., Sedmera, P. and Mach, K., *Methyl-Substituted Zirconocene-Bis(trimethylsilyl)acetylene Complexes (C₅H₅-nMen)₂Zr(Ĥ-2-Me₃SiCâ%ojCSiMe₃) (n = 2-5)*. Organometallics, 1996. **15**(17): p. 3752-3759.
- (54) Zachmanoglou, C. E., Docrat, A., Bridgewater, B. M., Parkin, G., Brandow, C. G., Bercaw, J. E., Jardine, C. N., Lyall, M., Green, J. C. and Keister, J. B., *The Electronic Influence of Ring Substituents and Ansa Bridges in Zirconocene Complexes as Probed by Infrared Spectroscopic, Electrochemical, and Computational Studies*. J. Am. Chem. Soc., 2002. **124**(32): p. 9525-9546.
- (55) Hofmann, P., Frede, M., Stauffert, P., Lasser, W. and Thewalt, U., *Monomeric, mononuclear zirconium enediolato complexes: molecular geometry and electronic structure of the products of reductive coupling of carbon monoxide on metal*. Angew. Chem., 1985. **97**(8): p. 693-4.
- (56) Piers, W. E., Whittall, R. M., Ferguson, G., Gallagher, J. F., Froese, R. D. J., Stronks, H. J. and Krygsman, P. H., *Structure and bonding in bis(stannylene) adducts of zirconocene and (1,1'-dimethyl)zirconocene*. Organometallics, 1992. **11**(12): p. 4015-22.
- (57) Berg, F. J. and Petersen, J. L., *Evidence of an alternative mechanism for the reductive coupling of isonitriles by electrophilic 1-sila-3-zirconacyclobutane complexes. Structural characterization of the bicyclic enediamido complexes [cyclic] Cp₂Zr(N(CMe₃)C(CH₂SiMe₂CH₂):CN(R)), where R = tert-butyl and 2,6-xylyl*. Organometallics, 1991. **10**(5): p. 1599-607.
- (58) Alt, H. G., Milius, W. and Palackal, S. J., *Bridged bis(fluorenyl) complexes of zirconium and hafnium as highly reactive catalysts in homogeneous olefin polymerization. The molecular structures of (C₁₃H₉-C₂H₄-C₁₃H₉) and (Ĥ-5:Ĥ-5-C₁₃H₈-C₂H₄-C₁₃H₈)ZrCl₂*. J. Organomet. Chem., 1994. **472**(1-2): p. 113-18.
- (59) Resconi, L., Jones, R. L., Rheingold, A. L. and Yap, G. P. A., *High-Molecular-Weight Atactic Polypropylene from Metallocene Catalysts. 1. Me₂Si(Ĥ-5-9-Flu)₂ZrX₂ (X = Cl, Me)*. Organometallics, 1996. **15**(3): p. 998-1005.
- (60) Alt, H. G. and Samuel, E., *Fluorenyl complexes of zirconium and hafnium as catalysts for olefin polymerization*. Chem. Soc. Rev., 1998. **27**(5): p. 323-329.
- (61) Chaudhari, M. A. and Sone, F. G. A., *Pentafluorophenyl derivatives of transition metals. V. Bis(Ĥ-cyclopentadienyl)bis(Ĥ-pentafluorophenyl)zirconium and related studies*. J. Chem. Soc. A, 1966(7): p. 838-41.
- (62) Dioumaev, V. K. and Harrod, J. F., *Studies of the Formation and Decomposition Pathways for Cationic Zirconocene Hydrido Silyl Complexes*. Organometallics, 1997. **16**: p. 2798 - 2807.
- (63) Stobenau, E. J., III and Jordan, R. F., *Nonchelated Alkene and Alkyne Complexes of d⁰ Zirconocene Pentafluorophenyl Cations*. J. Am. Chem. Soc., 2006. **128**(26): p. 8638-8650.

- (64) Mulhaupt, R., *Catalytic polymerization and post polymerization catalysis fifty years after the discovery of Ziegler's catalysts*. *Macromol. Chem. Phys.*, 2003. **204**(2): p. 289-327.
- (65) Allonas, Morlet, S., Lalevee and Fouassier, *A photodissociation reaction: Experimental and computational study of 2-hydroxy-2,2-dimethylacetophenone*. *Photochemistry and Photobiology*, 2006. **82**(1): p. 88 - 94.
- (66) Arnett, J. F., Newkome, G., Mattice, W. L. and McGlynn, S. P., *Excited electronic states of the α -dicarbonyls*. *J. Amer. Chem. Soc.*, 1974. **96**(14): p. 4385-92.
- (67) Koelsch and Hochman, *Journal of Organic Chemistry*, 1938. **3**: p. 503.
- (68) Hyatt, J. L., Wadkins, R. M., Tsurkan, L., Hicks, L. D., Hatfield, M. J., Edwards, C. C., Ross li, C. R., Cantalupo, S. A., Crundwell, G., Danks, M. K., Guy, R. K. and Potter, P. M., *Planarity and constraint of the carbonyl groups in 1,2-diones are determinants for selective inhibition of human carboxylesterase 1*. *Journal of Medicinal Chemistry*, 2007. **50**(23): p. 5727 - 5734.
- (69) Ganster, B., *Bathochrom verschobene Photoinitiatoren für Dentalformulierungen* Vienna University of Technology Institute of Applied Synthetic Chemistry. Ph.D. Thesis 2007: p. 224.
- (70) Page, P. C. B. and Rosenthal, S., *Simple preparation of α -bromoacylsilanes, α -ketoacylsilanes, and α -ketoesters from silyl acetylenes*. *Tetrahedron*, 1990. **46**(7): p. 2573-86.
- (71) Alaoui, I. M., Menzel, E. R., Farag, M., Cheng, K. H. and Murdock, R. H., *Mass spectra and time-resolved fluorescence spectroscopy of the reaction product of glycine with 1,2-indanedione in methanol*. *Forensic Sci. Int.*, 2005. **152**(2-3): p. 215-219.
- (72) Yamamoto, K., Hayashi, A., Suzuki, S. and Tsuji, J., *Preparation of substituted benzoyltrimethylsilanes and -germanes by the reaction of benzoyl chlorides with hexamethyldisilane or -digermane in the presence of palladium complexes as catalysts*. *Organometallics*, 1987. **6**(5): p. 974-9.
- (73) Schwetlick, K., *Organikum, 23. vollständig überarbeitete und aktualisierte Auflage*. 2009, Weinheim: Wiley-VCH.
- (74) Heaney, F., Fenlon, J., McArdle, P. and Cunningham, D., *α -Keto amides as precursors to heterocycles-generation and cycloaddition reactions of piperazin-5-one nitrones*. *Org. Biomol. Chem.*, 2003. **1**(7): p. 1122-1132.
- (75) Chen, J. T. and Sen, A., *Mechanism of transition-metal-catalyzed double carbonylation reactions. Synthesis and reactivity of benzoylformyl complexes of palladium(II) and platinum(II)*. *J. Am. Chem. Soc.*, 1984. **106**(5): p. 1506-7.
- (76) Eisch, J. J. and Foxton, M. W., *Organometallic compounds of Group III. XIX. Regiospecificity and stereochemistry in the hydralumination of unsymmetrical acetylenes. Controlled cis or trans reduction of 1-alkynyl derivatives*. *J. Org. Chem.*, 1971. **36**(23): p. 3520-6.
- (77) Koecher, J., Lehnig, M. and Neumann, W. P., *Chemistry of heavy carbene analogs R_2M ($M = Si, Ge, Sn$). 12. Concerted and nonconcerted insertion reactions of dimethylgermylene into the carbon-halogen bond*. *Organometallics*, 1988. **7**(5): p. 1201-7.
- (78) VanRheenen, V., Cha, D. Y. and Hartley, W. M., *Catalytic osmium tetroxide oxidation of olefins: cis-1,2-cyclohexanediol*. *Org. Synth.*, 1978. **58**: p. 43-52.
- (79) Hooton, K. A., Dissertation, Durham University

- (80) Groebel, B. T. and Seebach, D., *Umpolung of the reactivity of carbonyl compounds through sulfur-containing reagents*. *Synthesis*, 1977(6): p. 357-402.
- (81) Brook, A. G., Duff, J. M., Jones, P. F. and Davis, N. R., *Synthesis of Silyl and Germyl Ketones*. *Journal of the American Chemical Society*, 1967. **89**: p. 431,432, 433.
- (82) Piers, E. and Lemieux, R., *Reaction of (Trimethylgermyl)copper(I)-Dimethyl Sulfide with Acyl Chlorides: Efficient Syntheses of Functionalized Acyltrimethylgermanes*. *Organometallics*, 1995. **14**(11): p. 5011-12.
- (83) Marschner, C., *A new and easy route to polysilanylpotassium compounds*. *Eur. J. Inorg. Chem.*, 1998(2): p. 221-226.
- (84) Banwell, C. N., *Fundamentals of Molecular Spectroscopy*. 1966, London: McGraw Hill Book Co. Ltd.
- (85) Kelder, J. and Cerfontain, H., *Photodihydrodimerization of some cyclopropyl conjugated 1,2-diketones*. *Tetrahedron Lett.*, 1972(14): p. 1307-10.
- (86) Ogata, Y. and Takagi, K., *Photochemical reactions of some 1-aryl-1,2-propanediones*. *Bull. Chem. Soc. Jpn.*, 1974. **49**(7): p. 2255-9.
- (87) Peddle, G. J. D., *The preparation and properties of α -tin ketones*. *J. Organometal. Chem.*, 1968. **14**(1): p. 139-47.
- (88) Kosugi, M., Naka, H., Sano, H. and Migita, T., *Preparation and some properties of acyltin compounds*. *Bull. Chem. Soc. Jpn.*, 1987. **60**(9): p. 3462-4.
- (89) Villazana, R., Sharma, H., Cervantes-Lee, F. and Pannell, K. H., *Isolation, structural characterization, and photochemical study of an acylplumbane, Mes_3PbCOR ($R = methyl, phenyl$)*. *Organometallics*, 1993. **12**(11): p. 4278-9.
- (90) Singh, A. K. and Roy, M., *Photochemical reactivities of phenyl seleno and telluro esters*. *J. Photochem. Photobiol., A*, 1992. **69**(1): p. 49-52.
- (91) Gardner, S. A. and Gysling, H. J., *Synthesis And Properties of Tellurium(II) Compounds: Diaryltelluroesters, $ArCOTeEAR'$* . *Journal of Organometallic Chemistry*, 1980. **197**(1): p. 111 - 122.
- (92) Zhang, S. and Zhang, Y., *A Novel Method for the Synthesis of Telluroesters*. *Organic Preparations and Procedures International*, 1999. **31**(4): p. 450 - 453.
- (93) Crich, D., Chen, C., Hwang, J.-T., Yuan, H., Papadatos, A. and Walter, R. I., *Photoinduced Free Radical Chemistry of the Acyl Tellurides: Generation, Inter- and Intramolecular Trapping, and ESR Spectroscopic Identification of Acyl Radicals*. *J. Am. Chem. Soc.*, 1994. **116**(20): p. 8937-51.
- (94) Faoro, E., Manzoni, d. O. G., Lang, E. S. and Pereira, C. B., *Synthesis and structure of new aryltellurenyl halides derived from $(dmpTe)_2$ ($dmp = 2,6$ -dimethoxyphenyl)*. *J. Organomet. Chem.* **696**(3): p. 807-812.
- (95) Kato, S., Niyomura, O., Nakaiida, S., Kawahara, Y., Kanda, T., Yamada, R. and Hori, S., *First Isolation and Characterization of Sodium and Potassium Tellurocarboxylates: Structural Analysis of Te-Alkyl Telluroester*. *Inorg. Chem.*, 1999. **38**(3): p. 519-530.
- (96) Klemm, W., Sodomann, H. and Langmesser, P., *Z. Anorg. Allgem. Chemie*, 1939. **241**: p. 281.
- (97) Niyomura, O., Nakaiida, S., Yamada, R., Kato, S., Ishida, M., Ebihara, M., Ando, F. and Koketsu, J., *Diaroyl tellurides: synthesis, structure and NBO analysis of $(2-MeOC_6H_4CO)_2Te$ - comparison with its sulfur and selenium isologues. The first observation of $[MgBr][R(C=Te)O]$ salts*. *Molecules*, 2009. **14**(7): p. 2555-2572.

- (98) Nakamura, Y. and Yamago, S., *Organotellurium-mediated living radical polymerization under photoirradiation by a low-intensity light-emitting diode*. *Beilstein J. Org. Chem.*, 2013. **9**: p. 1607-1612, 6 pp.
- (99) Benedikt, S., Moszner, N. and Liska, R., *Benzoyl Phenyltelluride as Highly Reactive Visible-Light TERP-Reagent for Controlled Radical Polymerization*. *Macromolecules* (Washington, DC, U. S.), 2014. **47**(16): p. 5526-5531.
- (100) Matyjaszewski, K. and Xia, J., *Atom Transfer Radical Polymerization*. *Chem. Rev.* (Washington, D. C.), 2001. **101**(9): p. 2921-2990.
- (101) Hawker, C. J., Bosman, A. W. and Harth, E., *New Polymer Synthesis by Nitroxide Mediated Living Radical Polymerizations*. *Chem. Rev.* (Washington, D. C.), 2001. **101**(12): p. 3661-3688.
- (102) Chiefari, J., Chong, Y. K., Ercole, F., Krstina, J., Jeffery, J., Le, T. P. T., Mayadunne, R. T. A., Meijs, G. F., Moad, C. L., Moad, G., Rizzardo, E. and Thang, S. H., *Living Free-Radical Polymerization by Reversible Addition-Fragmentation Chain Transfer: The RAFT Process*. *Macromolecules*, 1998. **31**(16): p. 5559-5562.
- (103) Kong, H., Gao, C. and Yan, D., *Controlled functionalization of multiwalled carbon nanotubes by in situ atom transfer radical polymerization*. *J. Am. Chem. Soc.*, 2004. **126**(2): p. 412-413.
- (104) Bosman, A. W., Vestberg, R., Heumann, A., Frechet, J. M. J. and Hawker, C. J., *A modular approach toward functionalized three-dimensional macromolecules: from synthetic concepts to practical applications*. *J. Am. Chem. Soc.*, 2003. **125**(3): p. 715-728.
- (105) Bajpai, A. K., Shukla, S. K., Bhanu, S. and Kankane, S., *Responsive polymers in controlled drug delivery*. *Prog. Polym. Sci.*, 2008. **33**(11): p. 1088-1118.
- (106) Braunecker, W. A. and Matyjaszewski, K., *Controlled/living radical polymerization: Features, developments, and perspectives*. *Progress in Polymer Science*, 2007. **32**(1): p. 93-146.
- (107) Otsu, T. and Yoshida, M., *Role of initiator-transfer agent-terminator (iniferter) in radical polymerizations: polymer design by organic disulfides as iniferters*. *Makromol. Chem., Rapid Commun.*, 1982. **3**(2): p. 127-32.
- (108) Otsu, T., *Iniferter concept and living radical polymerization*. *J. Polym. Sci., Part A: Polym. Chem.*, 2000. **38**(12): p. 2121-2136.
- (109) Rohr, T., Hilder, E. F., Donovan, J. J., Svec, F. and Frechet, J. M. J., *Photografting and the Control of Surface Chemistry in Three-Dimensional Porous Polymer Monoliths*. *Macromolecules*, 2003. **36**(5): p. 1677-1684.
- (110) Choi, S.-J., Yoo, P. J., Baek, S. J., Kim, T. W. and Lee, H. H., *An Ultraviolet-Curable Mold for Sub-100-nm Lithography*. *J. Am. Chem. Soc.*, 2004. **126**(25): p. 7744-7745.
- (111) de Boer, B., Simon, H. K., Werts, M. P. L., van der Vegte, E. W. and Hadziioannou, G., *"Living" free radical photopolymerization initiated from surface-grafted iniferter monolayers*. *Macromolecules*, 2000. **33**(2): p. 349-356.
- (112) Schmelmer, U., Paul, A., Kueller, A., Steenackers, M., Ullman, A., Grunze, M., Goelzhaeuser, A. and Jordan, R., *Nanostructured polymer brushes*. *Small*, 2007. **3**(3): p. 459-465.
- (113) Lalevee, J., Blanchard, N., El-Roz, M., Allonas, X. and Fouassier, J. P., *New Photoiniferters: Respective Role of the Initiating and Persistent Radicals*. *Macromolecules* (Washington, DC, U. S.), 2008. **41**(7): p. 2347-2352.

- (114) Kuriyama, A. and Otsu, T., *Living radical polymerization of methyl methacrylate with a tetrafunctional photoiniferter: synthesis of a star polymer*. Polym. J. (Tokyo), 1984. **16**(6): p. 511-14.
- (115) Otsu, T. and Tazaki, T., *Living radical polymerization in homogeneous system with phenylazotriphenylmethane as a thermal iniferter*. Polym. Bull. (Berlin), 1986. **16**(4): p. 277-84.
- (116) Bertin, D., Boutevin, B., Gramain, P., Fabre, J.-M. and Montginoul, C., *Living radical polymerization of methyl methacrylate in the presence of piperidino-dithiocarbamate derivatives as photo-iniferters*. Eur. Polym. J., 1998. **34**(1): p. 85-90.
- (117) Lalevee, J., Allonas, X. and Fouassier, J. P., *A New Efficient Photoiniferter for Living Radical Photopolymerization*. Macromolecules, 2006. **39**(24): p. 8216-8218.
- (118) Lalevee, J., El-Roz, M., Allonas, X. and Fouassier, J. P., *Controlled photopolymerization reactions: the reactivity of new photoiniferters*. J. Polym. Sci., Part A: Polym. Chem., 2007. **45**(12): p. 2436-2442.
- (119) Bromme, T., Moebius, J., Schafer, S., Schmitz, C. and Strehmel, B., *Photocuring in a different light: crosslinking can be achieved by near infrared (NIR) radiation*. Eur. Coat. J., 2012(9): p. 20-21, 24-26, 27.
- (120) Goto, A., Tsujii, Y. and Fukuda, T., *Reversible chain transfer catalyzed polymerization (RTCP): A new class of living radical polymerization*. Polymer, 2008. **49**(24): p. 5177-5185.
- (121) Debuigne, A., Poli, R., Jerome, C., Jerome, R. and Detrembleur, C., *Overview of cobalt-mediated radical polymerization: Roots, state of the art and future prospects*. Prog. Polym. Sci., 2009. **34**(3): p. 211-239.
- (122) Yamago, S., *Precision Polymer Synthesis by Degenerative Transfer Controlled/Living Radical Polymerization Using Organotellurium, Organostibine, and Organobismuthine Chain-Transfer Agents*. Chem. Rev. (Washington, DC, U. S.), 2009. **109**(11): p. 5051-5068.
- (123) Yamago, S. and Nakamura, Y., *Recent progress in the use of photoirradiation in living radical polymerization*. Polymer, 2013. **54**(3): p. 981-994.
- (124) Yamago, S., Ukai, Y., Matsumoto, A. and Nakamura, Y., *Organotellurium-Mediated Controlled/Living Radical Polymerization Initiated by Direct C-Te Bond Photolysis*. J. Am. Chem. Soc., 2009. **131**(6): p. 2100-2101.
- (125) Yamago, S., Iida, K. and Yoshida, J., *Organotellurium Compounds as Novel Initiators for Controlled/Living Radical Polymerizations. Synthesis of Functionalized Polystyrenes and End-Group Modifications*. J. Am. Chem. Soc., 2002. **124**(12): p. 2874-2875.
- (126) Nakamura, Y., Kitada, Y., Kobayashi, Y., Ray, B. and Yamago, S., *Quantitative Analysis of the Effect of Azo Initiators on the Structure of α -Polymer Chain Ends in Degenerative Chain-Transfer-Mediated Living Radical Polymerization Reactions*. Macromolecules (Washington, DC, U. S.), 2011. **44**(21): p. 8388-8397.
- (127) Rang, K. and Sandstrom, J., *The N-(1-phenylethyl)dithiocarbamate anion. Electronic transitions, ultraviolet and CD spectra, reversible formation of its ammonium salts*. J. Chem. Soc., Perkin Trans. 2, 1999(4): p. 827-832.
- (128) Petrov, I. and Simonovska, B., *The UV spectra of ethylene-1,2-bisdithiocarbamates*. J. Mol. Struct., 1986. **142**: p. 167-70.
- (129) Qiu, J., Charleux, B. and Matyjaszewski, K., *Controlled/living radical polymerization in aqueous media: homogeneous and heterogeneous systems*. Prog. Polym. Sci., 2001. **26**(10): p. 2083-2134.

- (130) Kwak, Y., Tezuka, M., Goto, A., Fukuda, T. and Yamago, S., *Kinetic Study on Role of Ditelluride in Organotellurium-Mediated Living Radical Polymerization (TERP)*. *Macromolecules* (Washington, DC, U. S.), 2007. **40**(6): p. 1881-1885.
- (131) Benedikt, S., Wang, J., Markovic, M., Moszner, N., Dietliker, K., Ovsianikov, A., Grützmacher, H. and Liska, R., *Highly Efficient Water-Soluble Visible Light Photoinitiators*. *Journal of Polymer Science, Part A: Polymer Chemistry*, 2015.
- (132) El-Molla, M. M., *Synthesis of polyurethane acrylate oligomers as aqueous UV-curable binder for inks of ink jet in textile printing and pigment dyeing*. *Dyes Pigm.*, 2007. **74**(2): p. 371-379.
- (133) DeLong, S. A., Moon, J. J. and West, J. L., *Covalently immobilized gradients of bFGF on hydrogel scaffolds for directed cell migration*. *Biomaterials*, 2005. **26**(16): p. 3227-3234.
- (134) Du, J.-Z., Sun, T.-M., Weng, S.-Q., Chen, X.-S. and Wang, J., *Synthesis and characterization of photo-cross-linked hydrogels based on biodegradable polyphosphoesters and poly(ethylene glycol) copolymers*. *Biomacromolecules*, 2007. **8**(11): p. 3375-81.
- (135) Smith, R. C., Fischer, W. M. and Gin, D. L., *Ordered Poly(p-phenylenevinylene) Matrix Nanocomposites via Lyotropic Liquid-Crystalline Monomers*. *J. Am. Chem. Soc.*, 1997. **119**(17): p. 4092-4093.
- (136) Zhang, X., Jiang, X. N. and Sun, C., *Micro-stereolithography of polymeric and ceramic microstructures*. *Sens. Actuators, A*, 1999. **77**(2): p. 149-156.
- (137) Evans, E., Bowman, H., Leung, A., Needham, D. and Tirrell, D., *Biomembrane templates for nanoscale conduits and networks*. *Science* (Washington, D. C.), 1996. **273**(5277): p. 933-935.
- (138) Rijcken, C. J., Snel, C. J., Schiffelers, R. M., van Nostrum, C. F. and Hennink, W. E., *Hydrolysable core-crosslinked thermosensitive polymeric micelles: Synthesis, characterization and in vivo studies*. *Biomaterials*, 2007. **28**(36): p. 5581-5593.
- (139) Gray, D. H., Hu, S., Juang, E. and Gin, D. L., *Highly ordered polymer-inorganic nanocomposites via monomer self-assembly. In situ condensation approach*. *Adv. Mater.* (Weinheim, Ger.), 1997. **9**(9): p. 731-736.
- (140) Cheng, J., Jiang, S., Gao, Y., Wang, J. and Sun, F., *Tuning gradient property and initiating gradient photopolymerization of acrylamide aqueous solution of a hydrosoluble photocleavage polysiloxane-based photoinitiator*. *Polym. Adv. Technol.*, 2014. **25**(12): p. 1412-1418.
- (141) Lobry, E., Jasinski, F., Penconi, M., Chemtob, A., Croutxe-Barghorn, C., Oliveros, E., Braun, A. M. and Criqui, A., *Continuous-flow synthesis of polymer nanoparticles in a microreactor via miniemulsion photopolymerization*. *RSC Adv.*, 2014. **4**(82): p. 43756-43759.
- (142) Liu, M., Li, M.-D., Xue, J. and Phillips, D. L., *Time-Resolved Spectroscopic and Density Functional Theory Study of the Photochemistry of Irgacure-2959 in an Aqueous Solution*. *J. Phys. Chem. A*, 2014. **118**(38): p. 8701-8707.
- (143) Liska, R., *Photoinitiators with functional groups. V. New water-soluble photoinitiators containing carbohydrate residues and copolymerizable derivatives thereof*. *J. Polym. Sci., Part A: Polym. Chem.*, 2002. **40**(10): p. 1504-1518.
- (144) Akat, H., Gacal, B., Balta, D. K., Arsu, N. and Yagci, Y., *Poly(ethylene glycol)-thioxanthone prepared by Diels-Alder click chemistry as one-component polymeric photoinitiator for aqueous free-radical polymerization*. *J. Polym. Sci., Part A: Polym. Chem.*, 2010. **48**(10): p. 2109-2114.

- (145) Zhang, Y., Wang, Y., Wang, Y., Song, H. and Wang, Z., *PARA- OR MESO-FUNCTIONALIZED AROMATIC KETONE COMPOUNDS, PREPARATION METHODS THEREOF, AND PHOTOPOLYMERIZATION INITIATORS COMPRISING THE SAME*, Shenzhen Uv-Chemtech Co, L., Zhang, Y., Wang, Y., Wang, Y., Song, H., Wang, Z., Zhang, Y., Wang, Y., Wang, Y., Song, H. and Wang, Z., Editors. 2013.
- (146) Zhang, J., Dumur, F., Xiao, P., Graff, B., Bardelang, D., Gignes, D., Fouassier, J. P. and Lalevee, J., *Structure Design of Naphthalimide Derivatives: Toward Versatile Photoinitiators for Near-UV/Visible LEDs, 3D Printing, and Water-Soluble Photoinitiating Systems*. *Macromolecules* (Washington, DC, U. S.), 2015. **48**(7): p. 2054-2063.
- (147) Kork, S., Yilmaz, G. and Yagci, Y., *Poly(vinyl alcohol)-Thioxanthone as One-Component Type II Photoinitiator for Free Radical Polymerization in Organic and Aqueous Media*. *Macromol. Rapid Commun.*, 2015. **36**(10): p. 923-928.
- (148) Lougnot, D. J. and Fouassier, J. P., *Comparative reactivity of water soluble photoinitiators as viewed in terms of excited states processes*. *J. Polym. Sci., Part A: Polym. Chem.*, 1988. **26**(4): p. 1021-33.
- (149) Mueller, G., Gruetzmacher, H. and Dietliker, K., *Derivatives of bisacylphosphinic acid, their preparation and use as photoinitiators*. 2014, BASF SE, Germany . p. 107pp.
- (150) Mueller, G., Zalibera, M., Gescheidt, G., Rosenthal, A., Santiso-Quinones, G., Dietliker, K. and Grützmacher, H., *Simple One-Pot Syntheses of Water-Soluble Bis(acyl)phosphane Oxide Photoinitiators and Their Application in Surfactant-Free Emulsion Polymerization*. *Macromolecular Rapid Communications*, 2015.
- (151) Noe, R., Beck, E., Maase, M. and Henne, A., *Mono- and bisacylphosphine derivatives*. 2003. p. 70 pp.
- (152) Majima, T., Schnabel, W. and Weber, W., *Phenyl-2,4,6-trimethylbenzoylphosphinates as water-soluble photoinitiators. Generation and reactivity of O:P.(C₆H₅)(O⁻) radical anions*. *Makromol. Chem.*, 1991. **192**(10): p. 2307-15.
- (153) Fairbanks, B. D., Schwartz, M. P., Bowman, C. N. and Anseth, K. S., *Photoinitiated polymerization of PEG-diacrylate with lithium phenyl-2,4,6-trimethylbenzoylphosphinate: polymerization rate and cytocompatibility*. *Biomaterials*, 2009. **30**(35): p. 6702-6707.
- (154) Lin, H., Zhang, D., Alexander, P. G., Yang, G., Tan, J., Cheng, A. W.-M. and Tuan, R. S., *Application of visible light-based projection stereolithography for live cell-scaffold fabrication with designed architecture*. *Biomaterials*, 2013. **34**(2): p. 331-339.
- (155) Wagner, S., Ortwein, J., Rademann, J., Horatscheck, A., Kim, B. G., Lisurek, M., Beligny, S. and Schuetz, A., *Benzoylphosphonate-based photoactive phosphopeptide mimetics for modulation of protein tyrosine phosphatases and highly specific labeling of SH2 domains*. *Angewandte Chemie, International Edition*. **51**(37): p. 9441 - 9447,7.
- (156) Noe, R., Henne, A. and Maase, M., *Preparation of acyl and bisacyl phosphine derivatives*. 2003. p. 28 pp.
- (157) Bertz, A., Ehlers, J.-E., Woehl-Bruhn, S., Bunjes, H., Gericke, K.-H. and Menzel, H., *Mobility of Green Fluorescent Protein in Hydrogel-Based Drug-Delivery Systems Studied by Anisotropy and Fluorescence Recovery After Photobleaching*. *Macromol. Biosci.*, 2013. **13**(2): p. 215-226.

- (158) Nakamura, M., Yokono, H., Tomita, K.-I., Ouchi, M., Miki, M. and Dohno, R., *Substitution effect, absorption, and fluorescence behaviors of 11,12-benzo-1,7,10,13-tetraoxa-4-azacyclopentadec-11-ene (Benzoaza-15-crown-5) derivatives upon cation complexation in solvent extraction*. Journal of Organic Chemistry, 2002. **67**(10): p. 3533 - 3536.
- (159) Schultz, R. A., White, B. D. and Dishong, D. M., *12-, 15, and 18-Membered-Ring Nitrogen-Pivot Lariat Ethers: Syntheses, Properties, and Sodium and Ammonium Cation Binding Properties*. Journal of the American Chemical Society, 1985. **107**: p. 6659.
- (160) Van Den Bulcke, A. I., Bogdanov, B., De Rooze, N., Schacht, E. H., Cornelissen, M. and Berghmans, H., *Structural and Rheological Properties of Methacrylamide Modified Gelatin Hydrogels*. Biomacromolecules, 2000. **1**(1): p. 31-38.
- (161) Efe, H., Bicen, M., Kahraman, M. V. and Kayaman-Apohan, N., *Synthesis of 4-acryloylmorpholine-based hydrogels and investigation of their drug release behaviors*. J. Braz. Chem. Soc., 2013. **24**(5): p. 814-820.
- (162) Li, W., Nakayama, M., Akimoto, J. and Okano, T., *Effect of block compositions of amphiphilic block copolymers on the physicochemical properties of polymeric micelles*. Polymer, 2011. **52**(17): p. 3783-3790.
- (163) Fleckenstein, C. A. and Plenio, H., *The Role of Bidentate Fluorenylphosphines in Palladium-Catalyzed Cross-Coupling Reactions*. Organometallics, 2008. **27**(15): p. 3924-3932.
- (164) Nametkin, N. S., Durgar'yan, S. G., Tikhonova, L. I. and Filippova, V. G., *Polymerization transformation of substituted vinyl germanium compounds*. Polymer Science U.S.S.R, 1971. **13**: p. 191,192.
- (165) Jutzi, P. and Lorey, O., *Reactions of 2-trimethylsilyl-, -germyl-, -stannyl-1,3-dithianes with acid chlorides*. Phosphorus Sulfur, 1979. **7**(2): p. 203-9.
- (166) Armarego, W. L. F. and Chai, C. L. L., *Chapter 4 - Purification of Organic Chemicals*, in *Purification of Laboratory Chemicals (Sixth Edition)*, Chai, W.L.F.A.L.L., Editor. 2009, Butterworth-Heinemann: Oxford. p. 88-444.
- (167) Mautner, A., Dissertation, TU Wien
- (168) Gugg, A., Dissertation, Vienna University of Technology
- (169) Gorsche, C., Technische Universität Wien